Ph.D. Dissertation in Natural Sciences

Novel Secondary Metabolites from Marine Sediment-Derived Actinomycetes

해양퇴적물 유래 방선균에서 분리한 신규 이차대사산물

Inho Yang

February 2015

Laboratory of Marine Drugs
School of Earth and Environmental Sciences
Seoul National University

Novel Secondary Metabolites from Marine Sediment-Derived Actinomycetes
해양퇴적물 유래 방선균에서 분리한 신규 이차대사산물

지도교수 강 헌 중

이 논문을 이학박사 학위논문으로 제출함
2014 년 12 월

서울대학교 대학원
지구환경과학부
양 인 호

양인호의 이학박사 학위논문을 인준함
2014 년 12 월

위 원 장 _____ (인)
부 위 원 장 _____ (인)
위 원 _____ (인)
위 원 _____ (인)
위 원 _____ (인)

Abstract

Marine natural products are emerging source as an attractive drug pipeline based on its enormous biological diversity of origin. Technical advances like scuba diving, manned submarine boosted the interest to the marine natural products three decades ago and there are eight approved marine drugs now. Most of the approved drugs are based on marine natural products isolated from marine invertebrates, but recent study suggest that most of them are produced by microorganisms. In this study, actinomycetes were isolated from marine envirionments and investigated to discover a novel and bioactive marine natural products.

A chemical investigation of the actinomycetes, *Nocardiopsis* sp. CNQ115 isolated from marine sediment collected off the coast of southern California resulted in the isolation of two novel imidazole natural compounds nocarimidazoles A and B. The chemical structures of nocarimidazoles A and B were determined by interpretation of NMR data analyses. No significant antibacterial or cytotoxic activities were observed. Investigation of the chemical components of a *Streptomyces* sp. 10A085 isolated from mudflat sediments collected on the southern coast of the Korean peninsula led to isolation of four new compounds, anithiactins A – D. The chemical structures of anithiactins were determined by interpretation of NMR data analyses, while the chemical structure of anithiactin B was established from a combination of NMR spectroscopic and crystallographic data analysis. Anithiactins A – C displayed moderate acetylcholinesterase inhibitory activity with no significant cytotoxicity.

Key words

Marine natural products, Marine microorganisms, Marine actinomycetes, 2-phenylthiazole, 9,11-Secosterol

Student Number: 2010-30944

Table of Contents

List of Papers

This thesis is based on the following papers and unpublished data

Leutou, A.; **Yang, I.**; Kang, H.; Nam, S. Nocarimidazoles A and B from Marine–derived Actinomycetes *Nocardiopsis* sp. *manuscript in preparation.*

Kim, H.; **Yang, I.**; Patil, R.; Kang, S.; Lee, J.; Choi, H.; Kim, M.; Nam, S.; Kang, H. Anithiactins A-C, Modified 2-Phenylthiazoles from a Mudflat-Derived *Streptomyces* sp. *J. Nat. Prod*. **2014**. *77*, 2716-2719.

Yang, I.; Choi, H.; Won, D.; Nam, S.; Kang, H. An Antibacterial 9,11-Secosterol from a Marine Sponge *Irchinia* sp. *Bull. Korean Chem. Soc.* **2014**, *35*, 3360-3362.

List of other papers by the author not appended to this thesis

Wang, W.; Lee, T.; Patil, B.; Mun, B.; **Yang, I**.; Kim, H.; Hahn, D.; Won, D.; Lee, J.; Lee, Y.; Choi, C.; Nam, S.; Kang, H. Monanchosterols A and B, Bioactive Bicyclo[4,3,1]steroids from a Korean Sponge *Monanchora* sp. *J. Nat. Prod.* **2015**, *ASAP*

Mun, B.; Wang, W.; Kim, H.; Hahn, D.; **Yang**, **I.**; Won, D.; Kim, E.; Lee, J.; Han, C.; Kim, H.; Ekins, M.; Nam, S.; Choi, H.; Kang, H. Cytotoxic 5α,8α-epidioxy sterols from the marine sponge *Monanchora* sp. *Arch. Pharm. Res.* **2015**, *38*, 18-25.

Lee, Y.; Wang, W.; Kim, H.; Giri, A.; Won, D.; Hahn, D.; Baek, K.; Lee, J.; **Yang**, **I.**; Choi, H.; Nam, S.; Kang, H. Phorbaketals L–N, cytotoxic sesterterpenoids isolated from the marine sponge of the genus *Phorbas Bioorg. Med. Chem. Lett.* **2014**, *24*, 4095

Hahn, D.; Chin, J.; Kim, H.; **Yang**, **I.**; Won, D.; Ekins, M,; Choi, H.; Nam, S.; Kang, H. Sesquiterpenoids with PPARd agonistic effect from a Korean marine sponge *Ircinia* sp. *Tetrahedron. Lett.* **2014**, *55*, 4716

Lee, J.; H. Kim, H.; T. Lee, T.; **Yang**, **I.**; Won, D.; Choi, H.; Nam, S.; Kang, H. Anmindenols A and B, inducible nitric oxide synthase inhibitors from a marine-derived *Streptomyces* sp. *J. Nat. Prod*. **2014**, *77(6)*, 1528

Kim, H.; Chin, J.; Choi, H.; Baek, K.; Lee, T.; Park, S.; Wang, W.; Hahn, D.; **Yang**, **I.**; Lee, J.; Mun, B.; Ekins, M.; Nam, S.; Kang, H.
Phosphoiodyns A and B, Unique Phosphorus-Containing Iodinated Polyacetylenes from a Korean Sponge *Placospongia* sp. *Org. Lett.* **2013**, *15*, 100

Ham, J.; Hwang, H.; Kim, E.; Kim, J.; Cho, S.; Ko, J.; Lee, W.; Lee, J.; Holla, H,; Banerjee, J.; Kim, S.; **Yang**, **I.**; Lee, H.; Shin, K.; Choi, H.; Nam, S.; Tak, J.; Hahn, D.; Oh, T.; Won, D.; Lee, T.; Choi, J.; Park, M.; Seok, C.; Chin, J.; Kang, H. Discovery, design and synthesis of Y-shaped peroxisome proliferator-activated receptor d agonists as potent anti-obesity agents *in vivo Eur. J. Med. Chem.* **2012**, *53*, 190

List of Figures

List of Tables

List of Schemes

Chapter 1. Marine Natural Products as a New Pharmaceutical Pipeline

1.1 History of Natural Products as a Source for Drug Development

From old days, natural products have been used as a drug source. Before the modern age, natural products were used as a form of extract or plant materials. The oldest written record of medicinal plant was shown on the clay slab at Sumeria approximately 5,000 years ago which described 12 recipes for drug preparation from more than 250 different plants (Kelly, 2009). In China, medical usage of *Rhei rhisoma* (rhubarb), camphor, *Theae folium* (tea tree), ginseng, cinnamon bark, ephedra and many other medicinal plants were known since 2,500 BC, and these plant are still widely used over eastern and southern Asia (Bottcher, 1965; Wiart, 2006). After that, all through the history of mankind, continuous efforts to look for the healings were enormous and results were pass throughout the millennia (Petrovska, 2012).

After the advance of the science and technology in modern centuries, some of these medicinal plant become medicine after extraction, isolation and quantification. This technical improvement resulted in the development of many drugs such as khellin, metformin and verapamil. The khellin was isolated from plant *Ammi visnaga* Lamk and used as a bronchodilator. Efforts to reduce the side effects of khellin led to the development of chromolyn (used in the form of sodium chromoglycate). The galegine was isolated from the plant *Galega officinalis* L. as a major active ingredient of anti-hyperglycemia. The metformin was developed from galegine with

its main chemical structure maintained. The papaverine isolated from *Papaver somniferum* was advanced to verapamil to treat hypertension (Farbricant & Farnsworth, 2001). This medicinal plant is also well-known as a source of morphine and codeine (Buss & Waigh, 1995).

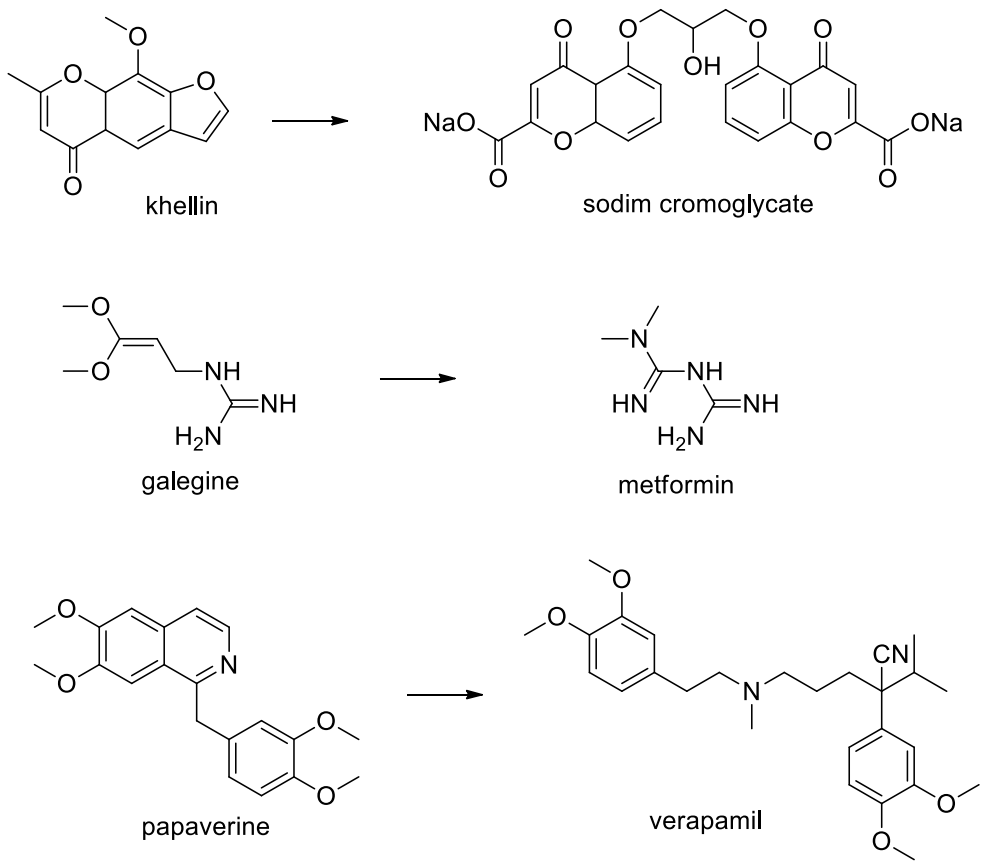

Figure 1.1 Drugs developed from medicinal plants

However, the most famous example of medicinal plant derived medicine would be the antimalarial drugs development. First generation antimalarial drugs, such as chloroquine and mefloquine, were developed from quinine which was isolated from the bark of *Cinchona* sp. This plant extracts was used to treat fevers around the Amazon region traditionally. Spread of quinine-class resistance malaria led to the

discovery of artemisinin isolated from the plant *Artemisia annua* and the development of artemisinin class antimalarial drugs. This plant has been used to treat fevers in China for a long time (Wongsrichanalai et al., 2002). Artemisinin class drugs are deployed to combat malaria all across the world, even though its mechanism of action not clear (O'Neill & Posner, 2004; O'Neill et al., 2010; Wang et al. 2010).

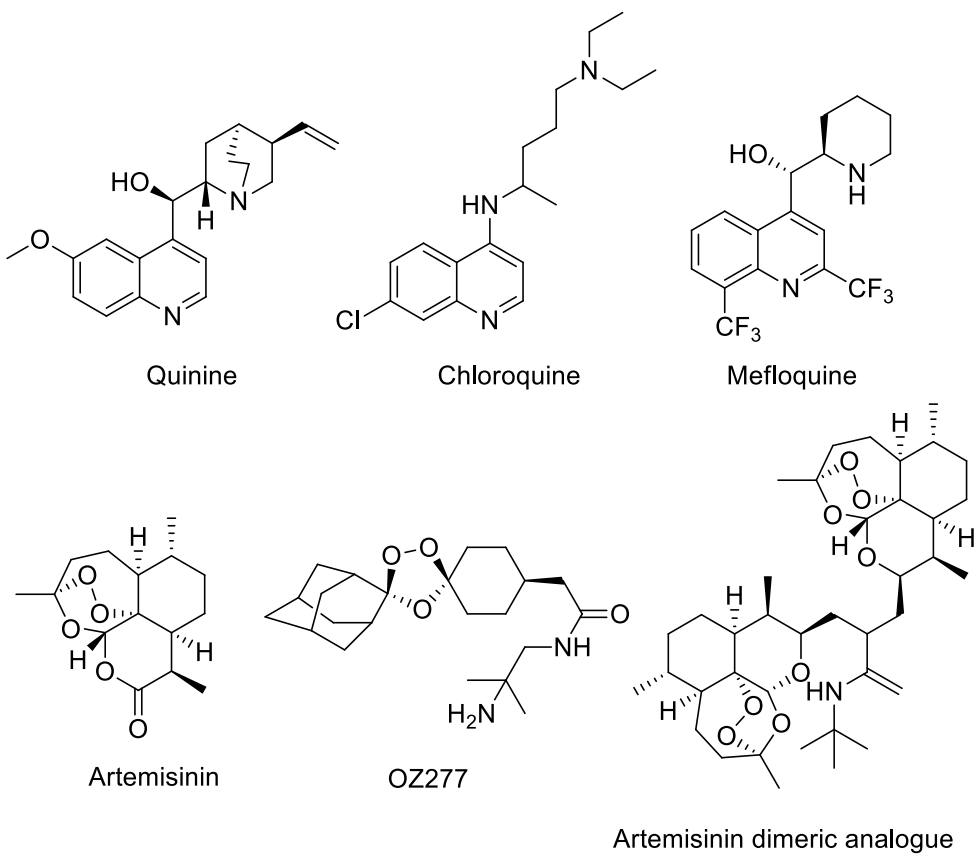

Figure 1.2 Antimararial drugs developed from medicinal plants

Likewise, using natural products as drug lead was deployed as useful tactics to combat other disease includes anticancer (Gueritte et al., 2005; Roussi et al., 2012) and antihypertensive (Cordell & Colyard, 2012). The analysis of the sources of small

molecule shows this trend clearly. Figure 1.3 is showing classified new drugs from 1981 to 2010 based on its origin as synthetic (*S*) or natural product (*N*). It revealed that two thirds of the small molecules are natural products or natural products inspired. Only one third can be categorized as truly synthetic (Newman & Cragg, 2012). Conclusively, natural products are major pipelines for developing drugs now and then (Cragg & Newman, 2013).

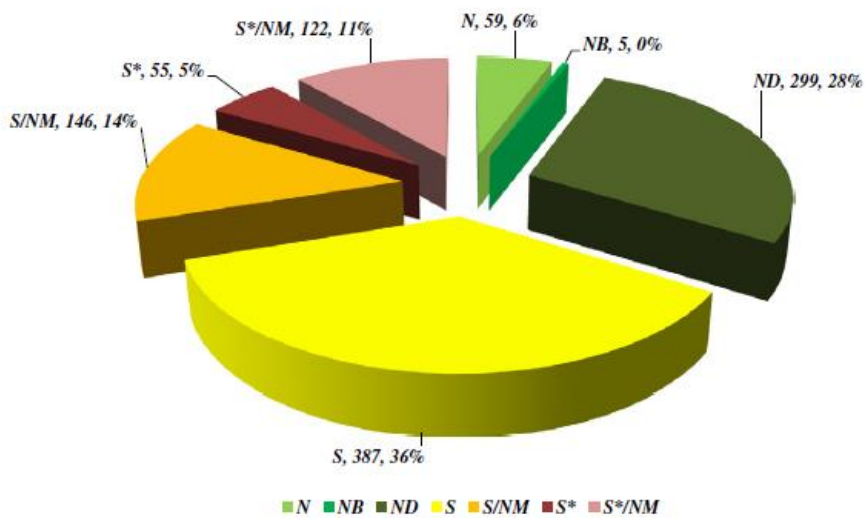

Figure 1.3 Sources of drugs [*N* (an unmodified natural product), *NB* (a natural product botanical), *ND* (a modified natural product), *S* (a synthetic compound with no natural product conception), S^*, S^*/NM (a synthetic compound with a natural product pharmacophore; */NM* indicating competitive inhibition), *S/NM* (a synthetic compound showing competitive inhibition of the natural product substrate)] (Cragg & Newman, 2013)

1.2 Marine Natural Products as a New Pharmaceutical Pipeline

1.2.1 Novelty of Marine Natural Products

Unlike its counter parts, marine resources were not used much as a medicinal sources for long time. Before scuba diving technique spread widely, collection of marine organisms under the water surface was very limited to specifically trained

professionals. Recent introduction of various technical advances like scuba, dredging, manned submarine and remotely operated vehicles gives more chance to address the marine resources. And this makes marine resources as a more attractive drug discovery pipeline. Currently, more than 30,000 marine natural products were reported and number is increasing (Blunt & Munro, 2008).

The most interesting character of the marine natural product is from biodiversity of marine organisms. For examples, there is only 1 terrestrial exclusive phylum among the 33 animal phyla. On the other hand, there are 15 of marine exclusive phyla and 5 of the rest phyla have more than 95% of their species in marine (Margulis & Schwarts, 1988). This enormous number of marine animal species and phyla may due to the oldness and wideness of the ocean environment then terrestrial one. As terrestrial organisms are descendants of marine life and 70% of the earth surface is covered with four thousand deep water.

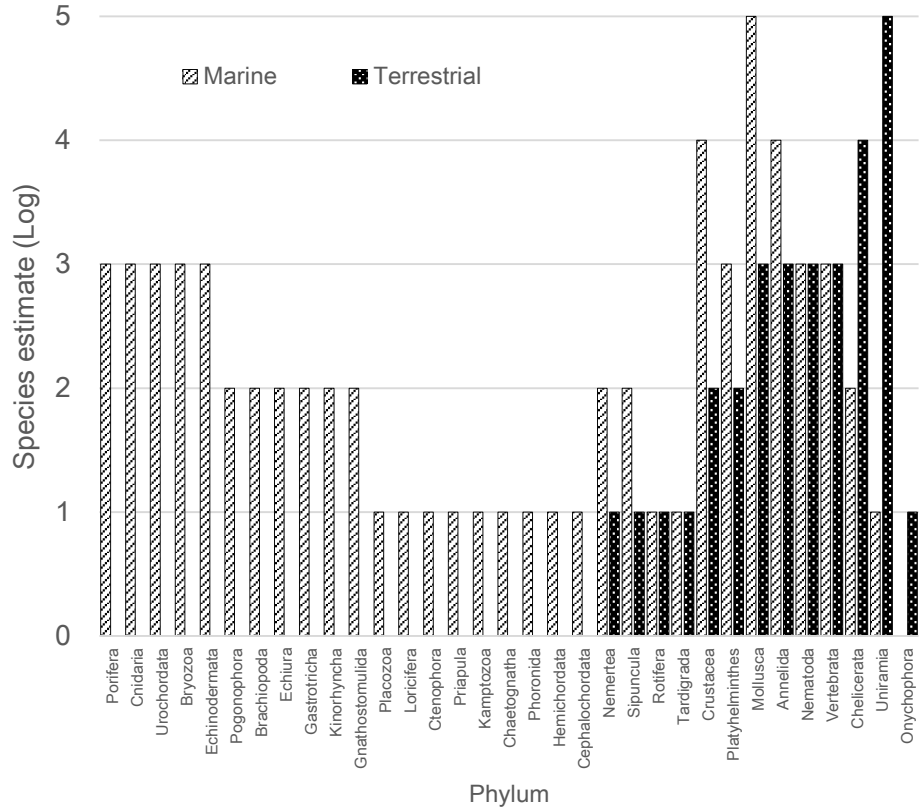

Figure 1.4 Number of estimated species of animal phyla in terrestrial and marine environment (Margulis & Schwarts, 1988, modified)

It is clear that more number of the species gives more chance to discover novel chemical structures. One of the Chinese chemistry group quantified the novelty of marine natural products (Kong et al., 2010). They categorized the known natural products from Dictionary of Natural Products and Dictionary of Marine Natural Products to the each of the specific 'scaffolds' which are defined as the contiguous ring systems with chains that link them. This scaffold analysis gave that there are 163,089 terrestrial natural products using 25,289 scaffolds and 31,772 marine natural products using 5276 scaffolds. And more than 70% of marine scaffolds are using less than two entities, 50% of the scaffolds are having only one compound.

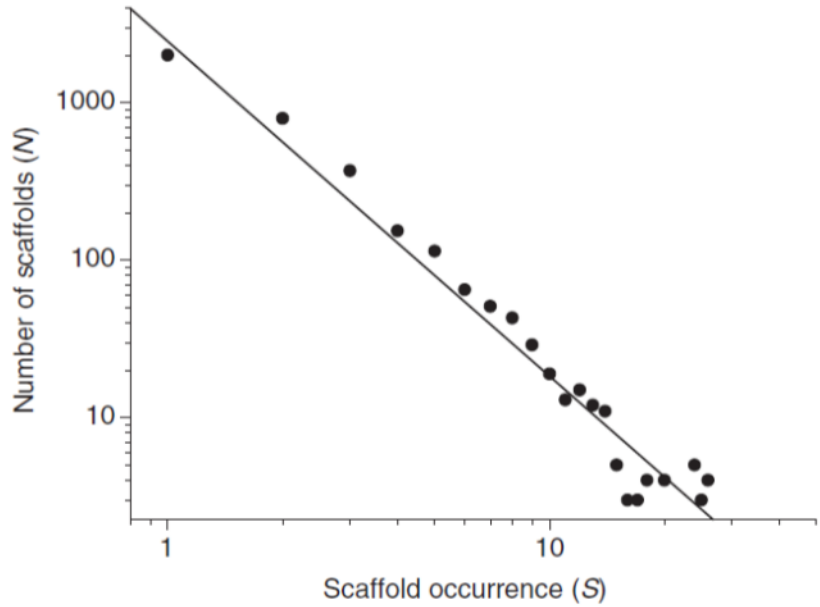

Figure 1.5 Number of scaffolds accord with number of marine natural products (Kong et al., 2010)

1.2.2 Marine Drugs on the Market

There are eight Food and Drug Administration (FDA) and European Medicines Agency (EMEA) approved drugs (Meyer, 2014). The four of marketed drugs are used to treat cancer (Adcetris, Cytoser-U, Halaven, Yondelis), two for virus (Carragelose, Vira-A) and each of one for hypertriglyceridemia and neuropathic pain (Lovaza and Prialt). Three of these are employed to drug as natural product itself (Prialt, Yondelis, Carragelos) and others took modifications to solve the supply and ADMET properties problems. Regarding origin of the drugs, six of marine drugs were obtained from marine invertebrates like tunicate, sea hare, marine snail and sponge (Martins et al., 2014). (Figure 1.6, Table 1.1)

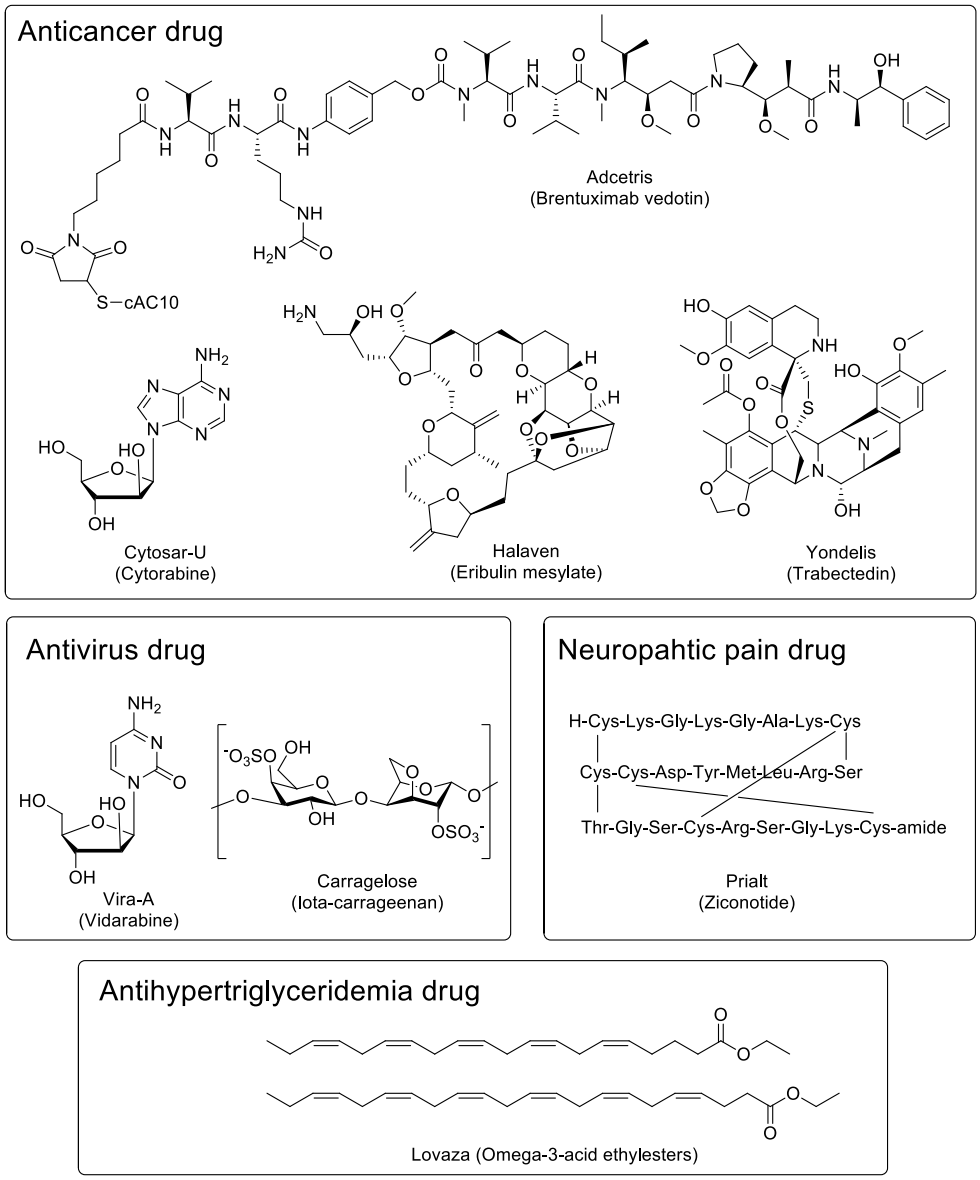

Figure 1.6 Chemical structures of marine drugs on the market divided by therapeutic area (Martins et al., 2014 modified)

Marine drug pipelines is listed with nine more drug candidates under clinical trials mainly treats cancer, include Aplidin and Zalypsis.

Table 1.1 The marine drugs on market (Martins et al., 2014)

Trademark (Compound Name).	**NP[a] or Derivative**	**Original NP / Source Organism**	**Therapeutic Area**	**Status (2013)**
Cytostar-U (Cytorabine)	NP derivative	Spongothymidine / Sponge *Cryptotethya crypta*	Cancer	FDA / EMEA approved
Vira-A (Vidarabine)	NP derivative	Spongouridine / Sponge Crptotethya crypta	Virus	FDA / EMEA approved US discontinued
Prialt (Ziconotide)	NP	ω-Conotoxin / Marine snail *Conus magus*	Neuropahtic Pain	FDA / EMEA approved
Lovaza (Omega-3-acid ethyl esters	NP derivative	Omega-3-fatty acids / fish	Hypertriglyceridemia	FDA / EMEA approved
Yondelis (Trabectedin)	NP	Ecteinascidin 743 / Tunicate *Ecteinascidia turbinata*	Cancer	FDA / EMEA approved
Halaven (Eribulin mesylate)	NP derivative	Halichondrin B / Sponge *Halichondria okadai*	Cancer	FDA / EMEA approved
Adcetris (Brentuximab vedotin)	NP derivative	Dolastatin 10 / Sea hare *Dolabella auricularia*	Cancer	FDA / EMEA approved
Carragelose (Iota-carrageenan)	NP	Iota-carrageenan / Red algee *Eucheuma / Cnondus*	Virus	Over-the-counter drug

[a]NP means natural product

Marine invertebrates are major supply for the marine drugs. It is because the many of marine natural products were obtained from marine invertebrates (Hu et al., 2011). (Figure 1.7) Within the marine invertebrate, sponge and coral were the main sources for the marine natural products. These animals are taking unique ecological roles to support the diversity of marine ecosystem. Coral reef are supporting up to 40% of all fish species while taking only 0.1% of ocean area around the tropical zone (Moyle & Cech, 2003). Sponges inhibit all around the ocean from polar area to the deep ocean trench bottom and associated with a wide variety of microorganisms (Taylor et al., 2007). It is known that from half to 80% of sponge weight is considered be that of associated bacteria. Both of these animals are filter-feeder, and providing physical shelters to around environment. However, the fact that marine invertebrates are main source of the marine drug is one of the main obstacle to overcome for the development of marine drugs that industrial scale cultivation technique for the most of the marine invertebrate are not available yet.

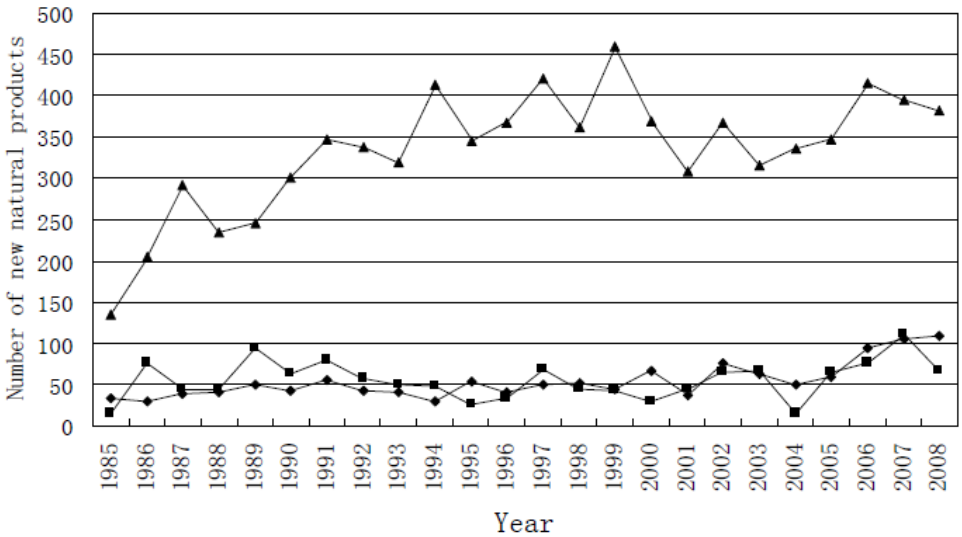

Figure 1.7 Temporal trends in the number of novel compounds isolated from different marine organisms between 1985 and 2008. [▲, marine invertebrate; ■, marine algae; ◆, Marine microorganisms (including phytoplankton).] (Hu et al. 2011)

1.2.3 Major Hurdle of Marine Natural Products derived Drug Discovery

As described ahead, marine natural products have potentials as attractive drug pipeline and are taking more and more interests. However, there are several problems to overcome. First of all, availability problems are still not neglectable. Despite of the introduction of many advanced methods, marine resource is not much close enough. Average depth of the open ocean is more than four thousand m, but general scuba technique allow us to only 40 m deep. Even with the most latest diving technique with atmospheric diving suit, depth reach is less than 700 m. The dredging is not considered these days for it is not eco-friendly and it is too much random sampling method. The budget for manned submarine is not available for most of the research group and even for the big pharmaceutical company. Recent introduce of

remotely operated vehicles can be a good alternative for most of the collection methods.

Second problem is biodiversity itself. As describe above, estimated number of marine organism is enormous. But there is not enough research infra to support that research. For example, sponge is one of the major source for the marine natural products for several decades, but convenient molecular level identification method like 16S RNA sequencing of microorganisms for this phylum is still under construction (Vargas et al., 2012). To have the desired result from this enormous resource, we need to set specific strategy considering ecological back ground and marine taxonomy.

Third and most important problem is supply. This issue can link with first addressed availability problem. As described above, most of the marine drugs were developed from invertebrate derived marine natural products. And most of those marine drug on market was 20 to 40 year after the first report of the natural products. It is mainly because of the supply problem that most of the industrial scale culture technique for marine invertebrate are not available yet. Those years are more than couple of decades longer than common process from terrestrial natural products. Most of these time gap used on the establishment of synthetic method for marine natural products supply. For example, Taxol was notorious for its supply problem. At early stage of discovery, 10 g of Taxol was isolated from 1,200 kg of *Taxus brevifolia* bark (Goodman & Walsh, 2001). Yield was low, but it was possible to do it. But it is not possible for marine natural products. There is no detailed research database of distribution of marine organisms as the forestry, also there is no industrial background to collect the marine organisms like the timber industry.

Yondelis is good example of marine drugs which solve the supply problem with creative way. It was first isolated from tunicate *Ecteinascidai turbinate* (sea squirt) and elucidated in 1984 (Rinehart, 2000). At the early stage of discovery, it was supplied from sea squirt at extremely low yield. Based on its anticancer activity and novel chemical structure, many synthetic preparation methods were developed to meet the requirement of this drug for clinical trials. But break-through was on other way. The Spanish pharmaceutical venture company PharmaMar devised semisynthetic process from Safracin B, which was obtained from bacterium *Pseudomonas fluorescens* by fermentation. This intuition from Yondelis with other recent discovery suggest that actual producer of most current marine drug from marine invertebrates are symbiotic microorganisms (Gerwick & Moore, 2012). This also emphasize the importance of marine microorganisms as attractive drug discovery pipeline.

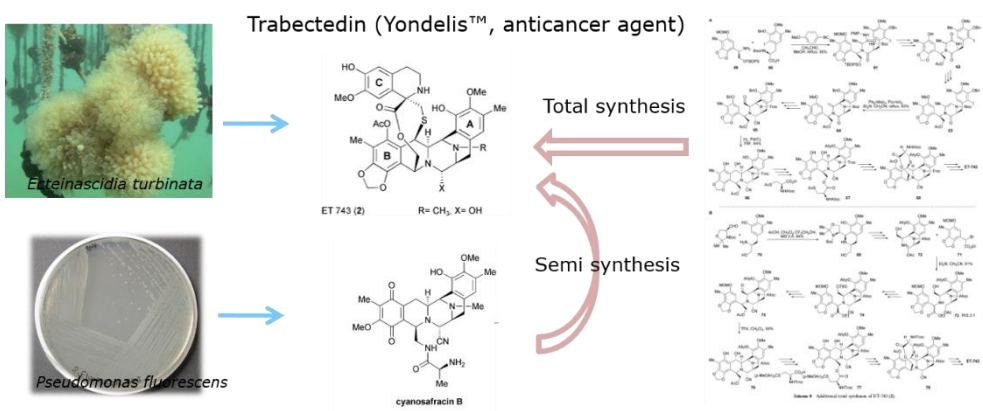

Figure 1.8 Supply of yondelis (Cuevas & Francesch, 2009)

In this study, sponge and marine microorganisms were screened to discover novel natural products. Sponge was screening target as the traditional marine natural products source. Marine microorganisms from bottom sediment were isolated and

screened. Mudflat was selected for new source of marine microorganisms, based on its environmental uniqueness, and isolated microorganisms were screened. Obtained marine natural products were studied with spectroscopic methods.

Chapter 2. Marine Natural Products from Sediment-Derived Actinomycetes

2.1 Introduction

Actinomycetes are the most economically and biotechnologically valuable prokaryotes due to the discovery of wide range of bioactive secondary metabolites, such as antibiotics, antitumor agents, and immunosuppressive agents (Ravikumar et al, 2011). More than 15,000 bioactive molecules were produced by these microbes including many that are used as drugs today. As the soil-derived microorganisms have been intensively investigated for discovering therapeutically important molecules over a half century (Fenical, 1993), the frequency of new compounds discovery has been decreased. Therefore, an unexplored environment needs to be searched for isolating different microorganisms found in terrestrial environments. Recently, microorganisms isolated from the marine environments including the deep sea sediments and marine organisms, have been considered as a good source for exploring new natural products (Takami et al., 1997). In particular, marine actinomycetes have different characteristics from those of terrestrial counterparts that produced unprecedentedly secondary metabolites with diverse biological activities (Imada et al., 2007; Fenical & Jenson, 2006).

2.2 Results and Discussion

2.2.1 Structure Elucidation of Nocarimidazoles from CNQ115

As part of our ongoing research to discover new bioactive compounds from marine-derived actinomycetes, strain CNQ115, identified as *Nocardiopsis* sp. from marine sediments collected off the coast of southern California was investigated. The genus *Nocardiopsis* has been shown to be phylogenetically coherent and to represent a distinct lineage within the order Actinomycetales (Rainey et al., 1996). *Nocardiopsis* strains are ubiquitous in the environment and are frequently isolated from habitats with moderate to high salt concentrations such as saline soils, marine sediments, and salterns (Sabry et al., 2004). The strains of *Nocardiopsis* have also been reported to produce a variety of biologically active agents including the cytotoxic antifungal antibiotic kalafungin (Bergy, 1968), the antibiotic 3-trehalosamine (Dolak et al., 1980), the protein kinase C inhibitor methylpendolmycin, and a staurosporine-like inhibitor of a cyclic AMP-dependent protein kinase (Peltola et al., 2001). LC-MS guided fractionations has led to two new natural products, nocarimidazols A (**1**) and B (**2**). Herein, we report the isolation and structure characterization of nocarimidazols A and B.

Imidazole derivatives were intensively studied for its pharmacological properties on various range of biological activities like analgesic and anti-inflammatory (Suzuki et al., 1992), anti-fungal (Johnson et al., 1999; Brewer et al., 1987) and anti-viral (Sharma et al., 2009). And many of prescription drugs have imidazole as a key pharmacophore (Zhang et al., 2014). Dacarbazine, well-known skin cancer and Hodgkin disease drug (Eggermont & Kirkwood, 2004), shares key chemical structure with nocarimidazoles, having carboxylic carbon and additional nitrogen at

4 and 5 position of imidazole ring. Also, many natural products with imidazole moiety have been reported (Jin, 2011). But, natural products which have 4-carboxylic carbon with imidazole ring is very rare. And imidazole natural products with 4-carboxylic carbon and 5-amine group is not reported yet.

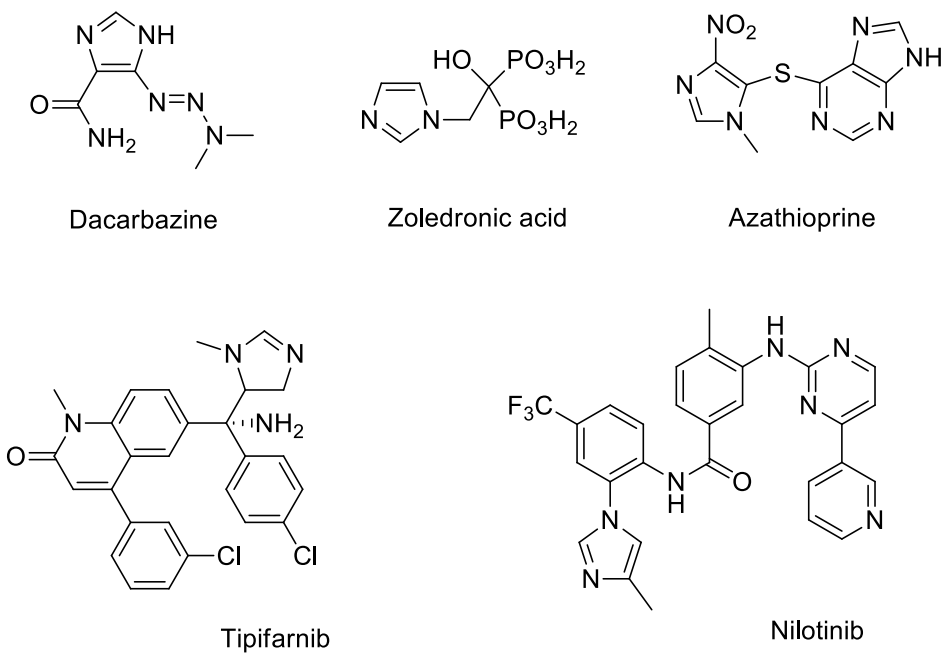

Figure 2.1 Imidazole-based anticancer drugs (Eggermont & Kirkwood, 2004)

2.2.1.1 Nocarimidazole A (**1**)

Actinomycete strain CNQ115, obtained from marine sediment sample collected off the coast of southern California, at a depth of 51 m, required seawater for growth. This strain shares 99.3% 16S rRNA gene sequence identity with its nearest neighbor, *Nocardiopsis* sp. The strain was cultured at 25 ℃ by rotary shaking in 8 replicate 2.5-L Ultra Yield Flasks each containing 1 L of the medium for seven days. The broth was extracted with EtOAc and evaporated under reduced pressure to yield an

extract, which was subjected to flash chromatography followed by HPLC to afford pure samples of nocarimidazols A (**1**) and B (**2**).

Nocarimidazols A (**1**) was obtained as a red amorphous solid. Its molecular formula was established as $C_{13}H_{23}N_3O$ based on HRESIMS (obsd $[M + H]^+$ at *m/z* 238.1918), implying 4 degrees of unsaturation. The UV spectrum of **1** displayed absorption bands at 300 nm, indicating the presence of a significant chromophore in the molecule. The IR spectrum of 1 showed the presence of a primary amine (3433 and 1640 cm^{-1}) and an α, β-unsaturated carbonyl group at 1678 cm^{-1}. Two substructures, a linear aliphatic chain and a imidazole moiety, were assigned by analyses of ^1H, ^{13}C, COSY, HSQC, and HMBC NMR spectroscopic data recorded in $CDCl_3$ (Tables 2.1). The ^1H NMR spectrum of **1** displayed a downfield singlet proton [(δ_H 7.80, s)]. The presence of alkyl chain moiety was suggested by a methyl doublet integrating for six hydrogens [δ_H 0.82, (d, J = 6.6 Hz)] and overlapping methylene proton signals [δ_H 1.03 - 1.32, (m)] and one methine proton [δ_H 1.46, (m)] and two downfield methylene proton [δ_H 1.62 (q, J =7.4 Hz), 2.68 (t, J = 7.4 Hz)]. The COSY cross peaks of H3-14 and H3-15 to H-13 indicated that these methyls were coupled to a methine proton (Table 2.1). The terminal gem dimethyl protons (H3-14 and H3-15) at δ_H 0.82, which showed HMBC correlations to C-13 (δ_C 27.9), and to C-12 (δ_C 38.9). The proton signal (δ_H 1.11) derived from H2-12 showed a HMBC correlation to C-11 (δ_C 27.2). These NMR data established a 2-methylbutane unit.

The proton signal (δ_H 2.68) derived from H2-7 showed a COSY correlation to an aliphatic methylene proton signal at δ_H 1.62 (H2-8), which in turn showed a COSY correlation to another aliphatic methylene proton signal at δ_H 1.29 (H2-9). The proton signal (δ_H 2.68) derived from H2-7 also showed HMBC correlations to a carbonyl C-6 (δ_C 190.9). These NMR data established a pentanone unit.

The alkyl chain moiety was final established by HMBC correlation from the methylene protons H2-11 to the carbons C-9. The HMBC correlations from the singlet proton H-2 (δ_H 7.80, s) to carbons C-4 (δ_C 146.9) and C-5 (δ_C 111.7) and the molecular formula of **1** allowed the construction of a imidazole ring moiety. Lastly, the connection between the alkyl chain moiety and the imidazole ring moiety was achieved by the long range HMBC correlations from an olefinic proton H-2 to carbonyl carbon C-6 allowed the assignment of nocarimidazols A to be completed, as shown in Figure 2.2.

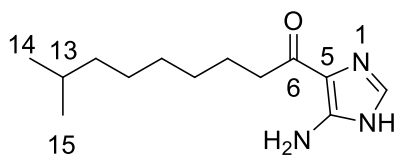

1

Figure 2.2 Chemical structure of nocarimidazole A (**1**)

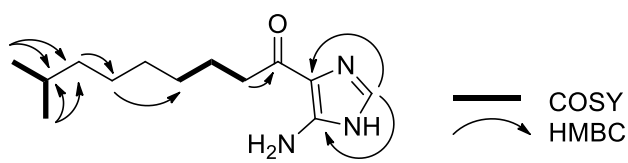

1

Figure 2.3. Key COSY and HMBC correlations of nocarimidazole A (**1)**

Table 2.1 Physical and spectral properties of nocarimidazole A (**1**)

Red amorphous solid
Molecular formula: $C_{13}H_{23}N_3O$,
HRFABMS: *m/z* 238.1918 $[M+H]^+$ (calcd for 238.1919)
IR (KBr) ν_{max}: 3433, 3054, 2928, 2360, 1678, 1640, 1384, 1265, 1201, 1140, 839, 749 cm^{-1}
^{1}H and ^{13}C NMR data[a] ($CDCl_3$)

	1	
No.	δ_C, mult.[b]	δ_H (*J* in Hz)
2	130.2, CH	7.80, s
4	146.9,C	
5	111.7,C	
6	190.9, C	
7	38.8, CH_2	2.68, t (*J* = 7.4)
8	24.1, CH_2	1.62, q (*J* = 7.4)
9	29.7, CH_2	1.29, m
10	38.8, CH_2	1.22, m
11	27.2, CH_2	1.24, m
12	38.9, CH_2	1.11, m
13	27.9, CH	1.47 dp (*J* = 13.1, 6.6)
14	22.5, CH_3	0.82, d (*J* = 6.6)
15	22.5, CH_3	0.82, d (*J* = 6.6)

[a] 500 MHz for ^{1}H NMR and 125 MHz for ^{13}C NMR
[b] Multiplicity was determined by the analysis of 2D NMR spectroscopic data

2.2.1.2 Nocarimidazole B (**2**)

Nocarimidazols B (**2**) was obtained as a red amorphous solid. Its molecular formula was established as $C_{14}H_{25}N_3O$ based on HRESIMS (obsd $[M + H]^+$ at *m/z* 252.2075), implying 4 degrees of unsaturation. The UV absorption spectrum of **2** showed an absorption band at 300 nm, which was identical with the UV data obtained from nocarimidazols A (**1**). The IR spectrum of **2** was also identical to that of **1**. The ^1H NMR spectrum of **2** was almost identical to that of **1** except for the presence of one additional methylene resonance and the presence of one methyl triplet (δ_H 0.84) and methyl doublet (δ_H 0.78). The ^{13}C NMR data of **2** were also similar to those of **1** except for additional carbon signals at C-14 [δ_C 36.5] (Table 2.2). The interpretation of 2D NMR spectroscopic data permitted the identification of the structure of **2**.

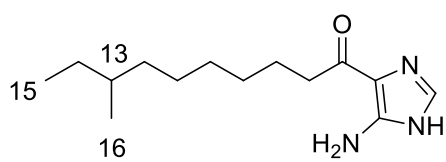

2

Figure 2.4 Chemical structure of nocarimidazole B (**2**)

To confirm the imidazole moiety of compound **2**, methyl derivative (**3**) was prepared with diazomethane. A down field singlet (δ_H 3.42) was observed at ^1H NMR spectrum of compound **3** and the HMBC correlations from the singlet proton 3-NCH_3 (δ_H 3.42) to C-2 (δ_C 130.9) and C-4 (δ_C 144.6) was clear to assign the position of N-3 within imidazole ring. However, to clarify the position of rest of nitrogen, dimethyl derivative of compound **2** was

prepared with iodomethane. This dimethyl derivative (**4**) of compound **2** showed two down field singlets and the HMBC correlations from the singlet proton 1-NCH_3 (δ_H 3.95) to C-2 (δ_C 130.6) and C-5 (δ_C 107.8) established the position of N-1 in imidazole ring. Those HMBC correlations observed from methyl derivatives of nocarimidazole B clarify the position of nitrogens and quaternary carbons within the imidazole ring as shown in Figure 2.5.

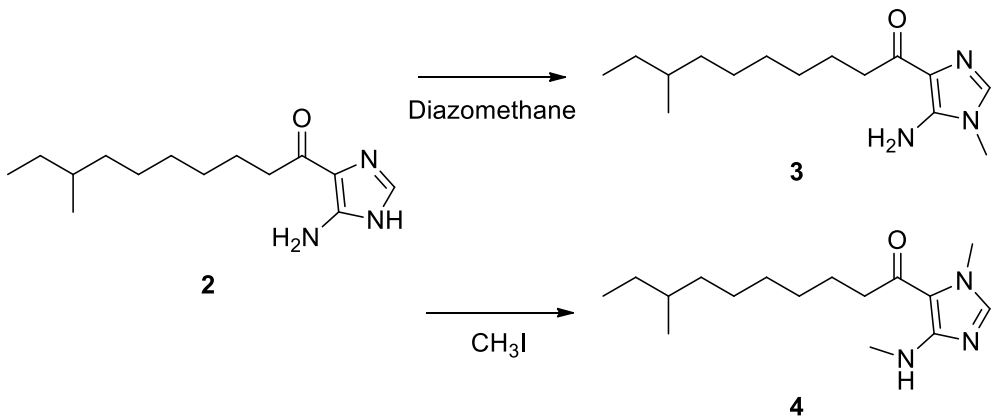

Scheme 2.1 Methylation reaction of nocarimidazole B (**2**)

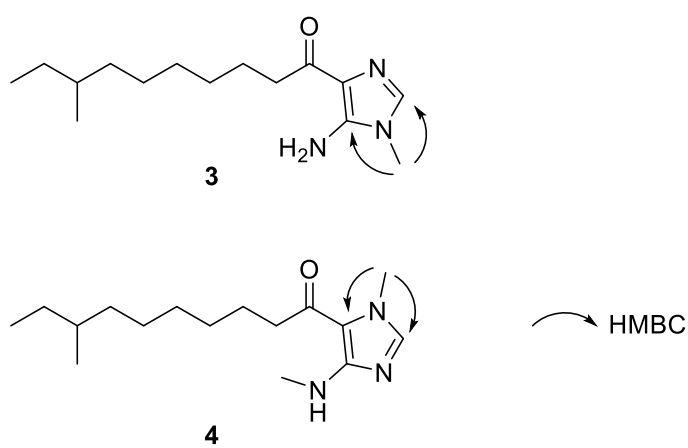

Figure 2.5 Key HMBC correlations of nocarimidazole B (**2**)

Table 2.2 Physical and spectral properties of nocarimidazole B (**2**)

Red amorphous solid

Molecular formula: $C_{14}H_{26}N_3O$,

HRFABMS: *m/z* 252.2075 $[M+H]^+$ (calcd for 252.2076)

IR (KBr) ν_{max}: 3433, 3054, 2926, 2855, 1678, 1548, 1455, 1384, 1203, 1140, 839, 722 cm^{-1}

$[\alpha]_D$ + 1.42° (*C* 0.42, MeOH)

^{1}H and ^{13}C NMR data[a] ($CDCl_3$)

	2	
No.	δ_C, mult.[b]	δ_H (*J* in Hz)
2	130.5, CH	7.75, s
4	147.2,C	
5	111.9, C	
6	190.8, C	
7	38.8, CH_2	2.68, t (*J* = 7.4)
8	24.1, CH_2	1.62, q (*J* =7.4)
9	26.9, CH_2	1.26,m
10	29.4, CH_2	1.07, m
11	29.5, CH_2	1.26, m
12	29.3, CH_2	1.26,m
13	34.3, CH	1.25, m
14	36.5, CH_2	1.05, m 1.23, m
15	11.3, CH_3	0.84, t (*J* = 9.0)
16	19.1, CH_3	0.78, d (*J* = 9.0)

[a] 500 MHz for ^{1}H NMR and 125 MHz for ^{13}C NMR

[b] Multiplicity was determined by the analysis of 2D NMR spectroscopic data

2.2.2 Bioactivities of Nocarimidazoles A and B

The cytotoxicities were evaluated with MTT assay on A498 and ACHN renal cancer cell lines, but no significant cytotoxicities were observed. There were no antibacterial activities either, on MIC assay. Interestingly, AChE inhibitory activity was obsereved but, activity was as weak as one of thousands compare with positive control.

2.3 Experimental

2.3.1 Instruments and Data Collection

The optical rotation was measured using a Autopol III (Rudolph Research, USA) polarimeter with a 5 cm cell. IR spectra were obtained with a Varian Scimitar Series. CD spectra were collected in a ChirascanTM-plus (Applied Photophysics, UK) spectrometer with a 0.5 mm pathlength rectangular cuvette. NMR spectra were recorded on Varian Inova NMR spectrometer (500 and 125 MHz for ^{1}H and ^{13}C NMR, respectively), using the signals of the residual solvent protons and the solvent carbons as internal references (δ_H 7.24 and δ_C 77.0 ppm for $CDCl_3$). EI-MS spectra were measured on a JEOL, JMS-AX505WA mass spectrometer. Low resolution LC-MS data were measured using an Agilent Technologies 6120 quadrupole LC/MS system with a reversed phase column (Phenomenex luna C18(2) 100 Å, 50 mm × 4.6 mm, 5 μm) at a flow rate of 1.0 mL/min. Column chromatography was performed using Silica gel 60 (0.040 ~ 0.063 mm, Merch), normal-phase methods. The fractions were separated by WATERSTM 616 quaternary HPLC pump, WATERSTM 996 photodiode array detector using an Phenomenex luna C18(2) (250 mm × 10 mm, 5 μm) reversed-phase HPLC column.

2.3.2 Microorganism Isolation and Fermentation

Nocardiopsis sp. (CNQ115) was isolated from marine sediments collected off the coast of southern California. It was classified according to 16S rRNA analysis with 99.3% identity. Strain CNQ115 was cultured in 8 2.5-L Ultra Yield Flasks each containing 1 L of the medium (10 g/L of soluble starch, 2 g/L of yeast, 4 g/L of peptone, 10 g/L of $CaCO_3$, 20 g/L of KBr, 8 g/L of $Fe_2(SO_4)_3 \cdot 4H_2O$ dissolved in 750

mL natural seawater and 250 mL of distilled water) at 25 ℃ with shaking at 150 rpm. After 7 days, the broth was extracted with EtOAc and evaporated under reduced pressure to yield an extract of CNQ115 (1.2 g).

2.3.3 Extraction and Compound Isolation

The crude extract (1.2 g) was subjected on open column chromatography on silica gel (30 g), eluted with a step gradient of dichloromethane and methanol. The dichloromethane/methanol (10:1) fraction contained a mixture of metabolites, which was purified by reversed-phase HPLC (Phenomenex Luna C-18 (2), 250×100 mm, 2.5 mL/min, 5 μm, 100 Å , UV = 254 nm) using an isocratic solvent system of 45% CH_3CN in H_2O to afford nocarimidazols A (**1**, 18.0 mg) and B (**2**, 25.0 mg).

2.3.4 Methylation Reactions

Nocarimidazole B Diazomethane Derivative (**3**); Freshly prepared diazomethane reagent (0.5 mL) was added to a 1 mL MeOH solution of **2** (5.0 mg) at 4 ˚C with stirring. This solution was gradually warmed to room temperature. After 2 h, the solvent was removed under vacuum to yield 3.0 mg of nocarimidazol B diazomethane derivative (**3**). ^{1}H NMR ($CDCl_3$): δ_H 6.94 (H-2, s, 1H), 3.42 (3-NCH_3, s, 3H), 2.84 (H-7, t, *J* =8.4 Hz, 2H), 1.68 (H-8, q, *J* =7.7, 2H), 1.26 (H-9, m, 2H), 1.26 (H-11, m, 2H), 1.26 (H-12, m, 2H), 1.24 (H-13, m, 1H), 1.07 (H-10, m, 2H), 1.05, 1.22 (H-14, m, 2H), 0.82 (H-15, t, *J* =8.4, 3H), 0.79 (H-16, d, *J* =7.0, 3H), EIMS *m/z* 266 $[M]^+$

Nocarimidazole Iodomethane Derivative (**4**); A solution of 6.0 mg (0.024 mmol) of nocarimidazol B in 0.5 mL of DMF An appropriate amount of 0.167 mmol of Potassium carbonate (7 eq) was added and the whole was methylated with 0.5 mL

of CH_3I. Then the mixture was heated to 60°C for 24 h to gave 4.0 mg of crude product (66% yield), which were purified by reversed-phase HPLC (Phenomenex Luna C-18 (2), 250×10 mm, 2.5 mL/min, 5 μm, 100 Å, UV = 254 nm) using an gradient solvent system of water and acetonitrile from 20% Acetonitrile to 100% Acetonitrile to afford a methyl nocarimidazol B (**4**, 1.5 mg) ^{1}H NMR ($CDCl_3$): δ_H 8.76 (H-2, s, 1H), 3.95 (1-NCH_3, s, 3H), 3.66 (4-$NHCH_3$, s, 3H), 2.66 (H-7, t, J =7.2 Hz, 2H), 1.64 (H-8, q, J =7.4, 2H), 1.29 (H-8, m, 2H), 1.26 (H-11, m, 2H), 1.26 (H-12, m, 2H), 1.25 (H-13, m, 1H), 1.23 (H-9, m, 2H), 1.05, 1.23 (H-14, m, 2H), 1.07 (H-10, m, 2H), 0.85-0.76 (H-15, H-16, m, 6H), EIMS *m/z* 280 $[M]^+$

2.3.5 Bioassay Procedures

2.3.5.1 Cytotoxicity Test

The cytotoxicity test was performed for two human cancer cell lines, A498 and ACHN renal cancer, according to a previously published method[19] with modifications. The cells were cultured in Dulbecco's modified Eagle's medium (DMEM) containing 10% fetal bovine serum (FBS) and 1% penicillin at 37℃ in a humidified atmosphere incubator (5% CO_2 in air). Wells with DMSO were used as negative controls, and temsirolimus, sunitinib and gemcitabine were used as positive controls

2.3.5.2 MIC Assay

A following seven bacterial strains were used: four Gram-positive (*Staphylococcus epidermidis* ATCC 12228, *Micrococcus lutes* ATCC 9341, *Bacillus subtilis* ATCC 6633, *S. aureus* ATCC 65381) and three Gram-negative (*Escherichia coli* ATCC 11775, *Salmonella typhimurium* ATCC 14028, *Klebsiella pneumonia* ATCC 4352).

These bacteria were inoculated in Mueller-Hinton agar media for 24 h at 37℃. The bacterial colony was cultivated into a 15 mL round tube containing 6 mL of Mueller-Hinton broth media at 37℃ and 225 rpm for 24 h. Test compound (**1**) and a positive control (gentamicin) dissolved in DMSO were added 100 µL of each to 96-well microtiter plate having 50 µL of Mueller-Hinton broth in rest well. The samples were serially diluted and 50 µL of bacterial Mueller-Hinton broth media adjusted to concentration of 1/100 diluted McFarland 0.5% standard. The 96-well was incubated for 24 h at 37℃. After then, the minimum inhibitory concentration (MIC) values were determined as the concentration of compounds at transparent well which inhibit the growth of bacteria.

2.3.5.3 Acetylcholinesterase Inhibitory Assay

The AChE inhibitory activity was measured using the modified method of Ellman et al. Briefly, a reaction mixture containing 140 μL of sodium phosphate buffer (pH 8.0), 20 μL of the test sample solution, and 20 μL of AChE was incubated for 15 min at 25℃. Following the incubation, the reaction was initiated by adding 10 μL of dithiobisnitrobenzoate (DTNB) and 10 μL of ACh and incubated for 10 min at 25℃. The hydrolysis of ACh was monitored and quantified in a spectrophotometer at 412 nm to measure the formation of DTNB with thiocholine released by the enzymatic hydrolysis of ACh. Donepezil hydrochloride (Santa Cruz Biotechnology) was used as a positive control. The 50% inhibitory concentration (IC_{50}) of the donepezil hydrochloride was 0.02 ± 0.004 μM. All reactions were performed in triplicate on 96-well plates and recorded using a VERSA max plate reader (Molecular Devices). The percentage of inhibition was calculated as (1 – S/E) × 100, where E and S are the enzyme activities with and without the sample.

Chapter 3. Marine Natural Products from Mudflat-Derived Actinomycetes

3.1 Introduction

Actinomycetes have been a promising source of bioactive natural compounds for several decades (Bérdy, 2005). Soil-derived actinomycetes have traditionally been the main source of bioactive natural products. In the 1980s, the first marine-derived actinomycete, *Rhodococcus marinonascens*, was described (Helmke & Weyland, 1984). Since then, marine sediments from beach sand to the deep sea bottom have been good environmental sources for isolating actinomycetes, which provide diverse bioactive secondary metabolites (Fenical & Jensen, 2006). Mudflats, also known as tidal flats, are intertidal zones with deposited mud, which create a unique ecological niche. This wetland is covered with salt water one to two times a day and is exposed to strong sunlight, which causes extreme environmental changes for the organisms living there. Despite these harsh environmental conditions, this zone is crowded with various microbial communities due to the rich nutrients available from the land and from the seawater. This unique ecological niche could also be an excellent environment for diverse bacterial species, including actinomycetes (Kim et al., 2004), a situation that often leads to unique chemical structures with diverse biological activities. Recently, our group reported that a *Streptomyces* sp. isolated from tidal flat sediments collected on Anmyeon Island, located on the west coast of Korea, produced

biologically active sesquiterpenoids with an indene moiety, anmindenols A and B (Lee et al., 2014).

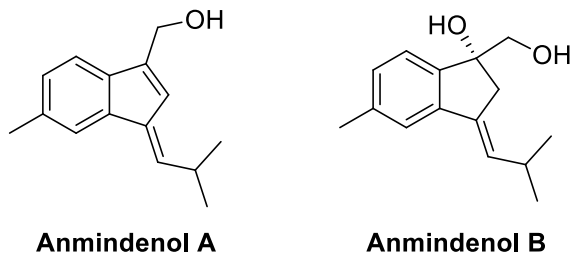

Figure 3.1 Sesquiterpenoids isolated from mudflat-drived actinomycetes

Actinomycete-derived natural products have not been examined extensively to combat neurodegenerative diseases, but specific efforts are ongoing. One of the diseases being studied is Alzheimer's disease (AD), which deteriorates cognitive function. The most common molecular target for drugs that act on the symptoms of AD is acetylcholinesterase (AChE) (Parsons et al., 2013). ChE inhibitors block the AChE enzyme and prevent the neurotransmitter acetylcholine (ACh) from being broken down by AChE, thereby increasing the level of ACh at the synapse and the duration and action of ACh. Thus far, few compounds that exhibit AChE inhibitory activity, such as geranylphenazinediol (Ohlendorf et al., 2012), elaiomycins B and C (Kim et al., 201), N98-1272A (Zheng et al., 2007), and cyclophostin (Kurokawa et al., 1993), have been isolated from *Streptomyces* species.

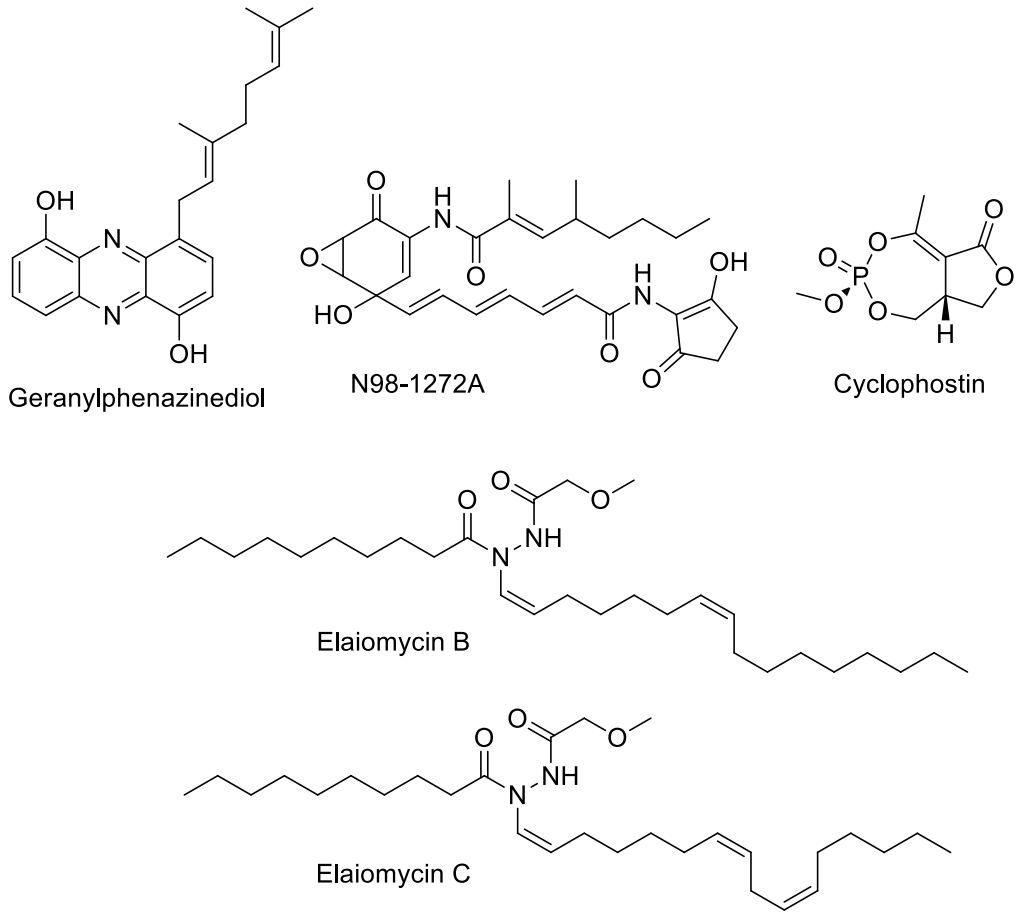

Figure 3.2 Acetylcholinesterase inhibitors isolated from actinomycetes

3.2 Results and Discussion

As part of our continued research into bioactive secondary metabolites from marine actinomycetes on the Korean peninsula, *Streptomyces* sp. 10A085 was isolated from a mudflat sediment sample. Chemical investigation of this strain yielded three new natural products, anithiactins A-D (**1**-**4**). Here, we present details of the isolation of anithiactins A-D and their biological activities in terms of AChE inhibition.

Anithiactins are members of the 2-phenylthiazole class of natural products. The representative natural products belonging to this class are aeruginoic acid (Yamada et al, 1970), aeruginol (Yang et al., 1993) and the pulicatins (Lin et al, 2010). In particular, the chemical structures of the anithiactins are closely related to those of aeruginoic acid and the pulicatins. Aeruginoic acid, a fluorescent natural product, was isolated from the culture medium of *Pseudomonas aeruginosa* and displayed antihypotensive activity (Imai et al., 1973). The pulicatins, isolated from a cone snail (*Conus pulicarius*) associate *Streptomyces* sp., showed G protein-coupled receptor 5-HT_{2B} inhibition activity in the micromolar range.[8] These natural products possess an OH group at C-2, whereas anithiactins have an *N*-methyl group. This aniline moiety is unusual within the 2-phenylthiazoline class of natural products.

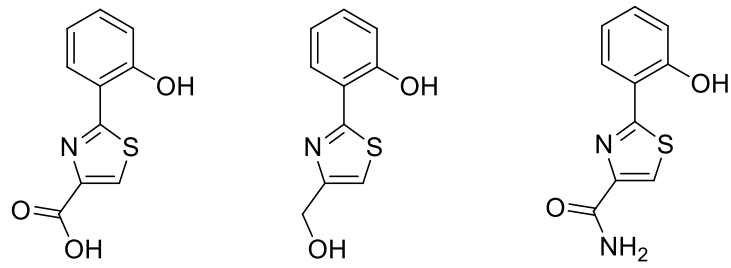

Figure 3.3 Known 2-phenylthiazole class natural products

3.2.1 Structure Elucidation of Anithiactins

3.2.1.1. Anithiactin A (**1**)

Anithiactin A (**1**) was obtained as a yellowish amorphous solid. The molecular formula of **1** was established as $C_{12}H_{12}N_2O_2S$ based on high resolution MS data. The ^{1}H NMR spectrum displayed a 1, 2-disubstituted benzene ring moiety [H-3 (δ_H 6.77, d, J = 7.8 Hz), H-4 (δ_H 7.32, ddd, J =7.8, 7.8, 1.3 Hz), H-5 (δ_H 6.67, dd, J = 7.8, 7.8 Hz), and H-6 (δ_H 7.63, dd, J = 7.8, 1.3 Hz)]. The ^{1}H NMR spectrum also showed a downfield singlet proton H-4′ (δ_H 8.04, s), and *N*-methyl and *O*-methyl singlets [2-NHMe (δ_H 3.01, s), 7′-OMe (δ_H 3.96, s)]. The HMBC correlations from the singlet proton H-4′ (δ_H 8.04, s) to carbons C-2′ (δ_C 170.1), C-5′ (δ_C 146.1) and C-7′ (δ_C 161.7) and the molecular formula of **1** allowed the construction of a thiazole ring moiety (Figure 3.4). The connection between the 1, 2-disubstituted benzene ring moiety and the thiazole ring moiety was achieved using HMBC correlations from the aromatic proton H-6 and the singlet proton H-4′ to C-2′. Lastly, the attachment of the *N*-methyl and the *O*-methyl groups at C-2 and C-7′, respectively, based on HMBC correlations from the *N*-methyl singlet to C-2 and the *O*-methyl singlet to C-7′ completed the assignment of the gross structure of **1**.

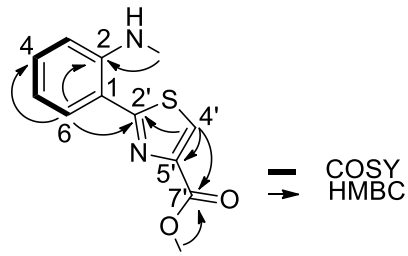

Figure 3.4 COSY and key HMBC correlations of anithiactin A (**1**)

Table 3.1 Physical and spectral properties of anithiactin A (**1)**

Yellowish amorphous solid
Molecular formula: $C_{12}H_{12}N_2O_2S$,
HRFABMS: *m/z* 249.0698 $[M+H]^+$ (calcd for 249.0698)
IR (film) ν_{max}: 3303, 3122, 1727, 1580, 1491, 1446, 1214, 1173, 1104, 906, 753, 738 cm^{-1}
UV (MeOH) λ_{max} (log ε): 209 (5.07), 222 (4.78), 247 (4.31), 286 (4.05), 383 (4.10) nm
^{1}H and ^{13}C NMR data[a] (CD_3OD)

	1	
No.	δ_C, mult.[b]	δ_H (*J* in Hz)
1	114.3, C	
2	147.5, C	
2-NHMe	29.8, CH_3	3.01, S
2-NH		8.43, br s
3	111.1, CH	6.77, d (7.8)
4	131.9, CH	7.32, ddd (7.8, 7.8, 1.3)
5	115.0, CH	6.67, dd (7.8, 7.8)
6	129.4, CH	7.63, dd (7.8, 1.3)
2′	170.1, C	
4′	125.1, CH	8.04, s
5′	146.1, C	
7′	161.7, C	
7′-OMe	52.3, CH_3	3.96, s

[a] 600 MHz for ^{1}H NMR and 125 MHz for ^{13}C NMR. [b] Numbers of attached protons were determined by analysis of 2D spectroscopic data.

3.2.1.2. Anithiactin B (**2**)

The molecular formula of anithiactin B (**2**) was obtained as $C_{11}H_{11}N_3OS$ on the interpretation of the protonated molecule at *m/z* 234.0701 $[M+H]^+$ in the HRFABMS data. The ^1H NMR spectrum of anithiactin B (**2**) was very similar to that of **1** except for the absence of an *O*-methyl singlet and the presence of two singlet protons (δ_H 5.73, δ_H 6.88). The analysis of the 2D NMR spectroscopic data and the molecular formula of **2** indicated that anithiactin B had an NH_2 group at C-7′ instead of a methyl ester. The structure of **2** was also confirmed using X-ray crystallographic data (Figure 3.6). Slow evaporation of a concentrated solution of **2** in hexane and $CHCl_3$ mixture yielded yellow needles.

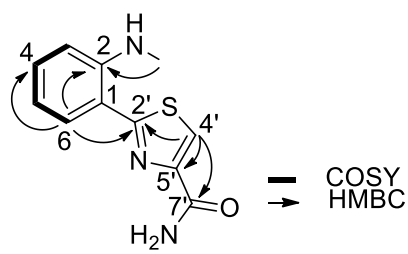

Figure 3.5. COSY and key HMBC correlations of anithiactin B (**2**)

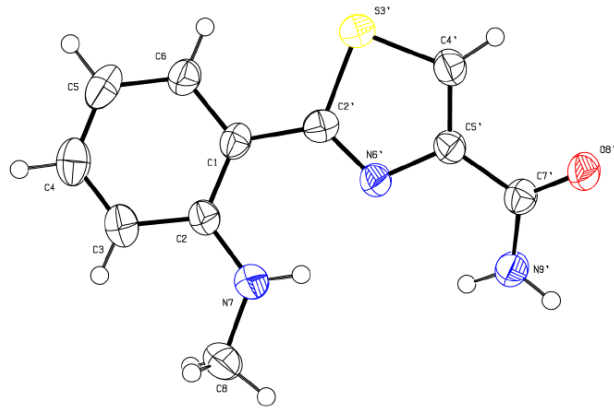

Figure 3.6 X-ray crystal structure of anithiactin B (**2**)

Table 3.2 Physical and spectral properties of anithiactin B (**2)**

Yellowish needle
Molecular formula: $C_{11}H_{11}N_3OS$,
HRFABMS: *m/z* 234.0701 $[M+H]^+$ (calcd for 234.0701)
IR (film) ν_{max}: 3415, 3321, 3193, 1650, 1609, 1581, 1485, 1367, 1215, 1175, 988, 804, 751 cm^{-1}
UV (MeOH) λ_{max} (log ε): 211 (4.67), 219 (4.41), 247 (3.91), 287 (3.67), 383 (3.70) nm
^{1}H and ^{13}C NMR data[a] (CD_3OD)

	2	
No.	δ_C, mult.[b]	δ_H (*J* in Hz)
1	114.9, C	
2	147.3, C	
2-NHMe	30.2, CH_3	3.00, d (5.0)
2-NH		7.74, br s
3	111.3, CH	6.77, d (7.8)
4	132.2, CH	7.35, ddd (7.8, 7.8, 1.4)
5	115.9, CH	6.71, dd (7.8, 7.8)
6	130.0, CH	7.64, dd (7.8, 1.4)
2′	170.5, C	
4′	122.9, CH	8.08 s
5′	149.2, C	
7′	162.9, C	
7′-NH_2		5.73, 6.88 br s

[a] 600 MHz for ^{1}H NMR and 125 MHz for ^{13}C NMR. [b] Numbers of attached protons were determined by analysis of 2D spectroscopic data.

3.2.1.3. Anithiactin C (**3**)

The ^{1}H NMR spectrum of anithiactin C (**3**) was almost identical to that of anithiactin A (**1**) except for the absence of the *O*-methyl group. The molecular formula of **3** was established as $C_{11}H_{10}N_2O_2S$ based on the HRFABMS data, indicating **3** had 14 Da less mass than anithiactin A. These data suggested that **3** had an OH group instead of an *O*-methyl group at C-7′. Interpretation of the 2D NMR spectroscopic data permitted the assignment of structure **3**.

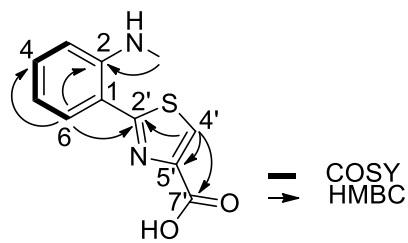

Figure 3.7 COSY and key HMBC correlations of anithiactin C (**3**)

Table 3.3 Physical and spectral properties of anithiactin C (**3)**

Yellowish amorphous solid
Molecular formula: $C_{11}H_{10}N_2O_2S$,
HRFABMS: *m/z* 235.0543 $[M+H]^+$ (calcd for 235.0541)
IR (film) ν_{max}: 3417, 2923, 1573, 1492, 1383, 1285, 1214, 1172, 750 cm^{-1}
UV (MeOH) λ_{max} (log ε): 211 (4.56), 219 (4.30), 261 (3.63), 286 (3.57), 379 (3.57) nm
^{1}H and ^{13}C NMR data[a] (CD_3OD)

	3	
No.	δ_C, mult.[b]	δ_H (*J* in Hz)
1	116.5, C	
2	148.8, C	
2-NHMe	29.9, CH_3	2.84, s
2-NH		4.51, br s
3	112.1, CH	6.64, d (7.8)
4	132.6, CH	7.14, ddd (7.8, 7.8, 1.3)
5	116.1, CH	6.49, dd (7.8, 7.8)
6	130.5, CH	7.50, dd (7.8, 1.3)
2′	170.3, C	
4′	123.1, CH	7.83, s
5′	154.9, C	
7′	170.2, C	

[a] 600 MHz for ^{1}H NMR and 125 MHz for ^{13}C NMR. [b] Numbers of attached protons were determined by analysis of 2D spectroscopic data.

3.2.1.4. Anithiactin D (**4**)

The LRMS of anithiactin D was 423 and 445, which suggest 422 as molecular weight. The 1H NMR spectrum displayed a 1, 2-disubstituted benzene ring moiety [H-6″ (δ_H 7.32, d, *J* = 7.8 Hz), H-7″ (δ_H 7.04, dd, *J* = 7.8, 7.8 Hz), H-8″ (δ_H 6.94, dd, *J* = 7.8, 7.8 Hz), and H-9″ (δ_H 7.48, d, *J* = 7.8 Hz)]. The 1H NMR spectrum also showed a 1, 2, 4-trisubstituted benzene ring moiety [H-3 (δ_H 6.74, d, *J* = 7.8 Hz), H-4 (δ_H 7.42, dd, *J* = 7.8, 1.3 Hz), and H-6 (δ_H 7.76, d, *J* = 1.3 Hz)]. The 1H NMR spectrum also showed downfield singlet protons H-4′ (δ_H 8.07), H-2″ (δ_H 7.27) and one *N*-methyl singlet [2-NHMe (δ_H 2.96, s)]. The upfield signals showed two methines [H-10″ (δ_H 4.27, d, *J* = 7.0 Hz) and H-11″ (δ_H 4.41, ddd, *J* = 7.0, 7.0, 4.2 Hz)] and one methylene [H-12″a (δ_H 3.61, dd, *J* = 7.0, 4.2 Hz) and H-12″b (δ_H 3.48, dd, *J* = 7.0, 4.2 Hz)]. The HMBC correlations from singlet proton H-4′ (δ_H 8.07, s) to carbons C-2′ (δ_C 171.7), C-5′ (δ_C 150.6) and C-6′ (δ_C 165.6) allowed the construction of a thiazole ring moiety. The HMBC correlations from H-6 (δ_H 7.76, s) to carbons C-2 (δ_C 147.0), C-4 (δ_C 134.2), C-5 (δ_C 130.8) and C-2′ (δ_C 171.7) attached thiazole ring with 1, 2, 4-trisubstituted benzene ring. The HMBC correlations from singlet proton H-2″ (δ_H 7.27, s) to carbons C-3″ (δ_C 117.8), C-4″ (δ_C 128.2), C-5″ (δ_C 137.9) and C-6″ (δ_C 112.2) with 1, 2-disubstituted benzene ring allowed the construction of a indole moiety. The connection between the indole moiety and phenyl thiazole was achieved using HMBC correlations from the methine proton H-10″ to carbons C-4, C-5, C-4′, C3″ and C-4″. The COSY correlations from H-11″ (δ_H 4.41, ddd, *J* = 7.0, 7.0, 4.2 Hz) to H-10″ (δ_H 4.27, d, *J* = 7.0 Hz) and H-12″ attached the rest of the carbons to achieve the chemical structure of anithiactin D.

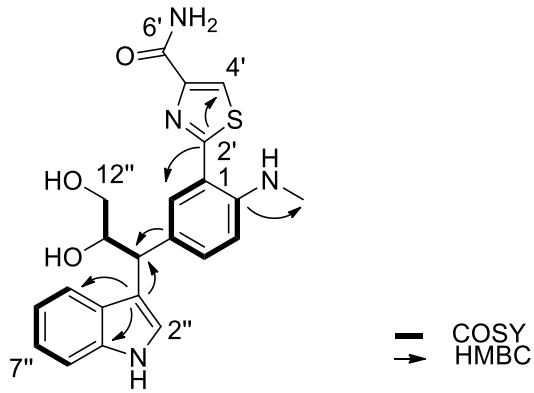

Figure 3.8 COSY and key HMBC correlations of anithiactin D (4)

Table 3.4 Physical and spectral properties of anithiactin D (**4)**

Yellowish amorphous solid
Molecular formula: $C_{22}H_{22}N_4O_3S$ (interpretation of NMR and LRMS data)
LRMS: *m/z* 423 / 445
^{1}H and ^{13}C NMR data[a] (CD_3OD)

	4	
No.	δ_C, mult.[b]	δ_H (*J* in Hz)
1	115.4, C	
2	147.0, C	
2-NHMe	30.0, CH_3	2.96, s
3	112.0, CH	6.74, d (7.8)
4	134.2, CH	7.42, dd (7.8, 1.3)
5	130.8, C	
6	131.3, CH	7.76, d (1.3)
2′	171.7, C	
4′	123.3, CH	8.07
5′	150.6, C	
6′	165.6, C	
2″	123.1, CH	7.27, s
3″	117.8, C	
4″	128.2, C	
5″	137.9, C	
6″	112.2, CH	7.32, d (7.8)
7″	122.3, CH	7.04, dd (7.8, 7.8)
8″	119.5, CH	6.94, dd (7.8, 7.8)
9″	119.8, CH	7.48, d (7.8)
10″	45.6, CH	4.27, d (7.0)
11″	75.6, CH	4.41, ddd (7.0, 7.0, 4.2)
12″	66.2, CH_2	3.61 d (7.0, 4.2)
		3.48 d (7.0, 4.2)

[a] 700 MHz for ^{1}H NMR and 150 MHz for ^{13}C NMR. [b] Numbers of attached protons were determined by analysis of 2D spectroscopic data.

3.2.2 Synthesis of Anithiactin A (**1**)

To further investigate the underlying biology of AChE inhibition using the anithiactins, a three -step synthetic route (Scheme 1) was developed for anithiactin A (**1**) using commercially available reagents. Thiobenzamide (**6**) was obtained from the sulfur substitution reaction of the anthranilamide (**5**) in 89% yield, which was then treated with bromopyruvate in dimethylformamide, a known thiazole ring formation reaction, to give thiazole **7** (Hoveyda et al., 2011). To achieve the selective *N*-monomethylation of **7**, we first attempted to use common methylation reagents, such as methyl iodide, *n*-butyl lithium and sodium cyanoborohydride. These methylation reagents gave the *N*-dimethyl product of thiazole **7**. Next, a solution of formaldehyde in dichloroethane and acetic acid was used as a mild methylation reagent for thiazole **7**. The reaction mixture was stirred overnight, and sodium triacetoxy borohydride at 0℃ was added. The mixture was left at room temperature for 2 h and yielded the *N*-monomethyl product (**1**) (Bonjouklian et al., 2004). The physical and spectroscopic data of the synthesized product were identical to the data for the natural product anithiactin A (**1**).

Scheme 3.1. Synthesis of anithiactin A (**1**)

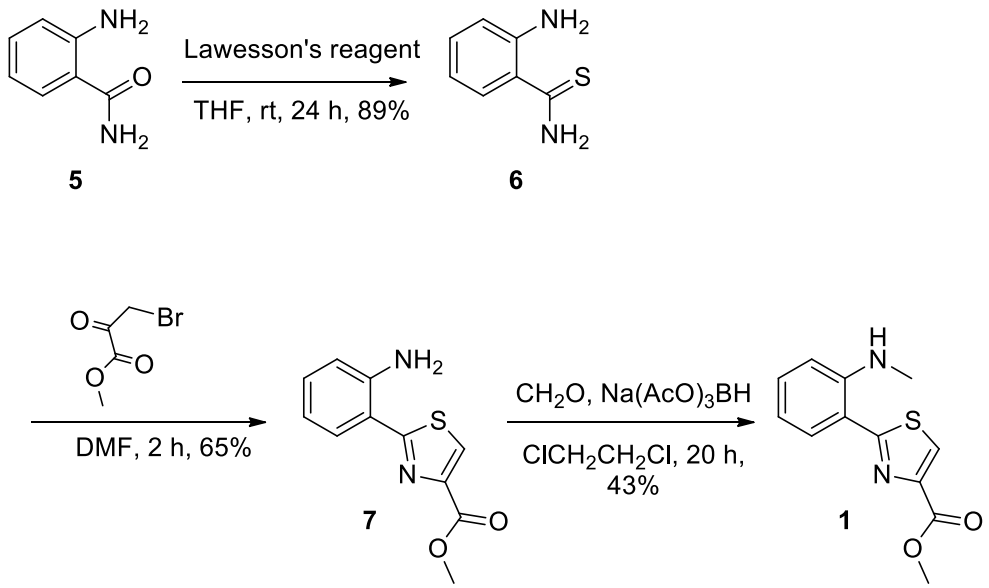

3.2.3 Bioactivities of Anithiactins

A number of previous studies demonstrated that AChE inhibitory activity was improved by replacing a phenyl or oxazole with the thiazole moiety (Nagal et al., 1995; Ronco et al., 2009). Recently, a thiazole containing AChE inhibitor, acotiamide (Acofide), was launched in Japan and is in preparation for phase III clinical trials in the EU (Nolan & Scott, 2013). Therefore, we examined the AChE inhibitory activities of anithiactins A-C (**1**-**3**) using the modified method of Ellman et al. (1961). Anithiactins A-C displayed AChE inhibitory effects with IC_{50} values of 63, 53, and 68 μM respectively. We also evaluated the cytotoxicity of the anithiactins against cancer cell lines. The three anithiactins did not show any significant cytotoxicity against A-498 and ACHN human cancer cell lines up to 200 μM with a modified MTT assay (Tran et al., 2012).

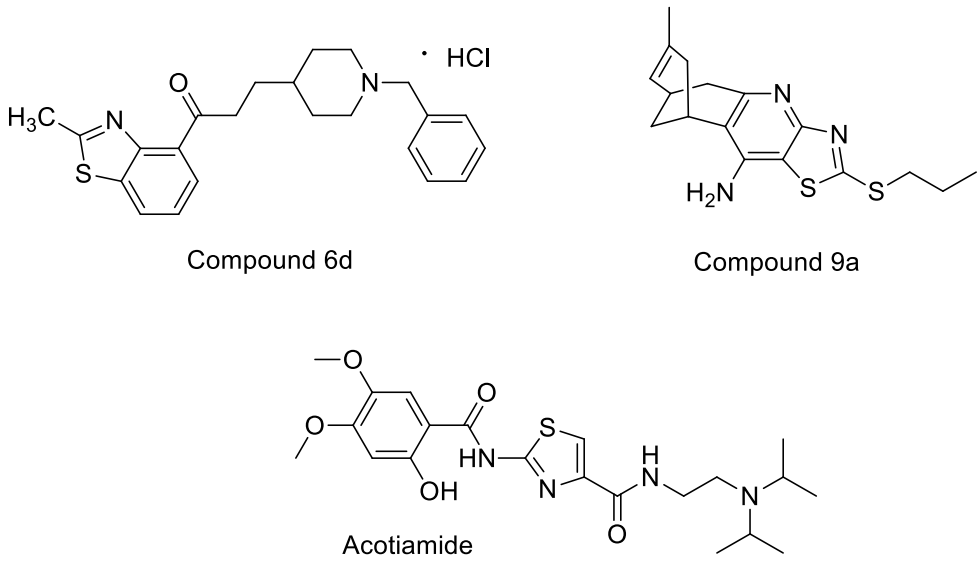

Figure 3.9 Acetylcholinesterase inhibitors containing thiazole moiety (Compound 6d: Nagal et al., Compound 9a: Ronco et al., Acotiamide: Nolan & Scott)

3.3 Experimental

3.3.1 Instruments and Data Collection

UV spectra were recorded in MeOH on a Scinco UVS-2100. The IR spectra were obtained using a Thermo Electron, Nicolet 5700 spectrometer. NMR spectra were obtained using Bruker Avance DPX-500 or DPX-600 spectrometers. $CHCl_3$ (δ_H 7.26; δ_C 77.0) and MeOH (δ_H 3.31; δ_C 49.3) resonances were used as internal references. The HRFABMS were determined on a JEOL, JMS-600W spectrometer. The solvents used were EP grade products from Dae-Jeong & Metals Co., Korea. HPLC grade solvents were purchased from Burdick & Jackson Co. Medium-pressure liquid chromatography was performed on EM Science silica gel (230−400 mesh). TLC was performed using EM Science precoated silica gel plates (Merck 60 F254). The separation of extracts using an HPLC Waters 515 pump and a Waters 996 photodiode array detector was carried out using MG2 C_{18} (250 × 10 mm, 5 μm). The chemical reagents used for synthesis were purchased from Aldrich and TCI. All culture media were purchased from BD.

3.3.2 Microorganism Isolation and Fermentation

Streptomyces sp. 10A085 was obtained from marine sediments from Jaebu Island, GyeongGi-Do, South Korea in 2010. The sampled mud sediments were dried in air for 24 h on a clean bench and given a heat shock at 55 ℃ for 5 min to eliminate other bacteria. Aggregated clumps were lightly mortared using a glass rod and stamped onto various solid agar substrates. Some of the dried samples were suspended in sterilized seawater, and the diluted suspension was spread on variously prepared solid agar substrates using a disposable plastic rod. These crude plates were placed

in a 27 ℃ chamber and monitored for 1 to 3 months to obtain unique actinomycete-like colonies. Strain 10A085 was picked from an ISP medium 4 agar plate containing white spores. The 16S gene was cloned using universal primers 27F and 1492R and showed 99% (1350/1357) similarity to *Streptomyces* sp. HV10 (accession no. KM881709).

3.3.3 Extraction and Compound Isolation

Strain 10A085 was cultured at 25 ℃ with shaking at 150 rpm in 24 Pyrex flasks, each containing 1 L of SYP medium (10 g soluble starch, 4 g yeast extract, and 2 g peptone dissolved in 1 L of 75% filtered natural seawater from Incheon, Korea). After 10 days, the broth was extracted twice using EtOAc, and the solvent was dried *in vacuo* to yield 2.6 g of extract. The extract (2.6 g) was separated using a silica column-equipped MPLC and step-gradient elution of MeOH in CH_2Cl_2 (0%, 1%, 2%, 5%, 10%, 20%, 50%, 90% and 100%). Fraction 1 was further purified using reversed-phase HPLC (MG2 C_{18} 250 × 10 mm, 5 m, 2.0 mL/min, UV = 210 and 280 nm; CH_3CN:H_2O = 70:30) to obtain 1.0 mg of anithiactin A (**1**). Fraction 3 was also purified using the same column, eluting with 98% CH_3CN in H_2O to afford anithiactin B (**2**, 3.0 mg). Anithiactin C (**3**, 3.0 mg) was isolated from fraction 8 with the same isolation procedure used for anithiactin B.

3.3.4 X-ray Crystallographic Analyses

The single-crystal X-ray diffraction data of the compound was collected with a Bruker SMART APEX CCD detector employing graphite-monochromated Mo Kα radiation (λ = 0.71073 Å) at 273(2)K. The data collection and integration were performed using SMART (Madison, WI, 2000) and SAINT-Plus (Madison, WI,

2001). The structure was solved using direct methods and refined using full-matrix least-squares on F^2 using SHELXTL (Madison, WI). All the non-hydrogen atoms were refined anisotropically, and hydrogen atoms were added to their geometrically ideal positions.

Anithiactin B (2): yellow needle; $C_{11}H_{11}N_3OS$, Mr = 233.30, monoclinic, a = 15.1825(12) Å, b = 5.2022(4) Å, c = 14.7674(12) Å, α = 90°, β = 111.728(2)°, γ = 90°, V = 1083.50(15) $Å^3$, space group P2(1)/c, Z = 4, Dx = 1.430 mg/m^3, μ(Cu Kα) = 0.279 mm^{-1}, and F(000) =488. Crystal dimensions: 0.18 × 0.14 × 0.12 mm^3. Independent reflections: 2677 (Rint = 0.0825). The final R1 values were 0.0644, wR2 = 0.1544 (I > 2σ(I)). CCDC number: 1022818.

3.3.5 Synthesis Procedures

Sulfur Substitution Reaction of Anthranilamide (5); A solution of anthranilamide (5, 200 mg, 1.47 mmol) and the Lawesson reagent (320 mg, 0.8 mmol) in THF (10 mL) was stirred under N_2 at r.t. for 24 h. The reaction mixture was partitioned between EtOAc (15 mL) and 2 N HCl (15 mL). A saturated aqueous NaHCO3 solution was added to the separated aqueous layer until pH 8 – 9 and extracted with EtOAc (2 × 20 mL). The combined organic layer was dried with $MgSO_4$ and filtered. The solvent was evaporated in vacuo and the thiobenzamide (6) was obtained after silica gel column chromatography (n-Hexane:EtOAc = 3:1).

Thiobenzamide (6): 200 mg (1.31 mmol, 89%), yellow amorphous solid; ^{1}H NMR (700 MHz, CD_3OD): δ ppm 6.67 (dd, *J* = 7.0, 7.0 Hz, 1 H), 6.78 (dd, *J* = 7.0, 1.2 Hz, 1 H), 7.14 (ddd, *J* = 7.0, 7.0, 1.2 Hz, 1 H), 7.26 (dd, *J* = 7.0, 1.2 Hz, 1 H); ^{13}C NMR (175 MHz, CD_3OD): δ ppm 118.4, 118.9, 126.9, 128.2, 132.5, 147.8, 203.8; LRESIMS *m/z* 153 $[M + H]^+$

Formation of Thiazole (7); To a solution of thiobenzamide (6, 100 mg, 0.66 mmol) in DMF (10 mL) was added bromopyruvate (70 μL, 0.66 mmol). The mixture was stirred under N_2 at 65 ˚C for 2 h. The reaction mixture was partitioned between EtOAc (20 mL) and saturated aqueous NH_4Cl solution (20 mL). The aqueous layer was extracted with EtOAc (2 × 20 mL) and combined organic layer was dried with $MgSO_4$ and filtered. The solvent was removed in vacuo and the thiazole (7) was obtained after silica gel column chromatography (nHexane:EtOAc = 3:1).

Thiazole (7): 100 mg (0.42 mmol, 65%), pale yellow amorphous solid; ^{1}H NMR (700 MHz, $CDCl_3$): δ ppm 3.94 (s, 3 H), 6.70 (dd, *J* = 7.0, 7.0 Hz, 1 H), 6.78 (d, *J* = 7.0 Hz, 1 H), 7.19 (dd, *J* = 7.0, 7.0 Hz, 1 H), 7.59 (d, *J* = 7.0 Hz, 1 H), 8.05 (s, 1H); ^{13}C NMR (175 MHz, $CDCl_3$): δ ppm 55.3, 114.7, 116.8, 116.9, 125.2, 129.1, 131.4, 145.9, 146.4, 161.7, 167.8; LRESIMS *m/z* 235 $[M+H]^+$

Monomethylation of Thiazole (7); Add formaldehyde (10 mg, 0.33 mmol) to a mixture of thiazole (7, 40 mg, 0.17 mmol), acetic acid (1 mL) and 1, 2-dichloroethane (10 mL). The reaction mixture was stirred overnight at r.t. and sodium triacetoxyborohydride (55 mg, 0.26 mmol) was added at 0℃. The reaction mixture was stirred for 2h at r.t. and partitioned between EtOAc (10 mL) and saturated aqueous NaHCO3 solution (20 mL). The aqueous layer was extracted with EtOAc (2 × 20 mL) and combined organic layer was dried with $MgSO^4$ and filtered. The solvent was removed in vacuo and the anithiactin (1) was obtained after silica gel column chromatography (n-Hexane:EtOAc = 4:1).

Anithiactin A (1): 18 mg (0.17 mmol, 43%), yellow amorphous solid; ^{1}H NMR (700 MHz, $CDCl_3$): δ ppm 3.01 (d, *J* = 7.4 Hz, 3 H), 3.96 (s, 3 H), 6.66 (dd, *J* = 7.0, 7.0 Hz, 1 H), 6.76 (d, *J* = 7.0 Hz, 1 H), 7.32 (dd, *J* = 7.0, 7.0 Hz, 1 H), 7.63 (d, *J* = 7.0 Hz, 1 H), 8.04 (s, 1 H), 8.41 (br, 1 H); ^{13}C NMR (175 MHz, $CDCl_3$): δ ppm 29.8,

52.3, 111.0, 114.3, 115.0, 125.1, 129.44, 131.9, 146.1, 147.6, 161.7, 170.2; LRESIMS *m/z* 249 $[M+H]^+$

3.3.6 Bioassay Procedures

3.3.6.1 Cytotoxcity test

The cytotoxicity test was performed for two human cancer cell lines, A498 and ACHN renal cancer, according to a previously published method[19] with modifications. The cells were cultured in Dulbecco's modified Eagle's medium (DMEM) containing 10% fetal bovine serum (FBS) and 1% penicillin at 37℃ in a humidified atmosphere incubator (5% CO_2 in air). Wells with DMSO were used as negative controls, and temsirolimus, sunitinib and gemcitabine were used as positive controls

3.3.6.2 Acetylcholinesterase Inhibitory Assay

The AChE inhibitory activity was measured using the modified method of Ellman et al. Briefly, a reaction mixture containing 140 μL of sodium phosphate buffer (pH 8.0), 20 μL of the test sample solution, and 20 μL of AChE was incubated for 15 min at 25℃. Following the incubation, the reaction was initiated by adding 10 μL of dithiobisnitrobenzoate (DTNB) and 10 μL of ACh and incubated for 10 min at 25℃. The hydrolysis of ACh was monitored and quantified in a spectrophotometer at 412 nm to measure the formation of DTNB with thiocholine released by the enzymatic hydrolysis of ACh. Donepezil hydrochloride (Santa Cruz Biotechnology) was used as a positive control. The 50% inhibitory concentration (IC_{50}) of the donepezil hydrochloride was 0.02 ± 0.004 μM. All reactions were performed in triplicate on 96-well plates and recorded using a VERSA max plate reader (Molecular Devices).

The percentage of inhibition was calculated as $(1 – S/E) \times 100$, where E and S are the enzyme activities with and without the sample.

References

Bérdy, J. *J. Antibiot.* **2005**, *58*, 1 – 26.

Bergy, M. E. *J. Antibiot*. **1968**, *21*, 454 – 457.

Bifulco, G.; Bruno, I.; Minale, L.; Riccio, R.; Debitus, C.; Bourdy, G.; Vassas, A.; Lavayre, J. *J. Nat. Prod.* **1995**, *58*, 1444 – 1449.

Blunt, J.; Munro, M. (Eds.) *Dictionary of Marine Natural Products*, Boca Raton, Florida, Chapman & Hall/CRC, **2008**.

Bonjouklian, R.; De Diego Gomez, J. E.; De Dios, A.; Hamdouchi, C. H.; Li, T.; Lopez De Uralde Garmendia, B.; Vieth, M.; York, J. S.; Dally, R. D.; Del Prado Catalina, M. F.; Jaramillo, C.; Martin Cabrejas, L. M.; Montero Salgado, C.; Pleite, S.; Sanchez-Martinez, C.; Shepherd, T. A.; Wikel, J. H. *PCT/US2003/019890*, **2004**

Bottcher, H. *Miracle drug*, Zagre, Zora, **1965**, pp. 23 – 139.

Brewer, M.D.; Dorgan, R.J.; Manger, B.R.; Mamalis, P.; Webster, R.A., *J. Med. Chem.* **1987**, *30*, 1848 – 1853.

Buss, A.; Waigh, R. *Natural products as leads for new pharmaceuticals*, in: Wolff, M. (Ed.), *Burger's medicinal chemistry and drug discovery. Principles and practice, vol. 1*, New York, John Wiley & Sons, Inc., **1995**, pp. 983 – 1033.

Cordell, G.; Colvard, M. *J. Nat. Prod.* **2012**, *75*, 514 – 525.

Cragg, G.M.; Newman, D.J. *Biochim. Biophys. Acta*, **2013**, *1830*, 3670 – 3695,

Cuevas, C.; Francesch, A. *Nat. Prod. Rep.* **2009**, *26*, 322 – 337.

Dolak, L. A.; Castle, T. M.; Laborde, A. L. *J. Antibiot*. **1980**, 33, 690 – 694.

Eggermont, A.; Kirkwood, J.M. *Euro. J. Cancer.* **2004**, *40*, 1825 – 1836.

Ellman, G. L.; Courtney, K. D.; Andres, V. Jr.; Feather-stone, R. M. *Biochempharmacol.* **1961**, *7*, 88 – 95.

Farbricant, D.; Farnsworth, N. *Environ. Health Perspect.* **2001**, *109*, 69 – 75.

Fenical, W. *Chemical Reviews* **1993**, *93*, 1673 – 1683.

Fenical, W.; Jensen, P. *Nat. Chem. Biol.* **2006**, *2*, 666 – 673.

Gerwick, W.; Moore, B. *Chem. & Biol.* **2012**, *19*, 85 - 98

Goodman, J.; Walsh, V. *The Story of Taxol: Nature and Politics in the Pursuit of an Anti-Cancer Drug.* Cambridge University Press., **2001**, pp. 17..

Gueritte, F.; Fahy, J. *The vinca alkaloids*, in: Cragg, G.; Kingston, D.; Newman, D. (Eds.) *Anticancer agents from natural products*, Boca Raton, Florida, Taylor and Francis, **2005**, pp. 123 – 135.

Helmke, E.; Weyland, H. *Int. J. Syst. Bacteriol*. **1984**, *34*, 127 – 138.

Hoveyda, H.; Marie-Ddile, R.; Lovat, F. G.; Guillaume, D. *PCT/EP2011/055218*, **2011**

Hu G.; Yuan, J.; Sun, L.; She, Z.; Wu, J.; Lan, X.; Zhu, X.; Lin, Y.; Chen, S. *Mar. Drugs* **2011**, *9*, 514 - 525.

Imada, C.; Koseki, N.; Kamata, M.; Kobayashi, T.; Hamada-Sato, N. *Actinomycetologica* **2007**, *21*, 27 – 31.

Imai, T.; Takahashi, M.; Seki, N.; Irie, Y. *US patent 3,729,378*, **1973**.

Jin, Z. *Nat. Prod. Rep.* **2011**, *28*, 1143 – 1191.

Johnson, R.A., Huong, S.M., Huang, E.S., *Antivir. Res.* **1999**, *41*, 101 – 111.

Kelly, K. *History of medicine*, New York, Facts on file, **2009**, pp. 29 – 50.

Kim, B.; Oh, H.; Kang, H.; Park, S.; Chun, J. *J. Microbiol. Biotechnol.* **2004**, *14*, 205 – 211.

Kim, B. Y.; Willbold, S.; Kulik, A.; Helaly, S. E.; Zinecker, H.; Wiese, J.; Imhoff, J. F.; Goodfellow, M.; Süssmuth, R. D.; Fiedler, H. P. *J. Antibiot. (Tokyo)*. **2011**, *64*, 595 – 597.

Kong, D.; Jiang, Y.; Zhang, H. *Drug Discov. Today* **2010**, *15*, 884 – 886.

Kurokawa, T.; Suzuki, K.; Hayaoka, T.; Nakagawa, T.; Izawa, T.; Kobayashi, M.; Harada, N. *J. Antibiot. (Tokyo).* **1993**, *46*, 1315 – 1318.

Lee, J.; Kim, H.; Lee, T.; Yang, I.; Won, D.; Choi, H.; Nam, S.-J.; Kang, H. *J. Nat. Prod.* **2014**, *77*, 1528 – 1531.

Lin, Z.; Antemano, R.; Hughen, R.; Tianero, M.; Peraud, O.; Haygood, M.; Concepcion, G.; Olivera, B.; Light, A.; Schmidt, E. *J. Nat. Prod.* **2010**, *73*, 1992 – 1926.

Margulis, L.; Schwartz, K. *Five kingdoms, an illustrated guide to the phyla of life on earth*, 2nd ed., New York, W. H. Freeman & Co., **1988**.

Martins, A.; Vieira, H.; Gaspar, H.; Santos, S. *Mar. Drugs* **2014**, *12*, 1066 - 1101.

Meyer, C.A. *The Global Marine Pharmaceuticals Pipeline.* http://marinepharmacology. midwestern.edu/

Moyle, P; Cech, J. *Fishes: An Introduction to Ichthyology*. New York, Benjamin Cummins, **2003**, pp. 744

Nagal, A.; Liston, D.; Jung, S.; Mahar, M.; Vincent, L.; Chapin, D.; Chen, Y.; Hubbard, S.; Ives, J.; Jones, S.; Nielsen, J.; Ramirez, A.; Shalaby, I.; Villalobas, A.; White, W. *J. Med. Chem.* **1995**, *38*, 1084 – 1089.

Newman, D.; Cragg, G. *J. Nat. Prod.* **2012**, *75*, 311 – 338.

Nolan, M.; Scott, L. *Drugs* **2013**, *73*, 1377 – 1383.

Ohlendorf, B.; Schulz, D.; Erhard, A.; Nagel, K.; Imhoff, J. F. *J. Nat. Prod*. **2012**, *75*, 1400 – 1404.

O'Neill, P.; Posner, G. *J. Med. Chem.* **2004**, *47*, 2945 – 2964.

O'Neill, P.; Barton, V.; Ward, S. **Molecules**, **2010**, *15*, 1705 – 1721.

Parsons, C. G.; Danysz, W.; Dekundy, A.; Pulte, I. *Neurotox. Res.* **2013**, *24*, 358 – 369.

Peltola, J. S.; Andersson, M. A.; Kampfer, P.; Augling, G.; Kroppenstedt, R. M.; Busse, H. U.; Salkinoja-Salonen, M. S.; Rainey. F. A. *Appl. Environ. Microbiol.* **2001**, *67*, 4293 – 2304.

Petrovska, B. *Pharmacogn. Rev.* **2012**, *6(11)*, 1 – 5.

Rainey, F. A.; Ward-Rainey, N.; Kroppenstedt, R. M.; Stackebrandt, E. *Int. J. Syst. Bacteriol.* **1996**, *46*, 1088 – 1092.

Ravikumar, S.; Inbaneson, S. J.; Uthiraselvam, M.; Priya, S. R.; Ramu, A.; Banerjee, M. B. *J. Pharm. Res.* **2011**, 4, 294 − 296.

Rinehart, K. *Med. Res. Rev.* **2000**, *20(1)*, 1 – 27.

Ronco, C.; Sorin, G.; Nachon, F.; Foucault, R.; Jean, L.; Romieu, A.; Renard, P. *Bioorg. Med. Chem.* **2009**, *17*, 4523 – 4536.

Roussi, F.; Gueritte, F.; Fahy, J. *The vinca alkaloids*, in: Cragg, G.; Kingston, D.; Newman, D. (Eds.) *Anticancer agents from natural products*, 2nd ed., Boca Raton, Florida, Taylor and Francis, **2012**, pp. 123 – 135.

Sabry, S. A.; Ghanem, N. B.; Abu-Ella, G. A.; Schumann, P.; Stackebrandt, E.; Kroppenstedt, R. M. *Int. J. Syst. EVol. Microbiol.* **2004**, *54*, 453 – 456.

Sharma, D.; Narasimhan, B.; Kumar, P.; Judge, V.; Narang, R.; Clercq, E.; Balzarini, J. *Euro. J. Med. Chem.* **2009**, *44*, 2347 – 2353.

Suzuki, F.; Kuroda, T.; Tamura, T.; Sato, S.; Ohmori, K.; Ichikawa, S. *J. Med. Chem.* **1992**, *35*, 2863 – 2870.

Takami, H.; Inoue, A.; Fuji, F.; Horikoshi, K. *FEMS Microbiol. Lett.* **1997**, *152*, 279 – 285.

Taylor, M.; Radax, R.; Steger, D.; Wagner, M. *Microbiol. Mol. Biol. Rev.* **2007**, *71(2)*, 295 – 347.

Tran, T. D.; Pham, N. B.; Fechner, G; Zencak, D.; Vu, H. T.; Hooper, J. N. A.; Quinn, R. J. *J. Nat. Prod*. **2012**, *75*, 2200 – 2208.

Vargas, S.; Schuster, A.; Sache, K.; Buttner, G.; Schatzel, S.; Lauchell, B.; Hall, K.; Hooper, J.; Erpenbeck, D.; Worheide, G. *Plos One* **2012**, *7*, e39345

Wang, J.; Huang L.; Li, J.; Fan, Q.; Long, Y.; Li, Y.; Zhou, B.; *PLoS One*, **2010**, *5* e9582.

Wiart, C. *Etnopharmacology of medicinal plants*, New Jersey, Humana Press, **2006**, pp. 1 – 50.

Wongsrichanalai, C.; Pickard, A.; Wernsdorfer, W.; Meshnick, S. *Lancet Infect. Dis.* **2002**, *2*, 209 –218.

Yamada, Y.; Seki, N.; Kitahara, T.; Takahashi, M.; Matsui, M. *Agric. Biol. Chem.* **1970**, *34*, 780 –783.

Yang, W.; Dostal, L.; Rosazza, J. *J. Nat. Prod.* **1993**, *56*, 1993 – 1994.

Zhang, L.; Peng, X.M; Damu, G. L. V.; Geng, R.X.; Zhou, C.H. *Med. Res. Rev*. **2014**, *34*, 340 – 437.

Zheng, Z. H.; Dong, Y. S.; Zhang, H.; Lu, X. H.; Ren, X.; Zhao, G.; He, J. G.; Si, S. Y. *J. Enzyme. Inhib. Med. Chem*. **2007**, *22*, 43 – 49.

Appendix A

List of Figures and Tables in Appendix A

A.1 Antibacterial Secosteroid from the Korean Sponge *Irchinia* sp.

A.1.1 Introduction

Marine Sponges are known as a source of structurally diverse natural products. This phylum of marine animal is possessing about 35% of reported marine natural products (Blunt et al., 2012). Many of the potent cytotoxins against cancer cell lines have been reported and some of them were developed as a lead of FDA approved drugs such as Cytosar-U®, and Halaven® (Martins et al., 2014). The antibacterial activity of marine sponge-derived metabolites are also well known such as discorhabdin Z (Jeon et al., 2010), agelasine D (Hertiani et al., 2010), 7,20-diisocyanoadociane (Wright et al., 2011), motualevic acid F (Keffer et al., 2009). In this regard, we have been investigated extracts of Korean marine sponges for the discovery of antibacterials. An extract of a Korean marine sponge in genus of *Ircinia* sp. showed antibacterial activities, and we continue the investigation of its bioactive constituents.

The genus *Ircinia* have been studied intensively and number of biologically active natural products have been reported such as antibacterials (Manes & Crews, 1986; Faulkner, 1973), cytotoxin (Kondo et al., 1992), ichthyotoxin (De Rosa et al., 1996), analgesic compound (Cimino et al., 1972; De Pasquale et al., 1991), multidrug resistance modulator (Kawakami et al., 2001), thrombin inhibitor (Nakao et al, 1995), angiotensin converting enzyme/aldose reductase inhibitor (Alfano et al., 1979), and inosine monophosphate dehydrogenase inhibitor (Cafieri et al., 1972; De Rosa et al., 1997).

Also, this *Ircinia* sp. is well known for its possession of divers terpenes such as ircinin-1,7 variabilin (De Rosa et al., 1996), fasciculation (Cafieri et al, 1972), and strobilinin (Rothberg & Shubiak, 1975). In addition, hydroquinones (Cimino et al, 1972a; Cimino et al. 1972b), chromans (Venkateswarlu & Reddy, 1994; Bifulco et al., 1995), and sterols (Venkateswarlu et al., 1996; Fu et al., 1999; Xu et al., 2008) have been reported. However, the organisms in *Ircinia* sp. was not reported for its secostrols.

Herein, we report the structure of an unprecedented secosterol with the 2-ene-1,4-dione as well as its antibacterial activity.

A.1.2 Results and Discussion

A.1.2.1 Structure Elucidation of 9,11-Secosterol (**1**)

The molecular formula of compound **1** was deduced as $C_{27}H_{44}O_5$, based on the analysis of HRFABMS data (a pseudomolecular ion peak at *m/z* 449.3271 $[M+H]^+$) and on the interpretation of ^{13}C NMR data. The ^1H NMR spectrum of **1** displayed an oxygenated methine proton [δ 4.04 (m)], an olefinic proton [δ 6.49 (br s)], and one downfielded methylene protons [δ 3.84 (m). 3.70 (m)]. The ^1H NMR spectrum also showed two methyl singlets [δ 1.23, 0.70] and three methyl doublets [δ 0.97 (d, *J* = 6.6 Hz), 0.88 (d, *J* = 2.3 Hz), 0.86 (d, *J* = 2.3 Hz)]. The ^{13}C NMR and HSQC spectra revealed five methyl, ten methylene, six methine, and six fully-substituted carbons. The 27 carbons, five methyl protons, and an oxygenated methine proton are characteristic of a cholesterol carbon skeleton. Furthermore, ^1H NMR signals of an olefinic proton δ 6.49 (s, 1H), oxymethylene protons [δ 3.70 (m, 1H), δ 3.84 (m, 1H)], a downfield proton [δ 3.52 (dd, 1H, *J* = 11.0, 8.5 Hz)], and five methyls [δ 0.70 (s, 3H), δ 1.23 (s, 3H), δ 0.97 (d, 3H, *J* = 6.6 Hz), δ 0.88 (d, 3H, *J* = 6.6 Hz), δ 0.86 (d, 3H, *J* = 6.6 Hz)] suggested that **1** was a 9, 11-secosterol.

Interpretation of 2D NMR spectroscopic data permitted the structure assignment of **1**. Analysis of COSY spectroscopic data of **1** revealed three fragments (a, b, and c) as shown in Figure A.1.1. In addition, the carbon chemical shifts of C-6 (δ 197.5), C-7 (δ 134.4), C-8 (δ 152.1), and C-9 (δ 203.1), and the HMBC correlations from an olefinic proton H-7 to carbons C-6, C-8, and C-9 supported the construction of an ene-dione moiety.

The connectivity of A/B ring including the fragment a and the ene-dione moiety for **1** was secured from HMBC correlations. The long-range HMBC correlations from

H-19 to carbons C-1, C-5, C-9, and C-10, and from H-4 to carbons C-2, C-5, and C-10, and from H-7 to the carbon C-5 allowed the A/B ring connectivity. The fragments b and c were also connected from the interpretation of HMBC correlations. A two-bond HMBC correlation from a methyl singlet proton H-18 to a carbon C-13, and three-bond HMBC correlations from H-18 to carbons C-12, C-17 permitted the C-12/C-13/C-17 connectivity. Lastly, the establishment of C-8/C-14 attachment based on the interpretation of three-bond HMBC correlations from the olefinic proton H-7 to a carbon C-14, and from the methyl singlet proton H-18 to a carbon C-14 allowed the completion of structure assignment of **1**. (Figure A.1.2)

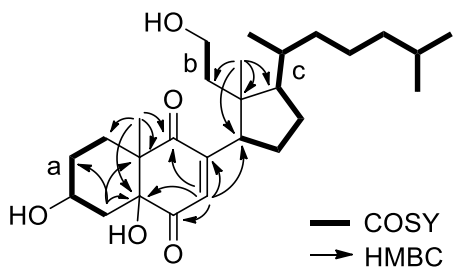

Figure A.1.1 COSY and key HMBC correlations of 9,11-secosterol (**1**)

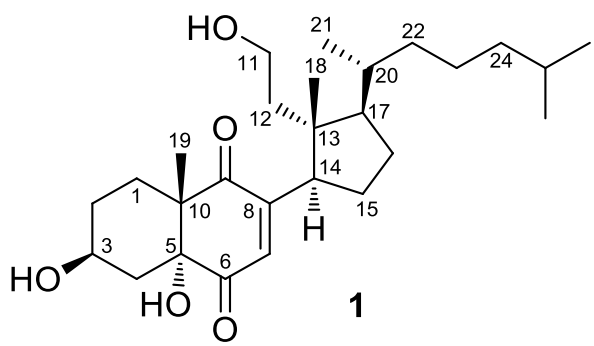

Figure A.1.2 Chemical structure of 9,11-secosterol (**1)**

The relative stereochemistry of the side chain and rings of **1** was identical to that of reported secosterols, which was determined by comparison with NMR data of known secosterols and by interpretation of NOESY correlations (Reddy et al., 1997; Lu & Faulkner, 1997). Briefly, NOESY correlations [H-7/H-14, H-14/H-12, H-12/H-21, H-18/H-20] were well corresponded to previously reported NOE correlations (Anta et al, 2002). The β-configuration of 3-hydroxy group at C-3 was defined from the coupling constants of H-4 (δ 2.16, dd, *J* = 13.1, 11.2 Hz) and NOESY correlations [H3/H4, H4 2.16)/H19]. (Figure A.1.3)

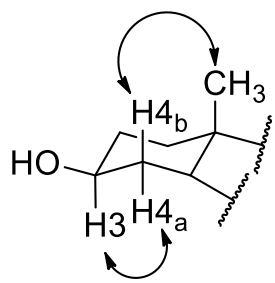

Figure A.1.3 Key NOESY correlations observed for 9,11-secosterol (**1**)

Table A.1.1 Physical and spectral properties of 9,11-secosterol (**1**)

Colorless needles
Molecular formula: $C_{27}H_{44}O_5$,
HRFABMS: *m/z* 449.3271 $[M+H]^+$ (calcd for 449.3275)
IR (film) ν_{max}: 3422, 2951, 2851, 1718, 1681, 1464, 1633 cm^{-1}
UV (MeOH) λ_{max} (log ε): 274 (3.96) nm
^{1}H, ^{13}C, COSY and HMBC NMR data[a] ($CDCl_3$)

No.	δ_C, m[b]	δ_H, m, *J* (Hz)	COSY	HMBC (J_{CH} = 10 Hz)
1	25.9, t	1.77 m	2	3, 5, 10, 19
		2.21 dt (11.2, 3.7)		
2	29.8, t	1.55 m	1, 3	
		2.00 m		
3	66.6, d	4.04 m	2, 4	
4	35.6, t	1.77 m	3	2, 5, 10
		2.16 dd (13.1, 11.2)		
5	80.5, s			
6	197.5, s			
7	134.4, d	6.49, s		5, 6, 8, 9, 14
8	152.1, s			
9	203.1, s			
10	52.1, s			
11	59.9, t	3.70 m;	12	
		3.84 m		
12	41.1, t	1.11 m	11	
		1.73 m		
13	47.5, s			
14	43.9, d	3.52 dd (11.0, 8.5)	15	7, 8, 9, 12, 13, 15, 18
15	26.3, t	1.75 m	14, 16	
		1.84 m		
16	26.6, t	1.68 m	15, 17	
		1.75 m		
17	50.1, d	1.73 m	16, 20	
18	17.7, q	0.70 s		12, 13, 14, 17
19	20.6, q	1.23 s		1, 5, 9, 10
20	34.5, d	1.41 m	17, 21, 22	
21	18.8, q	0.97 d (6.6)	20	17, 20, 22
22	35.6, t	0.99 m	20, 23	24
		1.35 m		
23	24.4, t	1.15 m	22, 24	
		1.35 m		
24	39.4, t	1.13 m	23, 25	
		1.15 m		
25	27.9, d	1.51 m	24, 26, 27	23
26	22.5, q	0.86 d (6.6)	25	24, 25, 27,
27	22.7, q	0.88 d (6.6)	25	24, 25, 26
5-OH		2.36 br s		

[a] 600 MHz for ^{1}H NMR and 150 MHz for ^{13}C NMR
[b] Multiplicity was determined by the analysis of 2D NMR spectroscopic data

A.1.2.2 Antibacterial Activity of Secosterol

Compound **1** was evaluated for antibacterial activity against seven pathogenic strains. (Table A.1.2) Compound **1** displayed the most potent activity on *Micrococcus lutes* ATCC 9341 and also showed the moderate activity against *Staphylococcus epidermidis* ATCC 12228 and *Bacillus subtilis* ATCC 6633 with MIC values of 3.1, 25 and 25 μg/mL, respectively. Meanwhile, **1** did not show any activity against gram negative strains include *Escherichia coli* ATCC 11775, *Salmonella typhimurium* ATCC 14028 and *Klebsiella pneumonia* ATCC 4352 up to 200 μg/mL. Interestingly, growth of one of the gram positive strain *Staphylococcus aureus* ATCC 65381 was not inhibited up to 200 μg/mL.

Table A.1.2 Antibacterial activity of 9,11-secosterol (**1**)

Strain	**1**[a]	Gentamicin [a]
Staphylococcus epidermidis ATCC 12228	25	0.2
Micrococcus lutes ATCC 9341	3.1	3.1
Bacillus subtilis ATCC 6633	25	0.2
S. aureus ATCC 65381	>200	0.2
Escherichia coli ATCC 11775	>200	0.8
Salmonella typhimurium ATCC 14028	>200	1.6
Klebsiella pneumonia ATCC 4352	>200	0.8

[a]Each experiment was repeated more than three times. MIC value in μg/mL

A.1.3 Experimental

A.1.3.1 Instruments and Data Collection

The optical rotation was measured using a Rudolph Research Autopol III polarimeter with a 5 cm cell. The UV spectrum was recorded in a Scinco UVS-2100 with a path length of 1 cm. Infrared spectra were recorded on a Thermo Electron Corporation spectrometer. NMR spectral spectroscopic data were obtained using Bruker Avance 600 MHz spectrometer [$CDCl_3$ (δ_H 7.26; δ_C 77.0) was used as an internal standard]. HRFABMS data were measured on a JEOL, JMS-AX505WA mass spectrometer.

A.1.3.2 Animal Material

The genus *Ircinia* sponge was collected by scuba diving at Yeongdeok-Gun in the East Sea. The sample was frozen immediately after collection with dry ice and stored in refrigerator at -20 ˚C before extraction.

A.1.3.3 Extraction and Isolation

The wet animal (3 kg) was extracted three times with 50% methanol (MeOH) in dichloromethane. These extracts were concentrated and partitioned three times between hexanes and MeOH. Then the MeOH-soluble layer was partitioned three times between ethylacetate (EtOAc) and water. The water-soluble fraction was further extracted thrice with n-butanol. The EtOAc-soluble layer (7.0 g) was subjected to silica flash column chromatography using step-gradient elution of EtOAc in hexanes (0%, 10%, 20%, 30%, 40%, 50%, 60%, 70%, 80%, 90%, and 100%) to afford seven fractions (Fr 1-Fr 11). Fr 5 (68.3 mg), which contained the

mixture of **1**, was further purified by reversed-phase HPLC (Polar-RP, 250 × 10 mm, 5 μm, 80 Å, 2.5 mL/min, UV detection = 210 nm), eluting with 70% acetonitrile in H_2O to afford compound **1** (2.7 mg), as colorless needles.

A.1.3.4 MIC Bioassay Procedures

The six microorganisms were obtained from the stock culture collection at the American Type Culture Collection (Maryland): The antibacterial activity was determined by the 2-fold microtiter broth dilution method (Wiegand & Hilpert, 2008). Dilutions of the test compounds dissolved in DMSO were added to each well of a 96-well microtiter plate containing a fixed volume of Mueller Hilton broth (final 0.64% DMSO). Each well was inoculated with an overnight culture of bacteria (5×10^5 cfu/mL), and the plate was incubated at 37 ˚C for 24 h. The minimum inhibitory concentration (MIC) was taken as the concentration at which no growth was observed.

References for Appendix A

Alfano, G.; Cimino, G.; De Stefano, S. *Experientia* **1979**, *35*, 1136 – 1137.

Anta, C.; González, N.; Rodriguez, J.; Jiménez, C. *J. Nat. Prod.* **2002**, *65*, 1357 – 1359.

Blunt, J.; Buchingham, J.; Munro, M. In *Handbook of Marine Natural Products*, Fattorusso, E.; Gerwick, W.; Taglialatela-Scafati, O. (Eds.) New York, Springer, **2012**, Vol. 1, pp. 4.

Cafieri, F.; Fattorusso, E.; Santocroce, C.; Minale, L. *Tetrahedron* **1972**, *28*, 1579 – 1583.

Cimino, G.; De Stefano, S.; Minale, L. *Experientia* **1972a**, *28*, 1401 – 1402.

Cimino, G.; De Stefano, S.; Minale, L. *Tetrahedron* **1972b**, *28*, 1315 – 1324.

De Pasquale, R.; Circosta, C.; Occhiuto, F.; De Rosa, S.; De Stefano, S. *Phytother. Res.* **1991**, *5*, 49 – 53.

De Rosa, S.; De giulio, A.; Crispino, A.; Iodice, C.; Tommonaro, G. *Nat. Prod. Lett.* **1997**, *10*, 7 – 12.

De Rosa, S.; Milone, A.; De Giulio, A.; Crispino, A.; Iodice, C. *Nat. Prod. Lett.* **1996**, *8*, 245 – 251.

Faulkner, D. *Tetrahedron Lett.* **1973**, *14*, 3821 – 3822.

Fu, X.; Ferreira, M. L. G.; Schmitz, F. J.; Kelly, M. *J. Org. Chem.* **1999**, *64*, 6706 – 6709.

Hertiani, T.; Edrada-Ebel, R.; Ortlepp, S.; van Soest, R.; de Voogd, N.; Wray, V.; Hentschel, U.; Kozytska, S.; Muller, W. E.; Proksch, P. *Bioorg. Med. Chem.* **2010**, *18*, 1297 – 1303.

Jeon, J.; Na, Z.; Jung, M.; Lee, H.; Sim, C.; Nahm, K.; Oh, K. B.; Shin, J. *J. Nat. Prod.* **2010**, *73*, 258 – 262.

Kawakami, A.; Miyamoto, T.; Higuchi, R.; Uchiumi, T.; Kuwano, M.; Van Soest, R. W. M. *Tetrahedron Lett.* **2001**, *42*, 3335 – 3337.

Keffer, J.; Plaza, A.; Bewley, C. A. *Org. Lett.* **2009**, *11*, 1087 – 1090.

Kondo, K.; Shigemori, H.; Kikuchi, Y.; Ishibashi, M.; Sasaki, T.;Kobayashi, J. *J. Org. Chem.* **1992**, *57*, 2480 – 2483.

Lu, Q.; Faulkner, D. J. *J. Nat. Prod.* **1997**, *60*, 195 – 198.

Manes, L.; Crews, P. *J. Nat. Prod.* **1986**, *49*, 787 – 793.

Martins, A.; Vieira, H.; Gaspar, H.; Santos, S. *Mar. Drugs* **2014**, *12*, 1066 - 1101.

Nakao, Y.; Matsunaga, S.; Fusetani, N. *Bioorg. Med. Chem.* **1995**, *3*, 1115 – 1122.

Reddy, M.; Harper, M.; Faulkner, D. *J. Nat. Prod.* **1997**, *60*, 41 – 43.

Rothberg, I.; Shubiak, P. *Tetrahedron Lett.* **1975**, *16*, 769 – 772.

Venkateswarlu, Y.; Reddy, M. V. R. *J. Nat. Prod.* **1994**, *57*, 1286 – 1289.

Venkateswarlu, Y.; Reddy, M. V. R.; Rao, M. R. *J. Nat. Prod.* **1996**, *59*, 876 – 887.

Wiegand, I.; Hilpert, K.; Hancock, R. *Nat. Protoc.* **2008**, *3*, 163 – 175.

Wright, A.; McCluskey, A.; Robertson, M.; MacGregor, K.; Gordon, C.; Guenther, J. *J. Org. Biomol. Chem.* **2011**, *9*, 400 – 407.

Xu, S.; Liao, X.; Du, B.; Zhou, X. L.; Huang, Q.; Wu, C. *Steroids* **2008**, *73*, 568 – 573.

A.2 NMR spectra of 9,11-Secosterol A

Figure A.2.1 ^{1}H NMR Spectrum of **9,11-Secosterol A** ($CDCl_3$, 600 MHz)

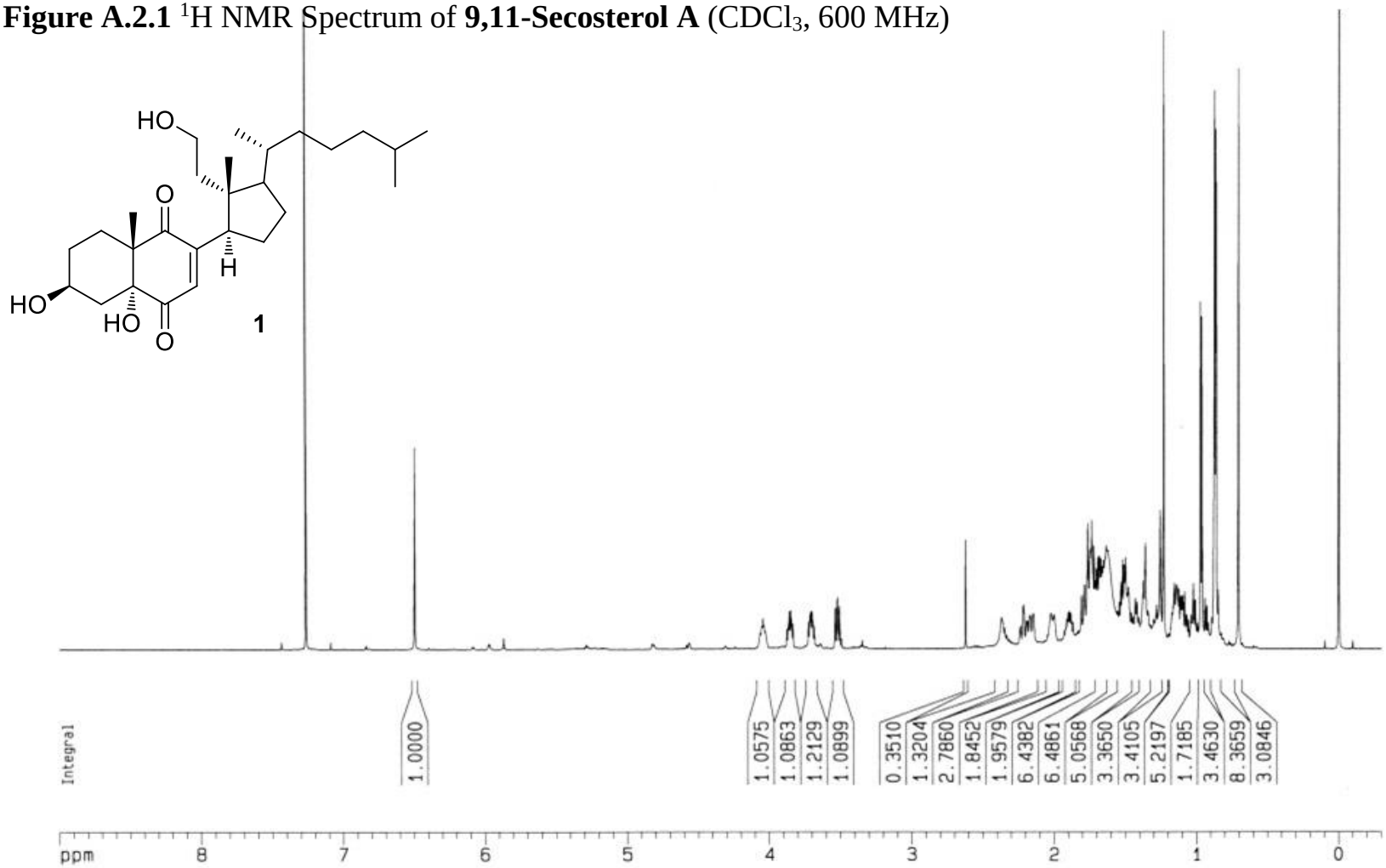

Figure A.2.2 ^{13}C NMR Spectrum of **9,11-Secosterol A** ($CDCl_3$, 150 MHz)

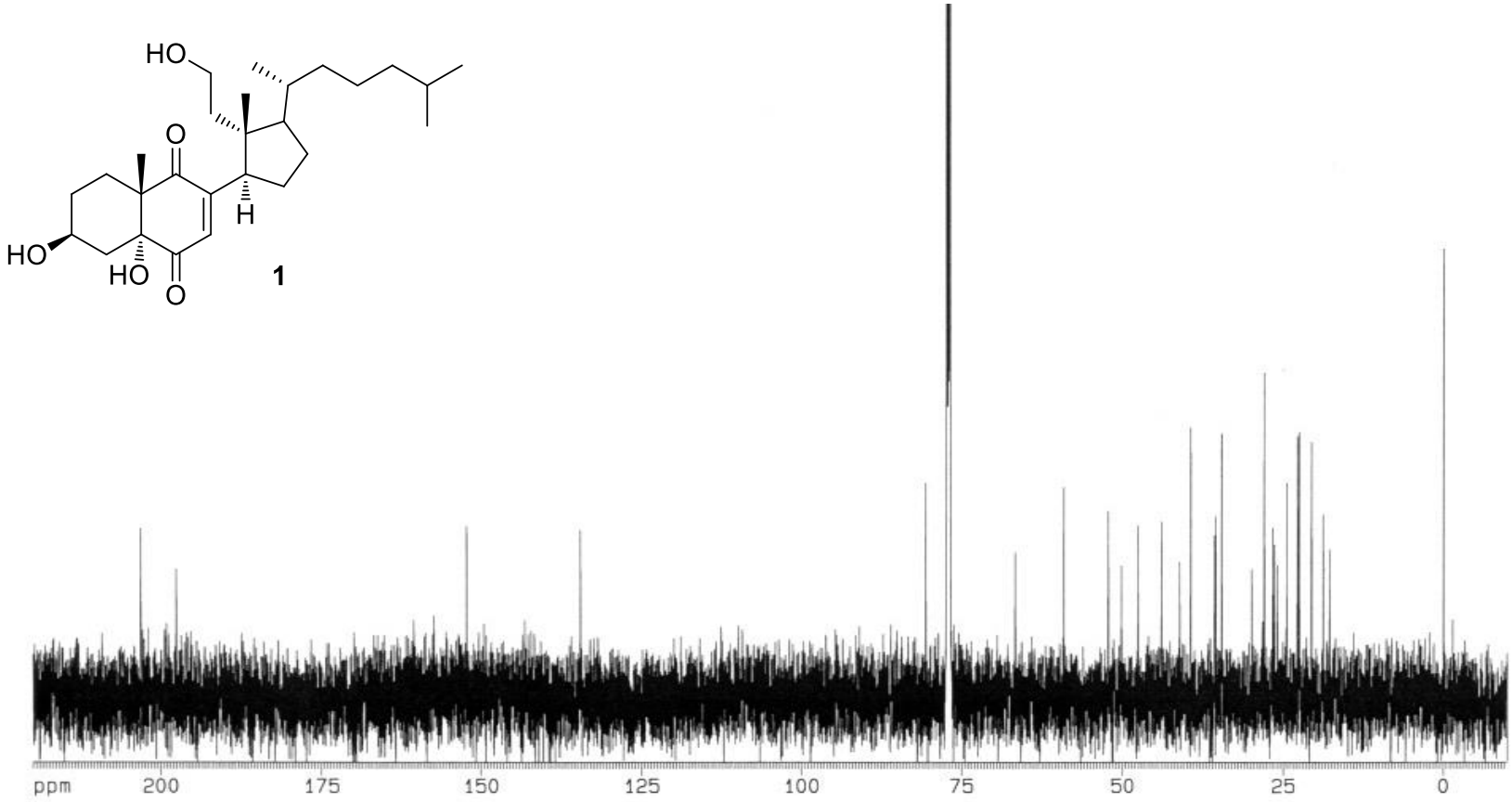

Figure A.2.3 COSY NMR Spectrum of **9,11-Secosterol A** ($CDCl_3$, 600 MHz)

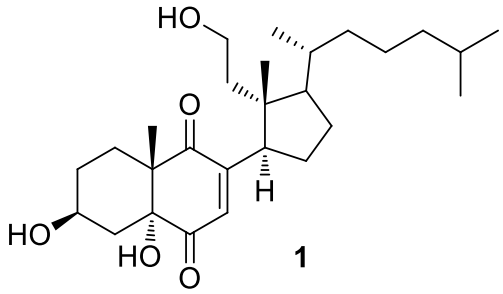

1

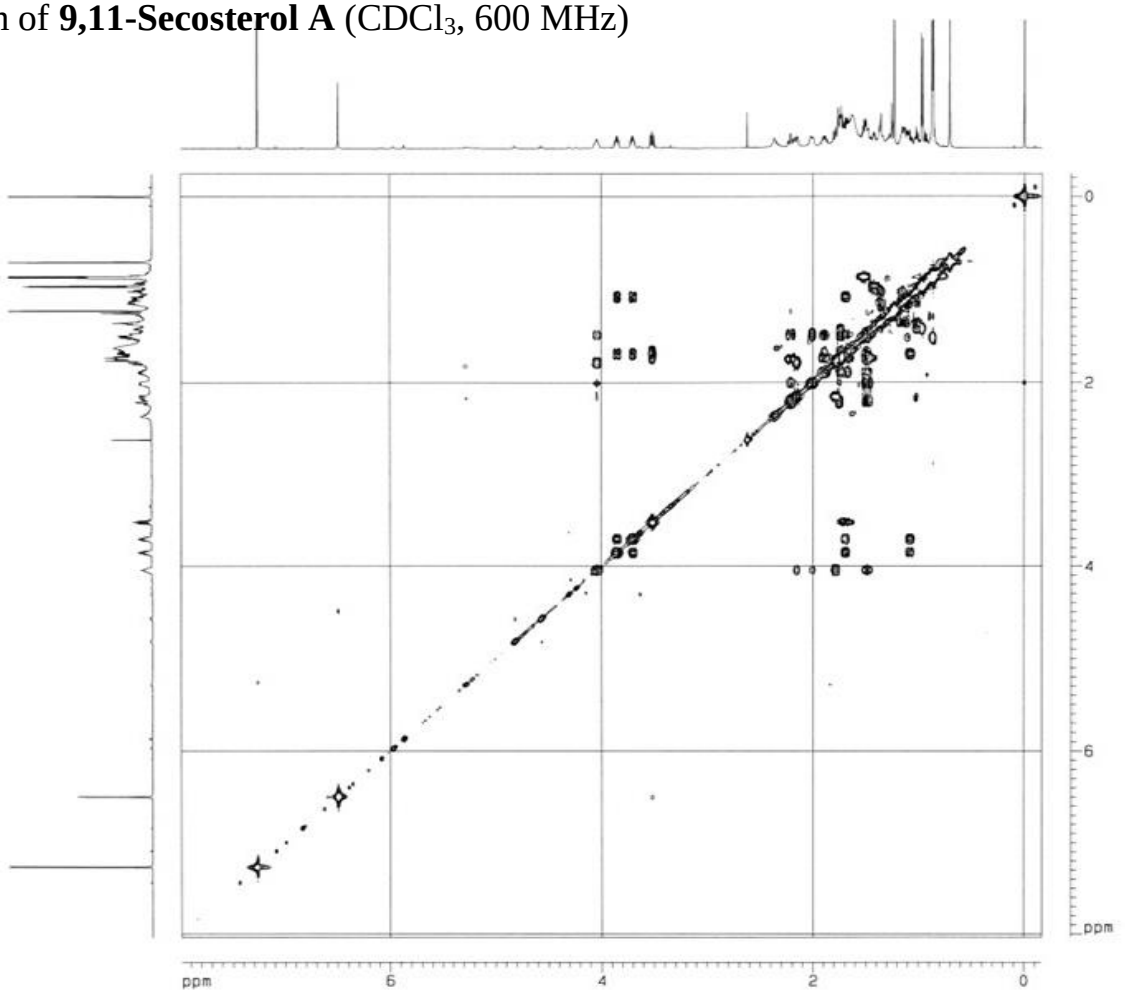

Figure A.2.4 HSQC Spectrum of **9,11-Secosterol A** ($CDCl_3$, 600 MHz)

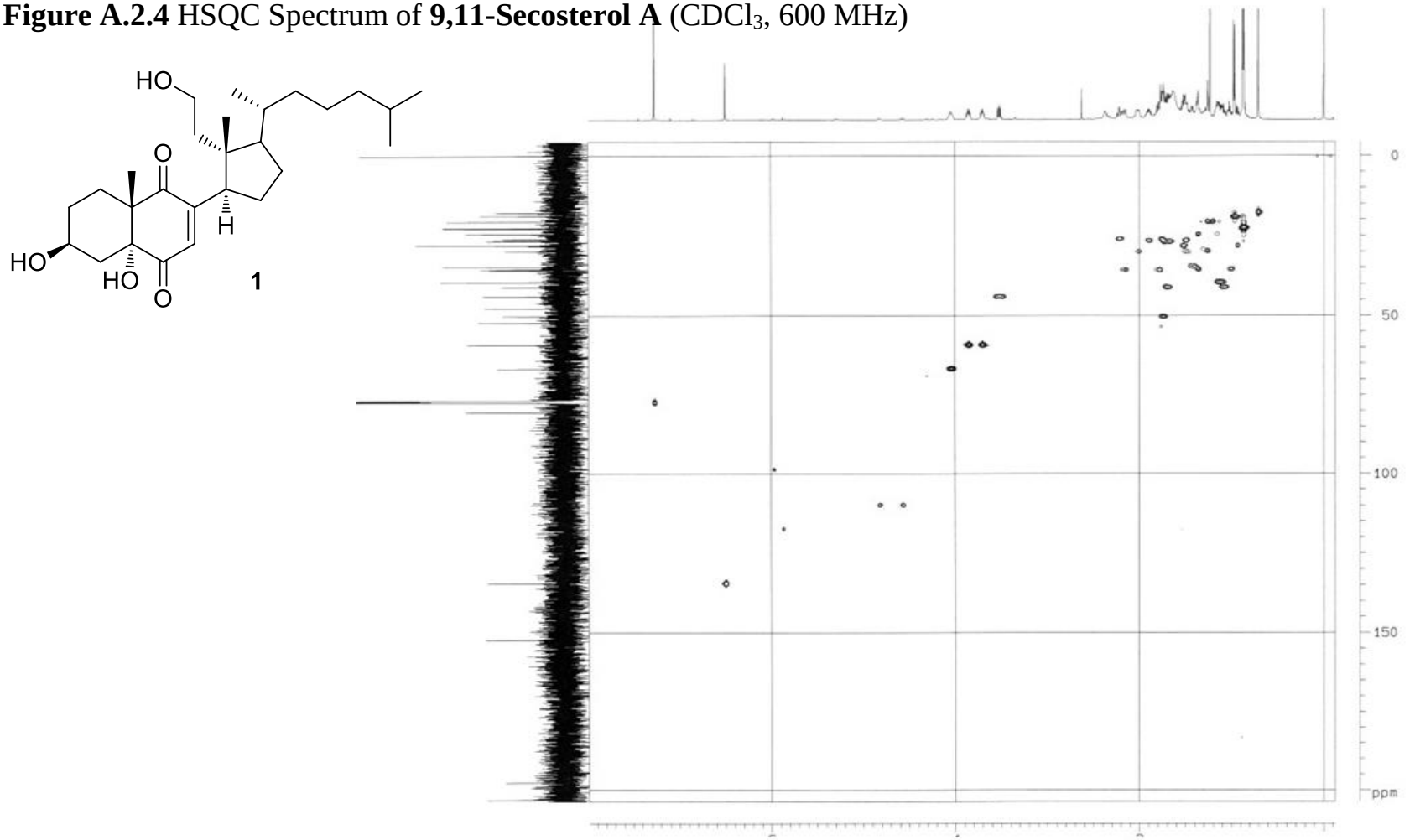

Figure A.2.5 HMBC NMR Spectrum of **9,11-Secosterol A** ($CDCl_3$, 600 MHz)

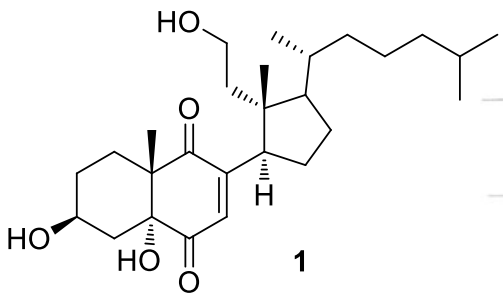

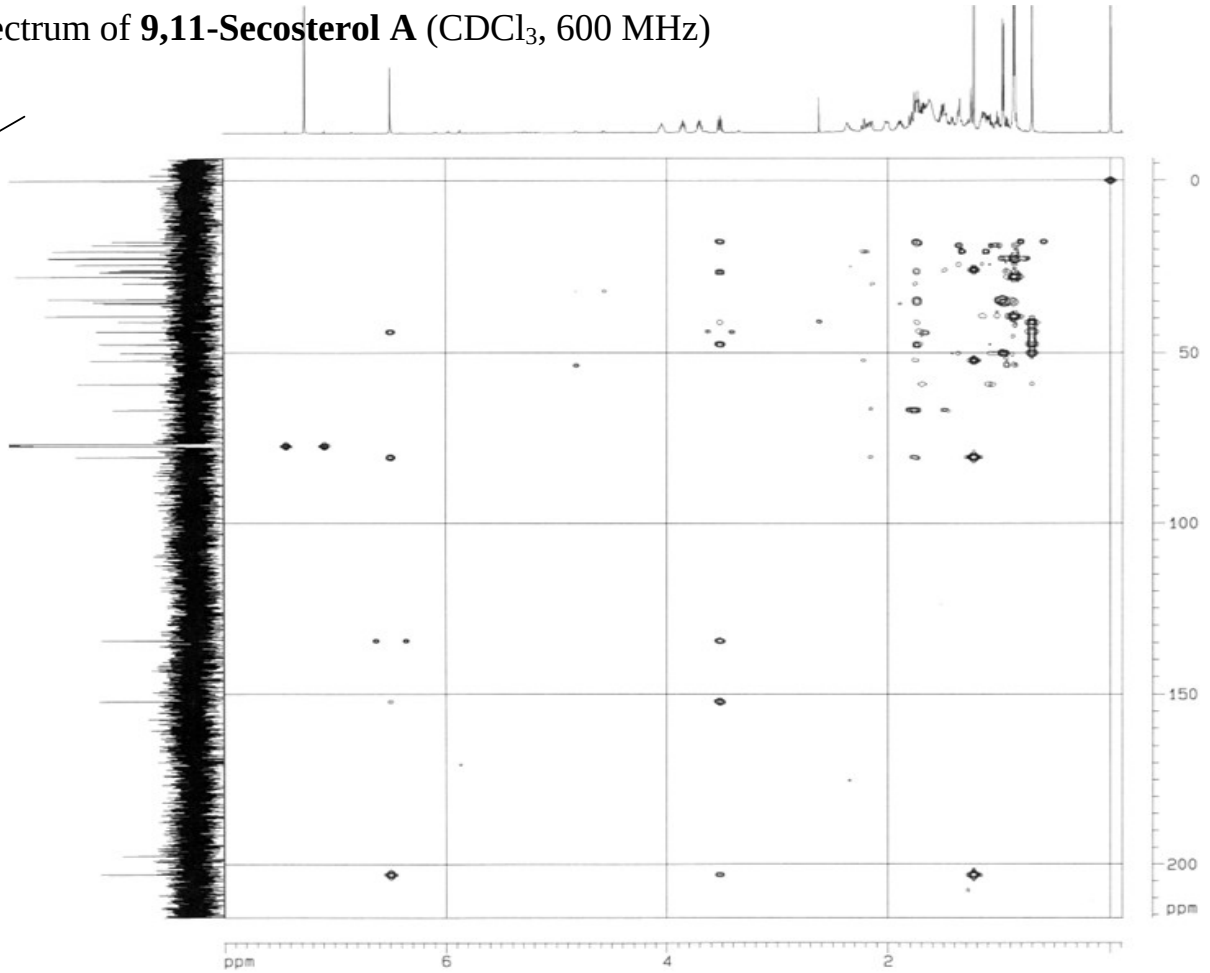

Figure A.2.6 NOESY NMR Spectrum of **9,11-Secosterol A** ($CDCl_3$, 600 MHz)

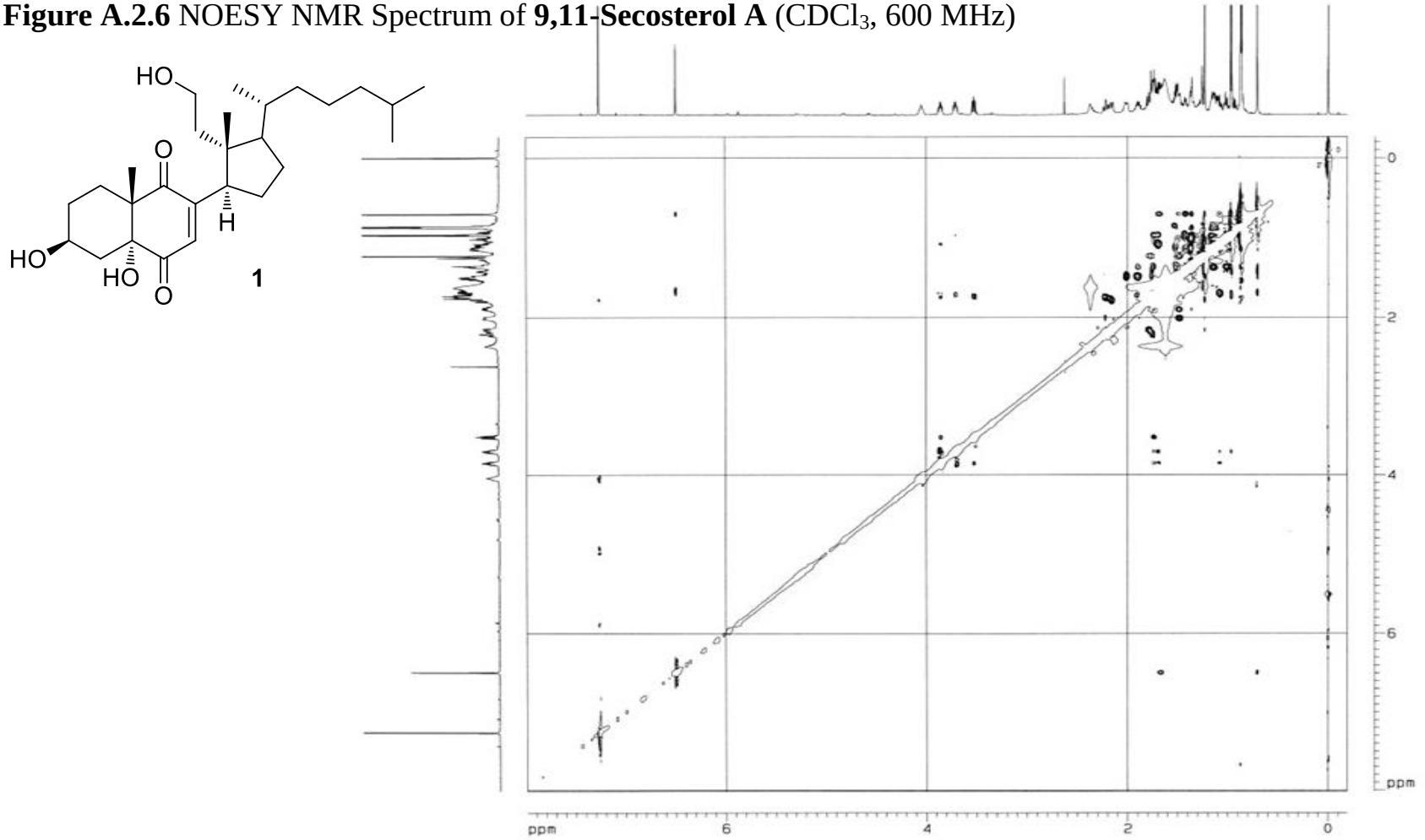

Appendix B

B.1 NMR Spectra of Nocrimidazoles A and B

Figure B.1.1 ^{1}H NMR Spectrum of Nocarimidazol A (**1**) ($CDCl_3$, 500 MHz)

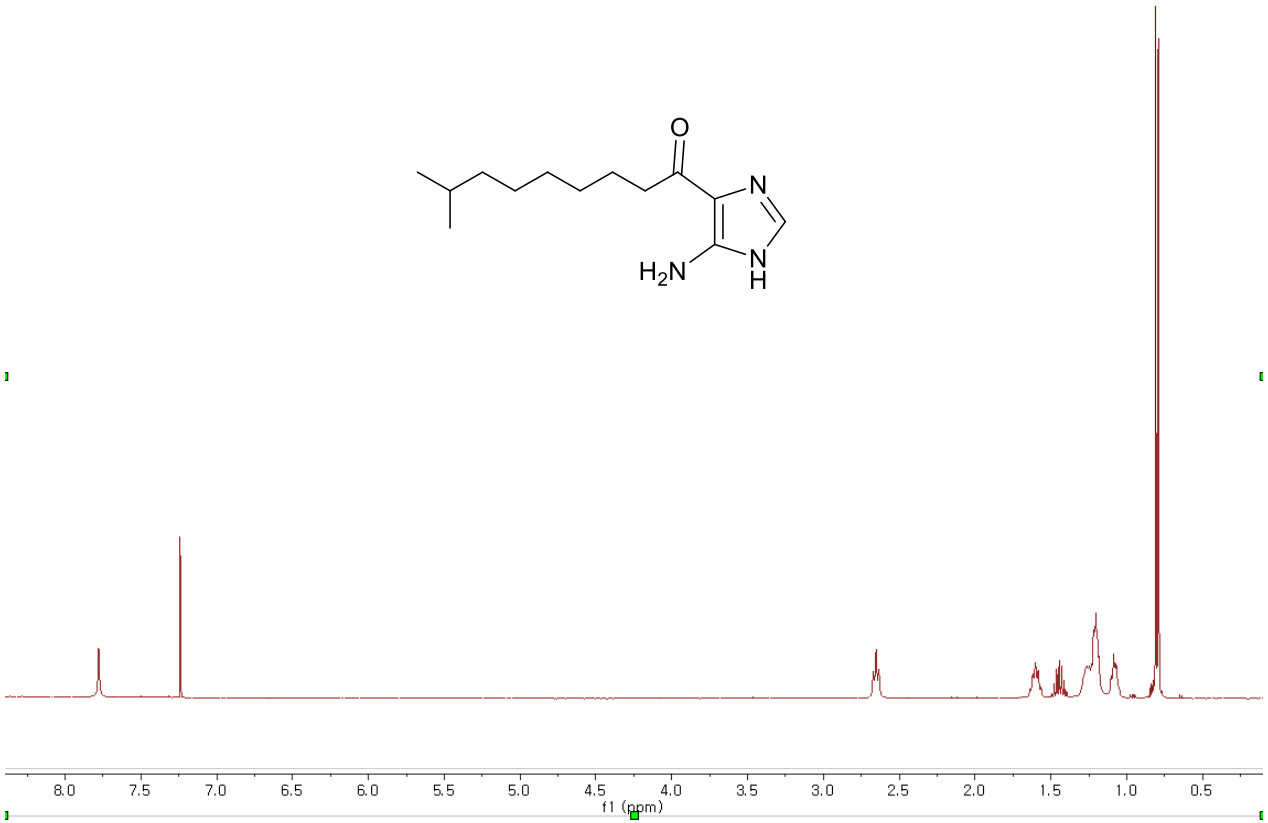

Figure B.1.2 ^{13}C NMR Spectrum of Nocarimidazol A (**1**) ($CDCl_3$, 125 MHz)

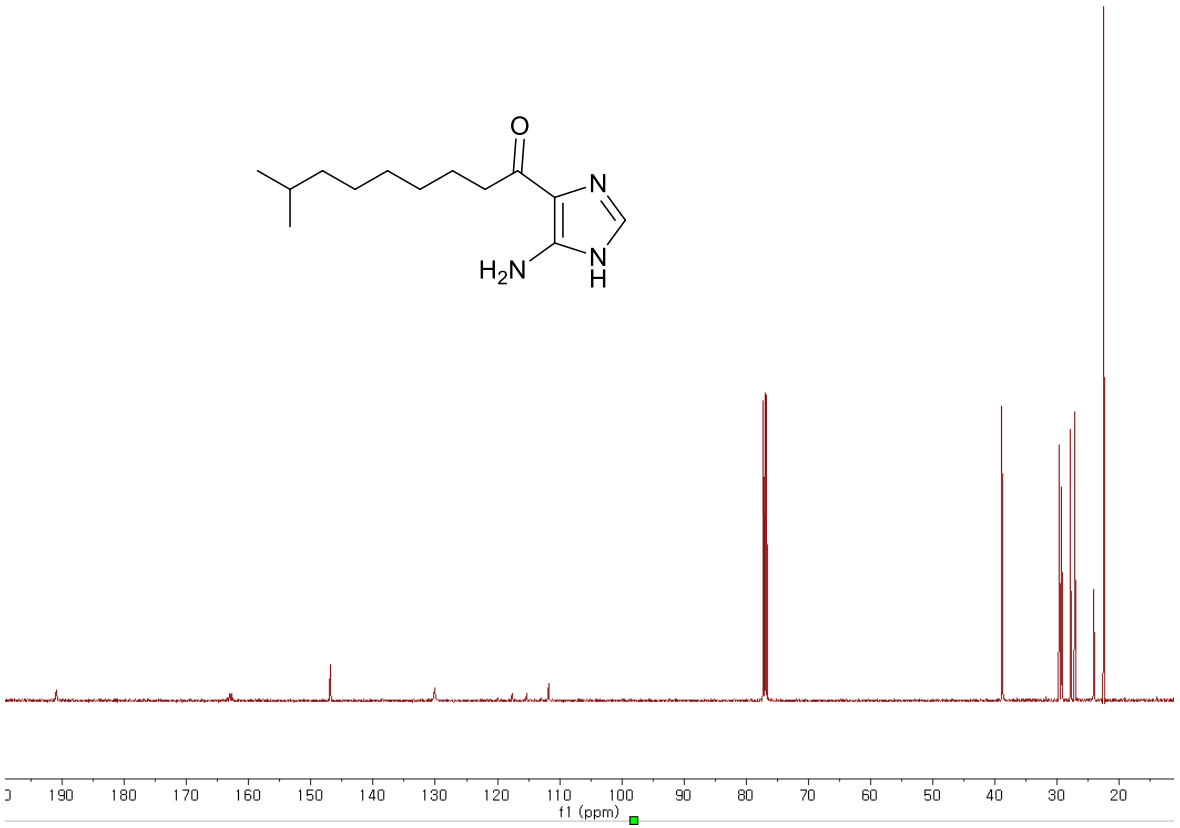

Figure B.1.3 COSY Spectrum of Nocarimidazol A (**1**) ($CDCl_3$, 500 MHz)

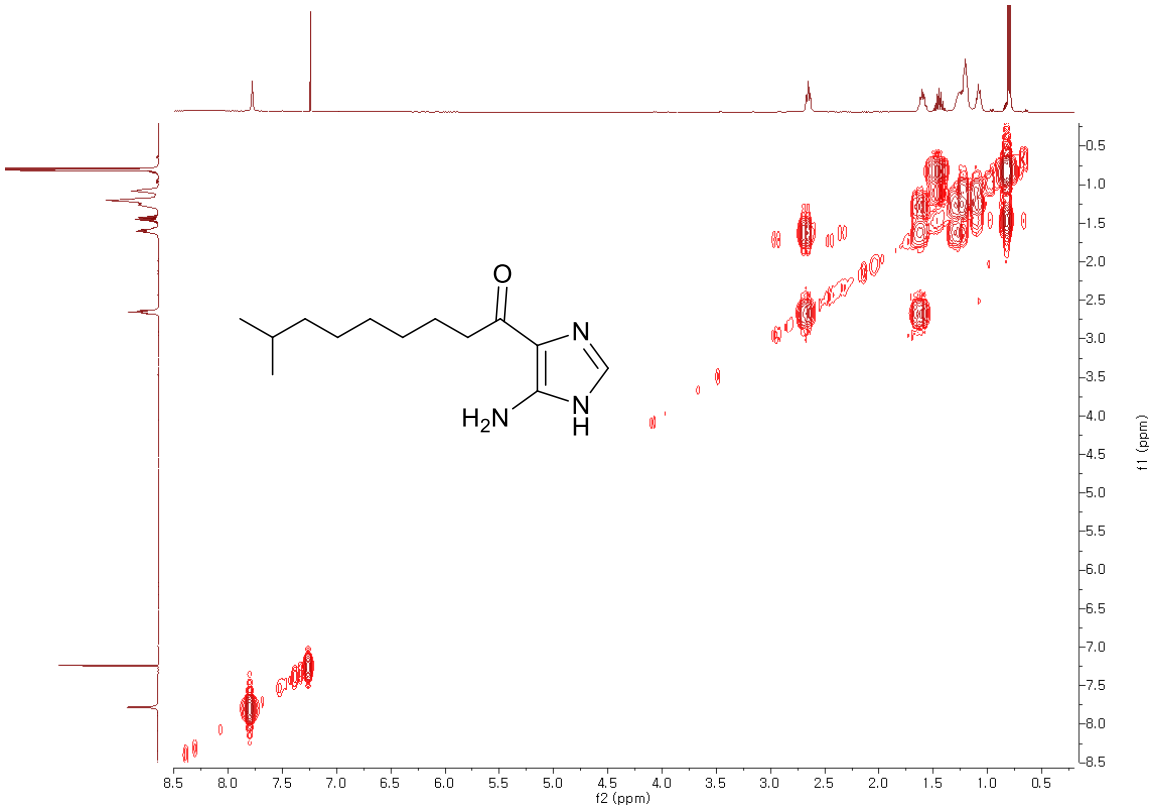

Figure B.1.4 HSQC Spectrum of Nocarimidazol A (**1**) ($CDCl_3$, 500 MHz)

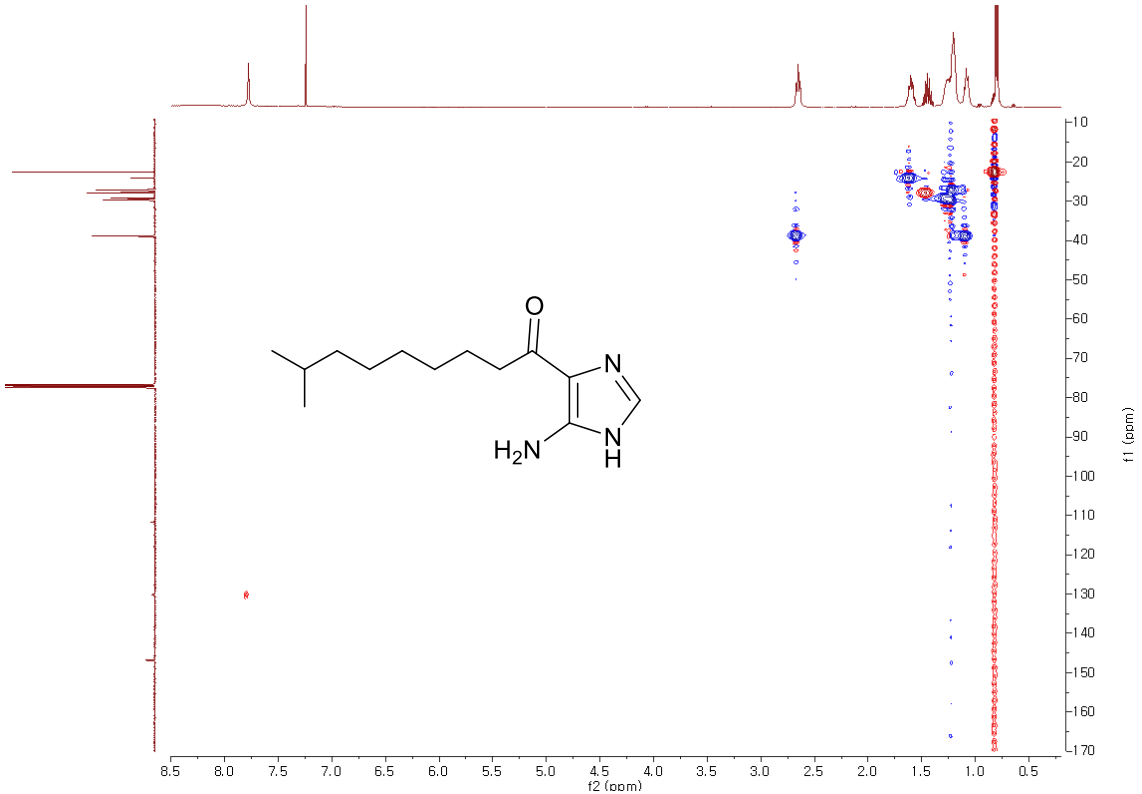

Figure B.1.5 HMBC Spectrum of Nocarimidazol A (**1**) ($CDCl_3$, 500 MHz)

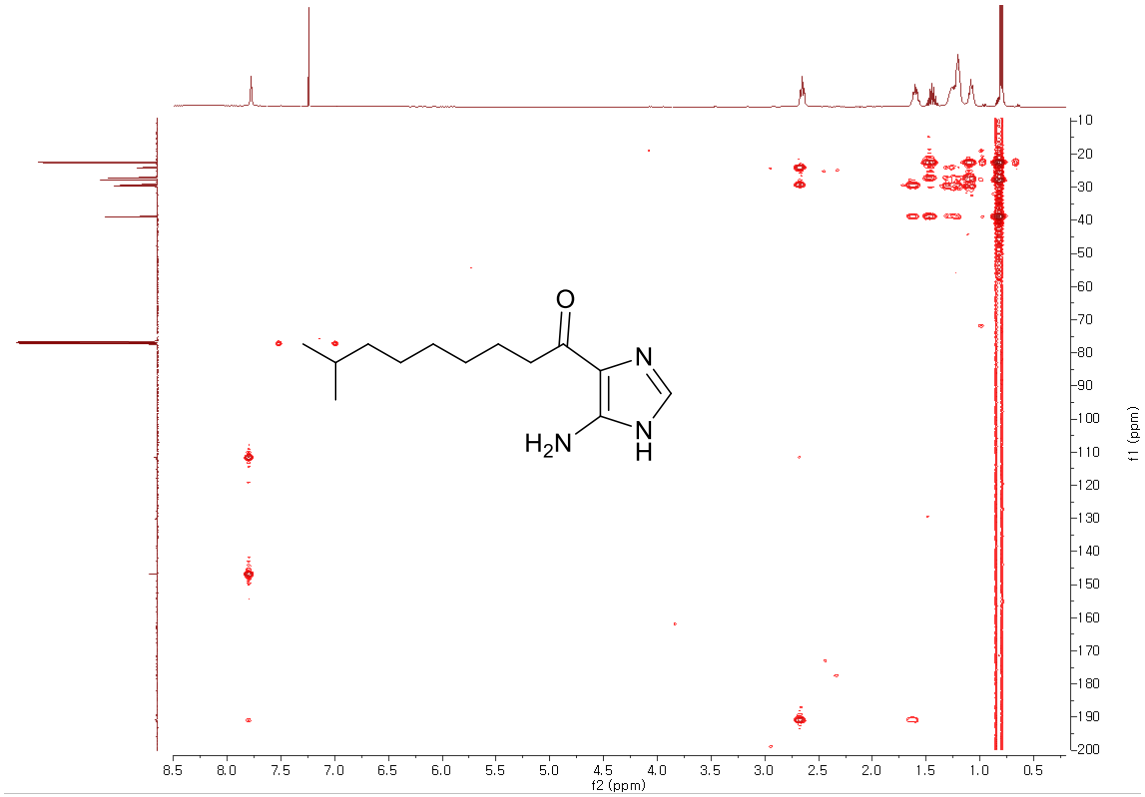

Figure B.1.6 ^{1}H NMR Spectrum of Nocarimidazol B (**2**) ($CDCl_3$, 500 MHz)

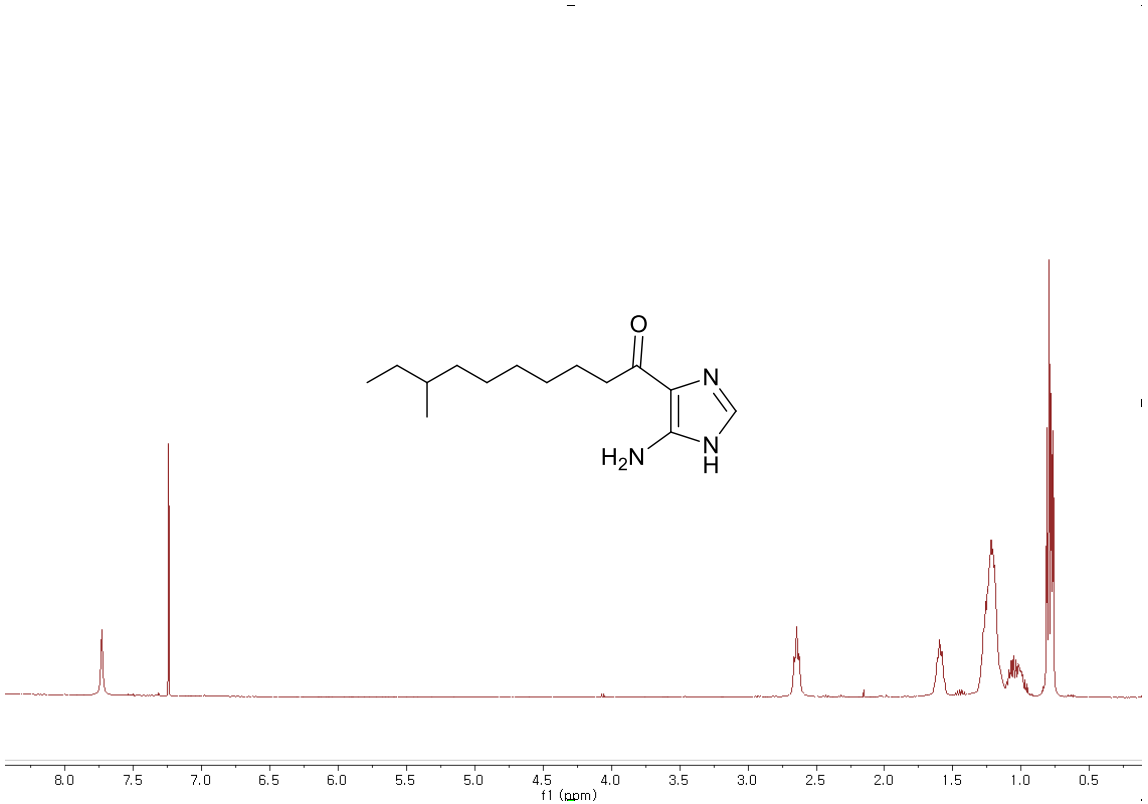

Figure B.1.**7** ^{13}C NMR Spectrum of Nocarimidazol B (**2**) ($CDCl_3$, 125 MHz)

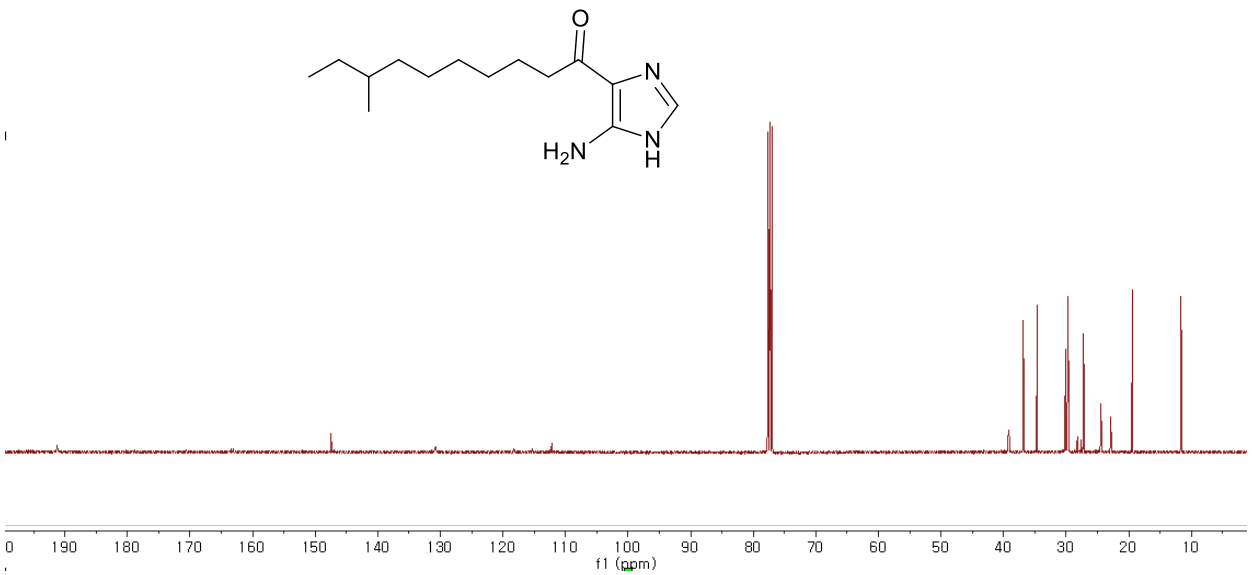

Figure B.1.8 COSY Spectrum of Nocarimidazol B (**2**) ($CDCl_3$, 500 MHz)

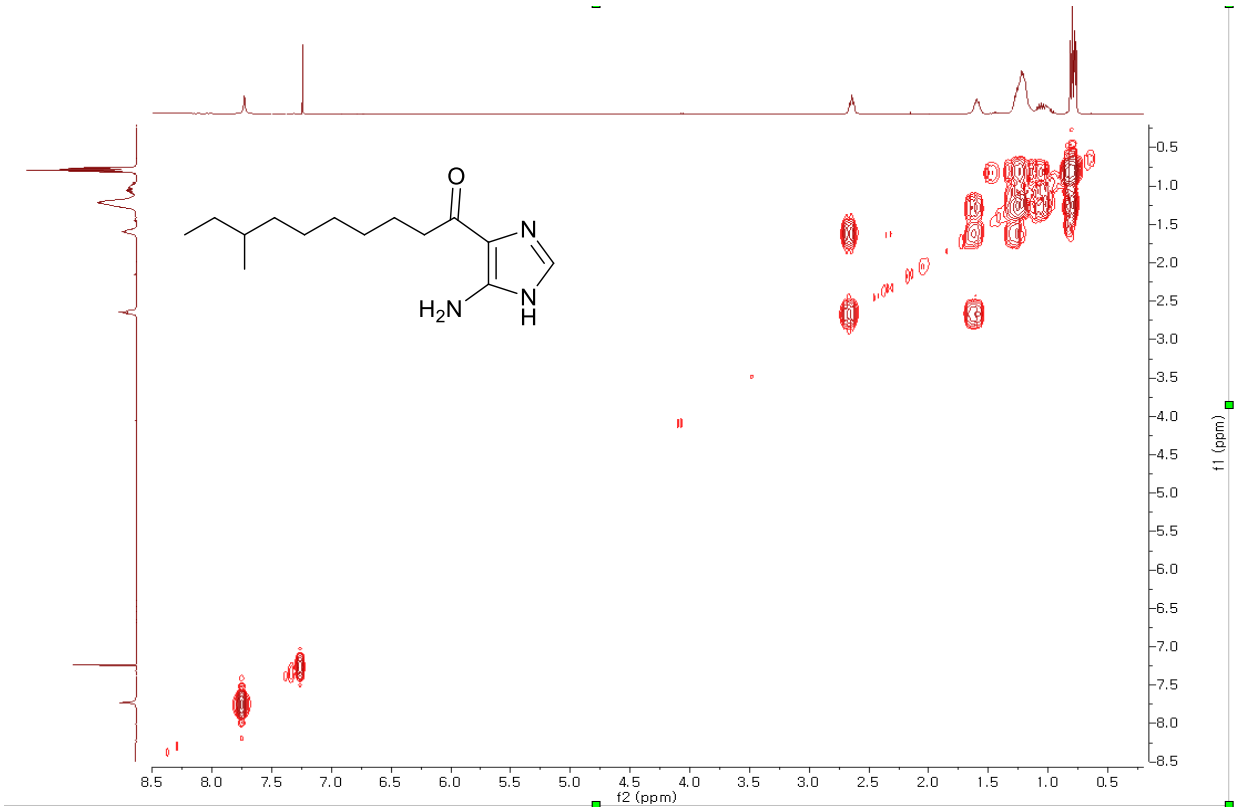

Figure B.1.9 HSQC Spectrum of Nocarimidazol B (**2**) ($CDCl_3$, 500 MHz)

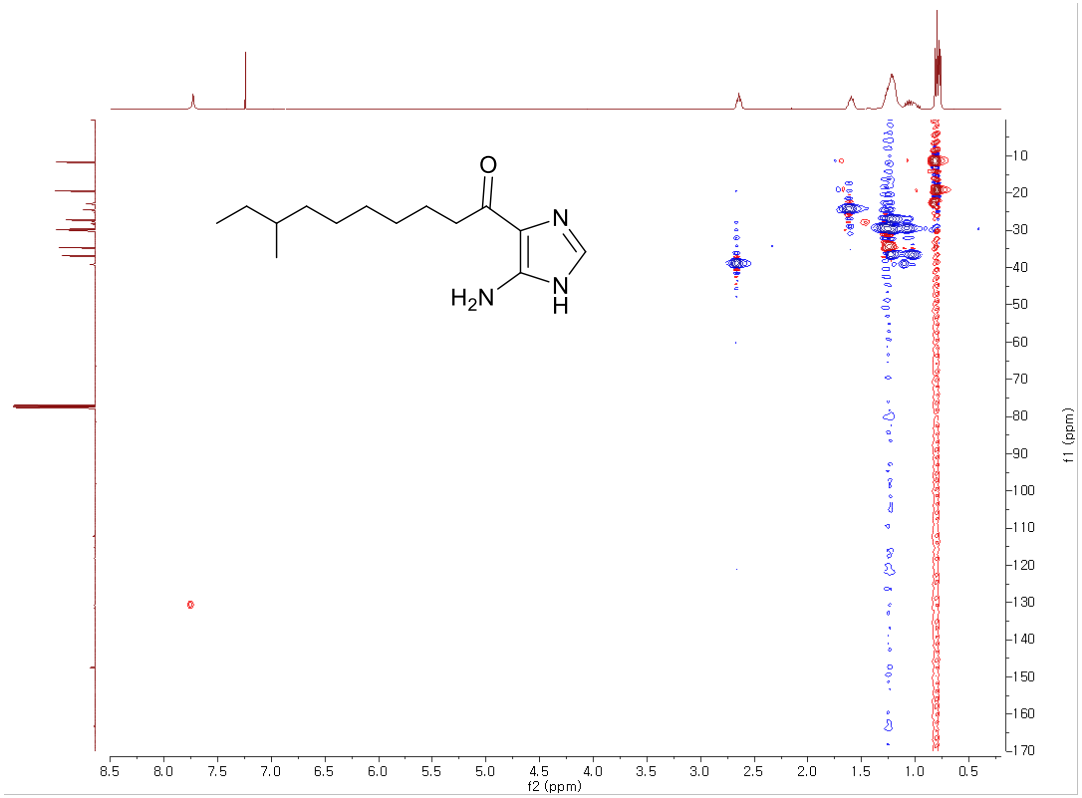

Figure B.1.10 HMBC Spectrum of Nocarimidazol B (**2**) ($CDCl_3$, 500 MHz)

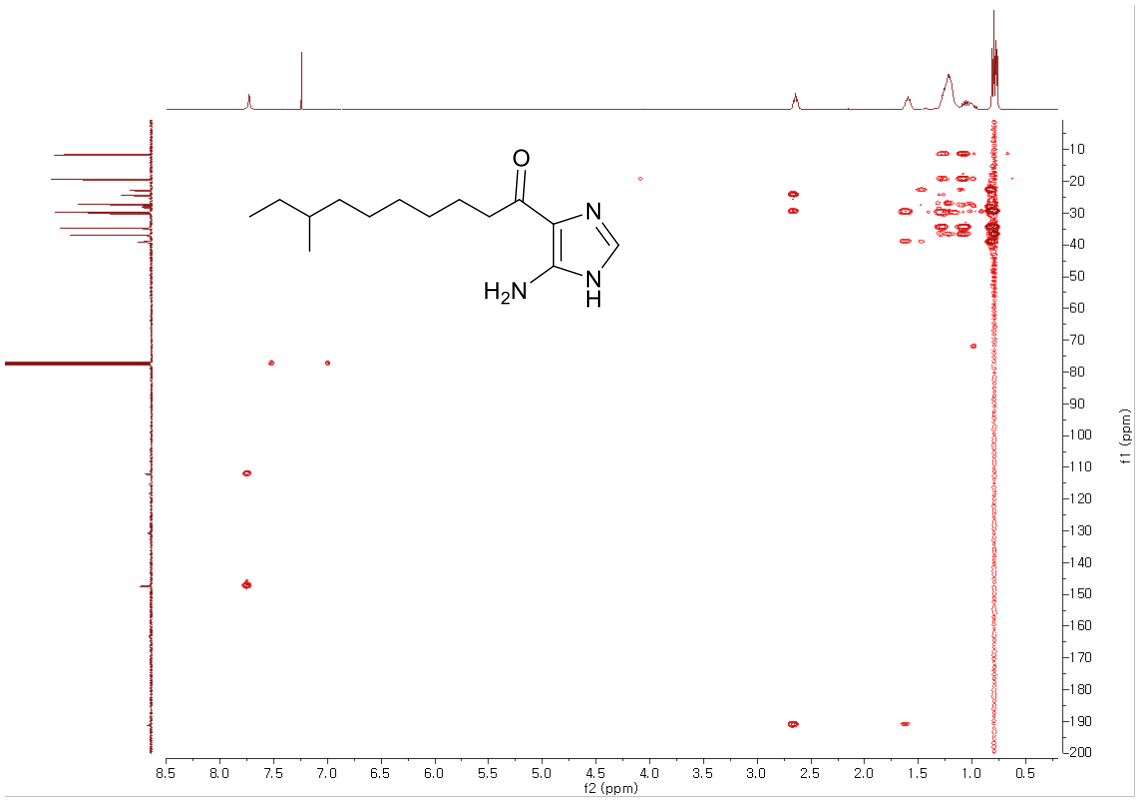

Figure B.1.11 ^{1}H NMR Spectrum of Nocarimidazole B Diazomethane derivative (**3**) ($CDCl_3$, 700 MHz)

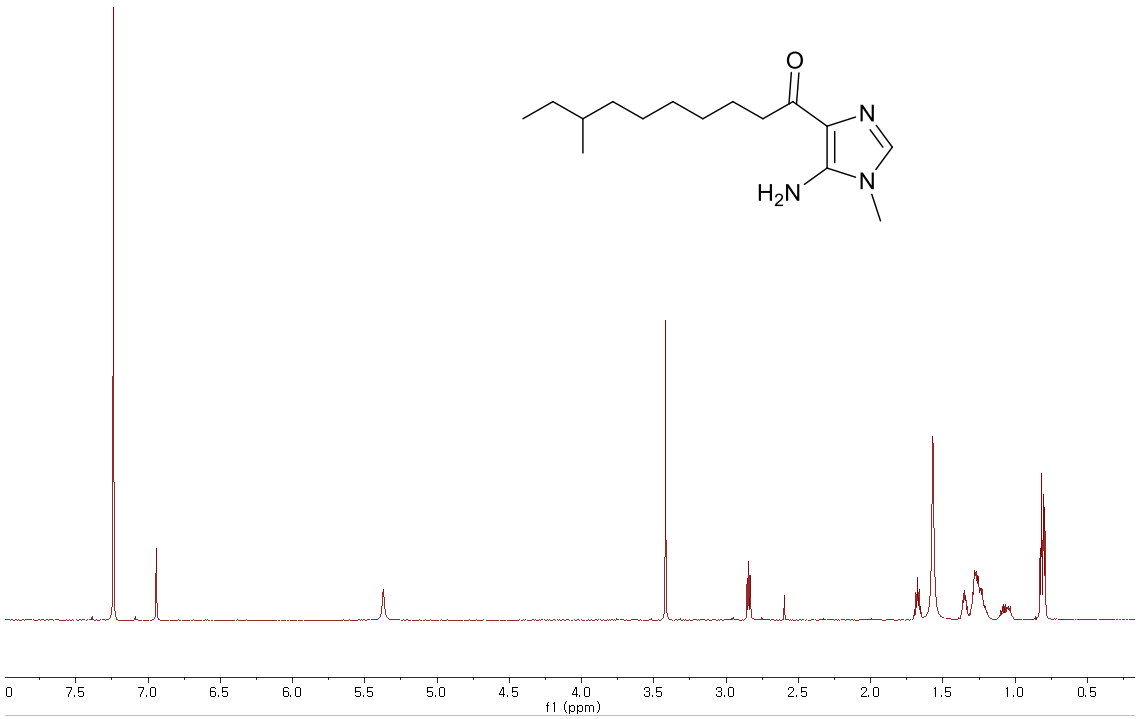

Figure B.1.12 COSY Spectrum of Nocarimidazole B Diazomethane derivative (**3**) ($CDCl_3$, 700 MHz)

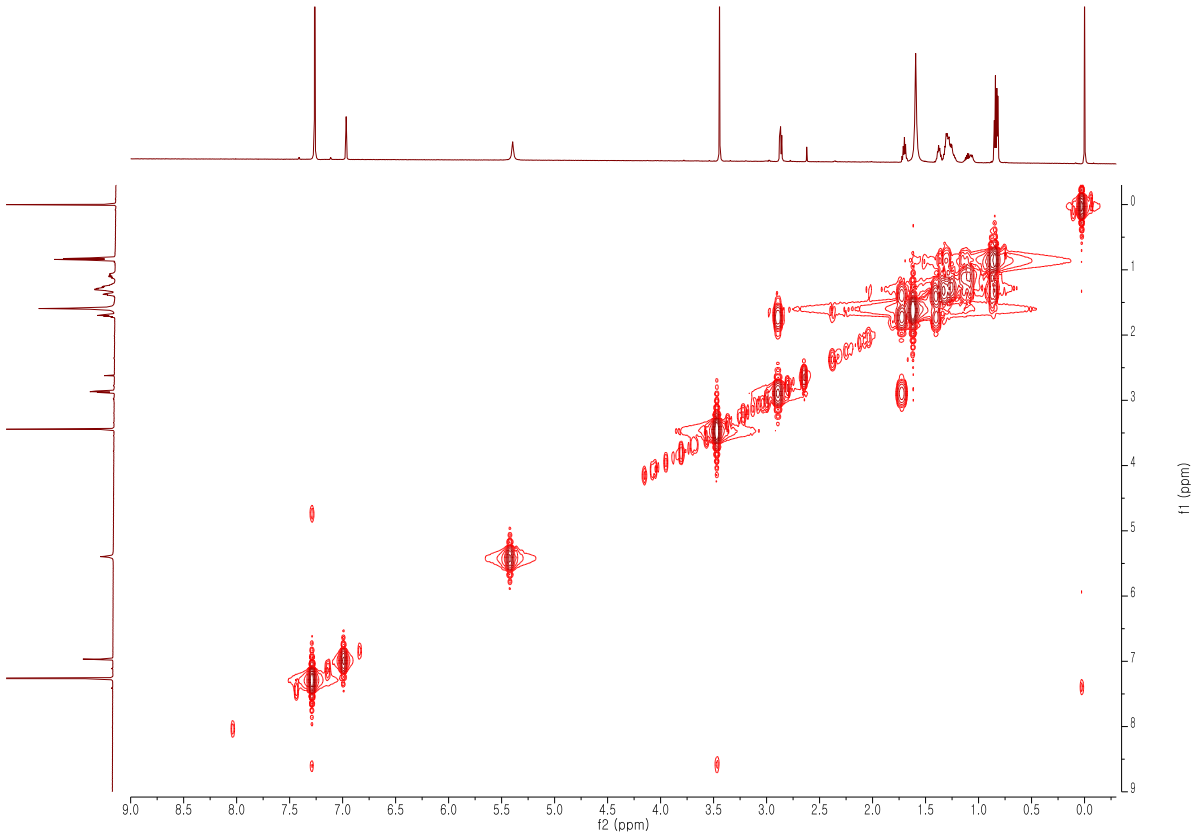

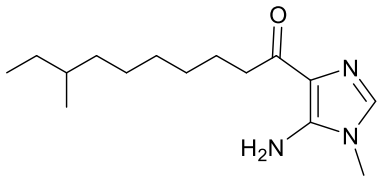

Figure B.1.13 HSQC Spectrum of Nocarimidazole B Diazomethane derivative (**3**) ($CDCl_3$, 700 MHz)

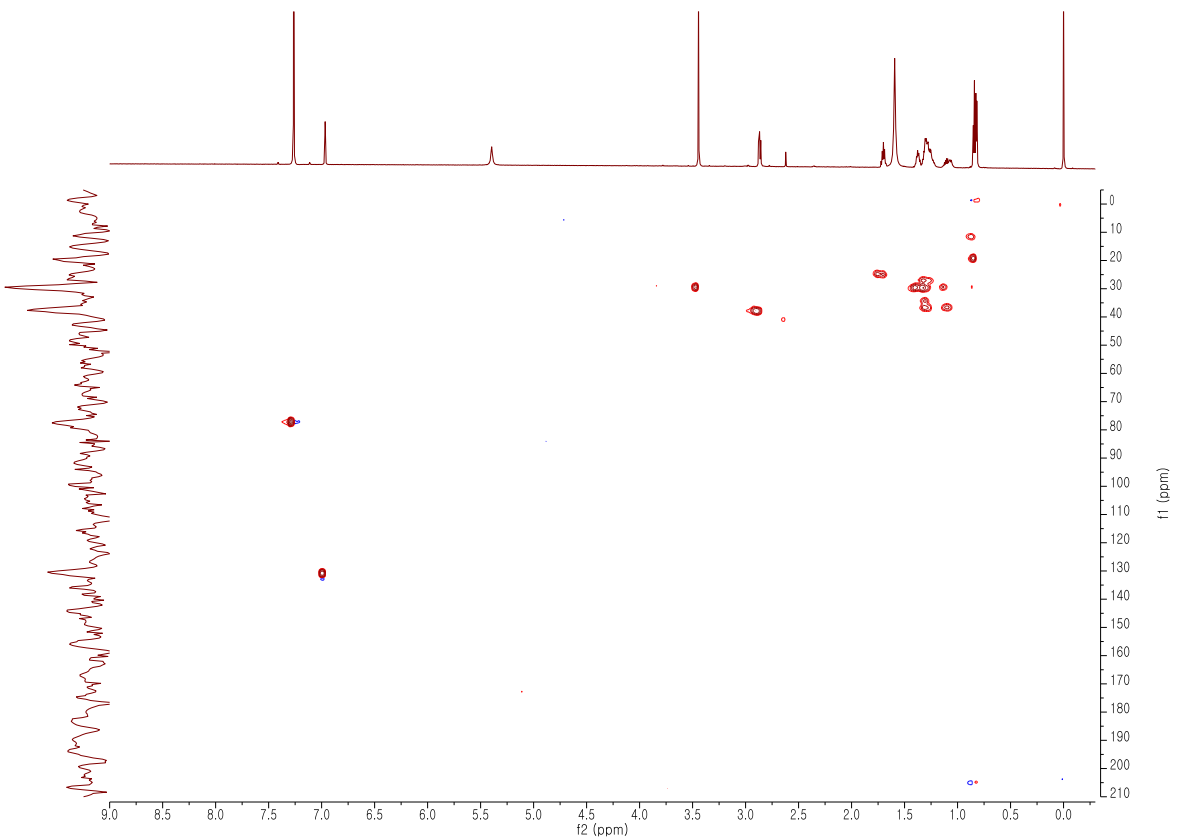

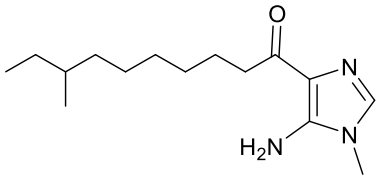

Figure B.1.14 HMBC Spectrum of Nocarimidazole B Diazomethane derivative (**3**) ($CDCl_3$, 700 MHz)

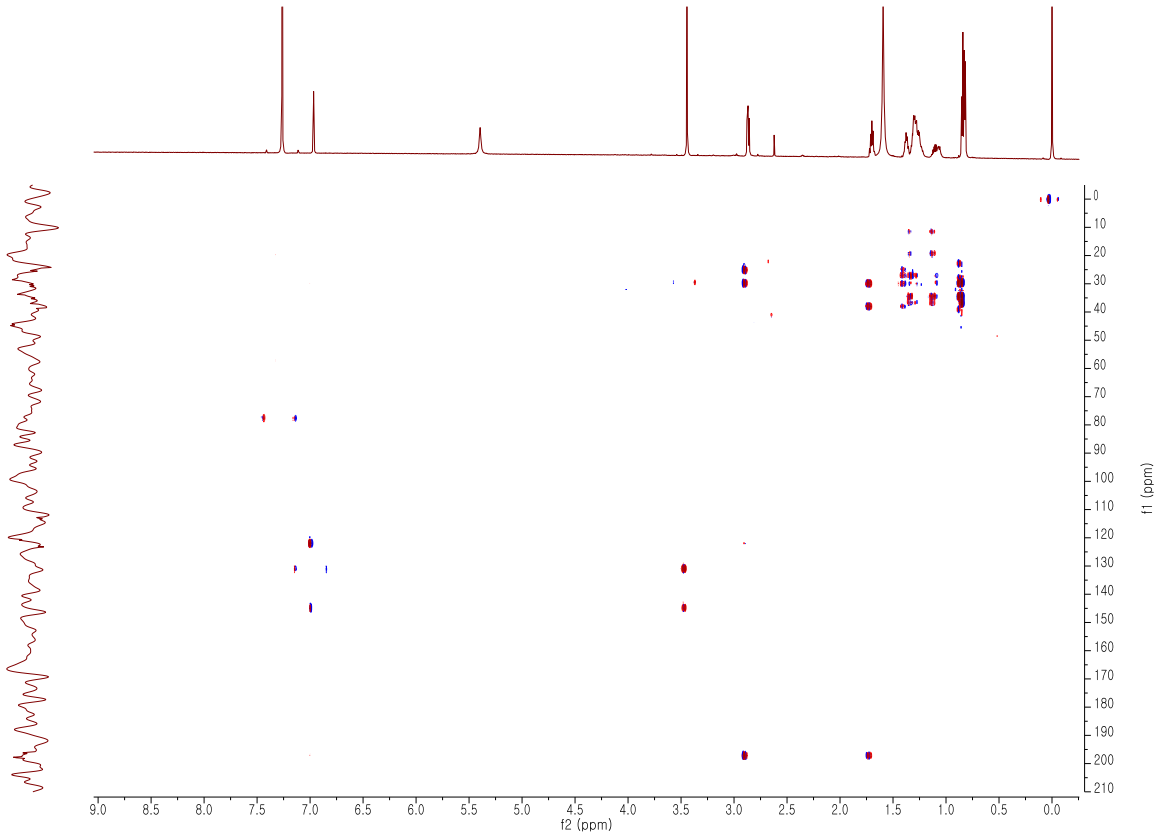

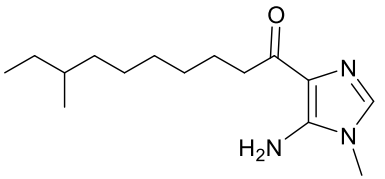

Figure B.1.15 ^{1}H NMR Spectrum of Nocarimidazole B Iodomethane Derivative (**4**) ($CDCl_3$, 700 MHz)

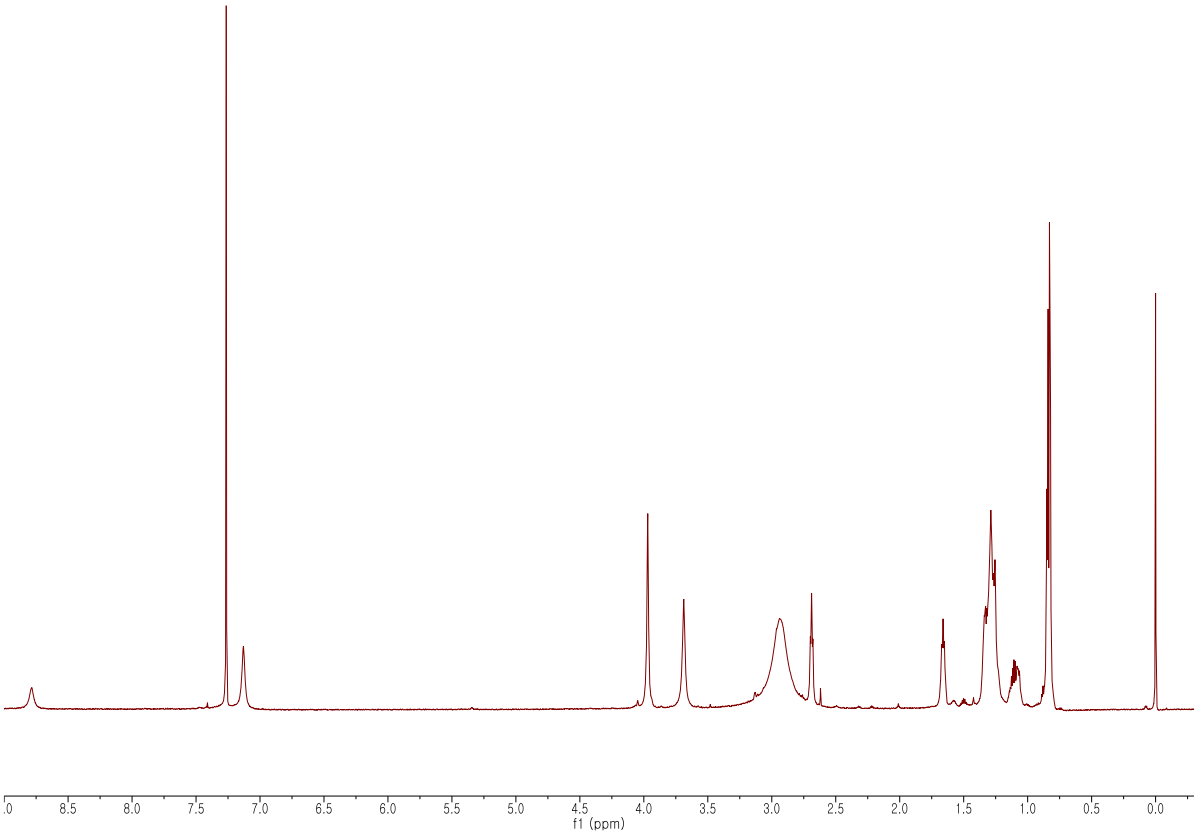

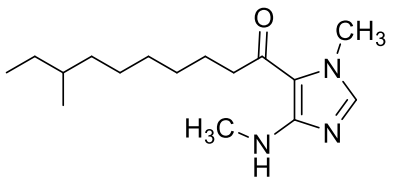

Figure B.1.16 COSY Spectrum of Nocarimidazole B Iodomethane Derivative (**4**) ($CDCl_3$, 700 MHz)

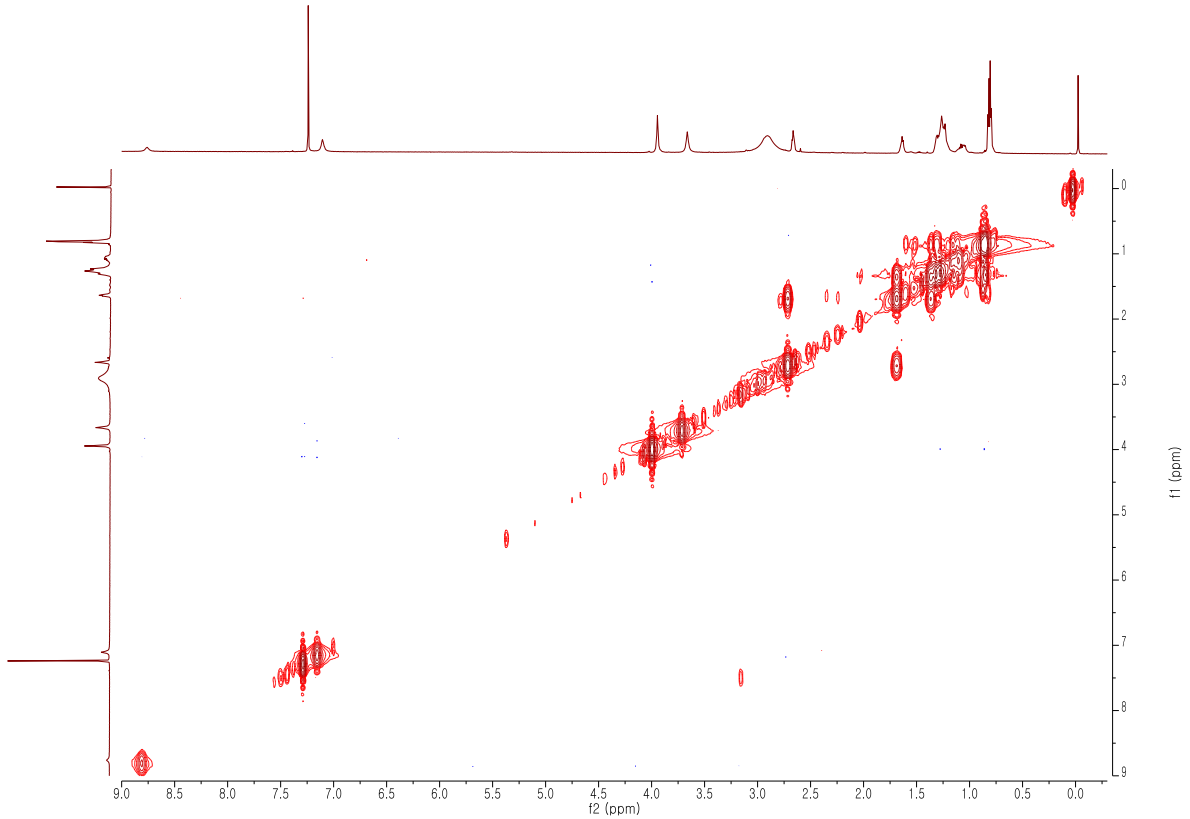

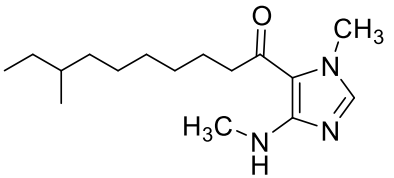

Figure B.1.17 HSQC Spectrum of Nocarimidazole B Iodomethane Derivative (**4**) ($CDCl_3$, 700 MHz)

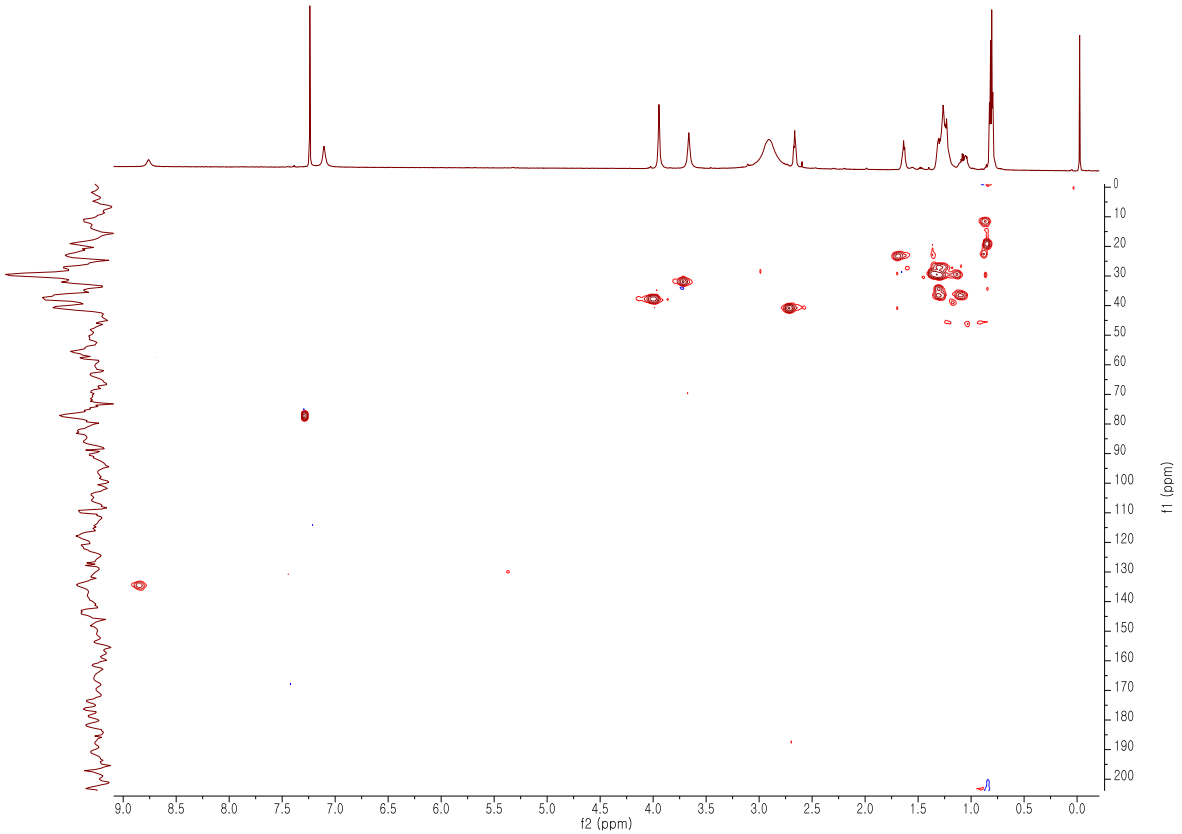

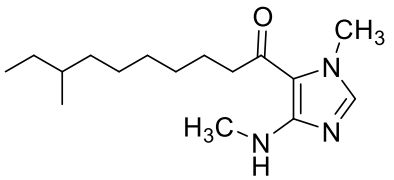

Figure B.1.18 HMBC Spectrum of Nocarimidazole B Iodomethane Derivative (**4**) ($CDCl_3$, 700 MHz)

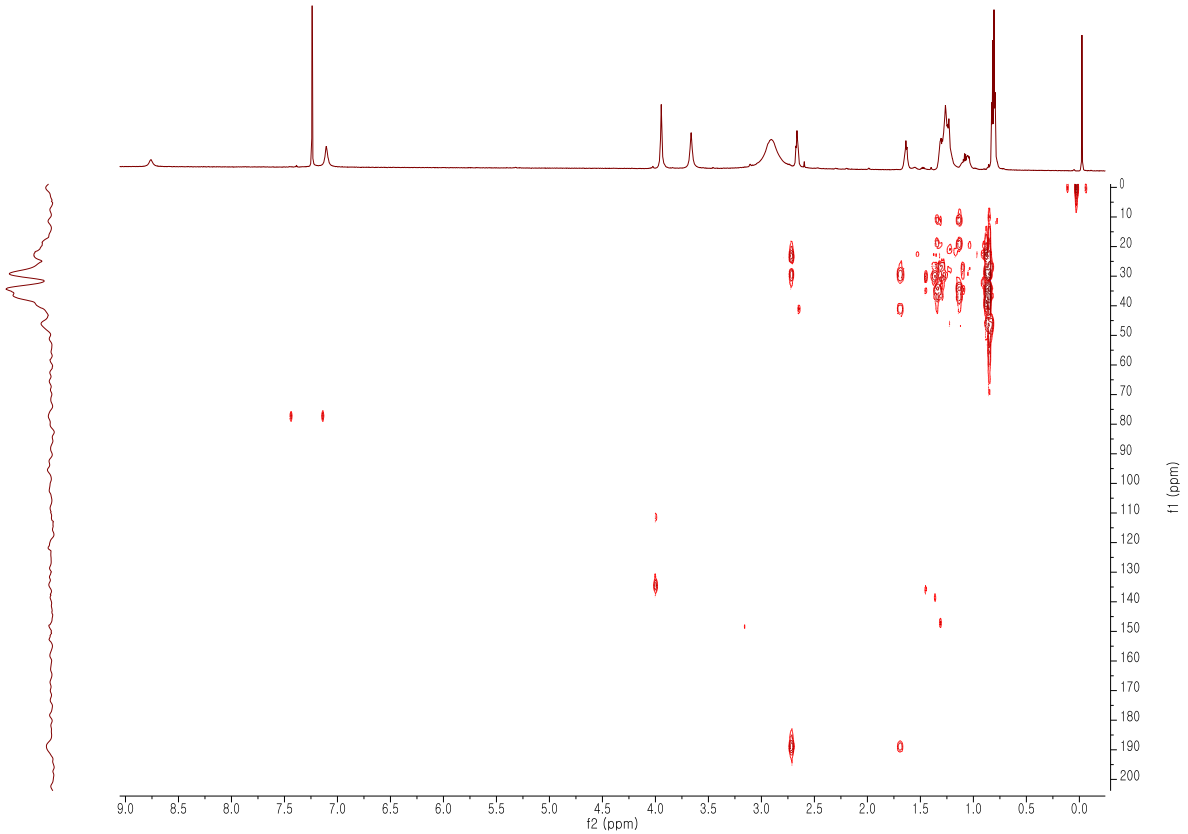

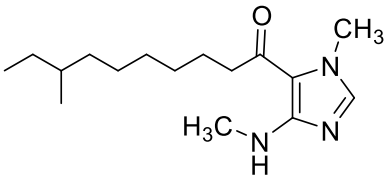

B.2 NMR Spectra of Anithiactins A-D

Figure B.2.1 ^{1}H NMR spectrum of Anithiactin A ($CDCl_3$, 600 MHz)

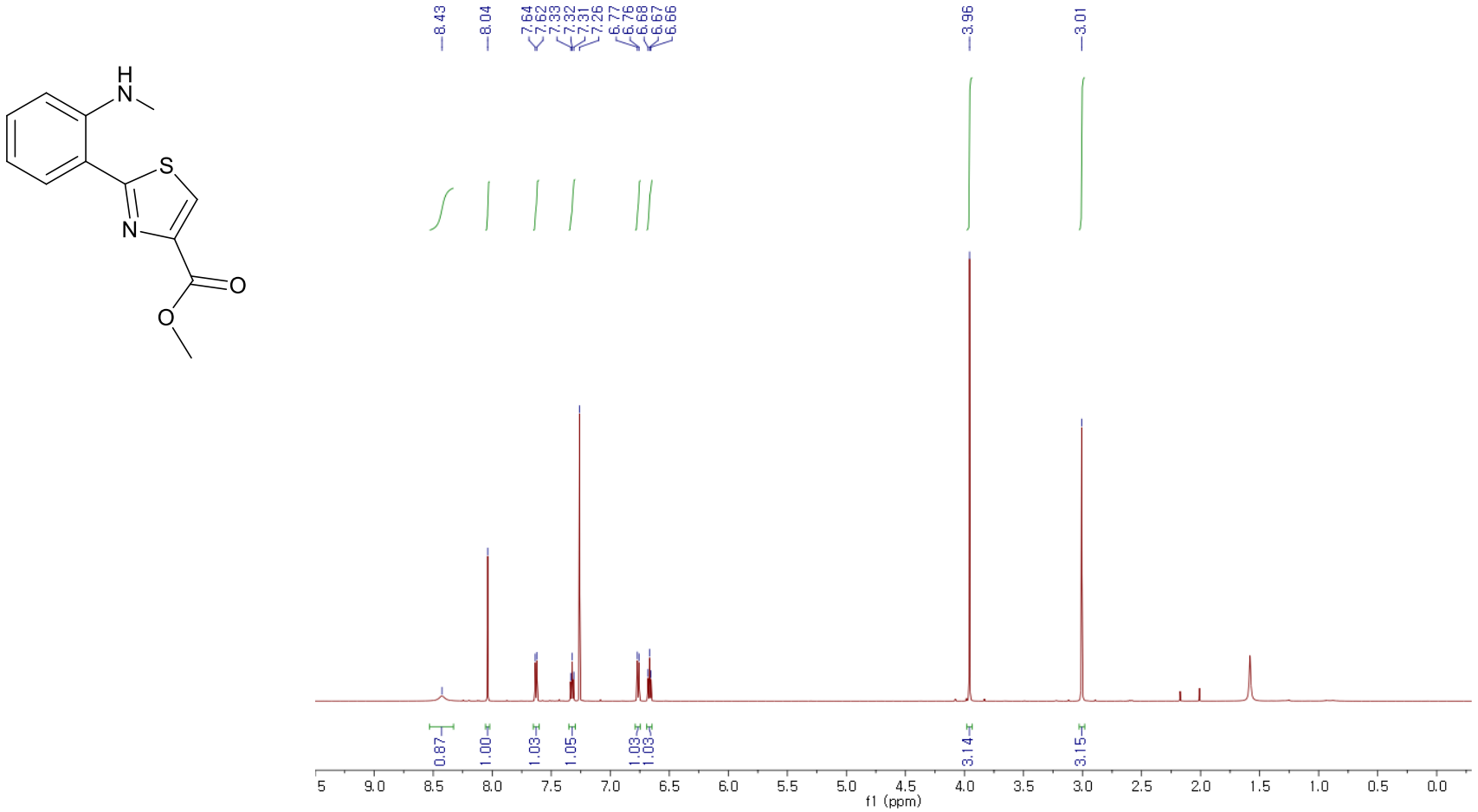

Figure B.2.2 ^{13}C NMR spectrum of Anithiactin A ($CDCl_3$, 600 MHz)

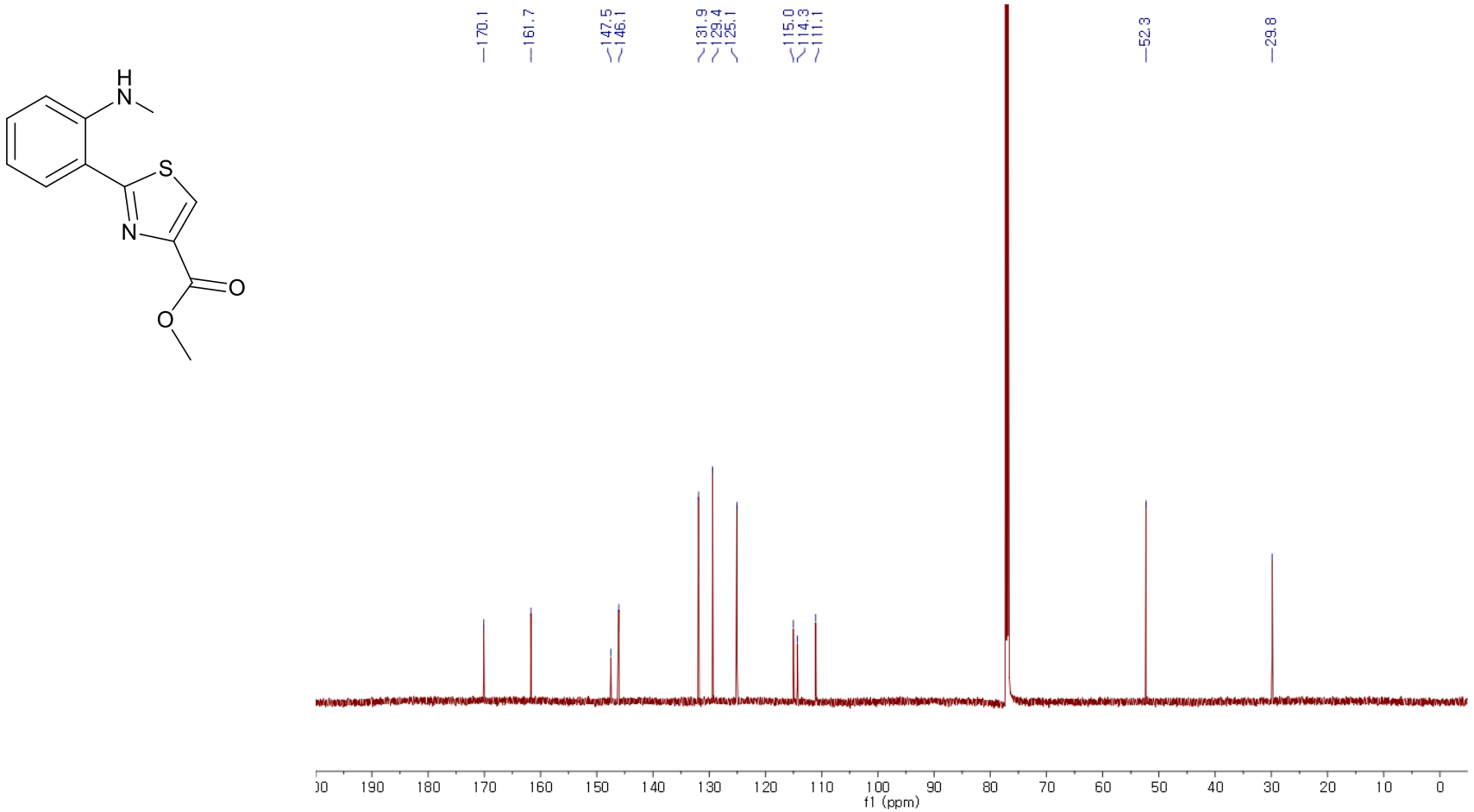

Figure B.2.3 COSY spectrum of Anithiactin A ($CDCl_3$, 600 MHz)

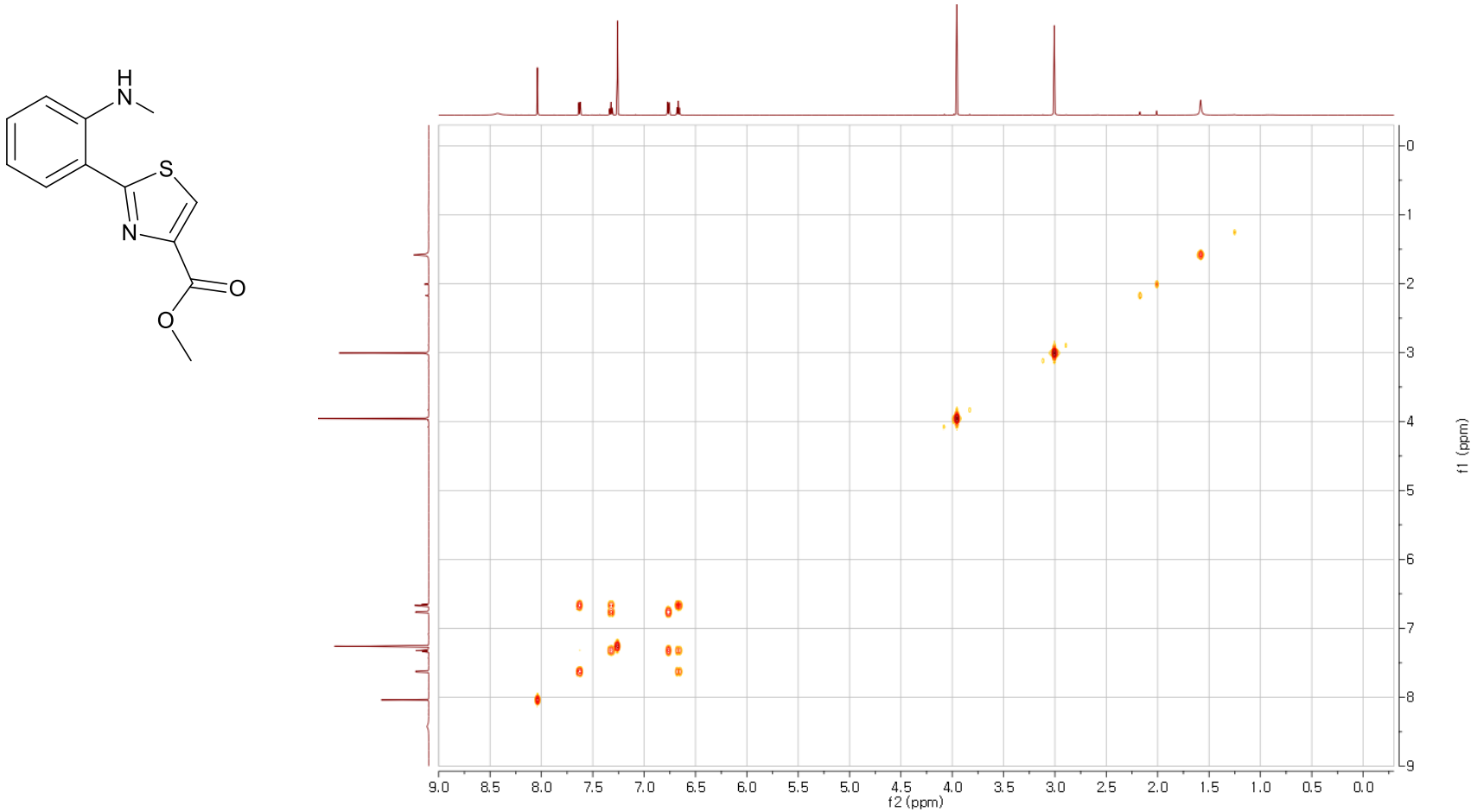

Figure B.2.4 HSQC NMR spectrum of Anithiactin A ($CDCl_3$, 600 MHz)

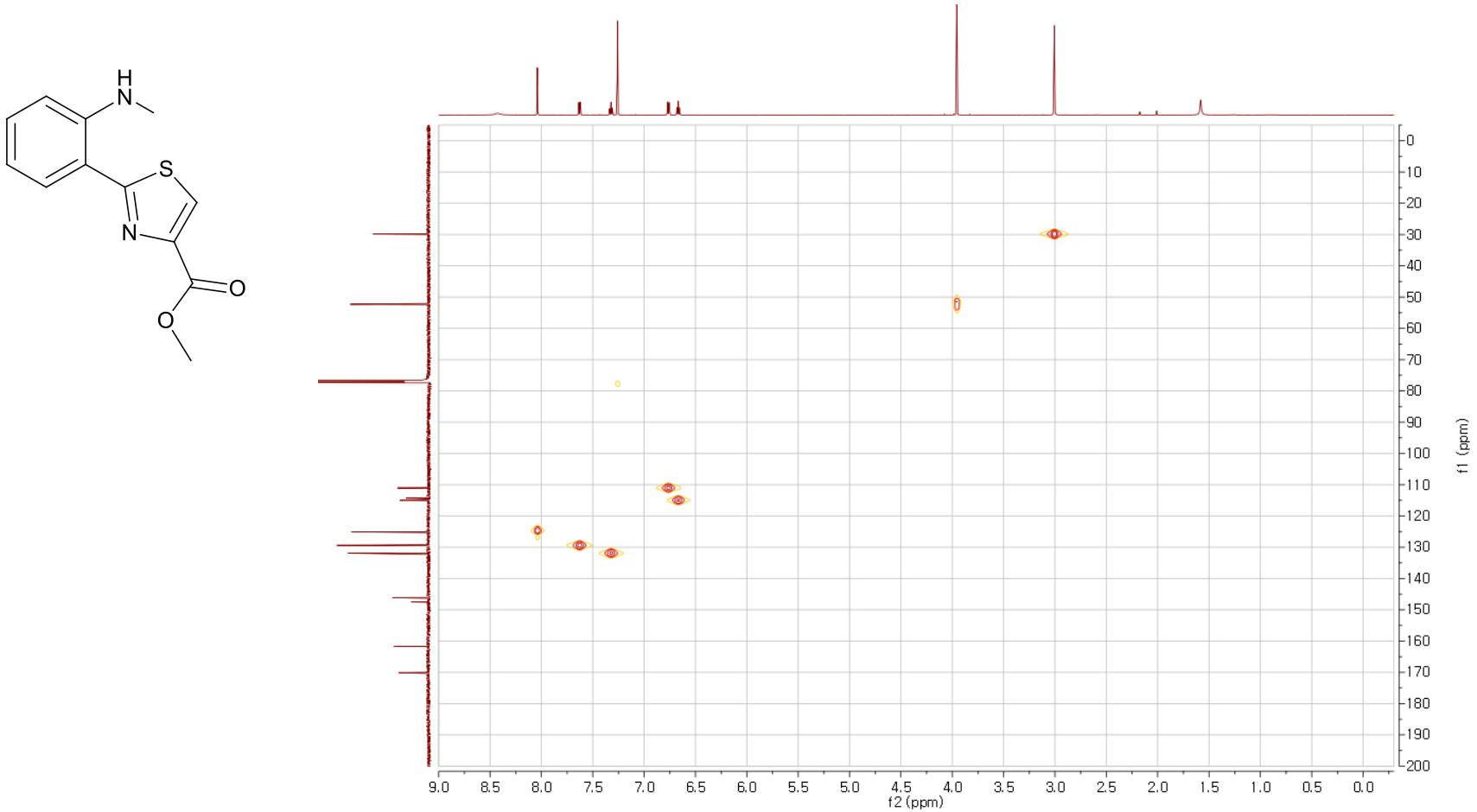

Figure B.2.5 HMBC NMR spectrum of Anithiactin A ($CDCl_3$, 600 MHz)

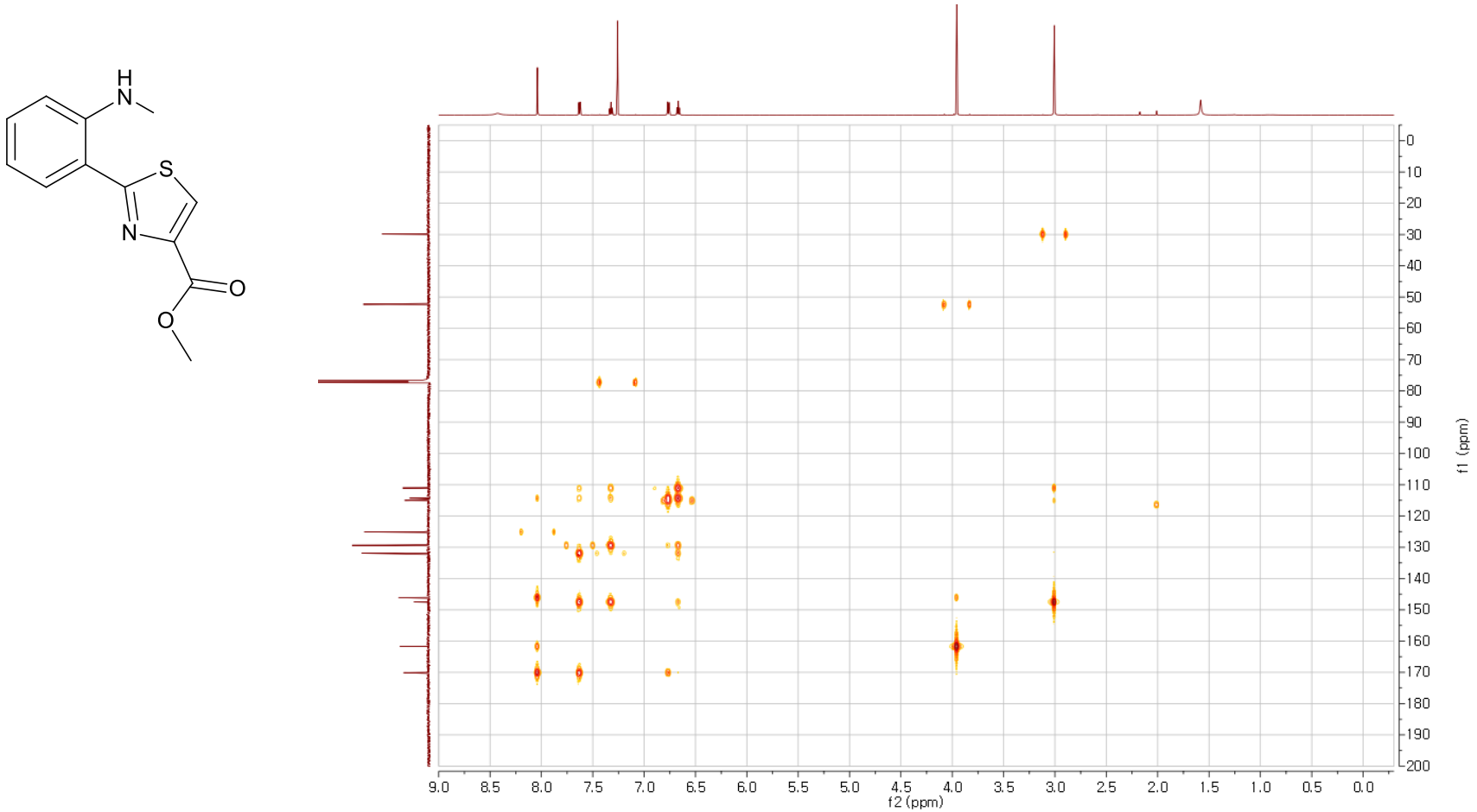

Figure B.2.6 ^{1}H NMR spectrum of Anithiactin B ($CDCl_3$, 600 MHz)

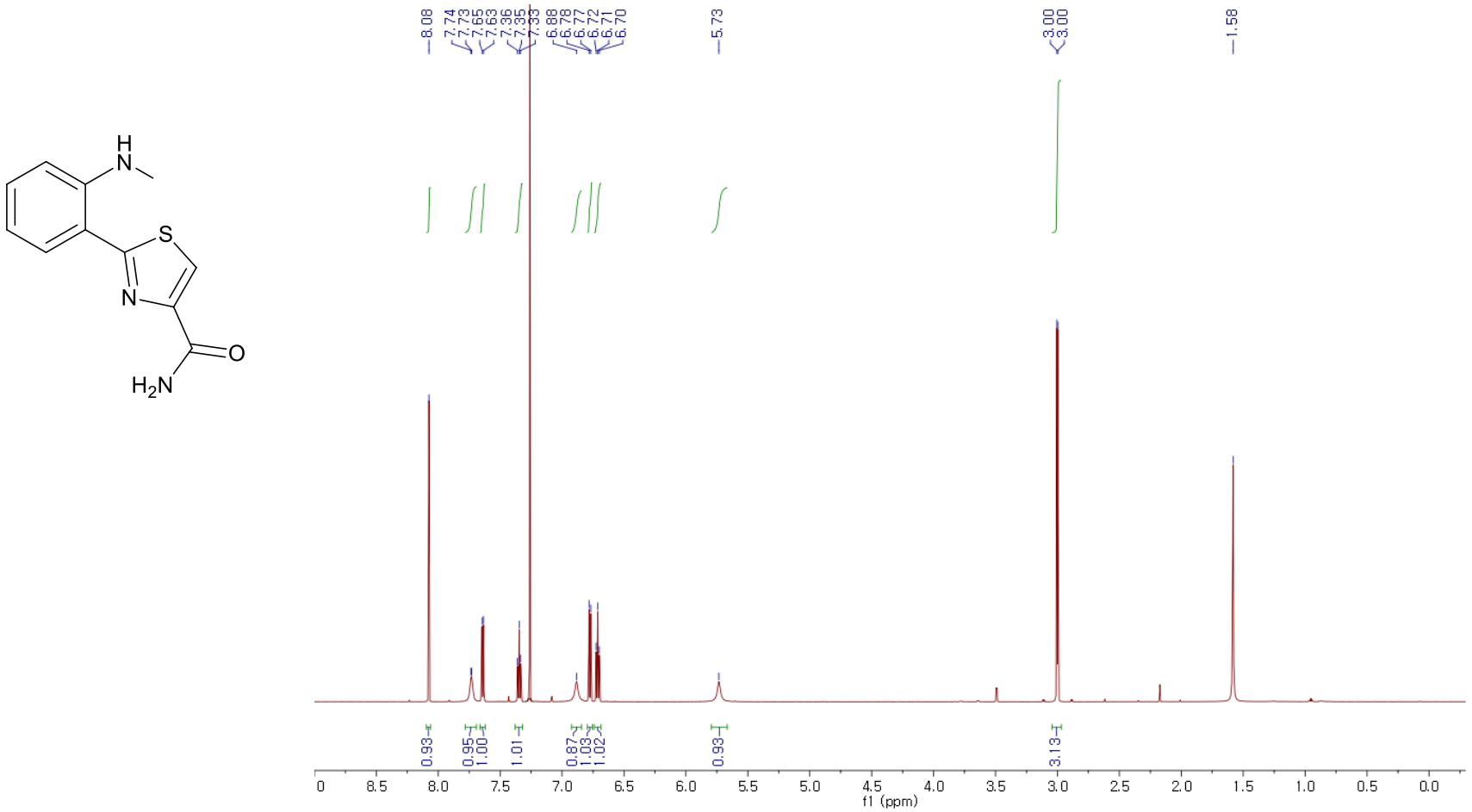

Figure B.2.7 ^{13}C NMR spectrum of Anithiactin B ($CDCl_3$, 600 MHz)

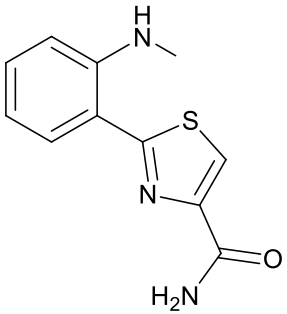

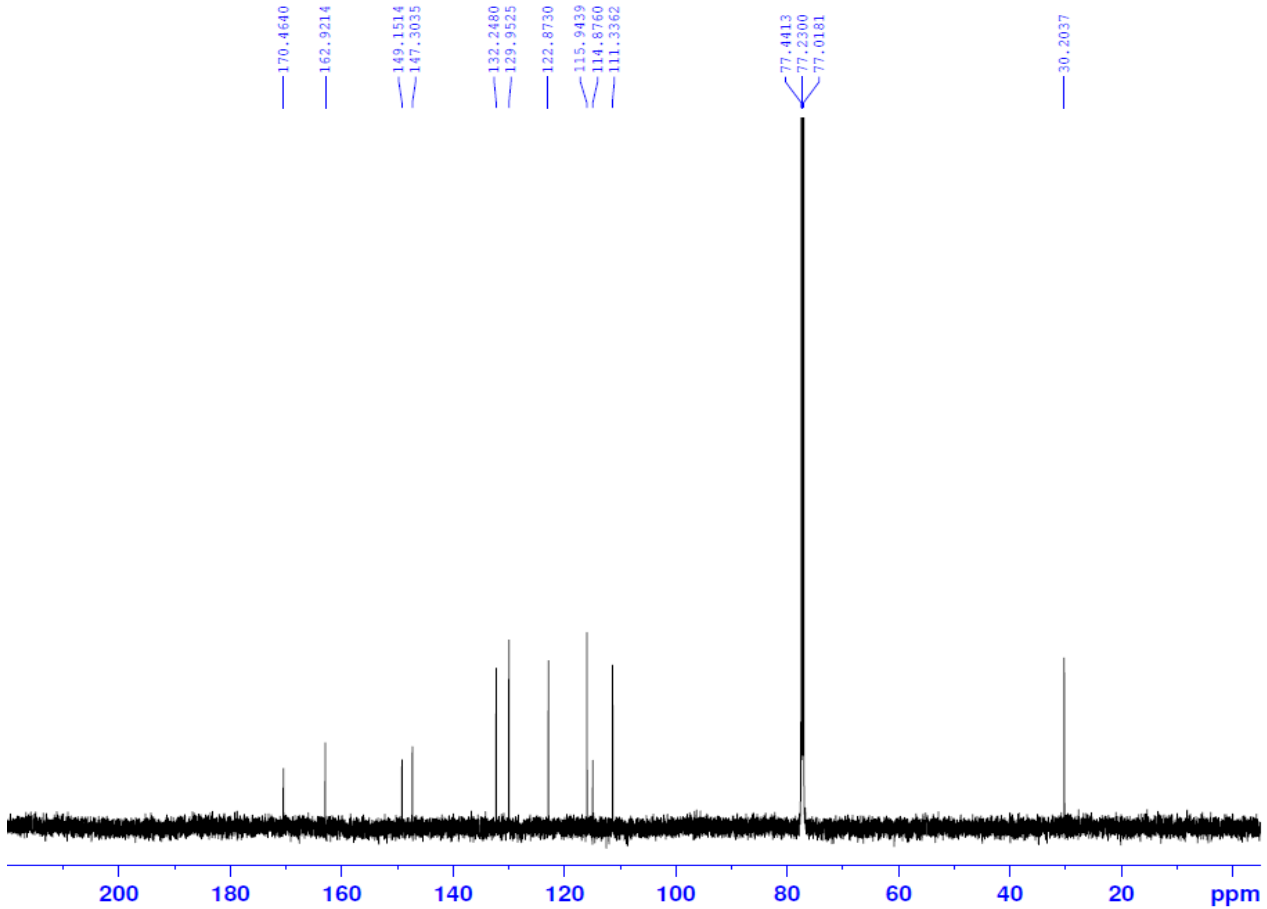

Figure B.2.8 ^{1}H NMR spectrum of Anithiactin C ($CDCl_3$, 600 MHz)

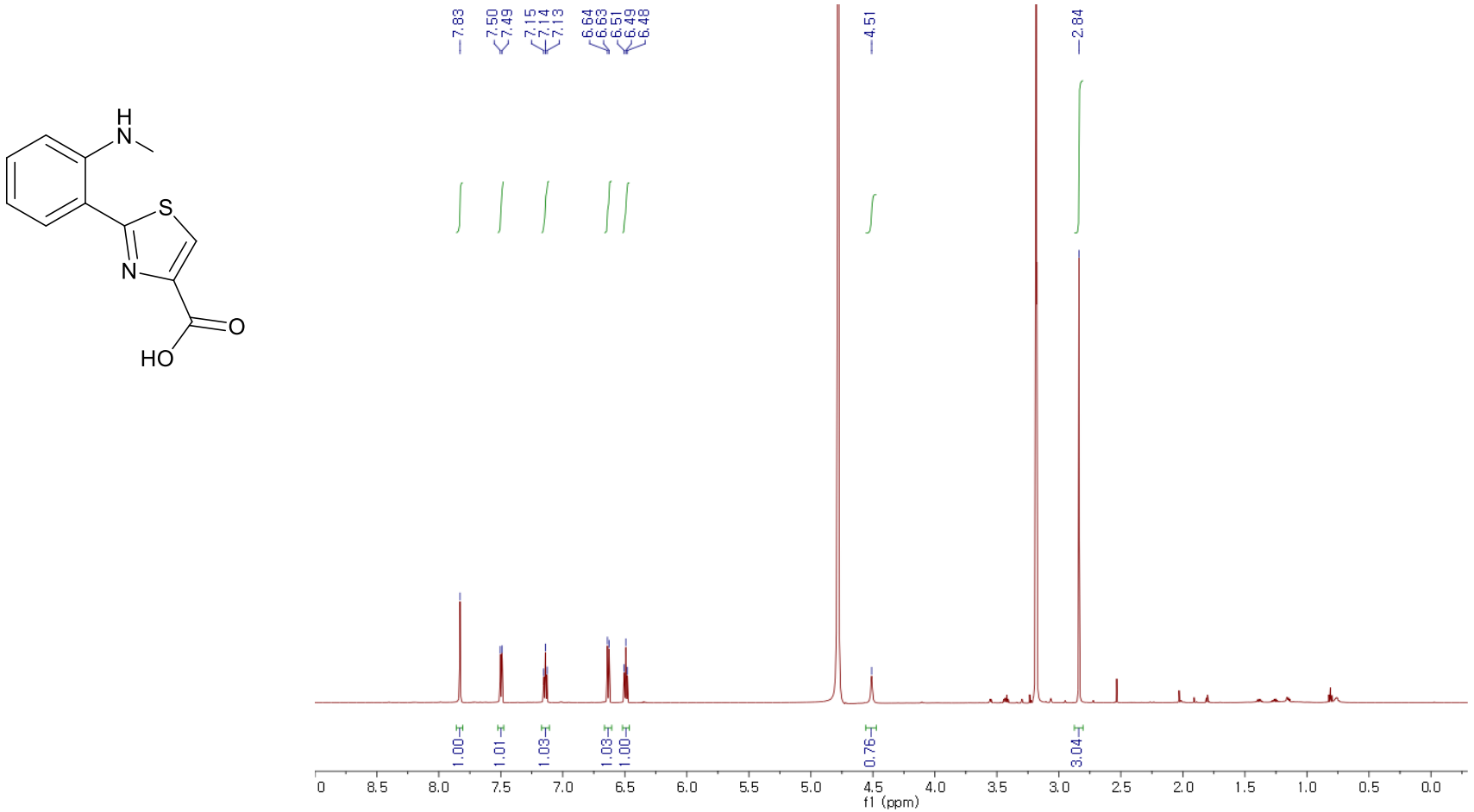

Figure B.2.9 ^{13}C NMR spectrum of Anithiactin C ($CDCl_3$, 600 MHz)

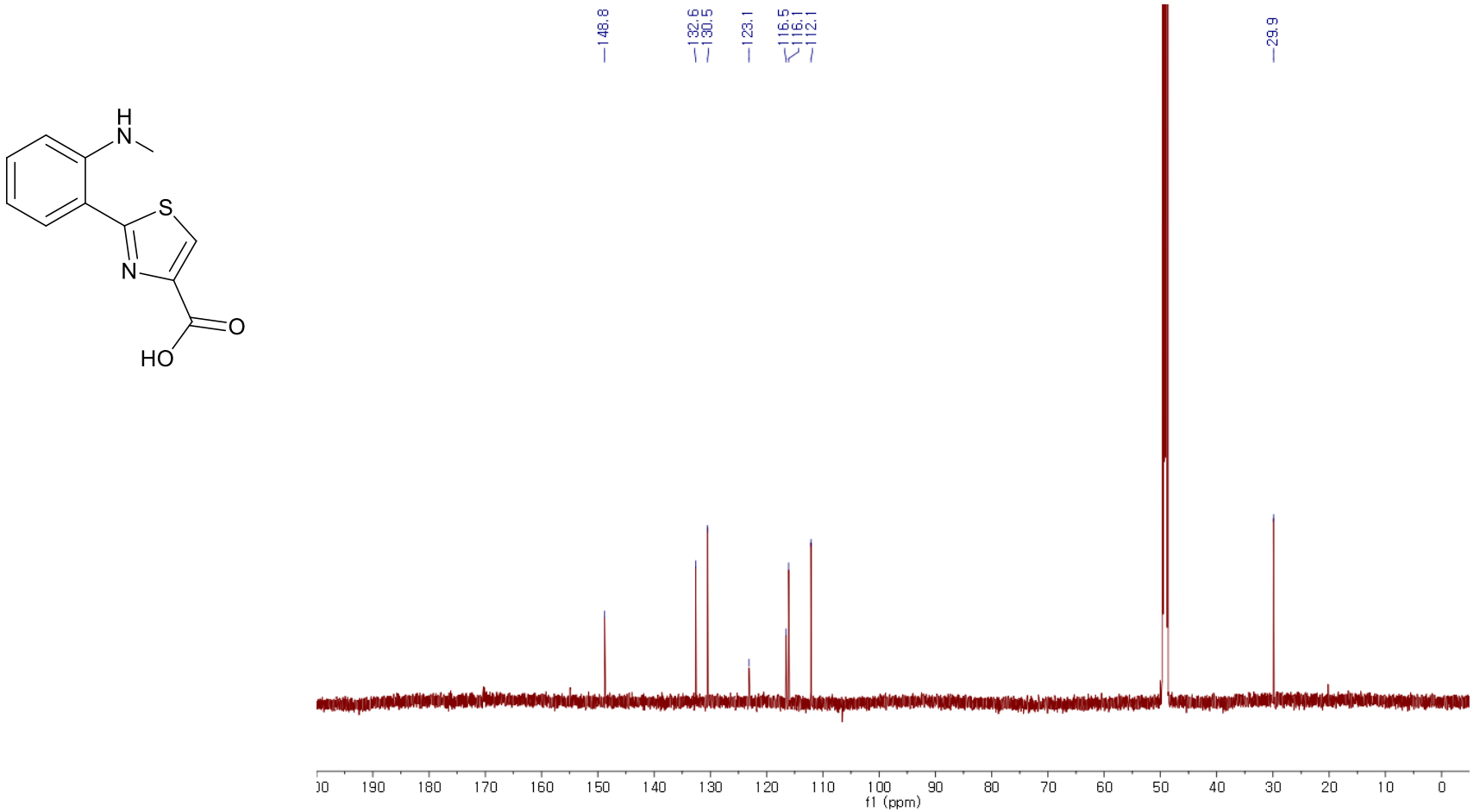

Figure B.2.10 ^{1}H NMR Spectrum of Anithiactin D (CD_3OD, 700 MHz)

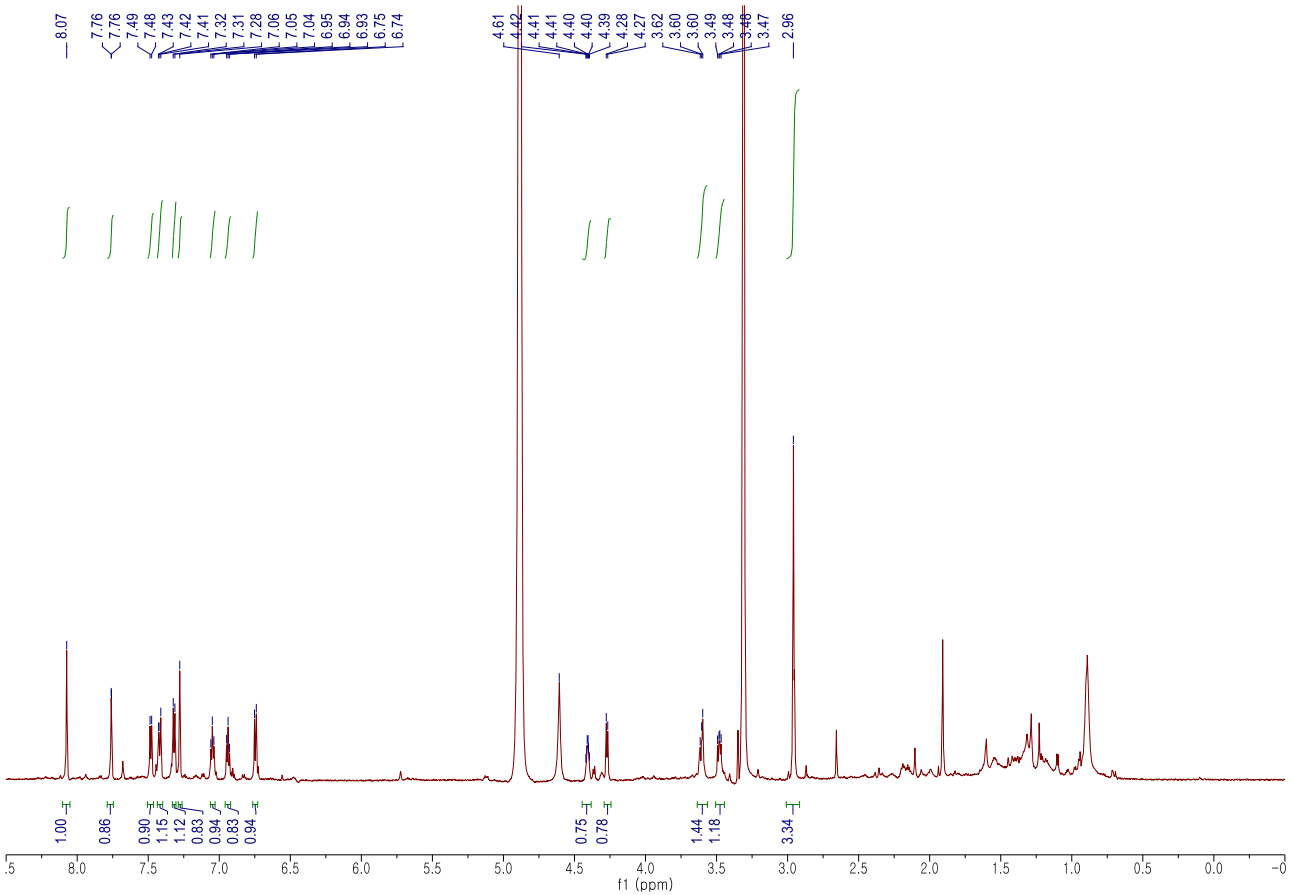

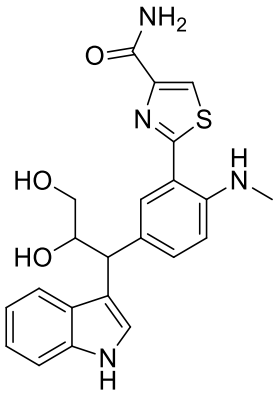

Figure B.2.11 COSY NMR Spectrum of Anithiactin D (CD_3OD, 700 MHz)

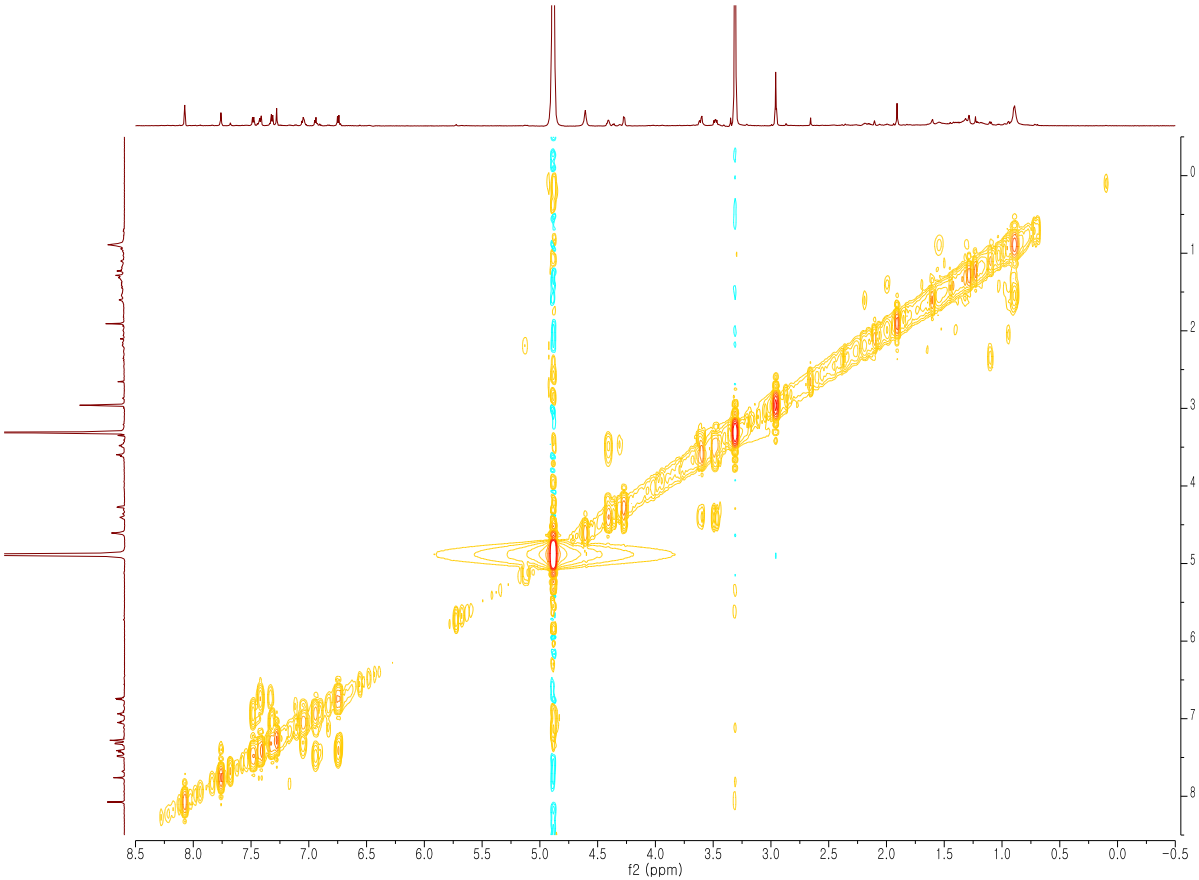

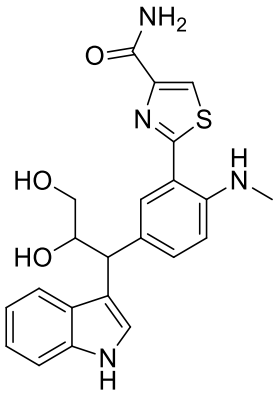

Figure B.2.12 HSQC NMR Spectrum of Anithiactin D (CD_3OD, 700 MHz)

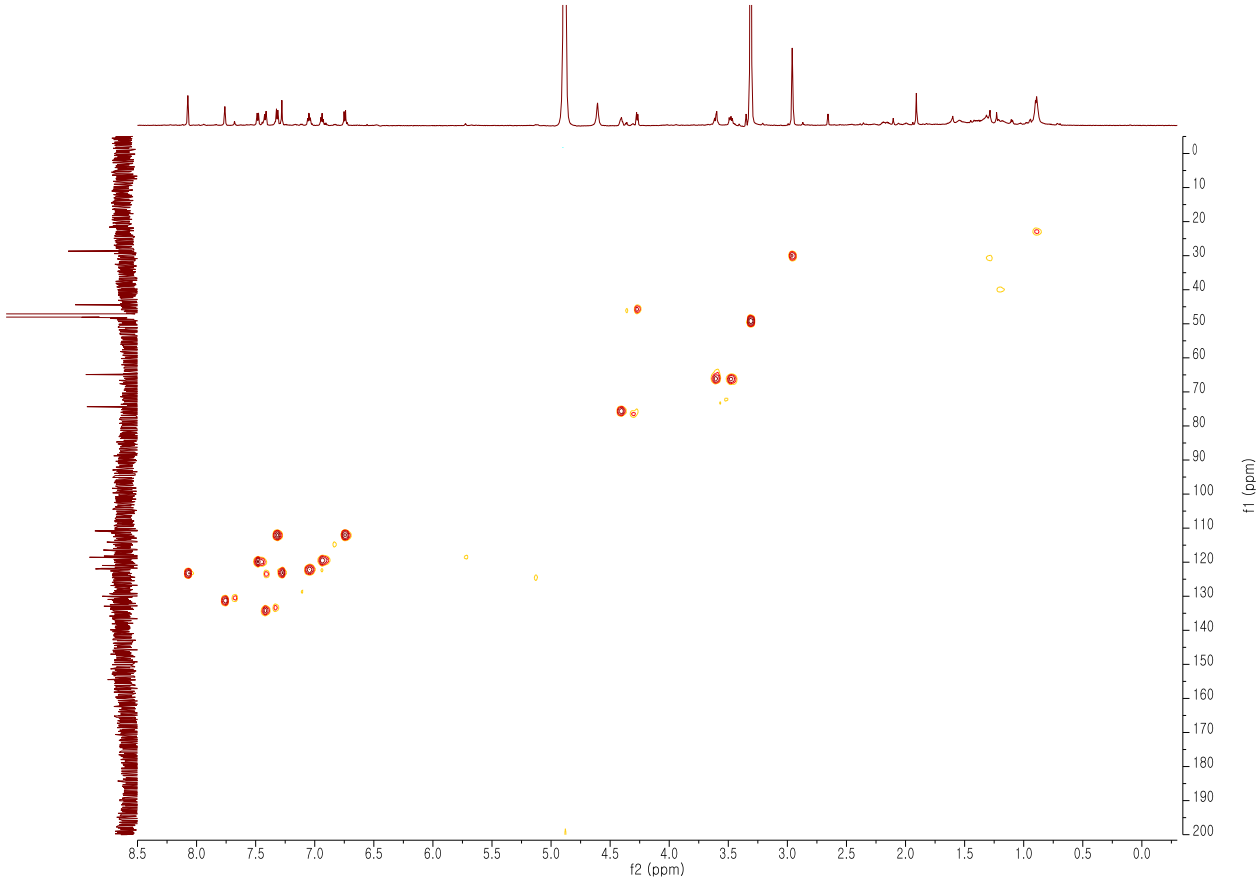

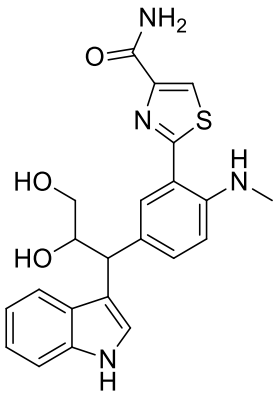

Figure B.2.13 HMBC NMR Spectrum of Anithiactin D (CD_3OD, 700 MHz)

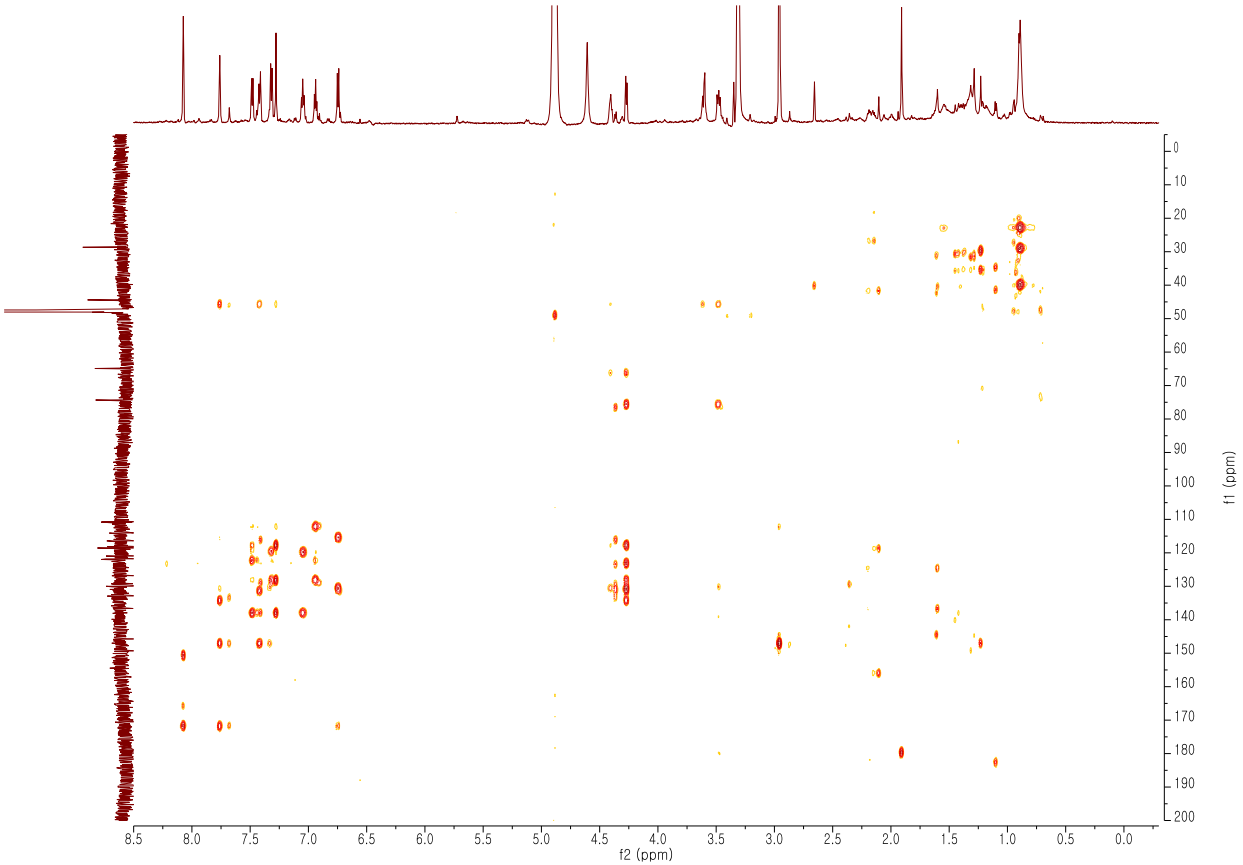

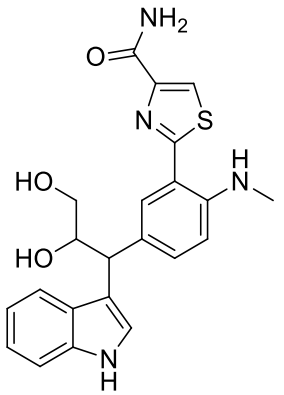

Figure B.2.14 ^{1}H NMR spectrum of synthetic intermediate 6 ($CDCl_3$, 600 MHz)

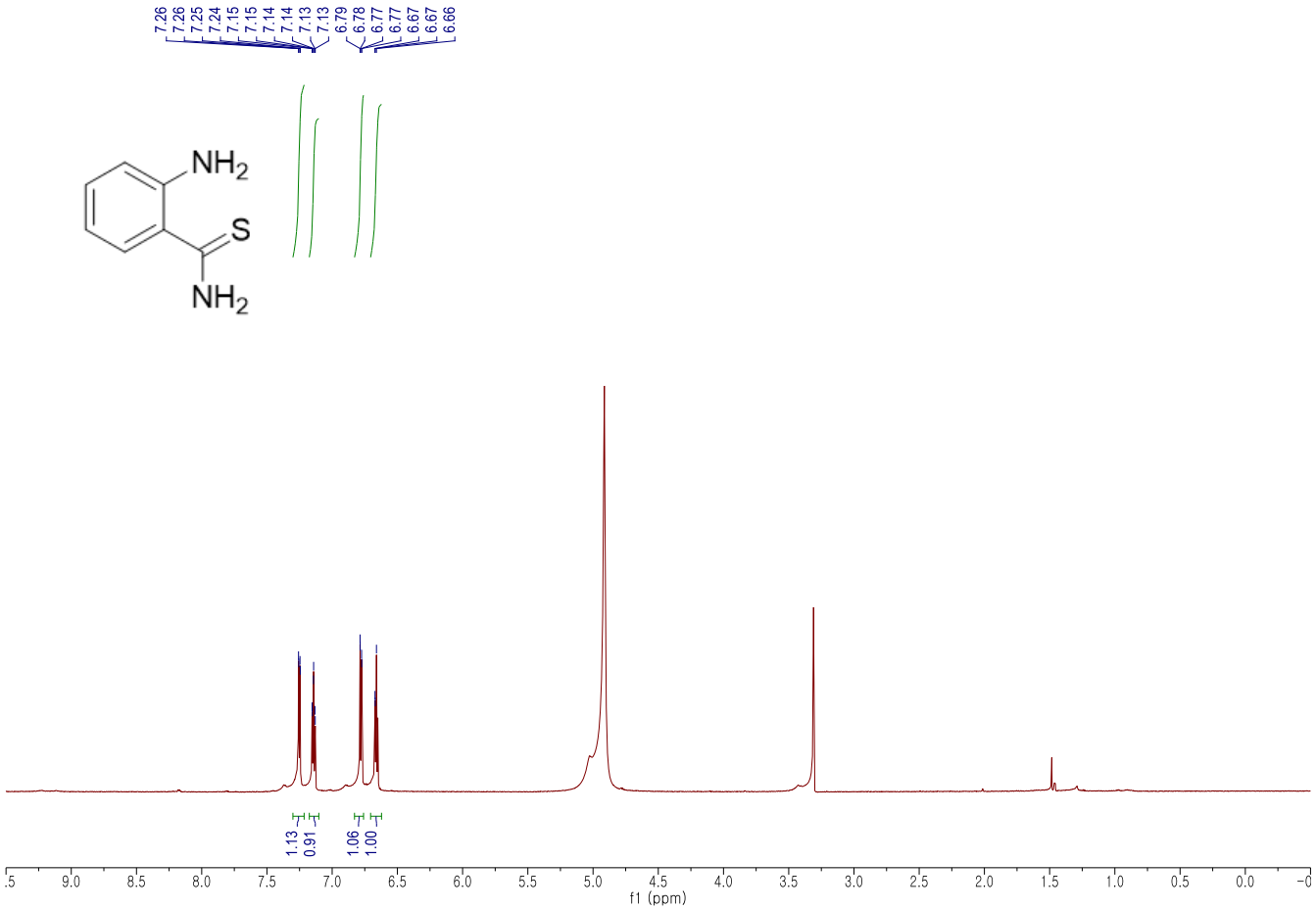

Figure B.2.15 ^{13}C NMR spectrum of synthetic intermediate 6 ($CDCl_3$, 600 MHz)

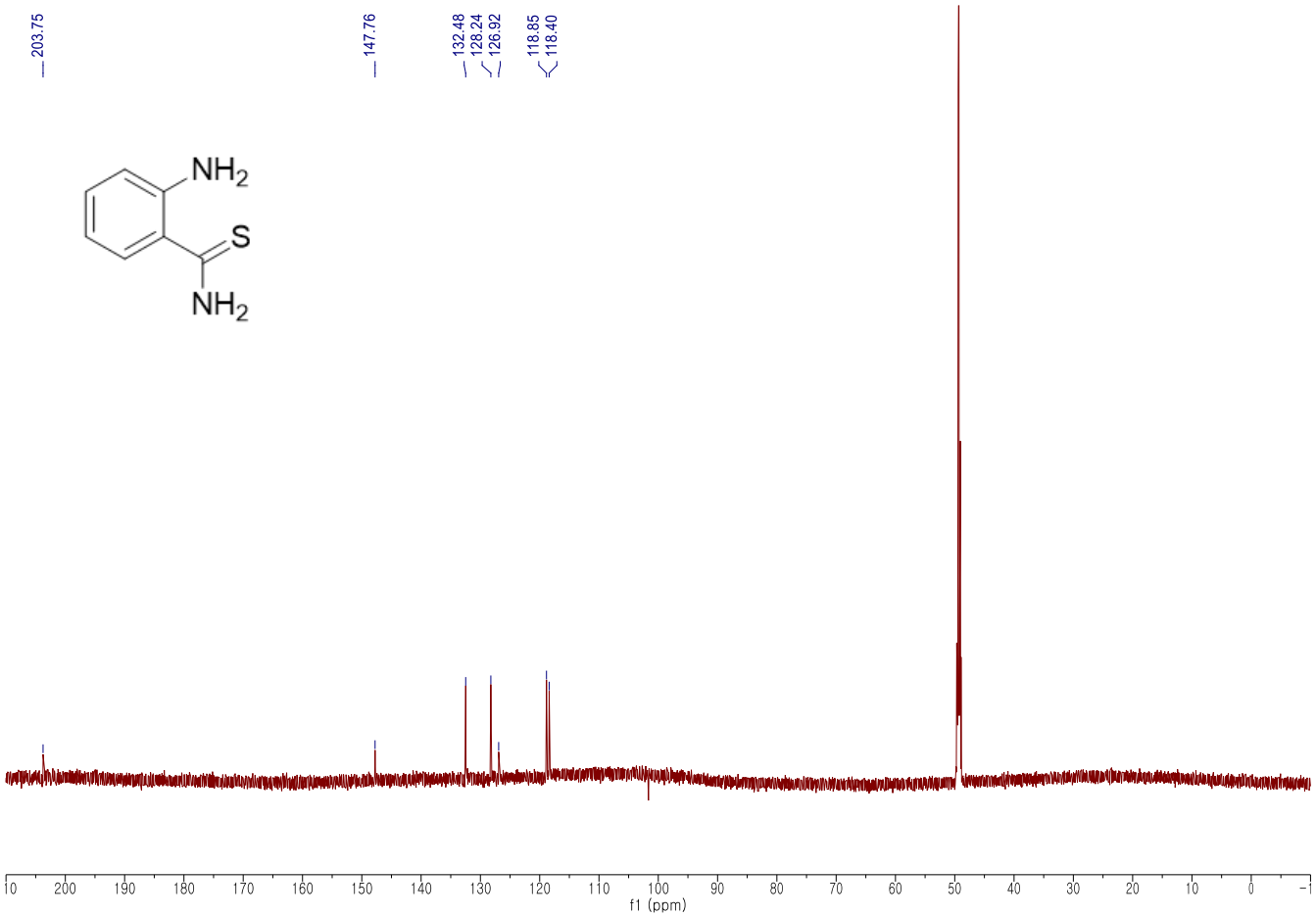

Figure B.2.16 ^{1}H NMR spectrum of synthetic intermediate 7 ($CDCl_3$, 600 MHz)

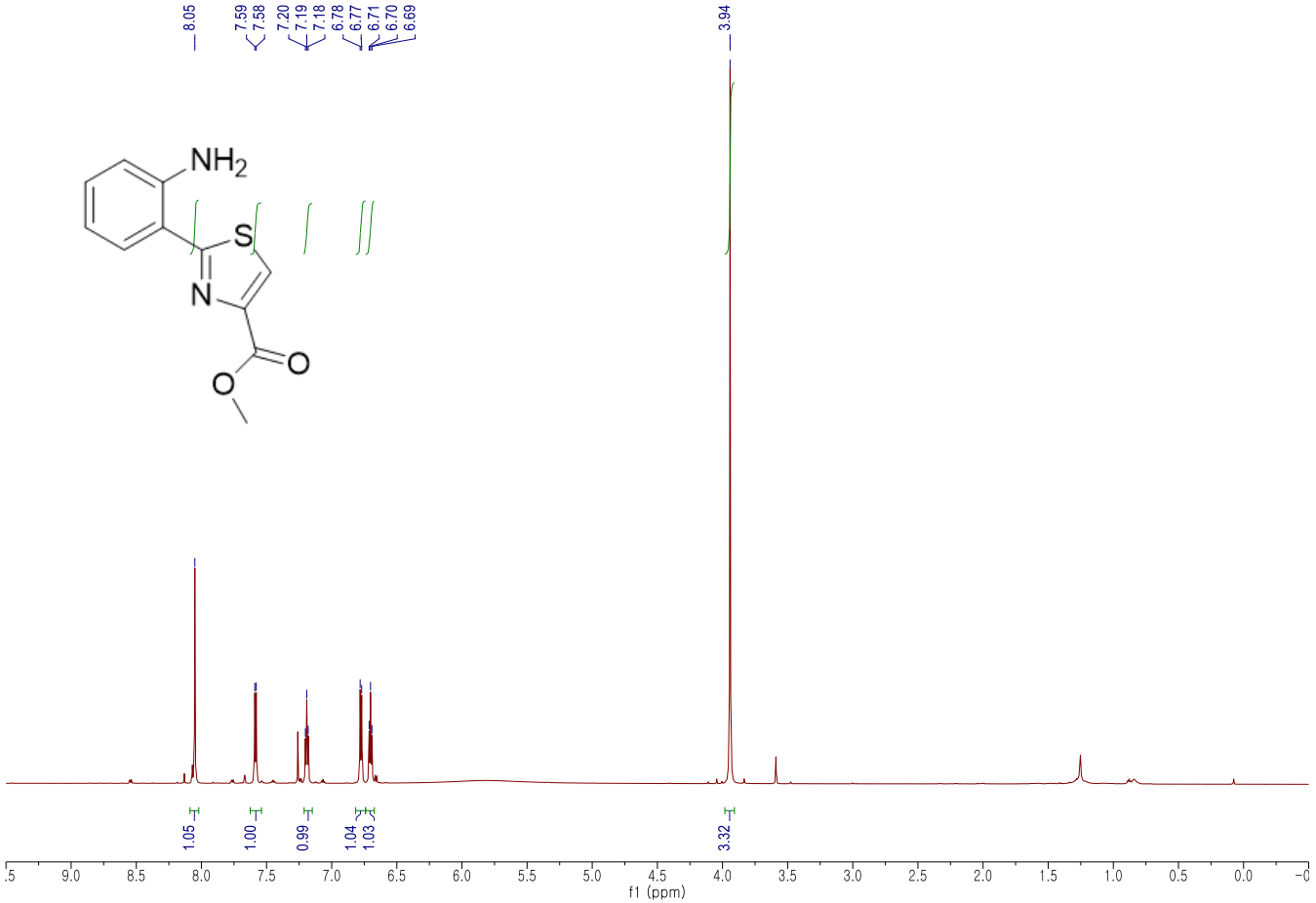

Figure B.2.17 ^{13}C NMR spectrum of synthetic intermediate 7 ($CDCl_3$, 600 MHz)

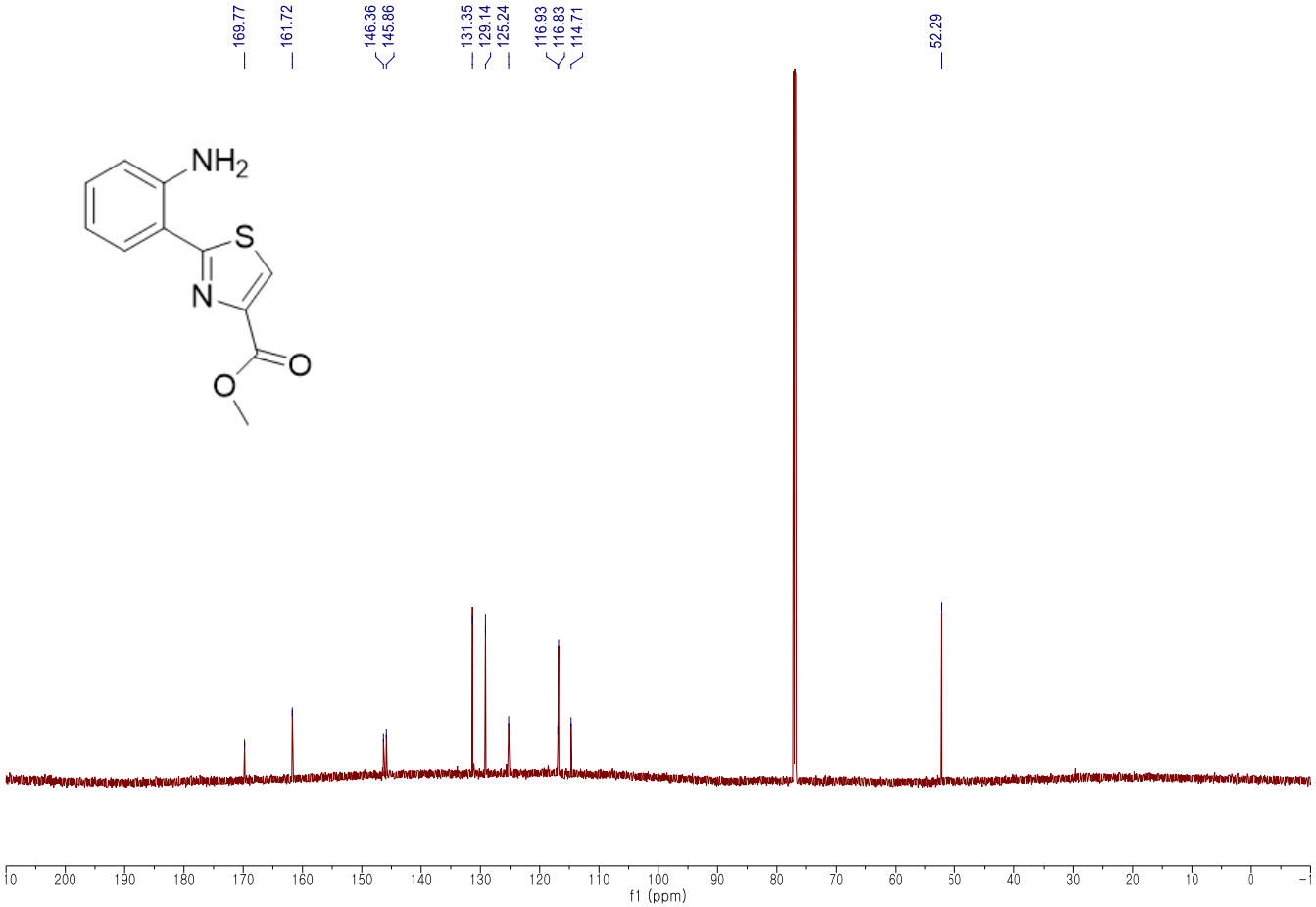

Figure B.2.18 ^{1}H NMR spectrum of synthetic Anithiactin A ($CDCl_3$, 600 MHz)

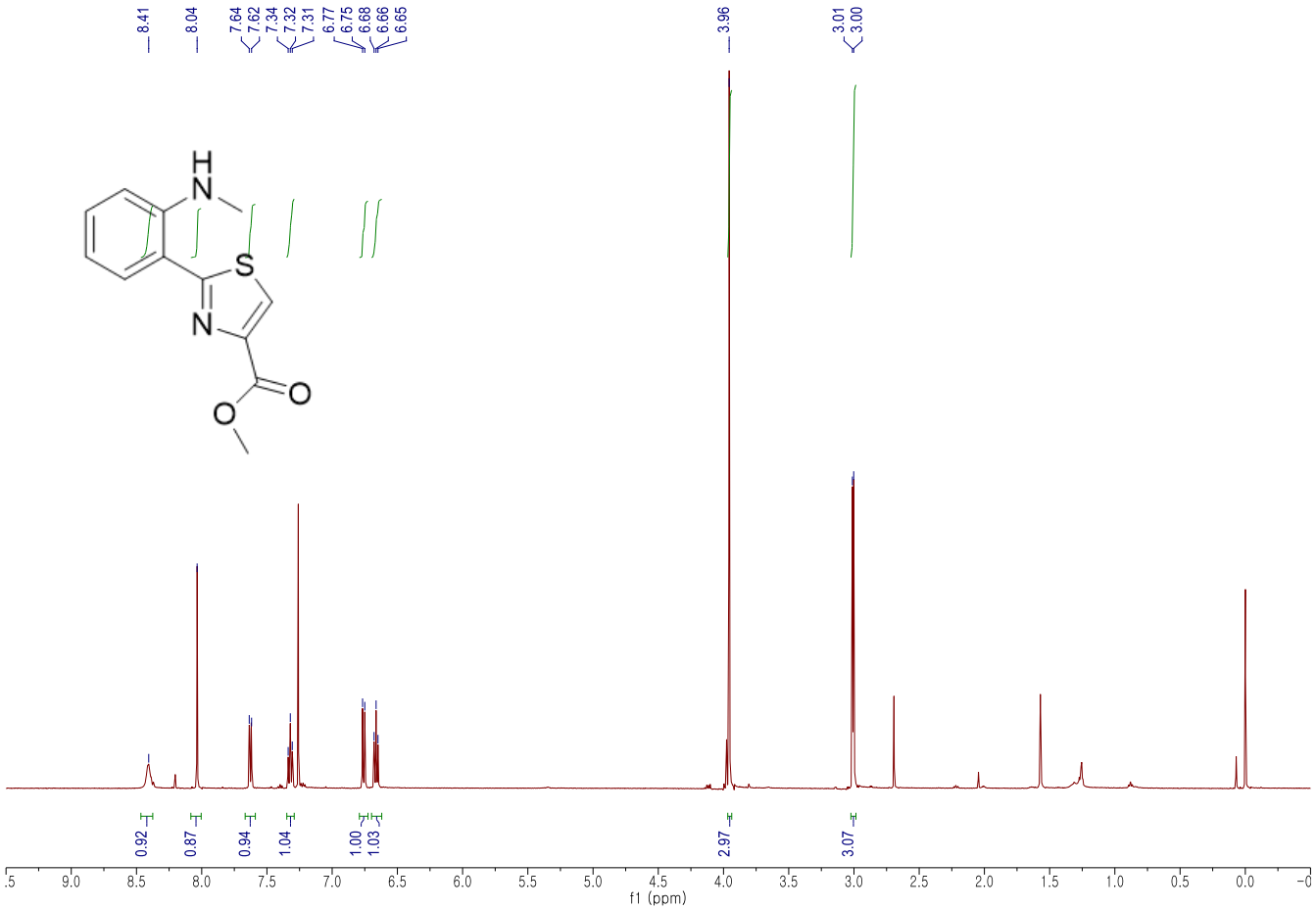

Figure B.2.19 ^{13}C NMR spectrum of synthetic Anithiactin A ($CDCl_3$, 600 MHz)

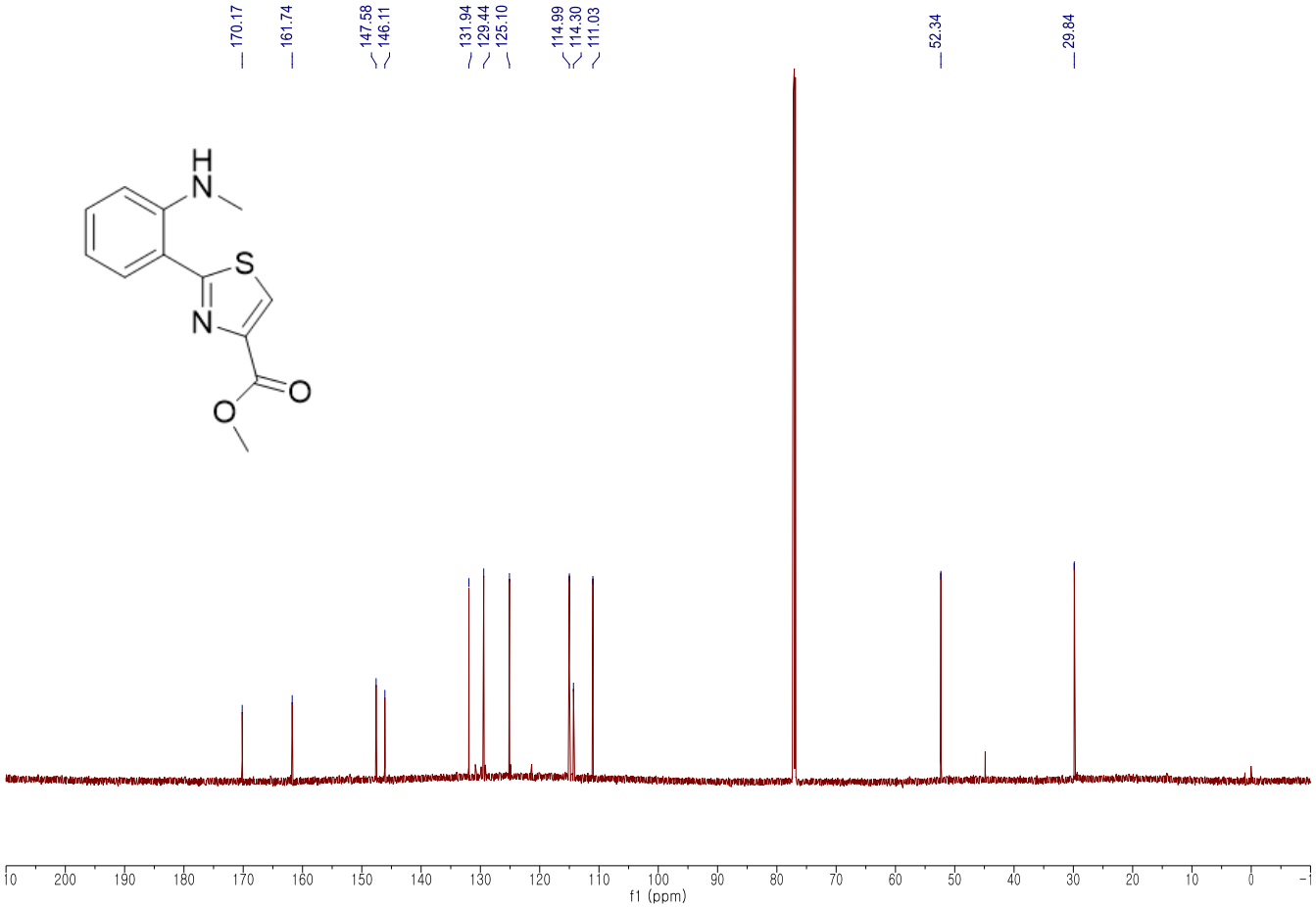

한글초록

해양천연물은 원천생물의 다양성에 기반한 신약후보물질의 새로운 공급원으로 각광받고 있다. 스쿠버다이빙이나 유인잠수정과 같은 기술의 발전에 힘입어 관심이 더해지고 있으며, 현재 8 종의 해양신약이 개발되었다. 대부분의 해양신약은 해양무척추동물로부터 분리된 해양천연물에 기반하여 개발되었으나, 최근에 들어 실제적인 생산자가 해양미생물인 것이 알려지게 되었다. 이 연구에서는 다양한 해양환경에서 분리된 방선균에서 신규한 생리활성 해양천연물을 분리하였다.

미국 캘리포니아 연안의 퇴적물에서 분리한 *Nocardiopsis* sp. CNQ115 에서 2 개의 새로운 이미다졸 천연물인 nocarimidazole A 와 B 를 분리하였다. Nocarimidazole A 와 B 의 화학구조를 NMR 을 이용하여 결정하였다. 항균활성과 항암활성을 확인하였으나, 주목할만하지 않다. 서해의 갯벌에서 *Streptomyces* sp. 10A085 를 분리하여 화학 조성물을 분석하였다. 새로운 티아졸 천연물 anithiactin A - D 를 분리하여 NMR 을 이용하여 화학구조를 결정하였다. Anithiactin B 는 X-ray 결정구조분석을 같이 수행하였다. Anithiactin A - C 는 acetylcholinesterase 를 저해하는 활성을 보였으며, 세포독성은 관찰되지 않았다.

Ph.D. Dissertation in Natural Sciences

Novel Secondary Metabolites from Marine Sediment-Derived Actinomycetes

해양퇴적물 유래 방선균에서 분리한 신규 이차대사산물

Inho Yang

February 2015

Laboratory of Marine Drugs
School of Earth and Environmental Sciences
Seoul National University

Novel Secondary Metabolites from Marine Sediment-Derived Actinomycetes
해양퇴적물 유래 방선균에서 분리한 신규 이차대사산물

지도교수 강 헌 중

이 논문을 이학박사 학위논문으로 제출함
2014 년 12 월

서울대학교 대학원
지구환경과학부
양 인 호

양인호의 이학박사 학위논문을 인준함
2014 년 12 월

위 원 장 _____ (인)
부 위 원 장 _____ (인)
위 원 _____ (인)
위 원 _____ (인)
위 원 _____ (인)

Abstract

Marine natural products are emerging source as an attractive drug pipeline based on its enormous biological diversity of origin. Technical advances like scuba diving, manned submarine boosted the interest to the marine natural products three decades ago and there are eight approved marine drugs now. Most of the approved drugs are based on marine natural products isolated from marine invertebrates, but recent study suggest that most of them are produced by microorganisms. In this study, actinomycetes were isolated from marine envirionments and investigated to discover a novel and bioactive marine natural products.

A chemical investigation of the actinomycetes, *Nocardiopsis* sp. CNQ115 isolated from marine sediment collected off the coast of southern California resulted in the isolation of two novel imidazole natural compounds nocarimidazoles A and B. The chemical structures of nocarimidazoles A and B were determined by interpretation of NMR data analyses. No significant antibacterial or cytotoxic activities were observed. Investigation of the chemical components of a *Streptomyces* sp. 10A085 isolated from mudflat sediments collected on the southern coast of the Korean peninsula led to isolation of four new compounds, anithiactins A – D. The chemical structures of anithiactins were determined by interpretation of NMR data analyses, while the chemical structure of anithiactin B was established from a combination of NMR spectroscopic and crystallographic data analysis. Anithiactins A – C displayed moderate acetylcholinesterase inhibitory activity with no significant cytotoxicity.

Key words

Marine natural products, Marine microorganisms, Marine actinomycetes, 2-phenylthiazole, 9,11-Secosterol

Student Number: 2010-30944

Table of Contents

List of Papers

This thesis is based on the following papers and unpublished data

Leutou, A.; **Yang, I.**; Kang, H.; Nam, S. Nocarimidazoles A and B from Marine–derived Actinomycetes *Nocardiopsis* sp. *manuscript in preparation.*

Kim, H.; **Yang, I.**; Patil, R.; Kang, S.; Lee, J.; Choi, H.; Kim, M.; Nam, S.; Kang, H. Anithiactins A-C, Modified 2-Phenylthiazoles from a Mudflat-Derived *Streptomyces* sp. *J. Nat. Prod*. **2014**. *77*, 2716-2719.

Yang, I.; Choi, H.; Won, D.; Nam, S.; Kang, H. An Antibacterial 9,11-Secosterol from a Marine Sponge *Irchinia* sp. *Bull. Korean Chem. Soc.* **2014**, *35*, 3360-3362.

List of other papers by the author not appended to this thesis

Wang, W.; Lee, T.; Patil, B.; Mun, B.; **Yang, I**.; Kim, H.; Hahn, D.; Won, D.; Lee, J.; Lee, Y.; Choi, C.; Nam, S.; Kang, H. Monanchosterols A and B, Bioactive Bicyclo[4,3,1]steroids from a Korean Sponge *Monanchora* sp. *J. Nat. Prod.* **2015**, *ASAP*

Mun, B.; Wang, W.; Kim, H.; Hahn, D.; **Yang**, **I.**; Won, D.; Kim, E.; Lee, J.; Han, C.; Kim, H.; Ekins, M.; Nam, S.; Choi, H.; Kang, H. Cytotoxic 5α,8α-epidioxy sterols from the marine sponge *Monanchora* sp. *Arch. Pharm. Res.* **2015**, *38*, 18-25.

Lee, Y.; Wang, W.; Kim, H.; Giri, A.; Won, D.; Hahn, D.; Baek, K.; Lee, J.; **Yang**, **I.**; Choi, H.; Nam, S.; Kang, H. Phorbaketals L–N, cytotoxic sesterterpenoids isolated from the marine sponge of the genus *Phorbas Bioorg. Med. Chem. Lett.* **2014**, *24*, 4095

Hahn, D.; Chin, J.; Kim, H.; **Yang**, **I.**; Won, D.; Ekins, M,; Choi, H.; Nam, S.; Kang, H. Sesquiterpenoids with PPARd agonistic effect from a Korean marine sponge *Ircinia* sp. *Tetrahedron. Lett.* **2014**, *55*, 4716

Lee, J.; H. Kim, H.; T. Lee, T.; **Yang**, **I.**; Won, D.; Choi, H.; Nam, S.; Kang, H. Anmindenols A and B, inducible nitric oxide synthase inhibitors from a marine-derived *Streptomyces* sp. *J. Nat. Prod*. **2014**, *77(6)*, 1528

Kim, H.; Chin, J.; Choi, H.; Baek, K.; Lee, T.; Park, S.; Wang, W.; Hahn, D.; **Yang**, **I.**; Lee, J.; Mun, B.; Ekins, M.; Nam, S.; Kang, H.
Phosphoiodyns A and B, Unique Phosphorus-Containing Iodinated Polyacetylenes from a Korean Sponge *Placospongia* sp. *Org. Lett.* **2013**, *15*, 100

Ham, J.; Hwang, H.; Kim, E.; Kim, J.; Cho, S.; Ko, J.; Lee, W.; Lee, J.; Holla, H,; Banerjee, J.; Kim, S.; **Yang**, **I.**; Lee, H.; Shin, K.; Choi, H.; Nam, S.; Tak, J.; Hahn, D.; Oh, T.; Won, D.; Lee, T.; Choi, J.; Park, M.; Seok, C.; Chin, J.; Kang, H. Discovery, design and synthesis of Y-shaped peroxisome proliferator-activated receptor d agonists as potent anti-obesity agents *in vivo Eur. J. Med. Chem.* **2012**, *53*, 190

List of Figures

List of Tables

List of Schemes

Chapter 1. Marine Natural Products as a New Pharmaceutical Pipeline

1.1 History of Natural Products as a Source for Drug Development

From old days, natural products have been used as a drug source. Before the modern age, natural products were used as a form of extract or plant materials. The oldest written record of medicinal plant was shown on the clay slab at Sumeria approximately 5,000 years ago which described 12 recipes for drug preparation from more than 250 different plants (Kelly, 2009). In China, medical usage of *Rhei rhisoma* (rhubarb), camphor, *Theae folium* (tea tree), ginseng, cinnamon bark, ephedra and many other medicinal plants were known since 2,500 BC, and these plant are still widely used over eastern and southern Asia (Bottcher, 1965; Wiart, 2006). After that, all through the history of mankind, continuous efforts to look for the healings were enormous and results were pass throughout the millennia (Petrovska, 2012).

After the advance of the science and technology in modern centuries, some of these medicinal plant become medicine after extraction, isolation and quantification. This technical improvement resulted in the development of many drugs such as khellin, metformin and verapamil. The khellin was isolated from plant *Ammi visnaga* Lamk and used as a bronchodilator. Efforts to reduce the side effects of khellin led to the development of chromolyn (used in the form of sodium chromoglycate). The galegine was isolated from the plant *Galega officinalis* L. as a major active ingredient of anti-hyperglycemia. The metformin was developed from galegine with

its main chemical structure maintained. The papaverine isolated from *Papaver somniferum* was advanced to verapamil to treat hypertension (Farbricant & Farnsworth, 2001). This medicinal plant is also well-known as a source of morphine and codeine (Buss & Waigh, 1995).

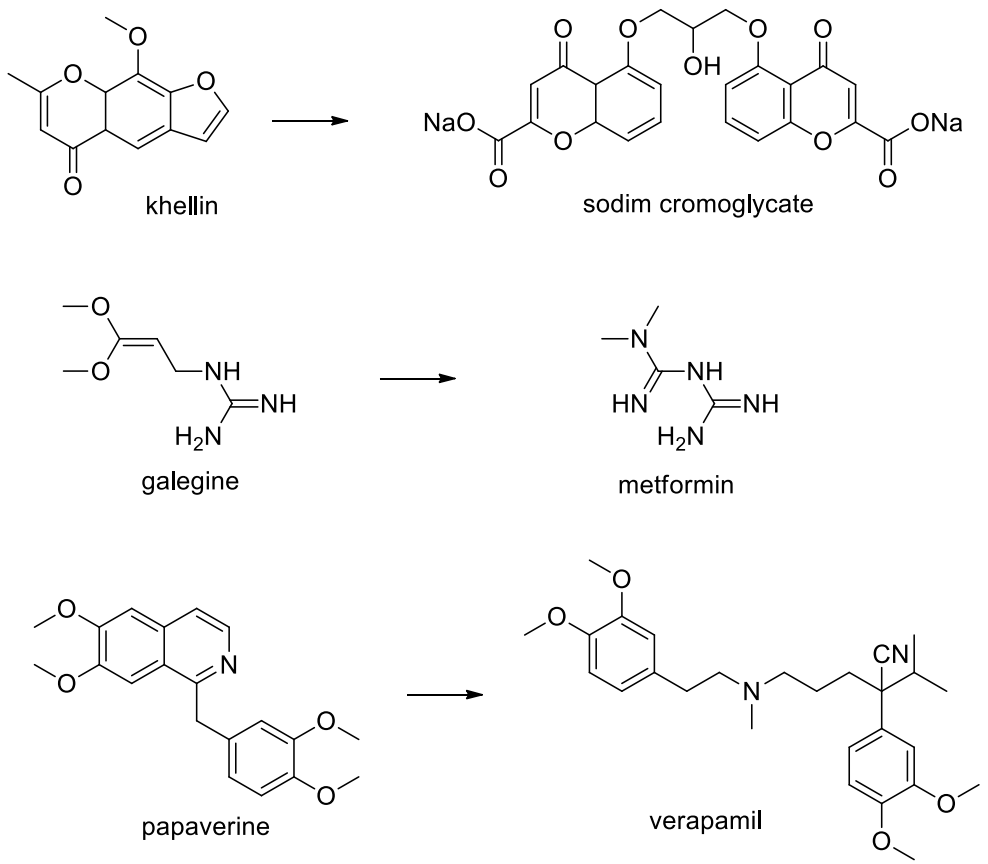

Figure 1.1 Drugs developed from medicinal plants

However, the most famous example of medicinal plant derived medicine would be the antimalarial drugs development. First generation antimalarial drugs, such as chloroquine and mefloquine, were developed from quinine which was isolated from the bark of *Cinchona* sp. This plant extracts was used to treat fevers around the Amazon region traditionally. Spread of quinine-class resistance malaria led to the

discovery of artemisinin isolated from the plant *Artemisia annua* and the development of artemisinin class antimalarial drugs. This plant has been used to treat fevers in China for a long time (Wongsrichanalai et al., 2002). Artemisinin class drugs are deployed to combat malaria all across the world, even though its mechanism of action not clear (O'Neill & Posner, 2004; O'Neill et al., 2010; Wang et al. 2010).

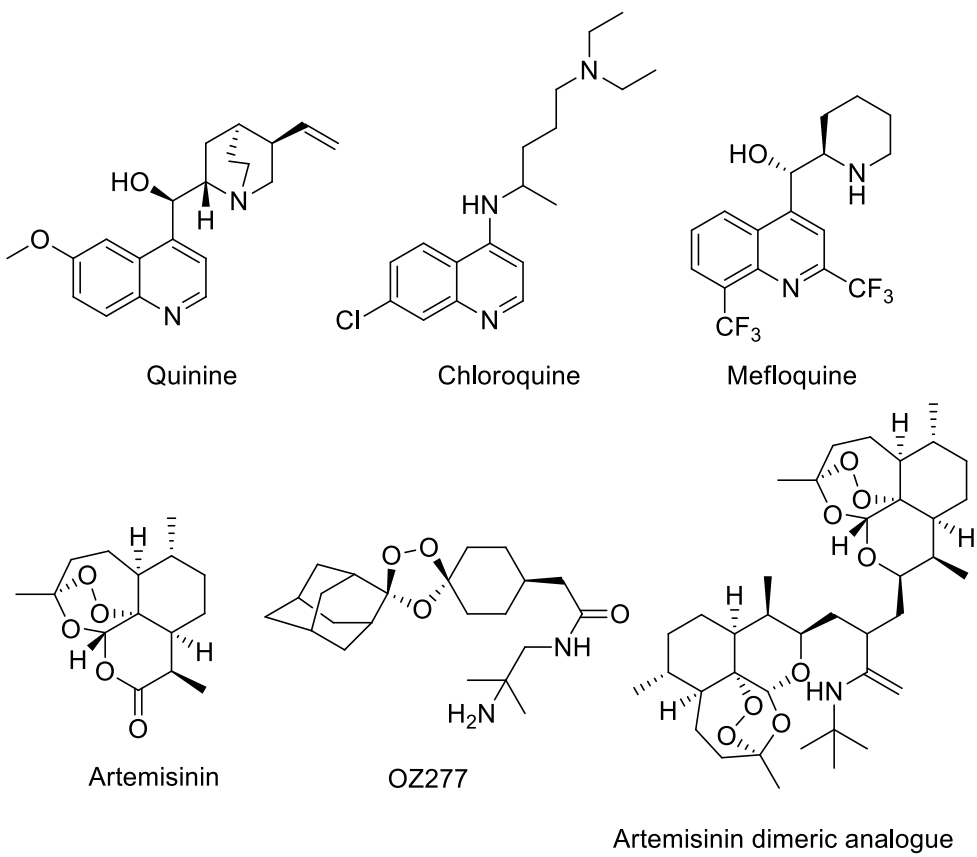

Figure 1.2 Antimararial drugs developed from medicinal plants

Likewise, using natural products as drug lead was deployed as useful tactics to combat other disease includes anticancer (Gueritte et al., 2005; Roussi et al., 2012) and antihypertensive (Cordell & Colyard, 2012). The analysis of the sources of small

molecule shows this trend clearly. Figure 1.3 is showing classified new drugs from 1981 to 2010 based on its origin as synthetic (*S*) or natural product (*N*). It revealed that two thirds of the small molecules are natural products or natural products inspired. Only one third can be categorized as truly synthetic (Newman & Cragg, 2012). Conclusively, natural products are major pipelines for developing drugs now and then (Cragg & Newman, 2013).

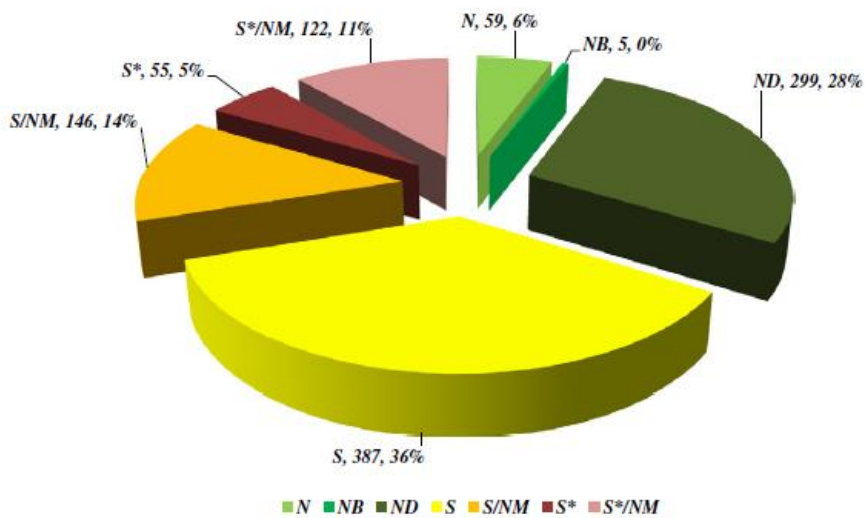

Figure 1.3 Sources of drugs [*N* (an unmodified natural product), *NB* (a natural product botanical), *ND* (a modified natural product), *S* (a synthetic compound with no natural product conception), S^*, S^*/NM (a synthetic compound with a natural product pharmacophore; */NM* indicating competitive inhibition), *S/NM* (a synthetic compound showing competitive inhibition of the natural product substrate)] (Cragg & Newman, 2013)

1.2 Marine Natural Products as a New Pharmaceutical Pipeline

1.2.1 Novelty of Marine Natural Products

Unlike its counter parts, marine resources were not used much as a medicinal sources for long time. Before scuba diving technique spread widely, collection of marine organisms under the water surface was very limited to specifically trained

professionals. Recent introduction of various technical advances like scuba, dredging, manned submarine and remotely operated vehicles gives more chance to address the marine resources. And this makes marine resources as a more attractive drug discovery pipeline. Currently, more than 30,000 marine natural products were reported and number is increasing (Blunt & Munro, 2008).

The most interesting character of the marine natural product is from biodiversity of marine organisms. For examples, there is only 1 terrestrial exclusive phylum among the 33 animal phyla. On the other hand, there are 15 of marine exclusive phyla and 5 of the rest phyla have more than 95% of their species in marine (Margulis & Schwarts, 1988). This enormous number of marine animal species and phyla may due to the oldness and wideness of the ocean environment then terrestrial one. As terrestrial organisms are descendants of marine life and 70% of the earth surface is covered with four thousand deep water.

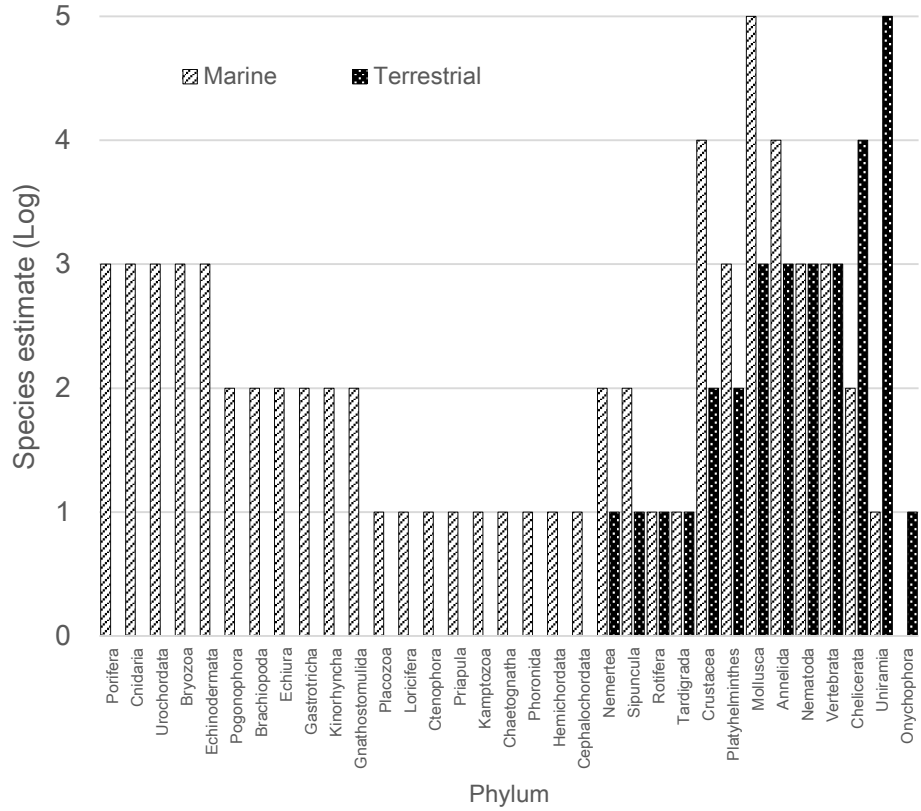

Figure 1.4 Number of estimated species of animal phyla in terrestrial and marine environment (Margulis & Schwarts, 1988, modified)

It is clear that more number of the species gives more chance to discover novel chemical structures. One of the Chinese chemistry group quantified the novelty of marine natural products (Kong et al., 2010). They categorized the known natural products from Dictionary of Natural Products and Dictionary of Marine Natural Products to the each of the specific 'scaffolds' which are defined as the contiguous ring systems with chains that link them. This scaffold analysis gave that there are 163,089 terrestrial natural products using 25,289 scaffolds and 31,772 marine natural products using 5276 scaffolds. And more than 70% of marine scaffolds are using less than two entities, 50% of the scaffolds are having only one compound.

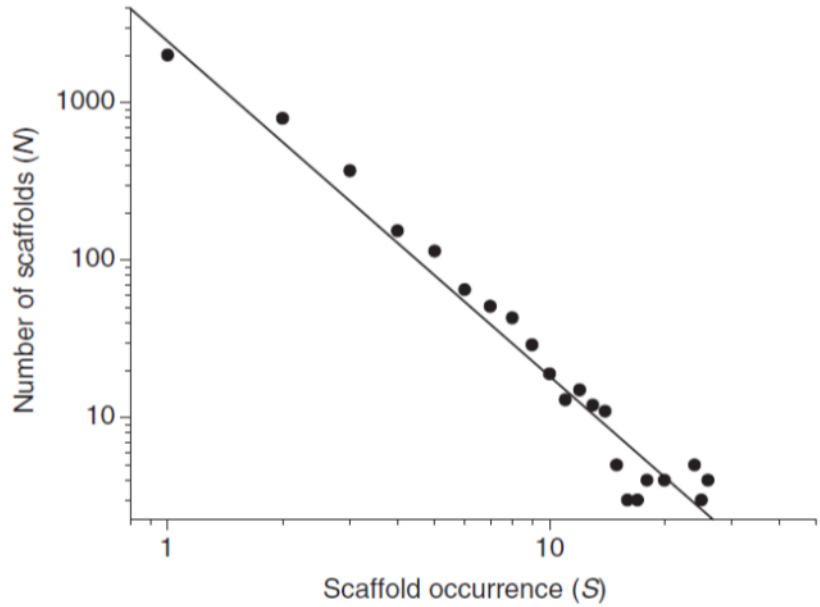

Figure 1.5 Number of scaffolds accord with number of marine natural products (Kong et al., 2010)

1.2.2 Marine Drugs on the Market

There are eight Food and Drug Administration (FDA) and European Medicines Agency (EMEA) approved drugs (Meyer, 2014). The four of marketed drugs are used to treat cancer (Adcetris, Cytoser-U, Halaven, Yondelis), two for virus (Carragelose, Vira-A) and each of one for hypertriglyceridemia and neuropathic pain (Lovaza and Prialt). Three of these are employed to drug as natural product itself (Prialt, Yondelis, Carragelos) and others took modifications to solve the supply and ADMET properties problems. Regarding origin of the drugs, six of marine drugs were obtained from marine invertebrates like tunicate, sea hare, marine snail and sponge (Martins et al., 2014). (Figure 1.6, Table 1.1)

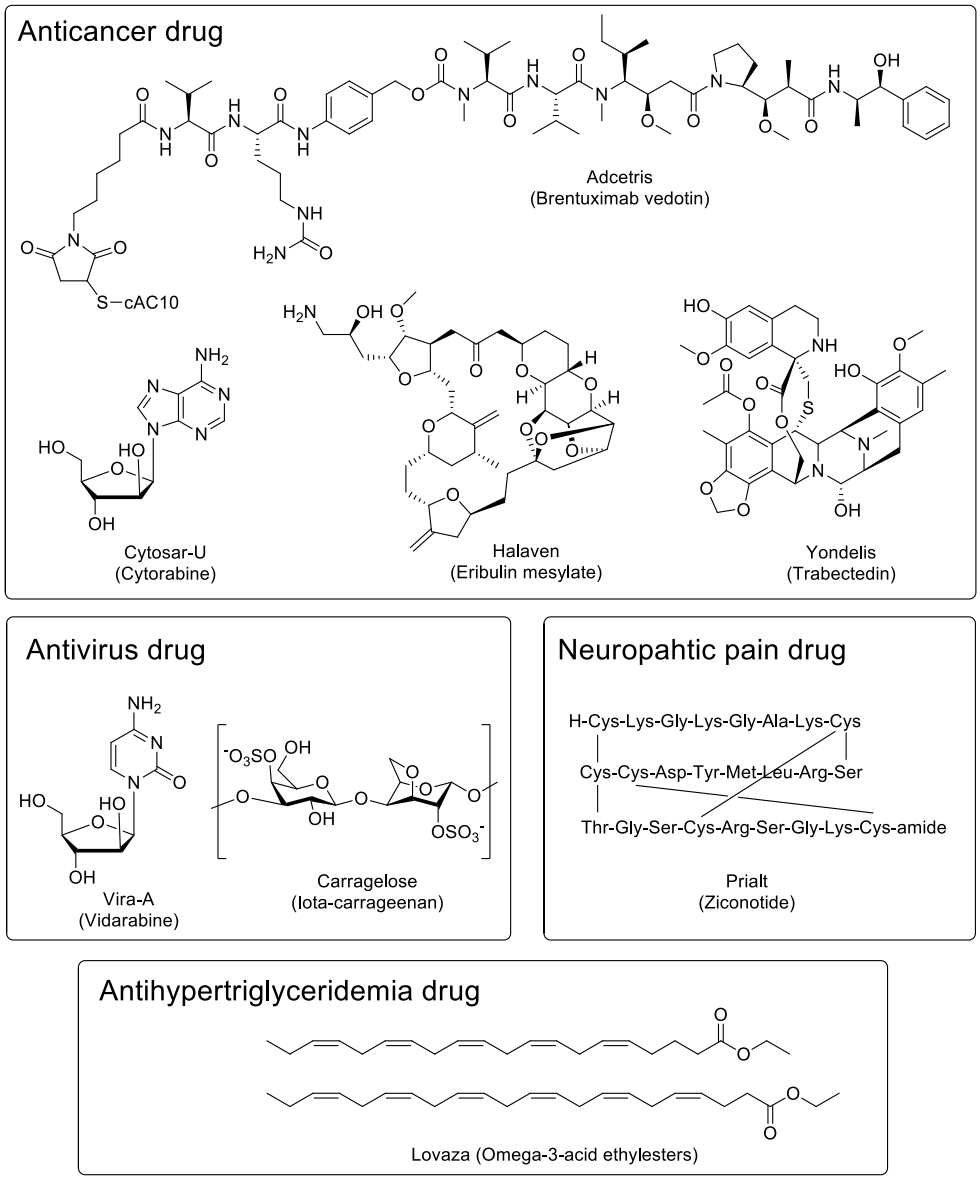

Figure 1.6 Chemical structures of marine drugs on the market divided by therapeutic area (Martins et al., 2014 modified)

Marine drug pipelines is listed with nine more drug candidates under clinical trials mainly treats cancer, include Aplidin and Zalypsis.

Table 1.1 The marine drugs on market (Martins et al., 2014)

Trademark (Compound Name).	**NP[a] or Derivative**	**Original NP / Source Organism**	**Therapeutic Area**	**Status (2013)**
Cytostar-U (Cytorabine)	NP derivative	Spongothymidine / Sponge *Cryptotethya crypta*	Cancer	FDA / EMEA approved
Vira-A (Vidarabine)	NP derivative	Spongouridine / Sponge Crptotethya crypta	Virus	FDA / EMEA approved US discontinued
Prialt (Ziconotide)	NP	ω-Conotoxin / Marine snail *Conus magus*	Neuropahtic Pain	FDA / EMEA approved
Lovaza (Omega-3-acid ethyl esters	NP derivative	Omega-3-fatty acids / fish	Hypertriglyceridemia	FDA / EMEA approved
Yondelis (Trabectedin)	NP	Ecteinascidin 743 / Tunicate *Ecteinascidia turbinata*	Cancer	FDA / EMEA approved
Halaven (Eribulin mesylate)	NP derivative	Halichondrin B / Sponge *Halichondria okadai*	Cancer	FDA / EMEA approved
Adcetris (Brentuximab vedotin)	NP derivative	Dolastatin 10 / Sea hare *Dolabella auricularia*	Cancer	FDA / EMEA approved
Carragelose (Iota-carrageenan)	NP	Iota-carrageenan / Red algee *Eucheuma / Cnondus*	Virus	Over-the-counter drug

[a]NP means natural product

Marine invertebrates are major supply for the marine drugs. It is because the many of marine natural products were obtained from marine invertebrates (Hu et al., 2011). (Figure 1.7) Within the marine invertebrate, sponge and coral were the main sources for the marine natural products. These animals are taking unique ecological roles to support the diversity of marine ecosystem. Coral reef are supporting up to 40% of all fish species while taking only 0.1% of ocean area around the tropical zone (Moyle & Cech, 2003). Sponges inhibit all around the ocean from polar area to the deep ocean trench bottom and associated with a wide variety of microorganisms (Taylor et al., 2007). It is known that from half to 80% of sponge weight is considered be that of associated bacteria. Both of these animals are filter-feeder, and providing physical shelters to around environment. However, the fact that marine invertebrates are main source of the marine drug is one of the main obstacle to overcome for the development of marine drugs that industrial scale cultivation technique for the most of the marine invertebrate are not available yet.

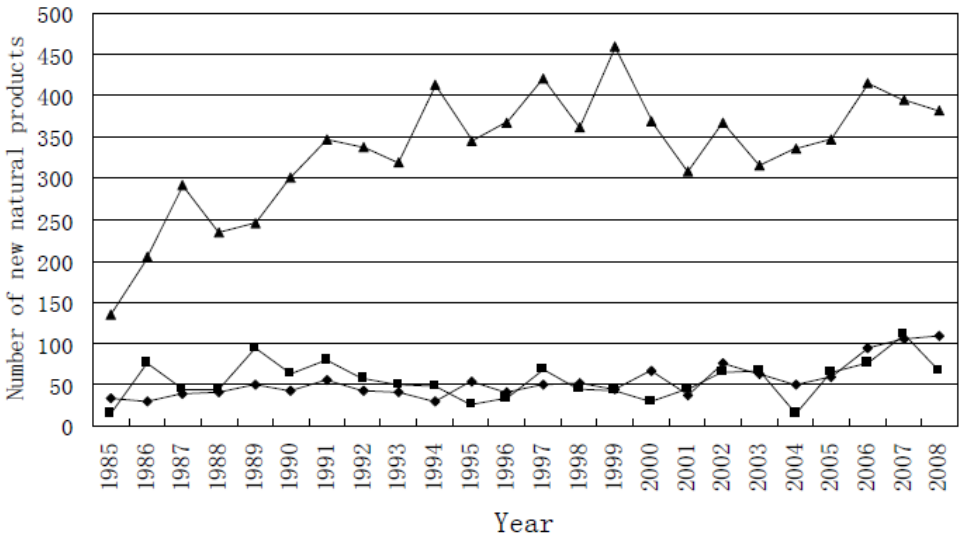

Figure 1.7 Temporal trends in the number of novel compounds isolated from different marine organisms between 1985 and 2008. [▲, marine invertebrate; ■, marine algae; ◆, Marine microorganisms (including phytoplankton).] (Hu et al. 2011)

1.2.3 Major Hurdle of Marine Natural Products derived Drug Discovery

As described ahead, marine natural products have potentials as attractive drug pipeline and are taking more and more interests. However, there are several problems to overcome. First of all, availability problems are still not neglectable. Despite of the introduction of many advanced methods, marine resource is not much close enough. Average depth of the open ocean is more than four thousand m, but general scuba technique allow us to only 40 m deep. Even with the most latest diving technique with atmospheric diving suit, depth reach is less than 700 m. The dredging is not considered these days for it is not eco-friendly and it is too much random sampling method. The budget for manned submarine is not available for most of the research group and even for the big pharmaceutical company. Recent introduce of

remotely operated vehicles can be a good alternative for most of the collection methods.

Second problem is biodiversity itself. As describe above, estimated number of marine organism is enormous. But there is not enough research infra to support that research. For example, sponge is one of the major source for the marine natural products for several decades, but convenient molecular level identification method like 16S RNA sequencing of microorganisms for this phylum is still under construction (Vargas et al., 2012). To have the desired result from this enormous resource, we need to set specific strategy considering ecological back ground and marine taxonomy.

Third and most important problem is supply. This issue can link with first addressed availability problem. As described above, most of the marine drugs were developed from invertebrate derived marine natural products. And most of those marine drug on market was 20 to 40 year after the first report of the natural products. It is mainly because of the supply problem that most of the industrial scale culture technique for marine invertebrate are not available yet. Those years are more than couple of decades longer than common process from terrestrial natural products. Most of these time gap used on the establishment of synthetic method for marine natural products supply. For example, Taxol was notorious for its supply problem. At early stage of discovery, 10 g of Taxol was isolated from 1,200 kg of *Taxus brevifolia* bark (Goodman & Walsh, 2001). Yield was low, but it was possible to do it. But it is not possible for marine natural products. There is no detailed research database of distribution of marine organisms as the forestry, also there is no industrial background to collect the marine organisms like the timber industry.

Yondelis is good example of marine drugs which solve the supply problem with creative way. It was first isolated from tunicate *Ecteinascidai turbinate* (sea squirt) and elucidated in 1984 (Rinehart, 2000). At the early stage of discovery, it was supplied from sea squirt at extremely low yield. Based on its anticancer activity and novel chemical structure, many synthetic preparation methods were developed to meet the requirement of this drug for clinical trials. But break-through was on other way. The Spanish pharmaceutical venture company PharmaMar devised semisynthetic process from Safracin B, which was obtained from bacterium *Pseudomonas fluorescens* by fermentation. This intuition from Yondelis with other recent discovery suggest that actual producer of most current marine drug from marine invertebrates are symbiotic microorganisms (Gerwick & Moore, 2012). This also emphasize the importance of marine microorganisms as attractive drug discovery pipeline.

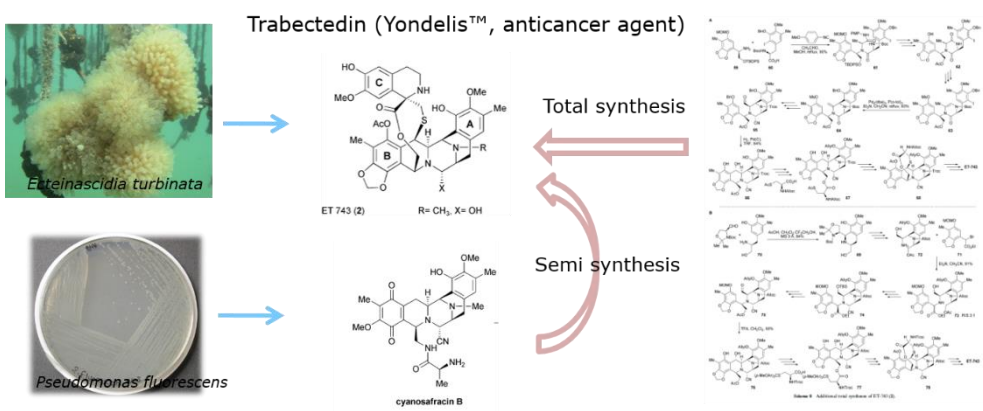

Figure 1.8 Supply of yondelis (Cuevas & Francesch, 2009)

In this study, sponge and marine microorganisms were screened to discover novel natural products. Sponge was screening target as the traditional marine natural products source. Marine microorganisms from bottom sediment were isolated and

screened. Mudflat was selected for new source of marine microorganisms, based on its environmental uniqueness, and isolated microorganisms were screened. Obtained marine natural products were studied with spectroscopic methods.

Chapter 2. Marine Natural Products from Sediment-Derived Actinomycetes

2.1 Introduction

Actinomycetes are the most economically and biotechnologically valuable prokaryotes due to the discovery of wide range of bioactive secondary metabolites, such as antibiotics, antitumor agents, and immunosuppressive agents (Ravikumar et al, 2011). More than 15,000 bioactive molecules were produced by these microbes including many that are used as drugs today. As the soil-derived microorganisms have been intensively investigated for discovering therapeutically important molecules over a half century (Fenical, 1993), the frequency of new compounds discovery has been decreased. Therefore, an unexplored environment needs to be searched for isolating different microorganisms found in terrestrial environments. Recently, microorganisms isolated from the marine environments including the deep sea sediments and marine organisms, have been considered as a good source for exploring new natural products (Takami et al., 1997). In particular, marine actinomycetes have different characteristics from those of terrestrial counterparts that produced unprecedentedly secondary metabolites with diverse biological activities (Imada et al., 2007; Fenical & Jenson, 2006).

2.2 Results and Discussion

2.2.1 Structure Elucidation of Nocarimidazoles from CNQ115

As part of our ongoing research to discover new bioactive compounds from marine-derived actinomycetes, strain CNQ115, identified as *Nocardiopsis* sp. from marine sediments collected off the coast of southern California was investigated. The genus *Nocardiopsis* has been shown to be phylogenetically coherent and to represent a distinct lineage within the order Actinomycetales (Rainey et al., 1996). *Nocardiopsis* strains are ubiquitous in the environment and are frequently isolated from habitats with moderate to high salt concentrations such as saline soils, marine sediments, and salterns (Sabry et al., 2004). The strains of *Nocardiopsis* have also been reported to produce a variety of biologically active agents including the cytotoxic antifungal antibiotic kalafungin (Bergy, 1968), the antibiotic 3-trehalosamine (Dolak et al., 1980), the protein kinase C inhibitor methylpendolmycin, and a staurosporine-like inhibitor of a cyclic AMP-dependent protein kinase (Peltola et al., 2001). LC-MS guided fractionations has led to two new natural products, nocarimidazols A (**1**) and B (**2**). Herein, we report the isolation and structure characterization of nocarimidazols A and B.

Imidazole derivatives were intensively studied for its pharmacological properties on various range of biological activities like analgesic and anti-inflammatory (Suzuki et al., 1992), anti-fungal (Johnson et al., 1999; Brewer et al., 1987) and anti-viral (Sharma et al., 2009). And many of prescription drugs have imidazole as a key pharmacophore (Zhang et al., 2014). Dacarbazine, well-known skin cancer and Hodgkin disease drug (Eggermont & Kirkwood, 2004), shares key chemical structure with nocarimidazoles, having carboxylic carbon and additional nitrogen at

4 and 5 position of imidazole ring. Also, many natural products with imidazole moiety have been reported (Jin, 2011). But, natural products which have 4-carboxylic carbon with imidazole ring is very rare. And imidazole natural products with 4-carboxylic carbon and 5-amine group is not reported yet.

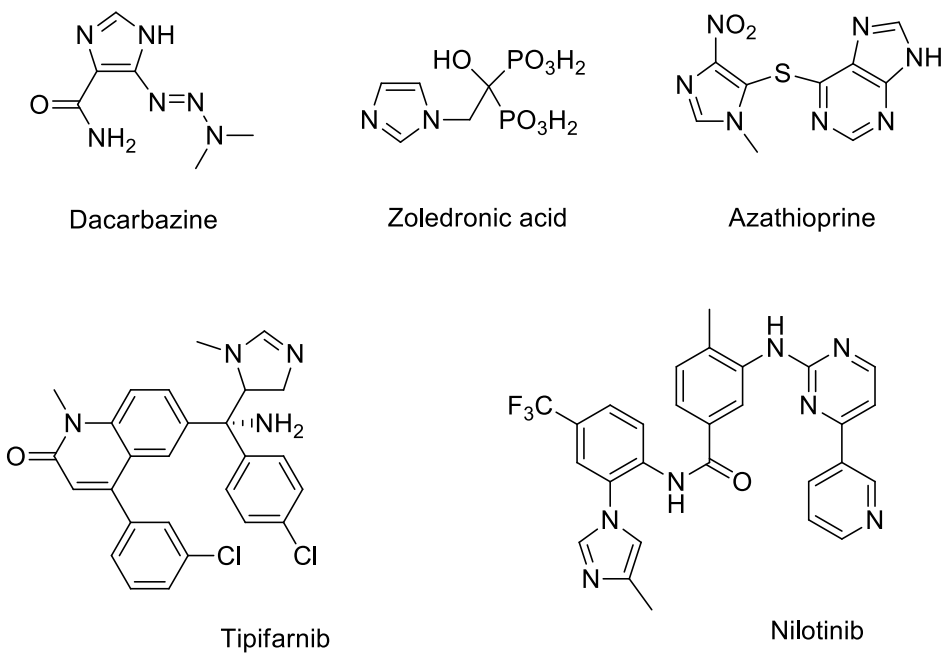

Figure 2.1 Imidazole-based anticancer drugs (Eggermont & Kirkwood, 2004)

2.2.1.1 Nocarimidazole A (**1**)

Actinomycete strain CNQ115, obtained from marine sediment sample collected off the coast of southern California, at a depth of 51 m, required seawater for growth. This strain shares 99.3% 16S rRNA gene sequence identity with its nearest neighbor, *Nocardiopsis* sp. The strain was cultured at 25 ℃ by rotary shaking in 8 replicate 2.5-L Ultra Yield Flasks each containing 1 L of the medium for seven days. The broth was extracted with EtOAc and evaporated under reduced pressure to yield an

extract, which was subjected to flash chromatography followed by HPLC to afford pure samples of nocarimidazols A (**1**) and B (**2**).

Nocarimidazols A (**1**) was obtained as a red amorphous solid. Its molecular formula was established as $C_{13}H_{23}N_3O$ based on HRESIMS (obsd $[M + H]^+$ at *m/z* 238.1918), implying 4 degrees of unsaturation. The UV spectrum of **1** displayed absorption bands at 300 nm, indicating the presence of a significant chromophore in the molecule. The IR spectrum of 1 showed the presence of a primary amine (3433 and 1640 cm^{-1}) and an α, β-unsaturated carbonyl group at 1678 cm^{-1}. Two substructures, a linear aliphatic chain and a imidazole moiety, were assigned by analyses of ^1H, ^{13}C, COSY, HSQC, and HMBC NMR spectroscopic data recorded in $CDCl_3$ (Tables 2.1). The ^1H NMR spectrum of **1** displayed a downfield singlet proton [(δ_H 7.80, s)]. The presence of alkyl chain moiety was suggested by a methyl doublet integrating for six hydrogens [δ_H 0.82, (d, J = 6.6 Hz)] and overlapping methylene proton signals [δ_H 1.03 - 1.32, (m)] and one methine proton [δ_H 1.46, (m)] and two downfield methylene proton [δ_H 1.62 (q, J =7.4 Hz), 2.68 (t, J = 7.4 Hz)]. The COSY cross peaks of H3-14 and H3-15 to H-13 indicated that these methyls were coupled to a methine proton (Table 2.1). The terminal gem dimethyl protons (H3-14 and H3-15) at δ_H 0.82, which showed HMBC correlations to C-13 (δ_C 27.9), and to C-12 (δ_C 38.9). The proton signal (δ_H 1.11) derived from H2-12 showed a HMBC correlation to C-11 (δ_C 27.2). These NMR data established a 2-methylbutane unit.

The proton signal (δ_H 2.68) derived from H2-7 showed a COSY correlation to an aliphatic methylene proton signal at δ_H 1.62 (H2-8), which in turn showed a COSY correlation to another aliphatic methylene proton signal at δ_H 1.29 (H2-9). The proton signal (δ_H 2.68) derived from H2-7 also showed HMBC correlations to a carbonyl C-6 (δ_C 190.9). These NMR data established a pentanone unit.

The alkyl chain moiety was final established by HMBC correlation from the methylene protons H2-11 to the carbons C-9. The HMBC correlations from the singlet proton H-2 (δ_H 7.80, s) to carbons C-4 (δ_C 146.9) and C-5 (δ_C 111.7) and the molecular formula of **1** allowed the construction of a imidazole ring moiety. Lastly, the connection between the alkyl chain moiety and the imidazole ring moiety was achieved by the long range HMBC correlations from an olefinic proton H-2 to carbonyl carbon C-6 allowed the assignment of nocarimidazols A to be completed, as shown in Figure 2.2.

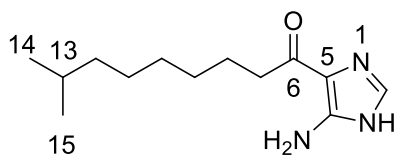

1

Figure 2.2 Chemical structure of nocarimidazole A (**1**)

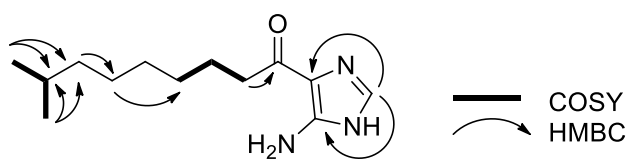

1

Figure 2.3. Key COSY and HMBC correlations of nocarimidazole A (**1)**

Table 2.1 Physical and spectral properties of nocarimidazole A (**1**)

Red amorphous solid
Molecular formula: $C_{13}H_{23}N_3O$,
HRFABMS: *m/z* 238.1918 $[M+H]^+$ (calcd for 238.1919)
IR (KBr) ν_{max}: 3433, 3054, 2928, 2360, 1678, 1640, 1384, 1265, 1201, 1140, 839, 749 cm^{-1}
^{1}H and ^{13}C NMR data[a] ($CDCl_3$)

	1	
No.	δ_C, mult.[b]	δ_H (*J* in Hz)
2	130.2, CH	7.80, s
4	146.9,C	
5	111.7,C	
6	190.9, C	
7	38.8, CH_2	2.68, t (*J* = 7.4)
8	24.1, CH_2	1.62, q (*J* = 7.4)
9	29.7, CH_2	1.29, m
10	38.8, CH_2	1.22, m
11	27.2, CH_2	1.24, m
12	38.9, CH_2	1.11, m
13	27.9, CH	1.47 dp (*J* = 13.1, 6.6)
14	22.5, CH_3	0.82, d (*J* = 6.6)
15	22.5, CH_3	0.82, d (*J* = 6.6)

[a] 500 MHz for ^{1}H NMR and 125 MHz for ^{13}C NMR
[b] Multiplicity was determined by the analysis of 2D NMR spectroscopic data

2.2.1.2 Nocarimidazole B (**2**)

Nocarimidazols B (**2**) was obtained as a red amorphous solid. Its molecular formula was established as $C_{14}H_{25}N_3O$ based on HRESIMS (obsd $[M + H]^+$ at *m/z* 252.2075), implying 4 degrees of unsaturation. The UV absorption spectrum of **2** showed an absorption band at 300 nm, which was identical with the UV data obtained from nocarimidazols A (**1**). The IR spectrum of **2** was also identical to that of **1**. The ^1H NMR spectrum of **2** was almost identical to that of **1** except for the presence of one additional methylene resonance and the presence of one methyl triplet (δ_H 0.84) and methyl doublet (δ_H 0.78). The ^{13}C NMR data of **2** were also similar to those of **1** except for additional carbon signals at C-14 [δ_C 36.5] (Table 2.2). The interpretation of 2D NMR spectroscopic data permitted the identification of the structure of **2**.

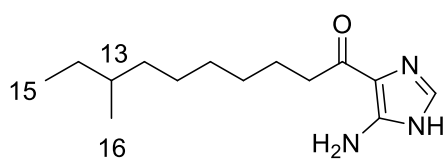

2

Figure 2.4 Chemical structure of nocarimidazole B (**2**)

To confirm the imidazole moiety of compound **2**, methyl derivative (**3**) was prepared with diazomethane. A down field singlet (δ_H 3.42) was observed at ^1H NMR spectrum of compound **3** and the HMBC correlations from the singlet proton 3-NCH_3 (δ_H 3.42) to C-2 (δ_C 130.9) and C-4 (δ_C 144.6) was clear to assign the position of N-3 within imidazole ring. However, to clarify the position of rest of nitrogen, dimethyl derivative of compound **2** was

prepared with iodomethane. This dimethyl derivative (**4**) of compound **2** showed two down field singlets and the HMBC correlations from the singlet proton 1-NCH_3 (δ_H 3.95) to C-2 (δ_C 130.6) and C-5 (δ_C 107.8) established the position of N-1 in imidazole ring. Those HMBC correlations observed from methyl derivatives of nocarimidazole B clarify the position of nitrogens and quaternary carbons within the imidazole ring as shown in Figure 2.5.

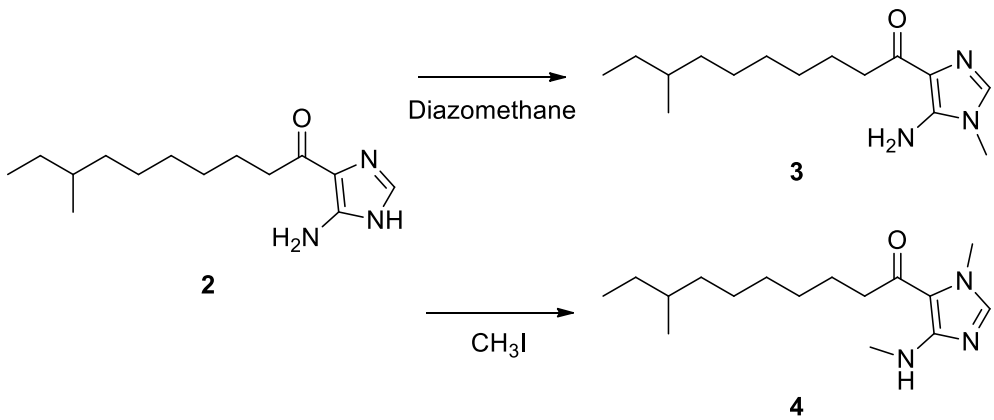

Scheme 2.1 Methylation reaction of nocarimidazole B (**2**)

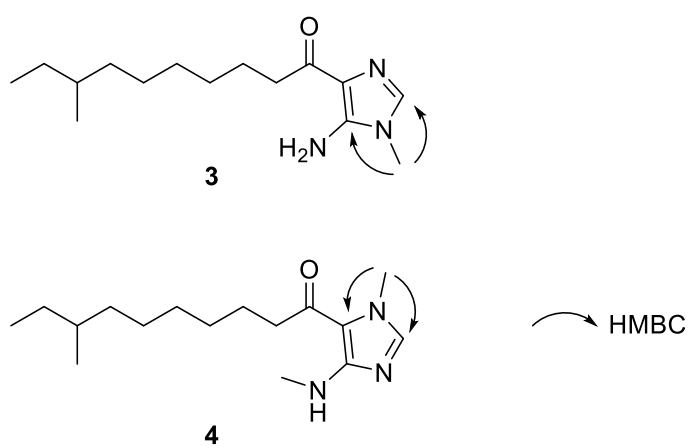

Figure 2.5 Key HMBC correlations of nocarimidazole B (**2**)

Table 2.2 Physical and spectral properties of nocarimidazole B (**2**)

Red amorphous solid

Molecular formula: $C_{14}H_{26}N_3O$,

HRFABMS: *m/z* 252.2075 $[M+H]^+$ (calcd for 252.2076)

IR (KBr) ν_{max}: 3433, 3054, 2926, 2855, 1678, 1548, 1455, 1384, 1203, 1140, 839, 722 cm^{-1}

$[\alpha]_D$ + 1.42° (*C* 0.42, MeOH)

^{1}H and ^{13}C NMR data[a] ($CDCl_3$)

	2	
No.	δ_C, mult.[b]	δ_H (*J* in Hz)
2	130.5, CH	7.75, s
4	147.2,C	
5	111.9, C	
6	190.8, C	
7	38.8, CH_2	2.68, t (*J* = 7.4)
8	24.1, CH_2	1.62, q (*J* =7.4)
9	26.9, CH_2	1.26,m
10	29.4, CH_2	1.07, m
11	29.5, CH_2	1.26, m
12	29.3, CH_2	1.26,m
13	34.3, CH	1.25, m
14	36.5, CH_2	1.05, m 1.23, m
15	11.3, CH_3	0.84, t (*J* = 9.0)
16	19.1, CH_3	0.78, d (*J* = 9.0)

[a] 500 MHz for ^{1}H NMR and 125 MHz for ^{13}C NMR

[b] Multiplicity was determined by the analysis of 2D NMR spectroscopic data

2.2.2 Bioactivities of Nocarimidazoles A and B

The cytotoxicities were evaluated with MTT assay on A498 and ACHN renal cancer cell lines, but no significant cytotoxicities were observed. There were no antibacterial activities either, on MIC assay. Interestingly, AChE inhibitory activity was obsereved but, activity was as weak as one of thousands compare with positive control.

2.3 Experimental

2.3.1 Instruments and Data Collection

The optical rotation was measured using a Autopol III (Rudolph Research, USA) polarimeter with a 5 cm cell. IR spectra were obtained with a Varian Scimitar Series. CD spectra were collected in a ChirascanTM-plus (Applied Photophysics, UK) spectrometer with a 0.5 mm pathlength rectangular cuvette. NMR spectra were recorded on Varian Inova NMR spectrometer (500 and 125 MHz for ^{1}H and ^{13}C NMR, respectively), using the signals of the residual solvent protons and the solvent carbons as internal references (δ_H 7.24 and δ_C 77.0 ppm for $CDCl_3$). EI-MS spectra were measured on a JEOL, JMS-AX505WA mass spectrometer. Low resolution LC-MS data were measured using an Agilent Technologies 6120 quadrupole LC/MS system with a reversed phase column (Phenomenex luna C18(2) 100 Å, 50 mm × 4.6 mm, 5 μm) at a flow rate of 1.0 mL/min. Column chromatography was performed using Silica gel 60 (0.040 ~ 0.063 mm, Merch), normal-phase methods. The fractions were separated by WATERSTM 616 quaternary HPLC pump, WATERSTM 996 photodiode array detector using an Phenomenex luna C18(2) (250 mm × 10 mm, 5 μm) reversed-phase HPLC column.

2.3.2 Microorganism Isolation and Fermentation

Nocardiopsis sp. (CNQ115) was isolated from marine sediments collected off the coast of southern California. It was classified according to 16S rRNA analysis with 99.3% identity. Strain CNQ115 was cultured in 8 2.5-L Ultra Yield Flasks each containing 1 L of the medium (10 g/L of soluble starch, 2 g/L of yeast, 4 g/L of peptone, 10 g/L of $CaCO_3$, 20 g/L of KBr, 8 g/L of $Fe_2(SO_4)_3 \cdot 4H_2O$ dissolved in 750

mL natural seawater and 250 mL of distilled water) at 25 ℃ with shaking at 150 rpm. After 7 days, the broth was extracted with EtOAc and evaporated under reduced pressure to yield an extract of CNQ115 (1.2 g).

2.3.3 Extraction and Compound Isolation

The crude extract (1.2 g) was subjected on open column chromatography on silica gel (30 g), eluted with a step gradient of dichloromethane and methanol. The dichloromethane/methanol (10:1) fraction contained a mixture of metabolites, which was purified by reversed-phase HPLC (Phenomenex Luna C-18 (2), 250×100 mm, 2.5 mL/min, 5 μm, 100 Å , UV = 254 nm) using an isocratic solvent system of 45% CH_3CN in H_2O to afford nocarimidazols A (**1**, 18.0 mg) and B (**2**, 25.0 mg).

2.3.4 Methylation Reactions

Nocarimidazole B Diazomethane Derivative (**3**); Freshly prepared diazomethane reagent (0.5 mL) was added to a 1 mL MeOH solution of **2** (5.0 mg) at 4 ˚C with stirring. This solution was gradually warmed to room temperature. After 2 h, the solvent was removed under vacuum to yield 3.0 mg of nocarimidazol B diazomethane derivative (**3**). ^{1}H NMR ($CDCl_3$): δ_H 6.94 (H-2, s, 1H), 3.42 (3-NCH_3, s, 3H), 2.84 (H-7, t, *J* =8.4 Hz, 2H), 1.68 (H-8, q, *J* =7.7, 2H), 1.26 (H-9, m, 2H), 1.26 (H-11, m, 2H), 1.26 (H-12, m, 2H), 1.24 (H-13, m, 1H), 1.07 (H-10, m, 2H), 1.05, 1.22 (H-14, m, 2H), 0.82 (H-15, t, *J* =8.4, 3H), 0.79 (H-16, d, *J* =7.0, 3H), EIMS *m/z* 266 $[M]^+$

Nocarimidazole Iodomethane Derivative (**4**); A solution of 6.0 mg (0.024 mmol) of nocarimidazol B in 0.5 mL of DMF An appropriate amount of 0.167 mmol of Potassium carbonate (7 eq) was added and the whole was methylated with 0.5 mL

of CH_3I. Then the mixture was heated to 60°C for 24 h to gave 4.0 mg of crude product (66% yield), which were purified by reversed-phase HPLC (Phenomenex Luna C-18 (2), 250×10 mm, 2.5 mL/min, 5 μm, 100 Å, UV = 254 nm) using an gradient solvent system of water and acetonitrile from 20% Acetonitrile to 100% Acetonitrile to afford a methyl nocarimidazol B (**4**, 1.5 mg) ^{1}H NMR ($CDCl_3$): δ_H 8.76 (H-2, s, 1H), 3.95 (1-NCH_3, s, 3H), 3.66 (4-$NHCH_3$, s, 3H), 2.66 (H-7, t, J =7.2 Hz, 2H), 1.64 (H-8, q, J =7.4, 2H), 1.29 (H-8, m, 2H), 1.26 (H-11, m, 2H), 1.26 (H-12, m, 2H), 1.25 (H-13, m, 1H), 1.23 (H-9, m, 2H), 1.05, 1.23 (H-14, m, 2H), 1.07 (H-10, m, 2H), 0.85-0.76 (H-15, H-16, m, 6H), EIMS *m/z* 280 $[M]^+$

2.3.5 Bioassay Procedures

2.3.5.1 Cytotoxicity Test

The cytotoxicity test was performed for two human cancer cell lines, A498 and ACHN renal cancer, according to a previously published method[19] with modifications. The cells were cultured in Dulbecco's modified Eagle's medium (DMEM) containing 10% fetal bovine serum (FBS) and 1% penicillin at 37℃ in a humidified atmosphere incubator (5% CO_2 in air). Wells with DMSO were used as negative controls, and temsirolimus, sunitinib and gemcitabine were used as positive controls

2.3.5.2 MIC Assay

A following seven bacterial strains were used: four Gram-positive (*Staphylococcus epidermidis* ATCC 12228, *Micrococcus lutes* ATCC 9341, *Bacillus subtilis* ATCC 6633, *S. aureus* ATCC 65381) and three Gram-negative (*Escherichia coli* ATCC 11775, *Salmonella typhimurium* ATCC 14028, *Klebsiella pneumonia* ATCC 4352).

These bacteria were inoculated in Mueller-Hinton agar media for 24 h at 37℃. The bacterial colony was cultivated into a 15 mL round tube containing 6 mL of Mueller-Hinton broth media at 37℃ and 225 rpm for 24 h. Test compound (**1**) and a positive control (gentamicin) dissolved in DMSO were added 100 µL of each to 96-well microtiter plate having 50 µL of Mueller-Hinton broth in rest well. The samples were serially diluted and 50 µL of bacterial Mueller-Hinton broth media adjusted to concentration of 1/100 diluted McFarland 0.5% standard. The 96-well was incubated for 24 h at 37℃. After then, the minimum inhibitory concentration (MIC) values were determined as the concentration of compounds at transparent well which inhibit the growth of bacteria.

2.3.5.3 Acetylcholinesterase Inhibitory Assay

The AChE inhibitory activity was measured using the modified method of Ellman et al. Briefly, a reaction mixture containing 140 μL of sodium phosphate buffer (pH 8.0), 20 μL of the test sample solution, and 20 μL of AChE was incubated for 15 min at 25℃. Following the incubation, the reaction was initiated by adding 10 μL of dithiobisnitrobenzoate (DTNB) and 10 μL of ACh and incubated for 10 min at 25℃. The hydrolysis of ACh was monitored and quantified in a spectrophotometer at 412 nm to measure the formation of DTNB with thiocholine released by the enzymatic hydrolysis of ACh. Donepezil hydrochloride (Santa Cruz Biotechnology) was used as a positive control. The 50% inhibitory concentration (IC_{50}) of the donepezil hydrochloride was 0.02 ± 0.004 μM. All reactions were performed in triplicate on 96-well plates and recorded using a VERSA max plate reader (Molecular Devices). The percentage of inhibition was calculated as (1 – S/E) × 100, where E and S are the enzyme activities with and without the sample.

Chapter 3. Marine Natural Products from Mudflat-Derived Actinomycetes

3.1 Introduction

Actinomycetes have been a promising source of bioactive natural compounds for several decades (Bérdy, 2005). Soil-derived actinomycetes have traditionally been the main source of bioactive natural products. In the 1980s, the first marine-derived actinomycete, *Rhodococcus marinonascens*, was described (Helmke & Weyland, 1984). Since then, marine sediments from beach sand to the deep sea bottom have been good environmental sources for isolating actinomycetes, which provide diverse bioactive secondary metabolites (Fenical & Jensen, 2006). Mudflats, also known as tidal flats, are intertidal zones with deposited mud, which create a unique ecological niche. This wetland is covered with salt water one to two times a day and is exposed to strong sunlight, which causes extreme environmental changes for the organisms living there. Despite these harsh environmental conditions, this zone is crowded with various microbial communities due to the rich nutrients available from the land and from the seawater. This unique ecological niche could also be an excellent environment for diverse bacterial species, including actinomycetes (Kim et al., 2004), a situation that often leads to unique chemical structures with diverse biological activities. Recently, our group reported that a *Streptomyces* sp. isolated from tidal flat sediments collected on Anmyeon Island, located on the west coast of Korea, produced

biologically active sesquiterpenoids with an indene moiety, anmindenols A and B (Lee et al., 2014).

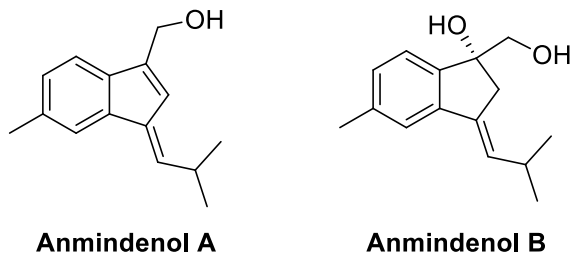

Figure 3.1 Sesquiterpenoids isolated from mudflat-drived actinomycetes

Actinomycete-derived natural products have not been examined extensively to combat neurodegenerative diseases, but specific efforts are ongoing. One of the diseases being studied is Alzheimer's disease (AD), which deteriorates cognitive function. The most common molecular target for drugs that act on the symptoms of AD is acetylcholinesterase (AChE) (Parsons et al., 2013). ChE inhibitors block the AChE enzyme and prevent the neurotransmitter acetylcholine (ACh) from being broken down by AChE, thereby increasing the level of ACh at the synapse and the duration and action of ACh. Thus far, few compounds that exhibit AChE inhibitory activity, such as geranylphenazinediol (Ohlendorf et al., 2012), elaiomycins B and C (Kim et al., 201), N98-1272A (Zheng et al., 2007), and cyclophostin (Kurokawa et al., 1993), have been isolated from *Streptomyces* species.

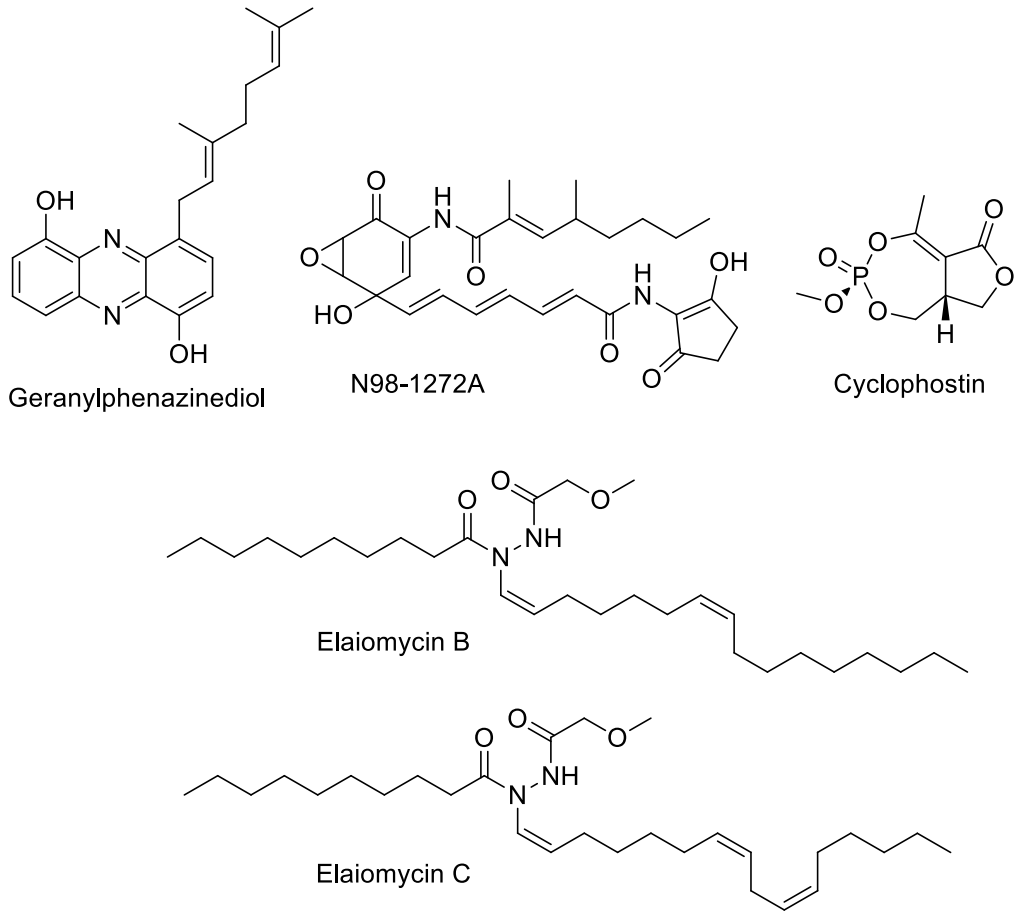

Figure 3.2 Acetylcholinesterase inhibitors isolated from actinomycetes

3.2 Results and Discussion

As part of our continued research into bioactive secondary metabolites from marine actinomycetes on the Korean peninsula, *Streptomyces* sp. 10A085 was isolated from a mudflat sediment sample. Chemical investigation of this strain yielded three new natural products, anithiactins A-D (**1**-**4**). Here, we present details of the isolation of anithiactins A-D and their biological activities in terms of AChE inhibition.

Anithiactins are members of the 2-phenylthiazole class of natural products. The representative natural products belonging to this class are aeruginoic acid (Yamada et al, 1970), aeruginol (Yang et al., 1993) and the pulicatins (Lin et al, 2010). In particular, the chemical structures of the anithiactins are closely related to those of aeruginoic acid and the pulicatins. Aeruginoic acid, a fluorescent natural product, was isolated from the culture medium of *Pseudomonas aeruginosa* and displayed antihypotensive activity (Imai et al., 1973). The pulicatins, isolated from a cone snail (*Conus pulicarius*) associate *Streptomyces* sp., showed G protein-coupled receptor 5-HT_{2B} inhibition activity in the micromolar range.[8] These natural products possess an OH group at C-2, whereas anithiactins have an *N*-methyl group. This aniline moiety is unusual within the 2-phenylthiazoline class of natural products.

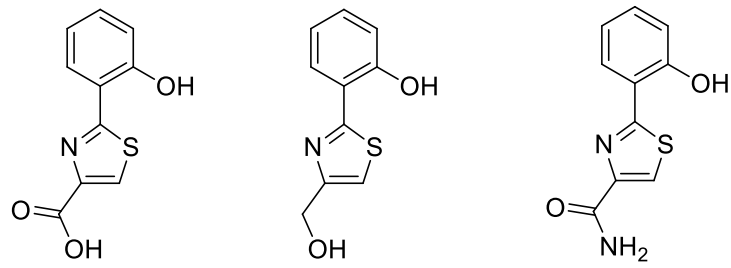

Figure 3.3 Known 2-phenylthiazole class natural products

3.2.1 Structure Elucidation of Anithiactins

3.2.1.1. Anithiactin A (**1**)

Anithiactin A (**1**) was obtained as a yellowish amorphous solid. The molecular formula of **1** was established as $C_{12}H_{12}N_2O_2S$ based on high resolution MS data. The ^{1}H NMR spectrum displayed a 1, 2-disubstituted benzene ring moiety [H-3 (δ_H 6.77, d, J = 7.8 Hz), H-4 (δ_H 7.32, ddd, J =7.8, 7.8, 1.3 Hz), H-5 (δ_H 6.67, dd, J = 7.8, 7.8 Hz), and H-6 (δ_H 7.63, dd, J = 7.8, 1.3 Hz)]. The ^{1}H NMR spectrum also showed a downfield singlet proton H-4′ (δ_H 8.04, s), and *N*-methyl and *O*-methyl singlets [2-NHMe (δ_H 3.01, s), 7′-OMe (δ_H 3.96, s)]. The HMBC correlations from the singlet proton H-4′ (δ_H 8.04, s) to carbons C-2′ (δ_C 170.1), C-5′ (δ_C 146.1) and C-7′ (δ_C 161.7) and the molecular formula of **1** allowed the construction of a thiazole ring moiety (Figure 3.4). The connection between the 1, 2-disubstituted benzene ring moiety and the thiazole ring moiety was achieved using HMBC correlations from the aromatic proton H-6 and the singlet proton H-4′ to C-2′. Lastly, the attachment of the *N*-methyl and the *O*-methyl groups at C-2 and C-7′, respectively, based on HMBC correlations from the *N*-methyl singlet to C-2 and the *O*-methyl singlet to C-7′ completed the assignment of the gross structure of **1**.

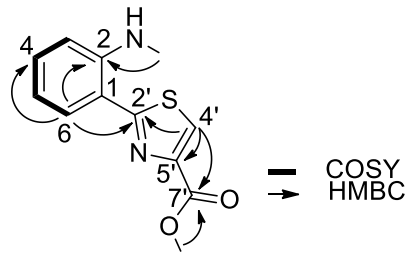

Figure 3.4 COSY and key HMBC correlations of anithiactin A (**1**)

Table 3.1 Physical and spectral properties of anithiactin A (**1)**

Yellowish amorphous solid
Molecular formula: $C_{12}H_{12}N_2O_2S$,
HRFABMS: *m/z* 249.0698 $[M+H]^+$ (calcd for 249.0698)
IR (film) ν_{max}: 3303, 3122, 1727, 1580, 1491, 1446, 1214, 1173, 1104, 906, 753, 738 cm^{-1}
UV (MeOH) λ_{max} (log ε): 209 (5.07), 222 (4.78), 247 (4.31), 286 (4.05), 383 (4.10) nm
^{1}H and ^{13}C NMR data[a] (CD_3OD)

	1	
No.	δ_C, mult.[b]	δ_H (*J* in Hz)
1	114.3, C	
2	147.5, C	
2-NHMe	29.8, CH_3	3.01, S
2-NH		8.43, br s
3	111.1, CH	6.77, d (7.8)
4	131.9, CH	7.32, ddd (7.8, 7.8, 1.3)
5	115.0, CH	6.67, dd (7.8, 7.8)
6	129.4, CH	7.63, dd (7.8, 1.3)
2′	170.1, C	
4′	125.1, CH	8.04, s
5′	146.1, C	
7′	161.7, C	
7′-OMe	52.3, CH_3	3.96, s

[a] 600 MHz for ^{1}H NMR and 125 MHz for ^{13}C NMR. [b] Numbers of attached protons were determined by analysis of 2D spectroscopic data.

3.2.1.2. Anithiactin B (**2**)

The molecular formula of anithiactin B (**2**) was obtained as $C_{11}H_{11}N_3OS$ on the interpretation of the protonated molecule at *m/z* 234.0701 $[M+H]^+$ in the HRFABMS data. The ^1H NMR spectrum of anithiactin B (**2**) was very similar to that of **1** except for the absence of an *O*-methyl singlet and the presence of two singlet protons (δ_H 5.73, δ_H 6.88). The analysis of the 2D NMR spectroscopic data and the molecular formula of **2** indicated that anithiactin B had an NH_2 group at C-7′ instead of a methyl ester. The structure of **2** was also confirmed using X-ray crystallographic data (Figure 3.6). Slow evaporation of a concentrated solution of **2** in hexane and $CHCl_3$ mixture yielded yellow needles.

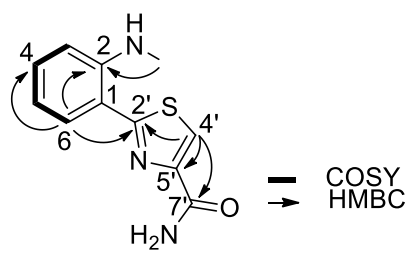

Figure 3.5. COSY and key HMBC correlations of anithiactin B (**2**)

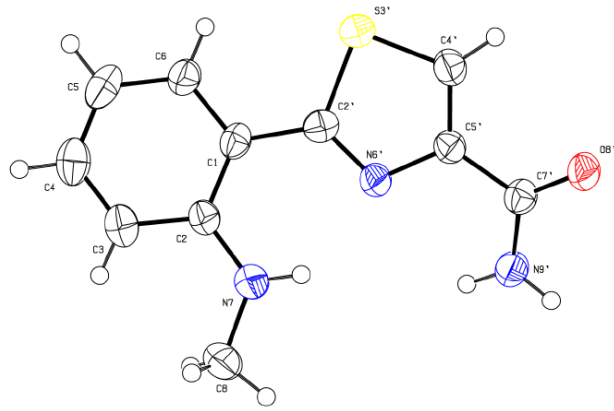

Figure 3.6 X-ray crystal structure of anithiactin B (**2**)

Table 3.2 Physical and spectral properties of anithiactin B (**2)**

Yellowish needle
Molecular formula: $C_{11}H_{11}N_3OS$,
HRFABMS: *m/z* 234.0701 $[M+H]^+$ (calcd for 234.0701)
IR (film) ν_{max}: 3415, 3321, 3193, 1650, 1609, 1581, 1485, 1367, 1215, 1175, 988, 804, 751 cm^{-1}
UV (MeOH) λ_{max} (log ε): 211 (4.67), 219 (4.41), 247 (3.91), 287 (3.67), 383 (3.70) nm
^{1}H and ^{13}C NMR data[a] (CD_3OD)

	2	
No.	δ_C, mult.[b]	δ_H (*J* in Hz)
1	114.9, C	
2	147.3, C	
2-NHMe	30.2, CH_3	3.00, d (5.0)
2-NH		7.74, br s
3	111.3, CH	6.77, d (7.8)
4	132.2, CH	7.35, ddd (7.8, 7.8, 1.4)
5	115.9, CH	6.71, dd (7.8, 7.8)
6	130.0, CH	7.64, dd (7.8, 1.4)
2′	170.5, C	
4′	122.9, CH	8.08 s
5′	149.2, C	
7′	162.9, C	
7′-NH_2		5.73, 6.88 br s

[a] 600 MHz for ^{1}H NMR and 125 MHz for ^{13}C NMR. [b] Numbers of attached protons were determined by analysis of 2D spectroscopic data.

3.2.1.3. Anithiactin C (**3**)

The ^{1}H NMR spectrum of anithiactin C (**3**) was almost identical to that of anithiactin A (**1**) except for the absence of the *O*-methyl group. The molecular formula of **3** was established as $C_{11}H_{10}N_2O_2S$ based on the HRFABMS data, indicating **3** had 14 Da less mass than anithiactin A. These data suggested that **3** had an OH group instead of an *O*-methyl group at C-7′. Interpretation of the 2D NMR spectroscopic data permitted the assignment of structure **3**.

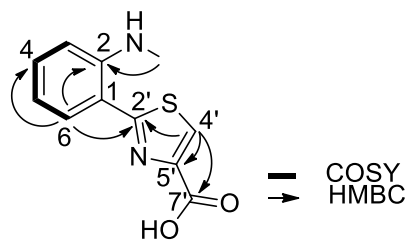

Figure 3.7 COSY and key HMBC correlations of anithiactin C (**3**)

Table 3.3 Physical and spectral properties of anithiactin C (**3)**

Yellowish amorphous solid
Molecular formula: $C_{11}H_{10}N_2O_2S$,
HRFABMS: *m/z* 235.0543 $[M+H]^+$ (calcd for 235.0541)
IR (film) ν_{max}: 3417, 2923, 1573, 1492, 1383, 1285, 1214, 1172, 750 cm^{-1}
UV (MeOH) λ_{max} (log ε): 211 (4.56), 219 (4.30), 261 (3.63), 286 (3.57), 379 (3.57) nm
^{1}H and ^{13}C NMR data[a] (CD_3OD)

	3	
No.	δ_C, mult.[b]	δ_H (*J* in Hz)
1	116.5, C	
2	148.8, C	
2-NHMe	29.9, CH_3	2.84, s
2-NH		4.51, br s
3	112.1, CH	6.64, d (7.8)
4	132.6, CH	7.14, ddd (7.8, 7.8, 1.3)
5	116.1, CH	6.49, dd (7.8, 7.8)
6	130.5, CH	7.50, dd (7.8, 1.3)
2′	170.3, C	
4′	123.1, CH	7.83, s
5′	154.9, C	
7′	170.2, C	

[a] 600 MHz for ^{1}H NMR and 125 MHz for ^{13}C NMR. [b] Numbers of attached protons were determined by analysis of 2D spectroscopic data.

3.2.1.4. Anithiactin D (**4**)

The LRMS of anithiactin D was 423 and 445, which suggest 422 as molecular weight. The 1H NMR spectrum displayed a 1, 2-disubstituted benzene ring moiety [H-6″ (δ_H 7.32, d, *J* = 7.8 Hz), H-7″ (δ_H 7.04, dd, *J* = 7.8, 7.8 Hz), H-8″ (δ_H 6.94, dd, *J* = 7.8, 7.8 Hz), and H-9″ (δ_H 7.48, d, *J* = 7.8 Hz)]. The 1H NMR spectrum also showed a 1, 2, 4-trisubstituted benzene ring moiety [H-3 (δ_H 6.74, d, *J* = 7.8 Hz), H-4 (δ_H 7.42, dd, *J* = 7.8, 1.3 Hz), and H-6 (δ_H 7.76, d, *J* = 1.3 Hz)]. The 1H NMR spectrum also showed downfield singlet protons H-4′ (δ_H 8.07), H-2″ (δ_H 7.27) and one *N*-methyl singlet [2-NHMe (δ_H 2.96, s)]. The upfield signals showed two methines [H-10″ (δ_H 4.27, d, *J* = 7.0 Hz) and H-11″ (δ_H 4.41, ddd, *J* = 7.0, 7.0, 4.2 Hz)] and one methylene [H-12″a (δ_H 3.61, dd, *J* = 7.0, 4.2 Hz) and H-12″b (δ_H 3.48, dd, *J* = 7.0, 4.2 Hz)]. The HMBC correlations from singlet proton H-4′ (δ_H 8.07, s) to carbons C-2′ (δ_C 171.7), C-5′ (δ_C 150.6) and C-6′ (δ_C 165.6) allowed the construction of a thiazole ring moiety. The HMBC correlations from H-6 (δ_H 7.76, s) to carbons C-2 (δ_C 147.0), C-4 (δ_C 134.2), C-5 (δ_C 130.8) and C-2′ (δ_C 171.7) attached thiazole ring with 1, 2, 4-trisubstituted benzene ring. The HMBC correlations from singlet proton H-2″ (δ_H 7.27, s) to carbons C-3″ (δ_C 117.8), C-4″ (δ_C 128.2), C-5″ (δ_C 137.9) and C-6″ (δ_C 112.2) with 1, 2-disubstituted benzene ring allowed the construction of a indole moiety. The connection between the indole moiety and phenyl thiazole was achieved using HMBC correlations from the methine proton H-10″ to carbons C-4, C-5, C-4′, C3″ and C-4″. The COSY correlations from H-11″ (δ_H 4.41, ddd, *J* = 7.0, 7.0, 4.2 Hz) to H-10″ (δ_H 4.27, d, *J* = 7.0 Hz) and H-12″ attached the rest of the carbons to achieve the chemical structure of anithiactin D.

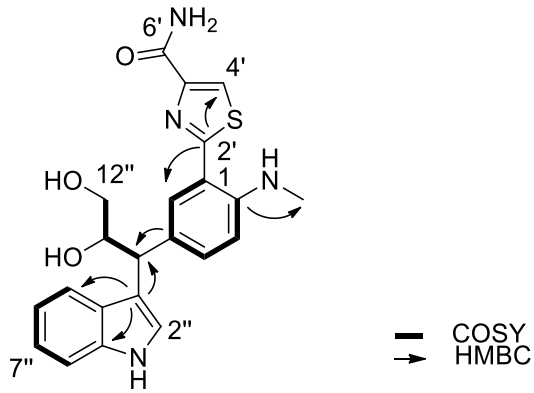

Figure 3.8 COSY and key HMBC correlations of anithiactin D (4)

Table 3.4 Physical and spectral properties of anithiactin D (**4)**

Yellowish amorphous solid
Molecular formula: $C_{22}H_{22}N_4O_3S$ (interpretation of NMR and LRMS data)
LRMS: *m/z* 423 / 445
^{1}H and ^{13}C NMR data[a] (CD_3OD)

	4	
No.	δ_C, mult.[b]	δ_H (*J* in Hz)
1	115.4, C	
2	147.0, C	
2-NHMe	30.0, CH_3	2.96, s
3	112.0, CH	6.74, d (7.8)
4	134.2, CH	7.42, dd (7.8, 1.3)
5	130.8, C	
6	131.3, CH	7.76, d (1.3)
2′	171.7, C	
4′	123.3, CH	8.07
5′	150.6, C	
6′	165.6, C	
2″	123.1, CH	7.27, s
3″	117.8, C	
4″	128.2, C	
5″	137.9, C	
6″	112.2, CH	7.32, d (7.8)
7″	122.3, CH	7.04, dd (7.8, 7.8)
8″	119.5, CH	6.94, dd (7.8, 7.8)
9″	119.8, CH	7.48, d (7.8)
10″	45.6, CH	4.27, d (7.0)
11″	75.6, CH	4.41, ddd (7.0, 7.0, 4.2)
12″	66.2, CH_2	3.61 d (7.0, 4.2)
		3.48 d (7.0, 4.2)

[a] 700 MHz for ^{1}H NMR and 150 MHz for ^{13}C NMR. [b] Numbers of attached protons were determined by analysis of 2D spectroscopic data.

3.2.2 Synthesis of Anithiactin A (**1**)

To further investigate the underlying biology of AChE inhibition using the anithiactins, a three -step synthetic route (Scheme 1) was developed for anithiactin A (**1**) using commercially available reagents. Thiobenzamide (**6**) was obtained from the sulfur substitution reaction of the anthranilamide (**5**) in 89% yield, which was then treated with bromopyruvate in dimethylformamide, a known thiazole ring formation reaction, to give thiazole **7** (Hoveyda et al., 2011). To achieve the selective *N*-monomethylation of **7**, we first attempted to use common methylation reagents, such as methyl iodide, *n*-butyl lithium and sodium cyanoborohydride. These methylation reagents gave the *N*-dimethyl product of thiazole **7**. Next, a solution of formaldehyde in dichloroethane and acetic acid was used as a mild methylation reagent for thiazole **7**. The reaction mixture was stirred overnight, and sodium triacetoxy borohydride at 0℃ was added. The mixture was left at room temperature for 2 h and yielded the *N*-monomethyl product (**1**) (Bonjouklian et al., 2004). The physical and spectroscopic data of the synthesized product were identical to the data for the natural product anithiactin A (**1**).

Scheme 3.1. Synthesis of anithiactin A (**1**)

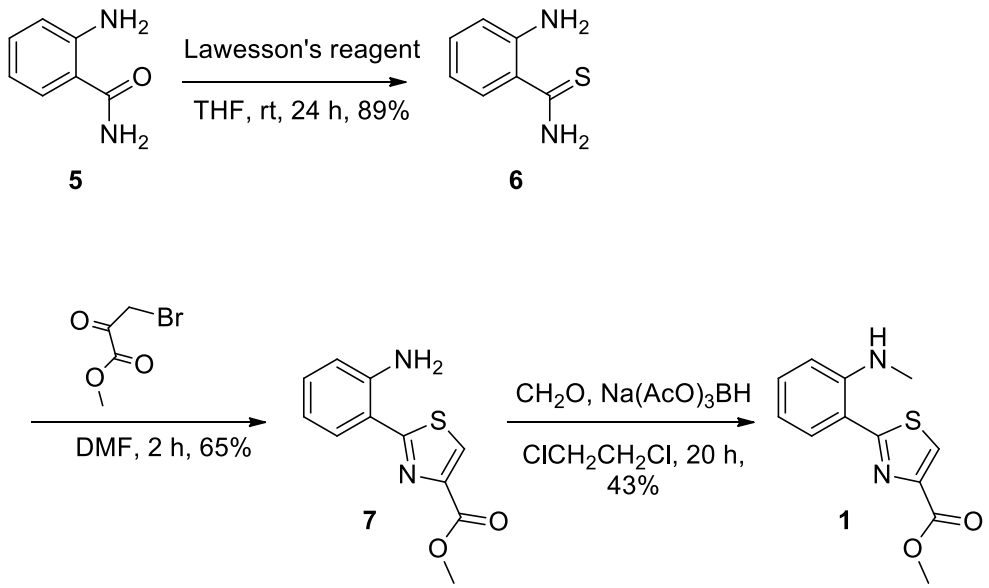

3.2.3 Bioactivities of Anithiactins

A number of previous studies demonstrated that AChE inhibitory activity was improved by replacing a phenyl or oxazole with the thiazole moiety (Nagal et al., 1995; Ronco et al., 2009). Recently, a thiazole containing AChE inhibitor, acotiamide (Acofide), was launched in Japan and is in preparation for phase III clinical trials in the EU (Nolan & Scott, 2013). Therefore, we examined the AChE inhibitory activities of anithiactins A-C (**1**-**3**) using the modified method of Ellman et al. (1961). Anithiactins A-C displayed AChE inhibitory effects with IC_{50} values of 63, 53, and 68 μM respectively. We also evaluated the cytotoxicity of the anithiactins against cancer cell lines. The three anithiactins did not show any significant cytotoxicity against A-498 and ACHN human cancer cell lines up to 200 μM with a modified MTT assay (Tran et al., 2012).

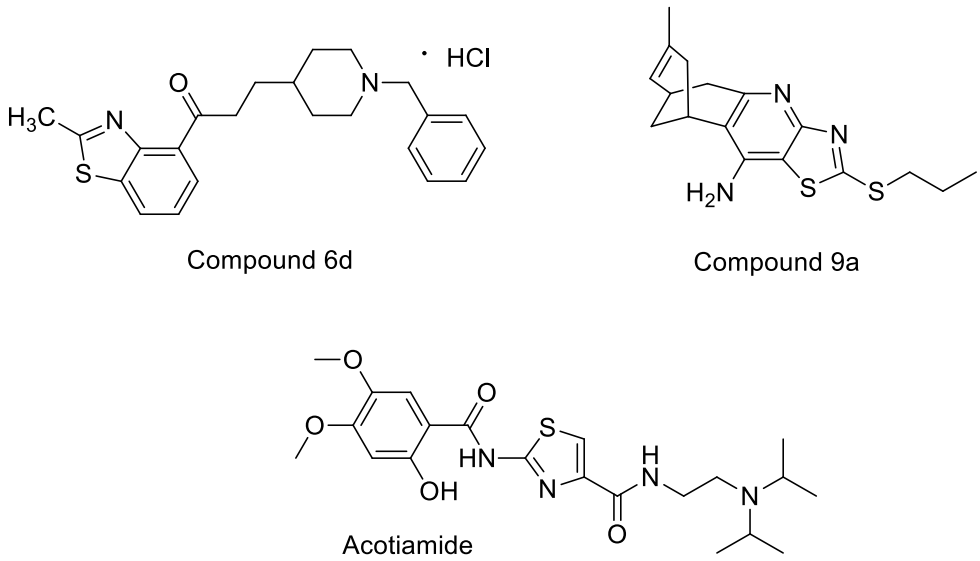

Figure 3.9 Acetylcholinesterase inhibitors containing thiazole moiety (Compound 6d: Nagal et al., Compound 9a: Ronco et al., Acotiamide: Nolan & Scott)

3.3 Experimental

3.3.1 Instruments and Data Collection

UV spectra were recorded in MeOH on a Scinco UVS-2100. The IR spectra were obtained using a Thermo Electron, Nicolet 5700 spectrometer. NMR spectra were obtained using Bruker Avance DPX-500 or DPX-600 spectrometers. $CHCl_3$ (δ_H 7.26; δ_C 77.0) and MeOH (δ_H 3.31; δ_C 49.3) resonances were used as internal references. The HRFABMS were determined on a JEOL, JMS-600W spectrometer. The solvents used were EP grade products from Dae-Jeong & Metals Co., Korea. HPLC grade solvents were purchased from Burdick & Jackson Co. Medium-pressure liquid chromatography was performed on EM Science silica gel (230−400 mesh). TLC was performed using EM Science precoated silica gel plates (Merck 60 F254). The separation of extracts using an HPLC Waters 515 pump and a Waters 996 photodiode array detector was carried out using MG2 C_{18} (250 × 10 mm, 5 μm). The chemical reagents used for synthesis were purchased from Aldrich and TCI. All culture media were purchased from BD.

3.3.2 Microorganism Isolation and Fermentation

Streptomyces sp. 10A085 was obtained from marine sediments from Jaebu Island, GyeongGi-Do, South Korea in 2010. The sampled mud sediments were dried in air for 24 h on a clean bench and given a heat shock at 55 ℃ for 5 min to eliminate other bacteria. Aggregated clumps were lightly mortared using a glass rod and stamped onto various solid agar substrates. Some of the dried samples were suspended in sterilized seawater, and the diluted suspension was spread on variously prepared solid agar substrates using a disposable plastic rod. These crude plates were placed

in a 27 ℃ chamber and monitored for 1 to 3 months to obtain unique actinomycete-like colonies. Strain 10A085 was picked from an ISP medium 4 agar plate containing white spores. The 16S gene was cloned using universal primers 27F and 1492R and showed 99% (1350/1357) similarity to *Streptomyces* sp. HV10 (accession no. KM881709).

3.3.3 Extraction and Compound Isolation

Strain 10A085 was cultured at 25 ℃ with shaking at 150 rpm in 24 Pyrex flasks, each containing 1 L of SYP medium (10 g soluble starch, 4 g yeast extract, and 2 g peptone dissolved in 1 L of 75% filtered natural seawater from Incheon, Korea). After 10 days, the broth was extracted twice using EtOAc, and the solvent was dried *in vacuo* to yield 2.6 g of extract. The extract (2.6 g) was separated using a silica column-equipped MPLC and step-gradient elution of MeOH in CH_2Cl_2 (0%, 1%, 2%, 5%, 10%, 20%, 50%, 90% and 100%). Fraction 1 was further purified using reversed-phase HPLC (MG2 C_{18} 250 × 10 mm, 5 m, 2.0 mL/min, UV = 210 and 280 nm; CH_3CN:H_2O = 70:30) to obtain 1.0 mg of anithiactin A (**1**). Fraction 3 was also purified using the same column, eluting with 98% CH_3CN in H_2O to afford anithiactin B (**2**, 3.0 mg). Anithiactin C (**3**, 3.0 mg) was isolated from fraction 8 with the same isolation procedure used for anithiactin B.

3.3.4 X-ray Crystallographic Analyses

The single-crystal X-ray diffraction data of the compound was collected with a Bruker SMART APEX CCD detector employing graphite-monochromated Mo Kα radiation (λ = 0.71073 Å) at 273(2)K. The data collection and integration were performed using SMART (Madison, WI, 2000) and SAINT-Plus (Madison, WI,

2001). The structure was solved using direct methods and refined using full-matrix least-squares on F^2 using SHELXTL (Madison, WI). All the non-hydrogen atoms were refined anisotropically, and hydrogen atoms were added to their geometrically ideal positions.

Anithiactin B (2): yellow needle; $C_{11}H_{11}N_3OS$, Mr = 233.30, monoclinic, a = 15.1825(12) Å, b = 5.2022(4) Å, c = 14.7674(12) Å, α = 90°, β = 111.728(2)°, γ = 90°, V = 1083.50(15) $Å^3$, space group P2(1)/c, Z = 4, Dx = 1.430 mg/m^3, μ(Cu Kα) = 0.279 mm^{-1}, and F(000) =488. Crystal dimensions: 0.18 × 0.14 × 0.12 mm^3. Independent reflections: 2677 (Rint = 0.0825). The final R1 values were 0.0644, wR2 = 0.1544 (I > 2σ(I)). CCDC number: 1022818.

3.3.5 Synthesis Procedures

Sulfur Substitution Reaction of Anthranilamide (5); A solution of anthranilamide (5, 200 mg, 1.47 mmol) and the Lawesson reagent (320 mg, 0.8 mmol) in THF (10 mL) was stirred under N_2 at r.t. for 24 h. The reaction mixture was partitioned between EtOAc (15 mL) and 2 N HCl (15 mL). A saturated aqueous NaHCO3 solution was added to the separated aqueous layer until pH 8 – 9 and extracted with EtOAc (2 × 20 mL). The combined organic layer was dried with $MgSO_4$ and filtered. The solvent was evaporated in vacuo and the thiobenzamide (6) was obtained after silica gel column chromatography (n-Hexane:EtOAc = 3:1).

Thiobenzamide (6): 200 mg (1.31 mmol, 89%), yellow amorphous solid; ^{1}H NMR (700 MHz, CD_3OD): δ ppm 6.67 (dd, *J* = 7.0, 7.0 Hz, 1 H), 6.78 (dd, *J* = 7.0, 1.2 Hz, 1 H), 7.14 (ddd, *J* = 7.0, 7.0, 1.2 Hz, 1 H), 7.26 (dd, *J* = 7.0, 1.2 Hz, 1 H); ^{13}C NMR (175 MHz, CD_3OD): δ ppm 118.4, 118.9, 126.9, 128.2, 132.5, 147.8, 203.8; LRESIMS *m/z* 153 $[M + H]^+$

Formation of Thiazole (7); To a solution of thiobenzamide (6, 100 mg, 0.66 mmol) in DMF (10 mL) was added bromopyruvate (70 μL, 0.66 mmol). The mixture was stirred under N_2 at 65 ˚C for 2 h. The reaction mixture was partitioned between EtOAc (20 mL) and saturated aqueous NH_4Cl solution (20 mL). The aqueous layer was extracted with EtOAc (2 × 20 mL) and combined organic layer was dried with $MgSO_4$ and filtered. The solvent was removed in vacuo and the thiazole (7) was obtained after silica gel column chromatography (nHexane:EtOAc = 3:1).

Thiazole (7): 100 mg (0.42 mmol, 65%), pale yellow amorphous solid; ^{1}H NMR (700 MHz, $CDCl_3$): δ ppm 3.94 (s, 3 H), 6.70 (dd, *J* = 7.0, 7.0 Hz, 1 H), 6.78 (d, *J* = 7.0 Hz, 1 H), 7.19 (dd, *J* = 7.0, 7.0 Hz, 1 H), 7.59 (d, *J* = 7.0 Hz, 1 H), 8.05 (s, 1H); ^{13}C NMR (175 MHz, $CDCl_3$): δ ppm 55.3, 114.7, 116.8, 116.9, 125.2, 129.1, 131.4, 145.9, 146.4, 161.7, 167.8; LRESIMS *m/z* 235 $[M+H]^+$

Monomethylation of Thiazole (7); Add formaldehyde (10 mg, 0.33 mmol) to a mixture of thiazole (7, 40 mg, 0.17 mmol), acetic acid (1 mL) and 1, 2-dichloroethane (10 mL). The reaction mixture was stirred overnight at r.t. and sodium triacetoxyborohydride (55 mg, 0.26 mmol) was added at 0℃. The reaction mixture was stirred for 2h at r.t. and partitioned between EtOAc (10 mL) and saturated aqueous NaHCO3 solution (20 mL). The aqueous layer was extracted with EtOAc (2 × 20 mL) and combined organic layer was dried with $MgSO^4$ and filtered. The solvent was removed in vacuo and the anithiactin (1) was obtained after silica gel column chromatography (n-Hexane:EtOAc = 4:1).

Anithiactin A (1): 18 mg (0.17 mmol, 43%), yellow amorphous solid; ^{1}H NMR (700 MHz, $CDCl_3$): δ ppm 3.01 (d, *J* = 7.4 Hz, 3 H), 3.96 (s, 3 H), 6.66 (dd, *J* = 7.0, 7.0 Hz, 1 H), 6.76 (d, *J* = 7.0 Hz, 1 H), 7.32 (dd, *J* = 7.0, 7.0 Hz, 1 H), 7.63 (d, *J* = 7.0 Hz, 1 H), 8.04 (s, 1 H), 8.41 (br, 1 H); ^{13}C NMR (175 MHz, $CDCl_3$): δ ppm 29.8,

52.3, 111.0, 114.3, 115.0, 125.1, 129.44, 131.9, 146.1, 147.6, 161.7, 170.2; LRESIMS *m/z* 249 $[M+H]^+$

3.3.6 Bioassay Procedures

3.3.6.1 Cytotoxcity test

The cytotoxicity test was performed for two human cancer cell lines, A498 and ACHN renal cancer, according to a previously published method[19] with modifications. The cells were cultured in Dulbecco's modified Eagle's medium (DMEM) containing 10% fetal bovine serum (FBS) and 1% penicillin at 37℃ in a humidified atmosphere incubator (5% CO_2 in air). Wells with DMSO were used as negative controls, and temsirolimus, sunitinib and gemcitabine were used as positive controls

3.3.6.2 Acetylcholinesterase Inhibitory Assay

The AChE inhibitory activity was measured using the modified method of Ellman et al. Briefly, a reaction mixture containing 140 μL of sodium phosphate buffer (pH 8.0), 20 μL of the test sample solution, and 20 μL of AChE was incubated for 15 min at 25℃. Following the incubation, the reaction was initiated by adding 10 μL of dithiobisnitrobenzoate (DTNB) and 10 μL of ACh and incubated for 10 min at 25℃. The hydrolysis of ACh was monitored and quantified in a spectrophotometer at 412 nm to measure the formation of DTNB with thiocholine released by the enzymatic hydrolysis of ACh. Donepezil hydrochloride (Santa Cruz Biotechnology) was used as a positive control. The 50% inhibitory concentration (IC_{50}) of the donepezil hydrochloride was 0.02 ± 0.004 μM. All reactions were performed in triplicate on 96-well plates and recorded using a VERSA max plate reader (Molecular Devices).

The percentage of inhibition was calculated as $(1 – S/E) \times 100$, where E and S are the enzyme activities with and without the sample.

References

Bérdy, J. *J. Antibiot.* **2005**, *58*, 1 – 26.

Bergy, M. E. *J. Antibiot*. **1968**, *21*, 454 – 457.

Bifulco, G.; Bruno, I.; Minale, L.; Riccio, R.; Debitus, C.; Bourdy, G.; Vassas, A.; Lavayre, J. *J. Nat. Prod.* **1995**, *58*, 1444 – 1449.

Blunt, J.; Munro, M. (Eds.) *Dictionary of Marine Natural Products*, Boca Raton, Florida, Chapman & Hall/CRC, **2008**.

Bonjouklian, R.; De Diego Gomez, J. E.; De Dios, A.; Hamdouchi, C. H.; Li, T.; Lopez De Uralde Garmendia, B.; Vieth, M.; York, J. S.; Dally, R. D.; Del Prado Catalina, M. F.; Jaramillo, C.; Martin Cabrejas, L. M.; Montero Salgado, C.; Pleite, S.; Sanchez-Martinez, C.; Shepherd, T. A.; Wikel, J. H. *PCT/US2003/019890*, **2004**

Bottcher, H. *Miracle drug*, Zagre, Zora, **1965**, pp. 23 – 139.

Brewer, M.D.; Dorgan, R.J.; Manger, B.R.; Mamalis, P.; Webster, R.A., *J. Med. Chem.* **1987**, *30*, 1848 – 1853.

Buss, A.; Waigh, R. *Natural products as leads for new pharmaceuticals*, in: Wolff, M. (Ed.), *Burger's medicinal chemistry and drug discovery. Principles and practice, vol. 1*, New York, John Wiley & Sons, Inc., **1995**, pp. 983 – 1033.

Cordell, G.; Colvard, M. *J. Nat. Prod.* **2012**, *75*, 514 – 525.

Cragg, G.M.; Newman, D.J. *Biochim. Biophys. Acta*, **2013**, *1830*, 3670 – 3695,

Cuevas, C.; Francesch, A. *Nat. Prod. Rep.* **2009**, *26*, 322 – 337.

Dolak, L. A.; Castle, T. M.; Laborde, A. L. *J. Antibiot*. **1980**, 33, 690 – 694.

Eggermont, A.; Kirkwood, J.M. *Euro. J. Cancer.* **2004**, *40*, 1825 – 1836.

Ellman, G. L.; Courtney, K. D.; Andres, V. Jr.; Feather-stone, R. M. *Biochempharmacol.* **1961**, *7*, 88 – 95.

Farbricant, D.; Farnsworth, N. *Environ. Health Perspect.* **2001**, *109*, 69 – 75.

Fenical, W. *Chemical Reviews* **1993**, *93*, 1673 – 1683.

Fenical, W.; Jensen, P. *Nat. Chem. Biol.* **2006**, *2*, 666 – 673.

Gerwick, W.; Moore, B. *Chem. & Biol.* **2012**, *19*, 85 - 98

Goodman, J.; Walsh, V. *The Story of Taxol: Nature and Politics in the Pursuit of an Anti-Cancer Drug.* Cambridge University Press., **2001**, pp. 17..

Gueritte, F.; Fahy, J. *The vinca alkaloids*, in: Cragg, G.; Kingston, D.; Newman, D. (Eds.) *Anticancer agents from natural products*, Boca Raton, Florida, Taylor and Francis, **2005**, pp. 123 – 135.

Helmke, E.; Weyland, H. *Int. J. Syst. Bacteriol*. **1984**, *34*, 127 – 138.

Hoveyda, H.; Marie-Ddile, R.; Lovat, F. G.; Guillaume, D. *PCT/EP2011/055218*, **2011**

Hu G.; Yuan, J.; Sun, L.; She, Z.; Wu, J.; Lan, X.; Zhu, X.; Lin, Y.; Chen, S. *Mar. Drugs* **2011**, *9*, 514 - 525.

Imada, C.; Koseki, N.; Kamata, M.; Kobayashi, T.; Hamada-Sato, N. *Actinomycetologica* **2007**, *21*, 27 – 31.

Imai, T.; Takahashi, M.; Seki, N.; Irie, Y. *US patent 3,729,378*, **1973**.

Jin, Z. *Nat. Prod. Rep.* **2011**, *28*, 1143 – 1191.

Johnson, R.A., Huong, S.M., Huang, E.S., *Antivir. Res.* **1999**, *41*, 101 – 111.

Kelly, K. *History of medicine*, New York, Facts on file, **2009**, pp. 29 – 50.

Kim, B.; Oh, H.; Kang, H.; Park, S.; Chun, J. *J. Microbiol. Biotechnol.* **2004**, *14*, 205 – 211.

Kim, B. Y.; Willbold, S.; Kulik, A.; Helaly, S. E.; Zinecker, H.; Wiese, J.; Imhoff, J. F.; Goodfellow, M.; Süssmuth, R. D.; Fiedler, H. P. *J. Antibiot. (Tokyo)*. **2011**, *64*, 595 – 597.

Kong, D.; Jiang, Y.; Zhang, H. *Drug Discov. Today* **2010**, *15*, 884 – 886.

Kurokawa, T.; Suzuki, K.; Hayaoka, T.; Nakagawa, T.; Izawa, T.; Kobayashi, M.; Harada, N. *J. Antibiot. (Tokyo).* **1993**, *46*, 1315 – 1318.

Lee, J.; Kim, H.; Lee, T.; Yang, I.; Won, D.; Choi, H.; Nam, S.-J.; Kang, H. *J. Nat. Prod.* **2014**, *77*, 1528 – 1531.

Lin, Z.; Antemano, R.; Hughen, R.; Tianero, M.; Peraud, O.; Haygood, M.; Concepcion, G.; Olivera, B.; Light, A.; Schmidt, E. *J. Nat. Prod.* **2010**, *73*, 1992 – 1926.

Margulis, L.; Schwartz, K. *Five kingdoms, an illustrated guide to the phyla of life on earth*, 2nd ed., New York, W. H. Freeman & Co., **1988**.

Martins, A.; Vieira, H.; Gaspar, H.; Santos, S. *Mar. Drugs* **2014**, *12*, 1066 - 1101.

Meyer, C.A. *The Global Marine Pharmaceuticals Pipeline.* http://marinepharmacology. midwestern.edu/

Moyle, P; Cech, J. *Fishes: An Introduction to Ichthyology*. New York, Benjamin Cummins, **2003**, pp. 744

Nagal, A.; Liston, D.; Jung, S.; Mahar, M.; Vincent, L.; Chapin, D.; Chen, Y.; Hubbard, S.; Ives, J.; Jones, S.; Nielsen, J.; Ramirez, A.; Shalaby, I.; Villalobas, A.; White, W. *J. Med. Chem.* **1995**, *38*, 1084 – 1089.

Newman, D.; Cragg, G. *J. Nat. Prod.* **2012**, *75*, 311 – 338.

Nolan, M.; Scott, L. *Drugs* **2013**, *73*, 1377 – 1383.

Ohlendorf, B.; Schulz, D.; Erhard, A.; Nagel, K.; Imhoff, J. F. *J. Nat. Prod*. **2012**, *75*, 1400 – 1404.

O'Neill, P.; Posner, G. *J. Med. Chem.* **2004**, *47*, 2945 – 2964.

O'Neill, P.; Barton, V.; Ward, S. **Molecules**, **2010**, *15*, 1705 – 1721.

Parsons, C. G.; Danysz, W.; Dekundy, A.; Pulte, I. *Neurotox. Res.* **2013**, *24*, 358 – 369.

Peltola, J. S.; Andersson, M. A.; Kampfer, P.; Augling, G.; Kroppenstedt, R. M.; Busse, H. U.; Salkinoja-Salonen, M. S.; Rainey. F. A. *Appl. Environ. Microbiol.* **2001**, *67*, 4293 – 2304.

Petrovska, B. *Pharmacogn. Rev.* **2012**, *6(11)*, 1 – 5.

Rainey, F. A.; Ward-Rainey, N.; Kroppenstedt, R. M.; Stackebrandt, E. *Int. J. Syst. Bacteriol.* **1996**, *46*, 1088 – 1092.

Ravikumar, S.; Inbaneson, S. J.; Uthiraselvam, M.; Priya, S. R.; Ramu, A.; Banerjee, M. B. *J. Pharm. Res.* **2011**, 4, 294 − 296.

Rinehart, K. *Med. Res. Rev.* **2000**, *20(1)*, 1 – 27.

Ronco, C.; Sorin, G.; Nachon, F.; Foucault, R.; Jean, L.; Romieu, A.; Renard, P. *Bioorg. Med. Chem.* **2009**, *17*, 4523 – 4536.

Roussi, F.; Gueritte, F.; Fahy, J. *The vinca alkaloids*, in: Cragg, G.; Kingston, D.; Newman, D. (Eds.) *Anticancer agents from natural products*, 2nd ed., Boca Raton, Florida, Taylor and Francis, **2012**, pp. 123 – 135.

Sabry, S. A.; Ghanem, N. B.; Abu-Ella, G. A.; Schumann, P.; Stackebrandt, E.; Kroppenstedt, R. M. *Int. J. Syst. EVol. Microbiol.* **2004**, *54*, 453 – 456.

Sharma, D.; Narasimhan, B.; Kumar, P.; Judge, V.; Narang, R.; Clercq, E.; Balzarini, J. *Euro. J. Med. Chem.* **2009**, *44*, 2347 – 2353.

Suzuki, F.; Kuroda, T.; Tamura, T.; Sato, S.; Ohmori, K.; Ichikawa, S. *J. Med. Chem.* **1992**, *35*, 2863 – 2870.

Takami, H.; Inoue, A.; Fuji, F.; Horikoshi, K. *FEMS Microbiol. Lett.* **1997**, *152*, 279 – 285.

Taylor, M.; Radax, R.; Steger, D.; Wagner, M. *Microbiol. Mol. Biol. Rev.* **2007**, *71(2)*, 295 – 347.

Tran, T. D.; Pham, N. B.; Fechner, G; Zencak, D.; Vu, H. T.; Hooper, J. N. A.; Quinn, R. J. *J. Nat. Prod*. **2012**, *75*, 2200 – 2208.

Vargas, S.; Schuster, A.; Sache, K.; Buttner, G.; Schatzel, S.; Lauchell, B.; Hall, K.; Hooper, J.; Erpenbeck, D.; Worheide, G. *Plos One* **2012**, *7*, e39345

Wang, J.; Huang L.; Li, J.; Fan, Q.; Long, Y.; Li, Y.; Zhou, B.; *PLoS One*, **2010**, *5* e9582.

Wiart, C. *Etnopharmacology of medicinal plants*, New Jersey, Humana Press, **2006**, pp. 1 – 50.

Wongsrichanalai, C.; Pickard, A.; Wernsdorfer, W.; Meshnick, S. *Lancet Infect. Dis.* **2002**, *2*, 209 –218.

Yamada, Y.; Seki, N.; Kitahara, T.; Takahashi, M.; Matsui, M. *Agric. Biol. Chem.* **1970**, *34*, 780 –783.

Yang, W.; Dostal, L.; Rosazza, J. *J. Nat. Prod.* **1993**, *56*, 1993 – 1994.

Zhang, L.; Peng, X.M; Damu, G. L. V.; Geng, R.X.; Zhou, C.H. *Med. Res. Rev*. **2014**, *34*, 340 – 437.

Zheng, Z. H.; Dong, Y. S.; Zhang, H.; Lu, X. H.; Ren, X.; Zhao, G.; He, J. G.; Si, S. Y. *J. Enzyme. Inhib. Med. Chem*. **2007**, *22*, 43 – 49.

Appendix A

List of Figures and Tables in Appendix A

A.1 Antibacterial Secosteroid from the Korean Sponge *Irchinia* sp.

A.1.1 Introduction

Marine Sponges are known as a source of structurally diverse natural products. This phylum of marine animal is possessing about 35% of reported marine natural products (Blunt et al., 2012). Many of the potent cytotoxins against cancer cell lines have been reported and some of them were developed as a lead of FDA approved drugs such as Cytosar-U®, and Halaven® (Martins et al., 2014). The antibacterial activity of marine sponge-derived metabolites are also well known such as discorhabdin Z (Jeon et al., 2010), agelasine D (Hertiani et al., 2010), 7,20-diisocyanoadociane (Wright et al., 2011), motualevic acid F (Keffer et al., 2009). In this regard, we have been investigated extracts of Korean marine sponges for the discovery of antibacterials. An extract of a Korean marine sponge in genus of *Ircinia* sp. showed antibacterial activities, and we continue the investigation of its bioactive constituents.

The genus *Ircinia* have been studied intensively and number of biologically active natural products have been reported such as antibacterials (Manes & Crews, 1986; Faulkner, 1973), cytotoxin (Kondo et al., 1992), ichthyotoxin (De Rosa et al., 1996), analgesic compound (Cimino et al., 1972; De Pasquale et al., 1991), multidrug resistance modulator (Kawakami et al., 2001), thrombin inhibitor (Nakao et al, 1995), angiotensin converting enzyme/aldose reductase inhibitor (Alfano et al., 1979), and inosine monophosphate dehydrogenase inhibitor (Cafieri et al., 1972; De Rosa et al., 1997).

Also, this *Ircinia* sp. is well known for its possession of divers terpenes such as ircinin-1,7 variabilin (De Rosa et al., 1996), fasciculation (Cafieri et al, 1972), and strobilinin (Rothberg & Shubiak, 1975). In addition, hydroquinones (Cimino et al, 1972a; Cimino et al. 1972b), chromans (Venkateswarlu & Reddy, 1994; Bifulco et al., 1995), and sterols (Venkateswarlu et al., 1996; Fu et al., 1999; Xu et al., 2008) have been reported. However, the organisms in *Ircinia* sp. was not reported for its secostrols.

Herein, we report the structure of an unprecedented secosterol with the 2-ene-1,4-dione as well as its antibacterial activity.

A.1.2 Results and Discussion

A.1.2.1 Structure Elucidation of 9,11-Secosterol (**1**)

The molecular formula of compound **1** was deduced as $C_{27}H_{44}O_5$, based on the analysis of HRFABMS data (a pseudomolecular ion peak at *m/z* 449.3271 $[M+H]^+$) and on the interpretation of ^{13}C NMR data. The ^1H NMR spectrum of **1** displayed an oxygenated methine proton [δ 4.04 (m)], an olefinic proton [δ 6.49 (br s)], and one downfielded methylene protons [δ 3.84 (m). 3.70 (m)]. The ^1H NMR spectrum also showed two methyl singlets [δ 1.23, 0.70] and three methyl doublets [δ 0.97 (d, *J* = 6.6 Hz), 0.88 (d, *J* = 2.3 Hz), 0.86 (d, *J* = 2.3 Hz)]. The ^{13}C NMR and HSQC spectra revealed five methyl, ten methylene, six methine, and six fully-substituted carbons. The 27 carbons, five methyl protons, and an oxygenated methine proton are characteristic of a cholesterol carbon skeleton. Furthermore, ^1H NMR signals of an olefinic proton δ 6.49 (s, 1H), oxymethylene protons [δ 3.70 (m, 1H), δ 3.84 (m, 1H)], a downfield proton [δ 3.52 (dd, 1H, *J* = 11.0, 8.5 Hz)], and five methyls [δ 0.70 (s, 3H), δ 1.23 (s, 3H), δ 0.97 (d, 3H, *J* = 6.6 Hz), δ 0.88 (d, 3H, *J* = 6.6 Hz), δ 0.86 (d, 3H, *J* = 6.6 Hz)] suggested that **1** was a 9, 11-secosterol.

Interpretation of 2D NMR spectroscopic data permitted the structure assignment of **1**. Analysis of COSY spectroscopic data of **1** revealed three fragments (a, b, and c) as shown in Figure A.1.1. In addition, the carbon chemical shifts of C-6 (δ 197.5), C-7 (δ 134.4), C-8 (δ 152.1), and C-9 (δ 203.1), and the HMBC correlations from an olefinic proton H-7 to carbons C-6, C-8, and C-9 supported the construction of an ene-dione moiety.

The connectivity of A/B ring including the fragment a and the ene-dione moiety for **1** was secured from HMBC correlations. The long-range HMBC correlations from

H-19 to carbons C-1, C-5, C-9, and C-10, and from H-4 to carbons C-2, C-5, and C-10, and from H-7 to the carbon C-5 allowed the A/B ring connectivity. The fragments b and c were also connected from the interpretation of HMBC correlations. A two-bond HMBC correlation from a methyl singlet proton H-18 to a carbon C-13, and three-bond HMBC correlations from H-18 to carbons C-12, C-17 permitted the C-12/C-13/C-17 connectivity. Lastly, the establishment of C-8/C-14 attachment based on the interpretation of three-bond HMBC correlations from the olefinic proton H-7 to a carbon C-14, and from the methyl singlet proton H-18 to a carbon C-14 allowed the completion of structure assignment of **1**. (Figure A.1.2)

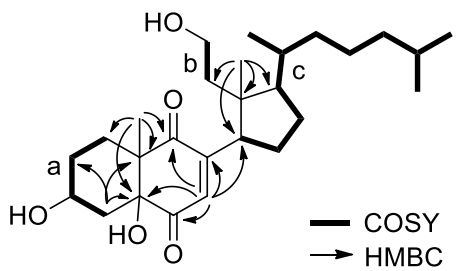

Figure A.1.1 COSY and key HMBC correlations of 9,11-secosterol (**1**)

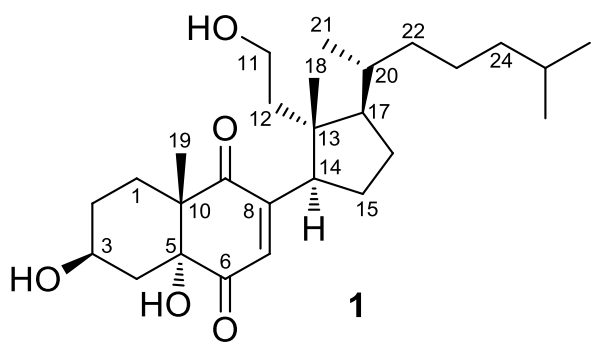

Figure A.1.2 Chemical structure of 9,11-secosterol (**1)**

The relative stereochemistry of the side chain and rings of **1** was identical to that of reported secosterols, which was determined by comparison with NMR data of known secosterols and by interpretation of NOESY correlations (Reddy et al., 1997; Lu & Faulkner, 1997). Briefly, NOESY correlations [H-7/H-14, H-14/H-12, H-12/H-21, H-18/H-20] were well corresponded to previously reported NOE correlations (Anta et al, 2002). The β-configuration of 3-hydroxy group at C-3 was defined from the coupling constants of H-4 (δ 2.16, dd, *J* = 13.1, 11.2 Hz) and NOESY correlations [H3/H4, H4 2.16)/H19]. (Figure A.1.3)

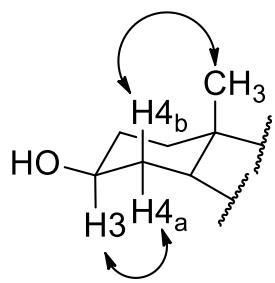

Figure A.1.3 Key NOESY correlations observed for 9,11-secosterol (**1**)

Table A.1.1 Physical and spectral properties of 9,11-secosterol (**1**)

Colorless needles
Molecular formula: $C_{27}H_{44}O_5$,
HRFABMS: *m/z* 449.3271 $[M+H]^+$ (calcd for 449.3275)
IR (film) ν_{max}: 3422, 2951, 2851, 1718, 1681, 1464, 1633 cm^{-1}
UV (MeOH) λ_{max} (log ε): 274 (3.96) nm
^{1}H, ^{13}C, COSY and HMBC NMR data[a] ($CDCl_3$)

No.	δ_C, m[b]	δ_H, m, *J* (Hz)	COSY	HMBC (J_{CH} = 10 Hz)
1	25.9, t	1.77 m	2	3, 5, 10, 19
		2.21 dt (11.2, 3.7)		
2	29.8, t	1.55 m	1, 3	
		2.00 m		
3	66.6, d	4.04 m	2, 4	
4	35.6, t	1.77 m	3	2, 5, 10
		2.16 dd (13.1, 11.2)		
5	80.5, s			
6	197.5, s			
7	134.4, d	6.49, s		5, 6, 8, 9, 14
8	152.1, s			
9	203.1, s			
10	52.1, s			
11	59.9, t	3.70 m;	12	
		3.84 m		
12	41.1, t	1.11 m	11	
		1.73 m		
13	47.5, s			
14	43.9, d	3.52 dd (11.0, 8.5)	15	7, 8, 9, 12, 13, 15, 18
15	26.3, t	1.75 m	14, 16	
		1.84 m		
16	26.6, t	1.68 m	15, 17	
		1.75 m		
17	50.1, d	1.73 m	16, 20	
18	17.7, q	0.70 s		12, 13, 14, 17
19	20.6, q	1.23 s		1, 5, 9, 10
20	34.5, d	1.41 m	17, 21, 22	
21	18.8, q	0.97 d (6.6)	20	17, 20, 22
22	35.6, t	0.99 m	20, 23	24
		1.35 m		
23	24.4, t	1.15 m	22, 24	
		1.35 m		
24	39.4, t	1.13 m	23, 25	
		1.15 m		
25	27.9, d	1.51 m	24, 26, 27	23
26	22.5, q	0.86 d (6.6)	25	24, 25, 27,
27	22.7, q	0.88 d (6.6)	25	24, 25, 26
5-OH		2.36 br s		

[a] 600 MHz for ^{1}H NMR and 150 MHz for ^{13}C NMR
[b] Multiplicity was determined by the analysis of 2D NMR spectroscopic data

A.1.2.2 Antibacterial Activity of Secosterol

Compound **1** was evaluated for antibacterial activity against seven pathogenic strains. (Table A.1.2) Compound **1** displayed the most potent activity on *Micrococcus lutes* ATCC 9341 and also showed the moderate activity against *Staphylococcus epidermidis* ATCC 12228 and *Bacillus subtilis* ATCC 6633 with MIC values of 3.1, 25 and 25 μg/mL, respectively. Meanwhile, **1** did not show any activity against gram negative strains include *Escherichia coli* ATCC 11775, *Salmonella typhimurium* ATCC 14028 and *Klebsiella pneumonia* ATCC 4352 up to 200 μg/mL. Interestingly, growth of one of the gram positive strain *Staphylococcus aureus* ATCC 65381 was not inhibited up to 200 μg/mL.

Table A.1.2 Antibacterial activity of 9,11-secosterol (**1**)

Strain	**1**[a]	Gentamicin [a]
Staphylococcus epidermidis ATCC 12228	25	0.2
Micrococcus lutes ATCC 9341	3.1	3.1
Bacillus subtilis ATCC 6633	25	0.2
S. aureus ATCC 65381	>200	0.2
Escherichia coli ATCC 11775	>200	0.8
Salmonella typhimurium ATCC 14028	>200	1.6
Klebsiella pneumonia ATCC 4352	>200	0.8

[a]Each experiment was repeated more than three times. MIC value in μg/mL

A.1.3 Experimental

A.1.3.1 Instruments and Data Collection

The optical rotation was measured using a Rudolph Research Autopol III polarimeter with a 5 cm cell. The UV spectrum was recorded in a Scinco UVS-2100 with a path length of 1 cm. Infrared spectra were recorded on a Thermo Electron Corporation spectrometer. NMR spectral spectroscopic data were obtained using Bruker Avance 600 MHz spectrometer [$CDCl_3$ (δ_H 7.26; δ_C 77.0) was used as an internal standard]. HRFABMS data were measured on a JEOL, JMS-AX505WA mass spectrometer.

A.1.3.2 Animal Material

The genus *Ircinia* sponge was collected by scuba diving at Yeongdeok-Gun in the East Sea. The sample was frozen immediately after collection with dry ice and stored in refrigerator at -20 ˚C before extraction.

A.1.3.3 Extraction and Isolation

The wet animal (3 kg) was extracted three times with 50% methanol (MeOH) in dichloromethane. These extracts were concentrated and partitioned three times between hexanes and MeOH. Then the MeOH-soluble layer was partitioned three times between ethylacetate (EtOAc) and water. The water-soluble fraction was further extracted thrice with n-butanol. The EtOAc-soluble layer (7.0 g) was subjected to silica flash column chromatography using step-gradient elution of EtOAc in hexanes (0%, 10%, 20%, 30%, 40%, 50%, 60%, 70%, 80%, 90%, and 100%) to afford seven fractions (Fr 1-Fr 11). Fr 5 (68.3 mg), which contained the

mixture of **1**, was further purified by reversed-phase HPLC (Polar-RP, 250 × 10 mm, 5 μm, 80 Å, 2.5 mL/min, UV detection = 210 nm), eluting with 70% acetonitrile in H_2O to afford compound **1** (2.7 mg), as colorless needles.

A.1.3.4 MIC Bioassay Procedures

The six microorganisms were obtained from the stock culture collection at the American Type Culture Collection (Maryland): The antibacterial activity was determined by the 2-fold microtiter broth dilution method (Wiegand & Hilpert, 2008). Dilutions of the test compounds dissolved in DMSO were added to each well of a 96-well microtiter plate containing a fixed volume of Mueller Hilton broth (final 0.64% DMSO). Each well was inoculated with an overnight culture of bacteria (5×10^5 cfu/mL), and the plate was incubated at 37 ˚C for 24 h. The minimum inhibitory concentration (MIC) was taken as the concentration at which no growth was observed.

References for Appendix A

Alfano, G.; Cimino, G.; De Stefano, S. *Experientia* **1979**, *35*, 1136 – 1137.

Anta, C.; González, N.; Rodriguez, J.; Jiménez, C. *J. Nat. Prod.* **2002**, *65*, 1357 – 1359.

Blunt, J.; Buchingham, J.; Munro, M. In *Handbook of Marine Natural Products*, Fattorusso, E.; Gerwick, W.; Taglialatela-Scafati, O. (Eds.) New York, Springer, **2012**, Vol. 1, pp. 4.

Cafieri, F.; Fattorusso, E.; Santocroce, C.; Minale, L. *Tetrahedron* **1972**, *28*, 1579 – 1583.

Cimino, G.; De Stefano, S.; Minale, L. *Experientia* **1972a**, *28*, 1401 – 1402.

Cimino, G.; De Stefano, S.; Minale, L. *Tetrahedron* **1972b**, *28*, 1315 – 1324.

De Pasquale, R.; Circosta, C.; Occhiuto, F.; De Rosa, S.; De Stefano, S. *Phytother. Res.* **1991**, *5*, 49 – 53.

De Rosa, S.; De giulio, A.; Crispino, A.; Iodice, C.; Tommonaro, G. *Nat. Prod. Lett.* **1997**, *10*, 7 – 12.

De Rosa, S.; Milone, A.; De Giulio, A.; Crispino, A.; Iodice, C. *Nat. Prod. Lett.* **1996**, *8*, 245 – 251.

Faulkner, D. *Tetrahedron Lett.* **1973**, *14*, 3821 – 3822.

Fu, X.; Ferreira, M. L. G.; Schmitz, F. J.; Kelly, M. *J. Org. Chem.* **1999**, *64*, 6706 – 6709.

Hertiani, T.; Edrada-Ebel, R.; Ortlepp, S.; van Soest, R.; de Voogd, N.; Wray, V.; Hentschel, U.; Kozytska, S.; Muller, W. E.; Proksch, P. *Bioorg. Med. Chem.* **2010**, *18*, 1297 – 1303.

Jeon, J.; Na, Z.; Jung, M.; Lee, H.; Sim, C.; Nahm, K.; Oh, K. B.; Shin, J. *J. Nat. Prod.* **2010**, *73*, 258 – 262.

Kawakami, A.; Miyamoto, T.; Higuchi, R.; Uchiumi, T.; Kuwano, M.; Van Soest, R. W. M. *Tetrahedron Lett.* **2001**, *42*, 3335 – 3337.

Keffer, J.; Plaza, A.; Bewley, C. A. *Org. Lett.* **2009**, *11*, 1087 – 1090.

Kondo, K.; Shigemori, H.; Kikuchi, Y.; Ishibashi, M.; Sasaki, T.;Kobayashi, J. *J. Org. Chem.* **1992**, *57*, 2480 – 2483.

Lu, Q.; Faulkner, D. J. *J. Nat. Prod.* **1997**, *60*, 195 – 198.

Manes, L.; Crews, P. *J. Nat. Prod.* **1986**, *49*, 787 – 793.

Martins, A.; Vieira, H.; Gaspar, H.; Santos, S. *Mar. Drugs* **2014**, *12*, 1066 - 1101.

Nakao, Y.; Matsunaga, S.; Fusetani, N. *Bioorg. Med. Chem.* **1995**, *3*, 1115 – 1122.

Reddy, M.; Harper, M.; Faulkner, D. *J. Nat. Prod.* **1997**, *60*, 41 – 43.

Rothberg, I.; Shubiak, P. *Tetrahedron Lett.* **1975**, *16*, 769 – 772.

Venkateswarlu, Y.; Reddy, M. V. R. *J. Nat. Prod.* **1994**, *57*, 1286 – 1289.

Venkateswarlu, Y.; Reddy, M. V. R.; Rao, M. R. *J. Nat. Prod.* **1996**, *59*, 876 – 887.

Wiegand, I.; Hilpert, K.; Hancock, R. *Nat. Protoc.* **2008**, *3*, 163 – 175.

Wright, A.; McCluskey, A.; Robertson, M.; MacGregor, K.; Gordon, C.; Guenther, J. *J. Org. Biomol. Chem.* **2011**, *9*, 400 – 407.

Xu, S.; Liao, X.; Du, B.; Zhou, X. L.; Huang, Q.; Wu, C. *Steroids* **2008**, *73*, 568 – 573.

A.2 NMR spectra of 9,11-Secosterol A

Figure A.2.1 ^{1}H NMR Spectrum of **9,11-Secosterol A** ($CDCl_3$, 600 MHz)

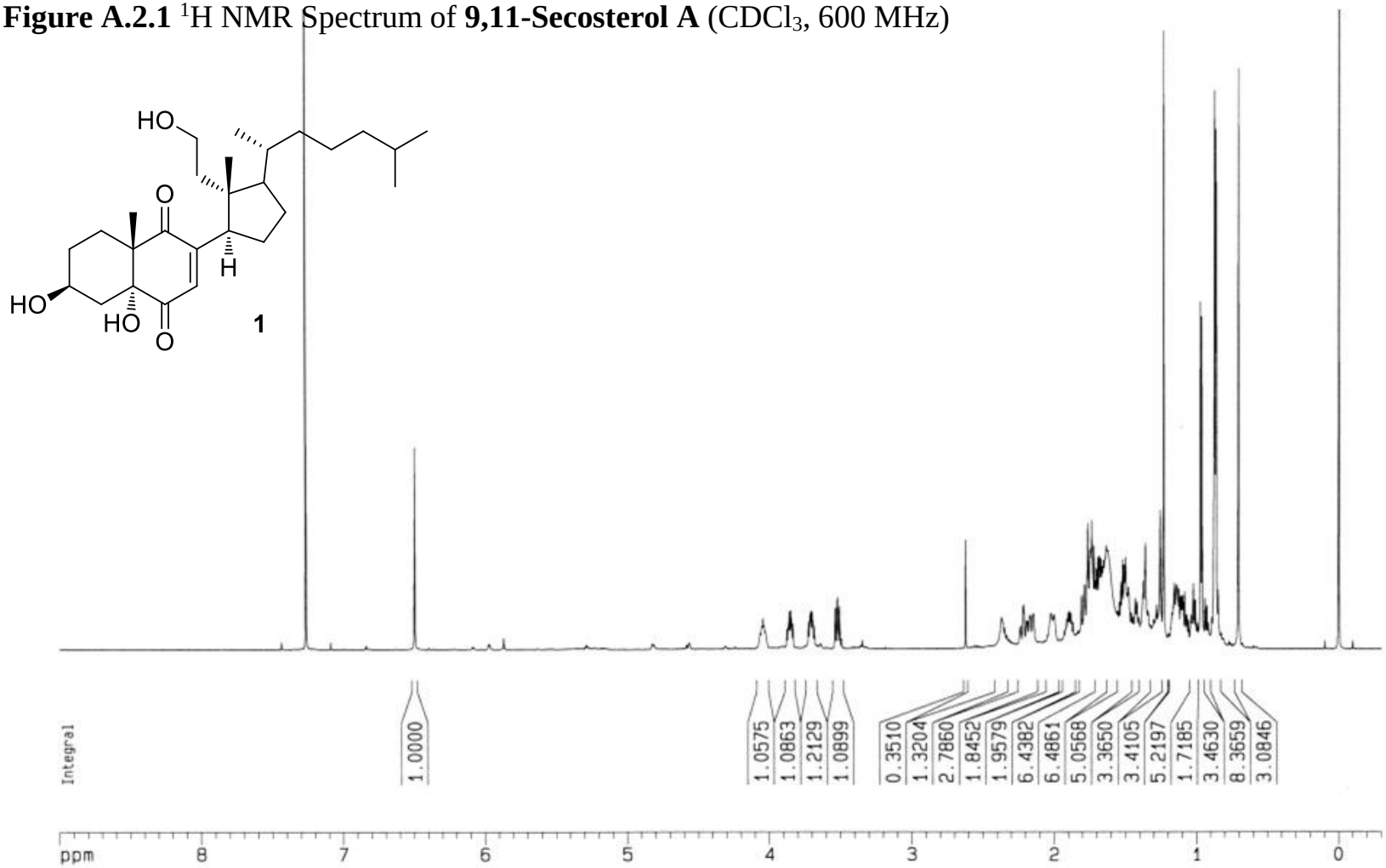

Figure A.2.2 ^{13}C NMR Spectrum of **9,11-Secosterol A** ($CDCl_3$, 150 MHz)

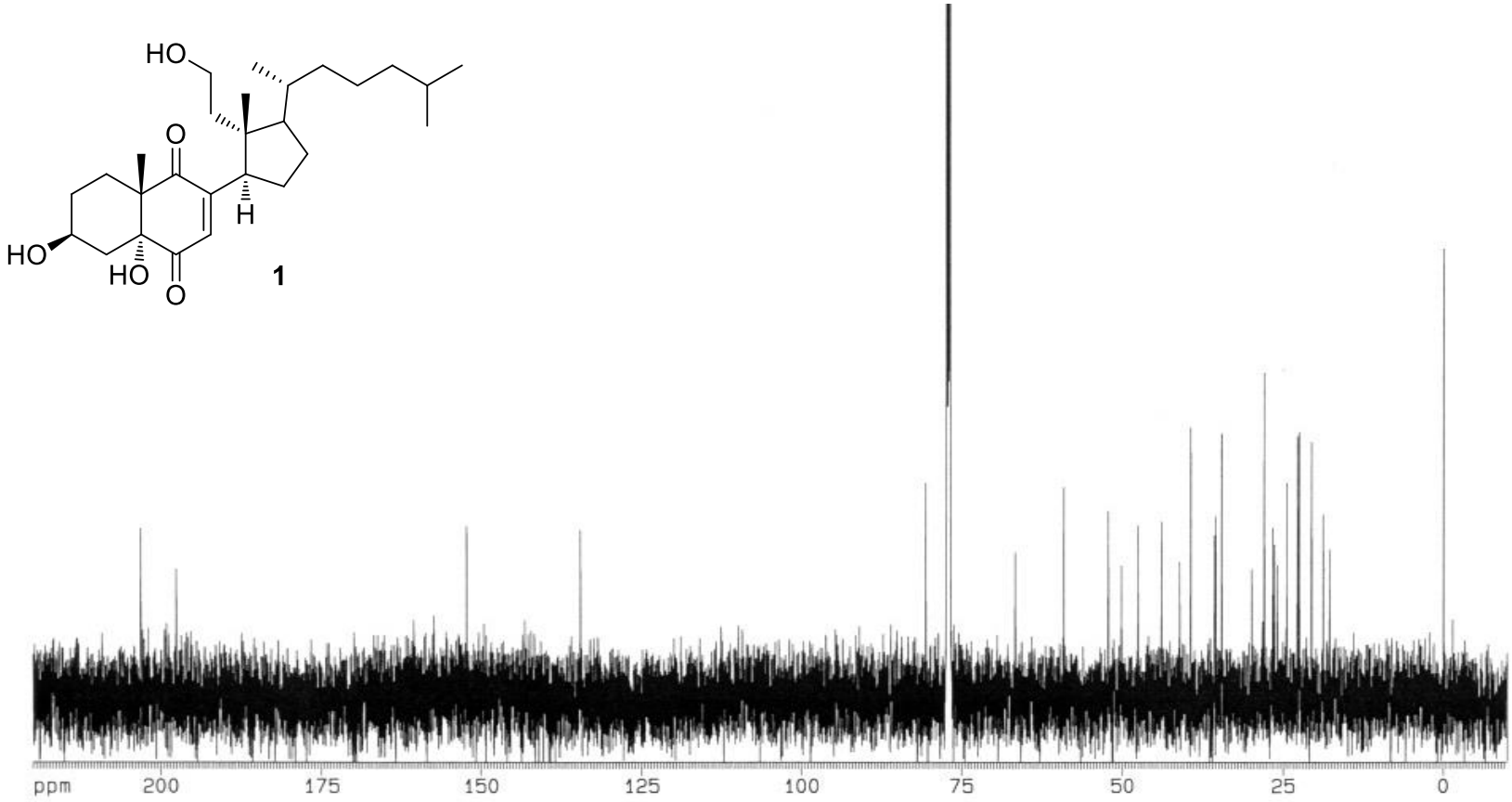

Figure A.2.3 COSY NMR Spectrum of **9,11-Secosterol A** ($CDCl_3$, 600 MHz)

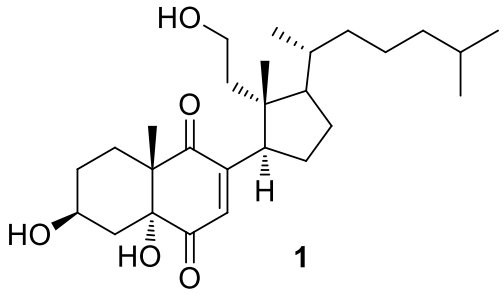

1

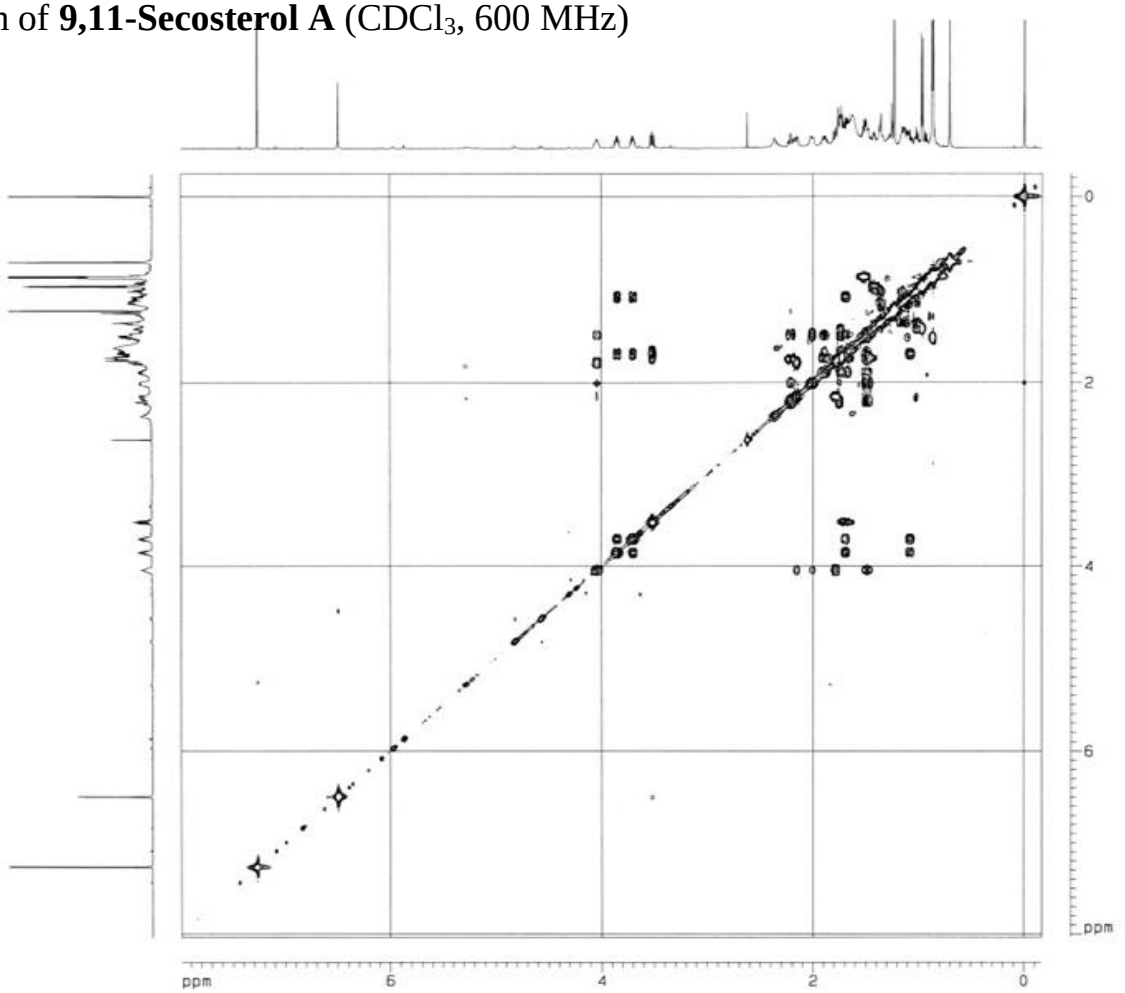

Figure A.2.4 HSQC Spectrum of **9,11-Secosterol A** ($CDCl_3$, 600 MHz)

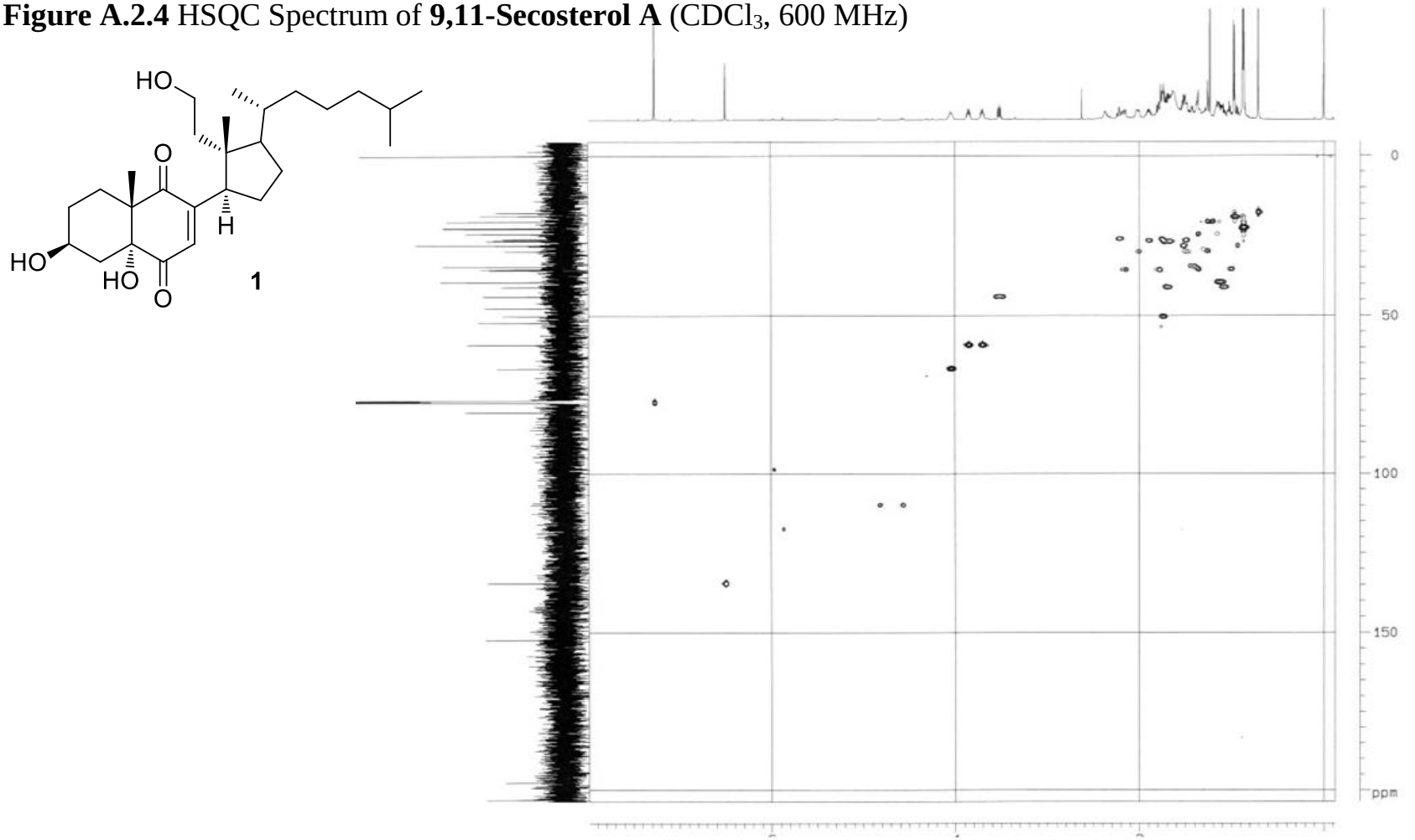

Figure A.2.5 HMBC NMR Spectrum of **9,11-Secosterol A** ($CDCl_3$, 600 MHz)

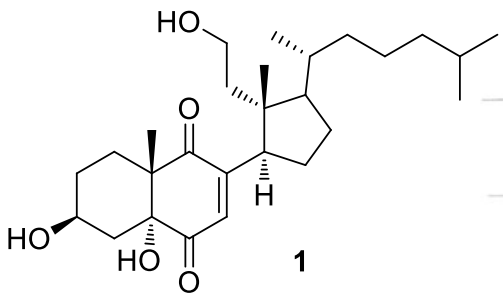

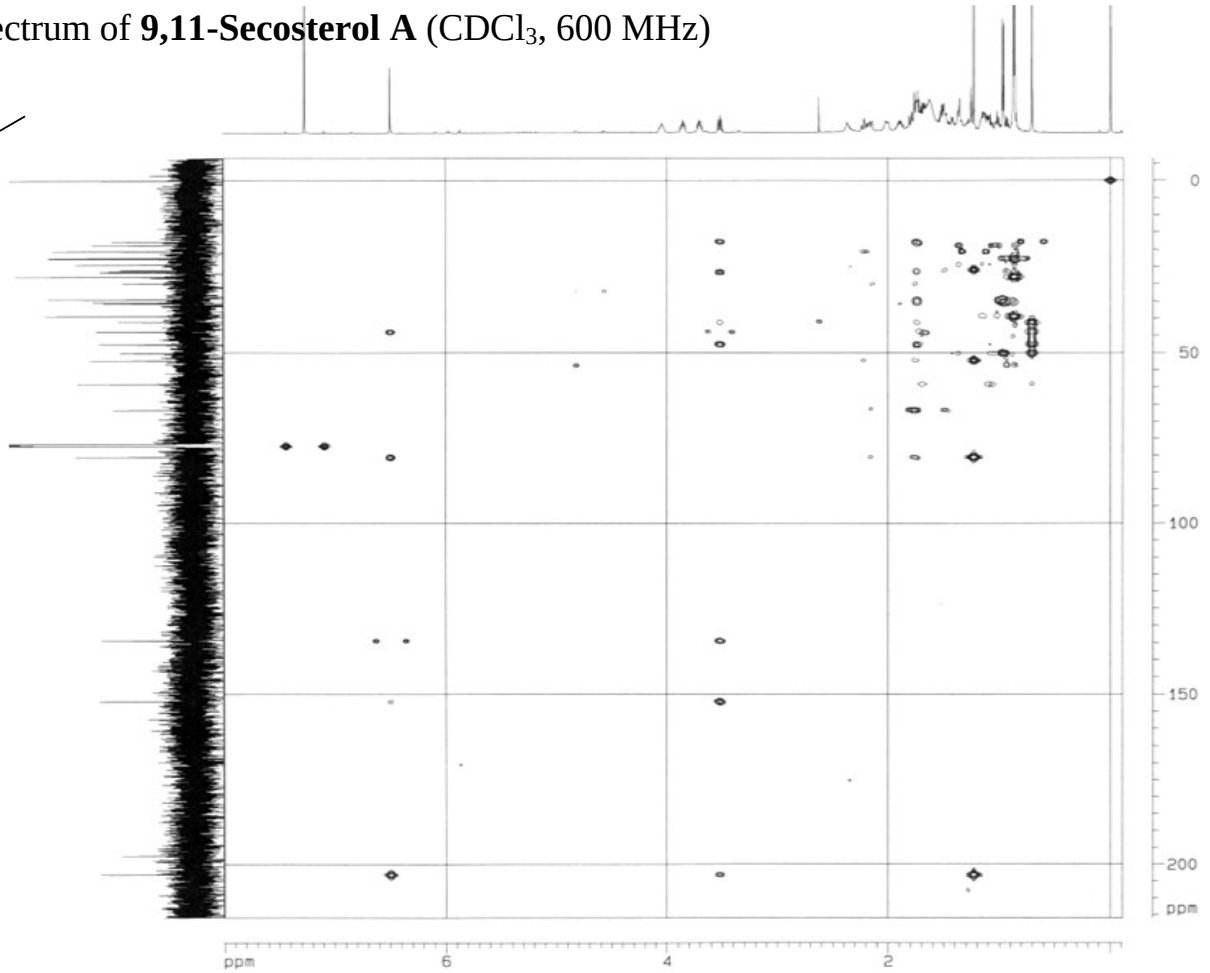

Figure A.2.6 NOESY NMR Spectrum of **9,11-Secosterol A** ($CDCl_3$, 600 MHz)

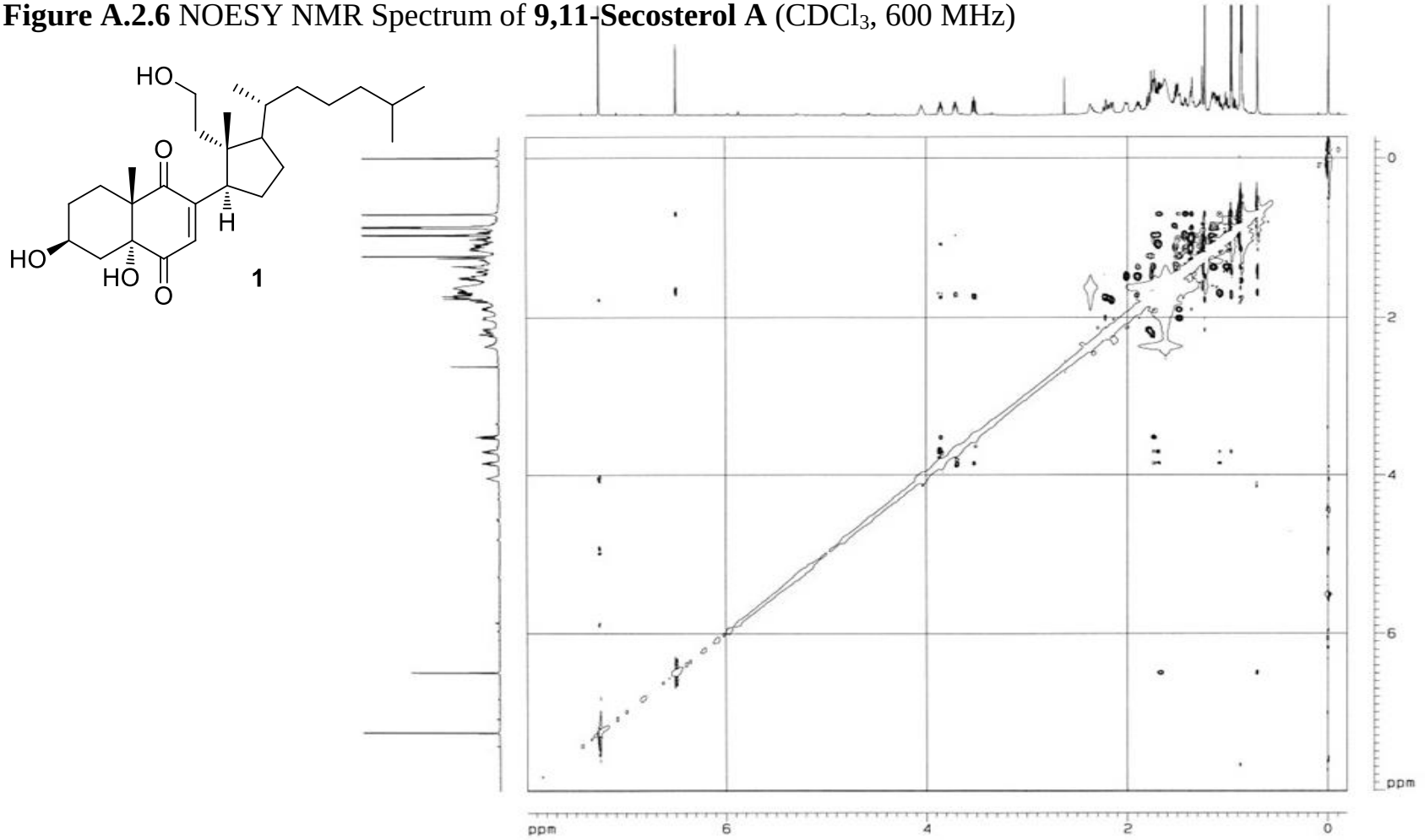

Appendix B

B.1 NMR Spectra of Nocrimidazoles A and B

Figure B.1.1 ^{1}H NMR Spectrum of Nocarimidazol A (**1**) ($CDCl_3$, 500 MHz)

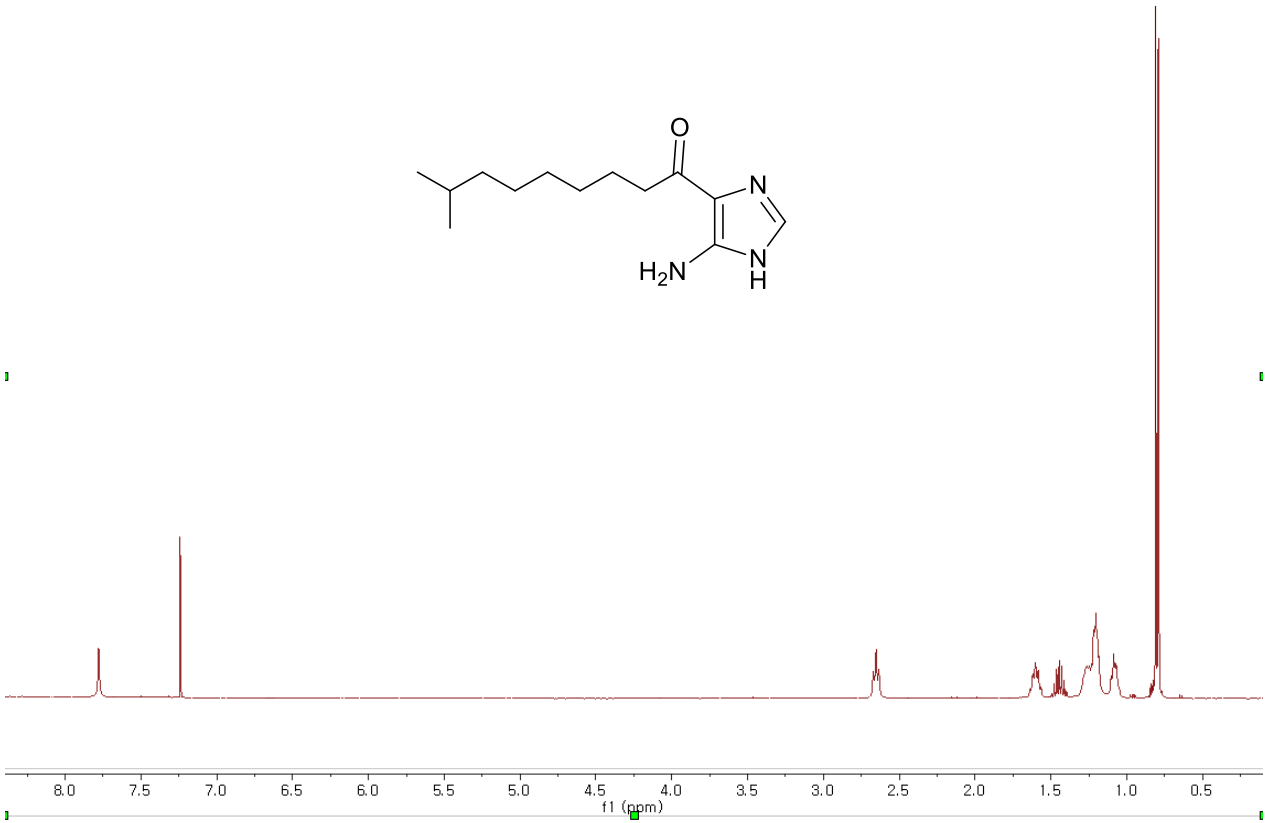

Figure B.1.2 ^{13}C NMR Spectrum of Nocarimidazol A (**1**) ($CDCl_3$, 125 MHz)

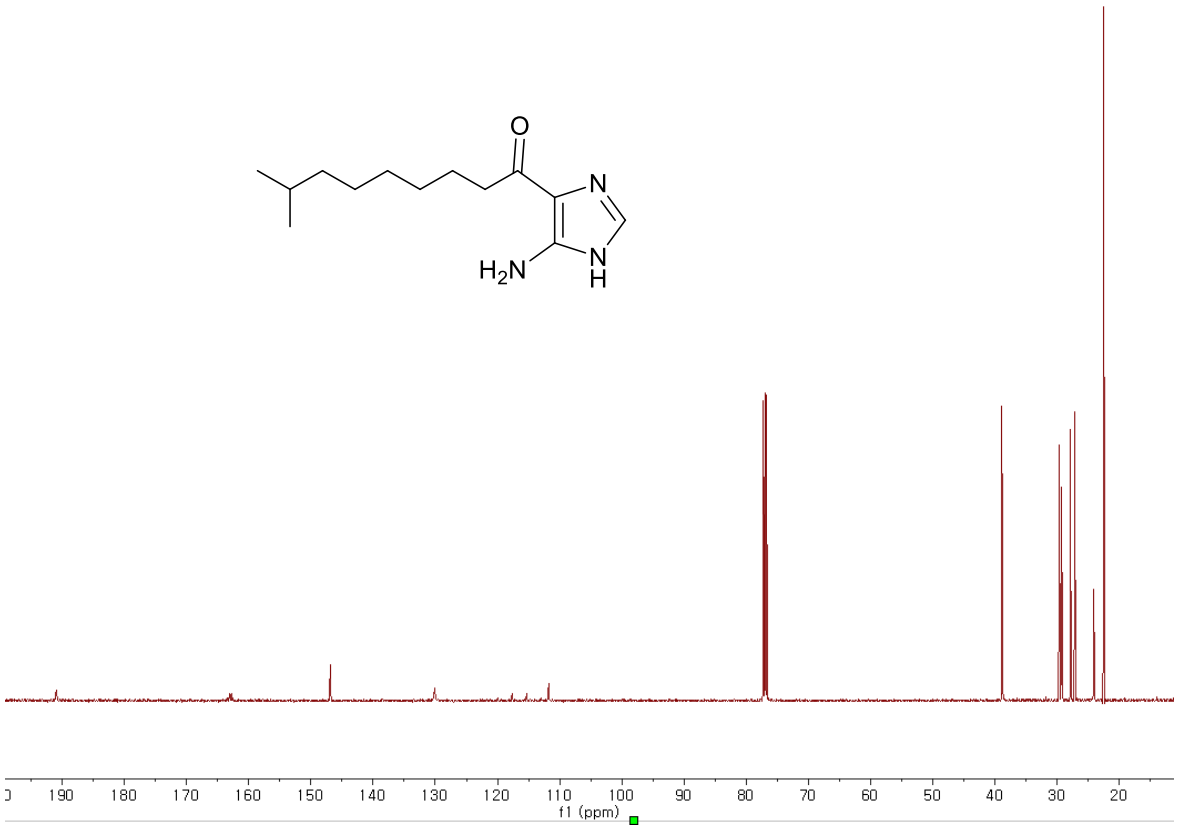

Figure B.1.3 COSY Spectrum of Nocarimidazol A (**1**) ($CDCl_3$, 500 MHz)

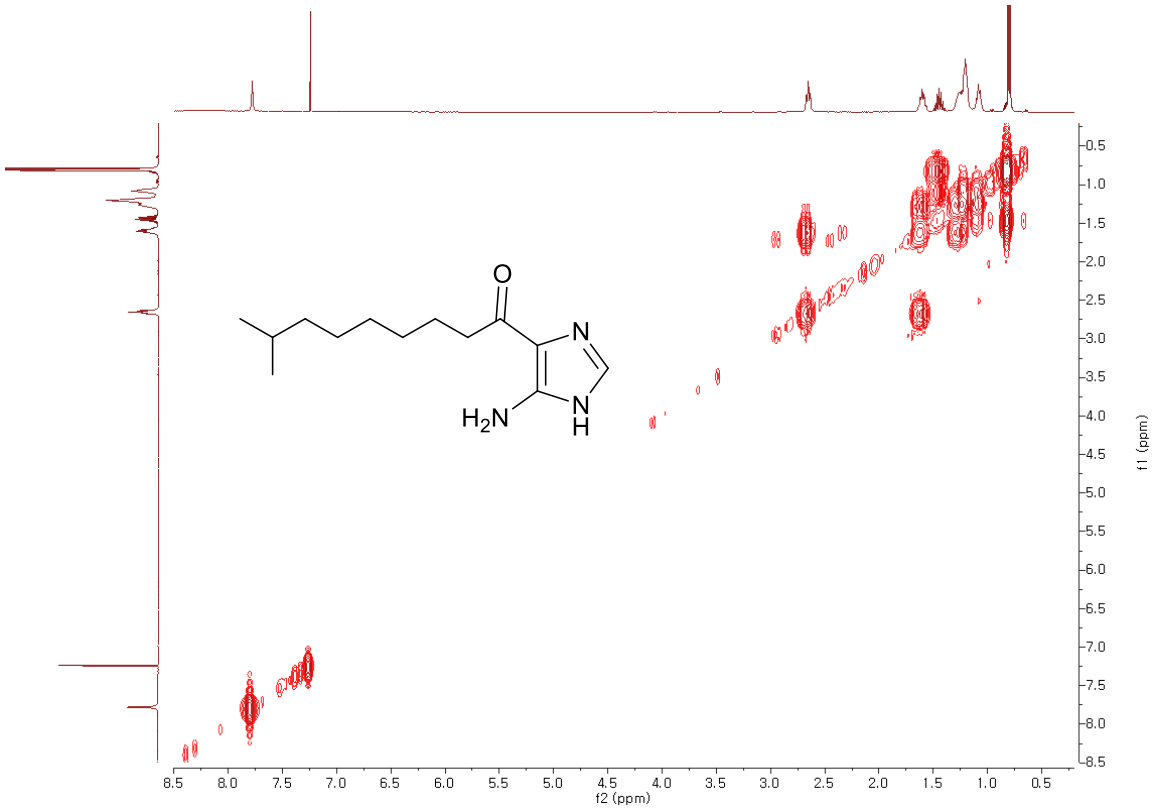

Figure B.1.4 HSQC Spectrum of Nocarimidazol A (**1**) ($CDCl_3$, 500 MHz)

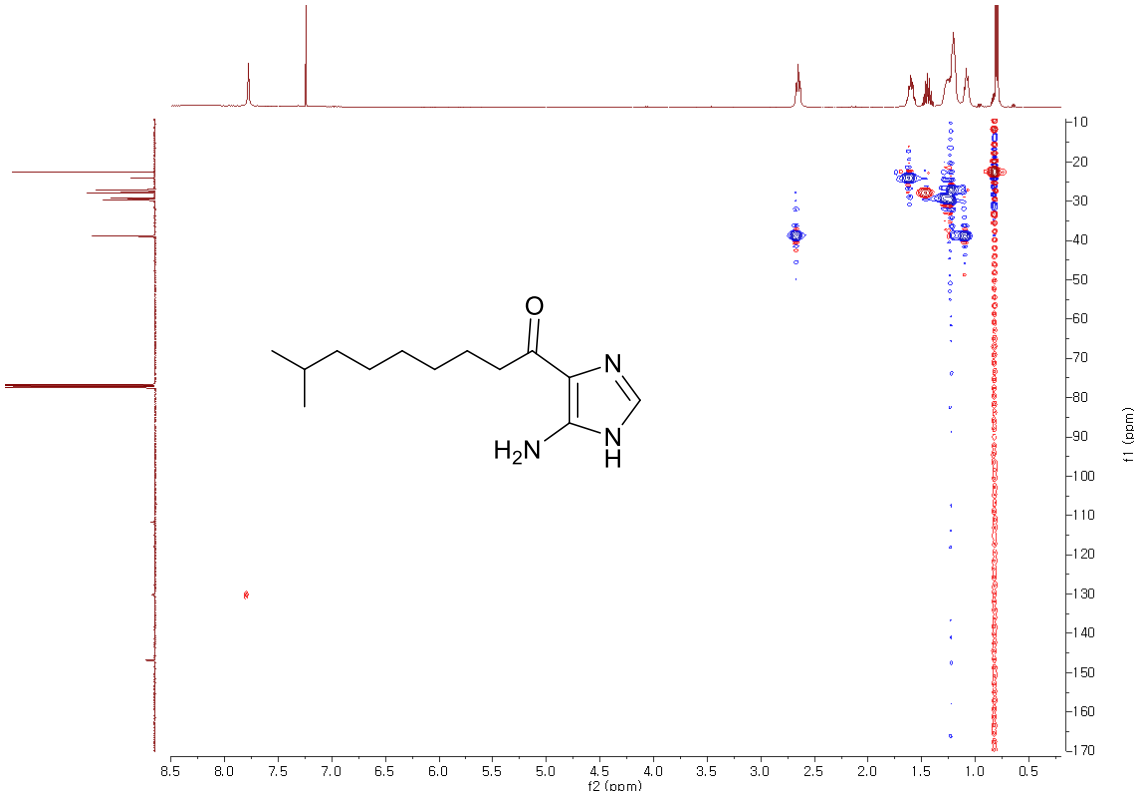

Figure B.1.5 HMBC Spectrum of Nocarimidazol A (**1**) ($CDCl_3$, 500 MHz)

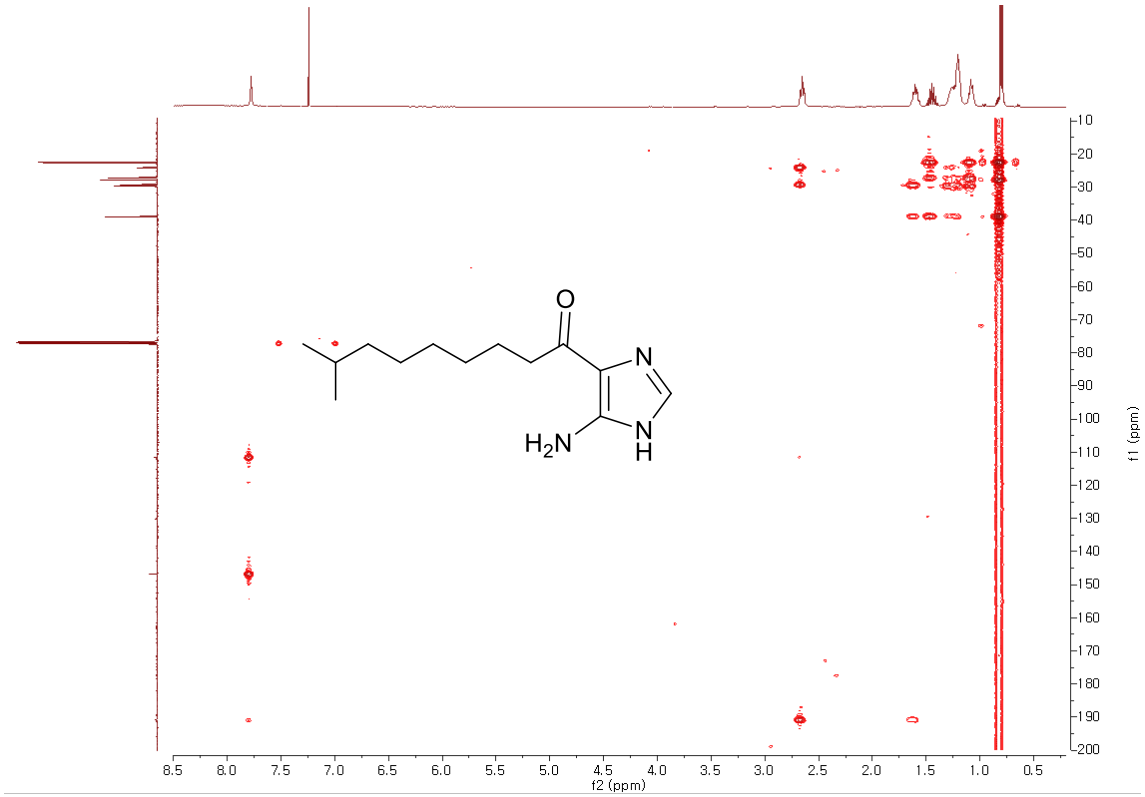

Figure B.1.6 ^{1}H NMR Spectrum of Nocarimidazol B (**2**) ($CDCl_3$, 500 MHz)

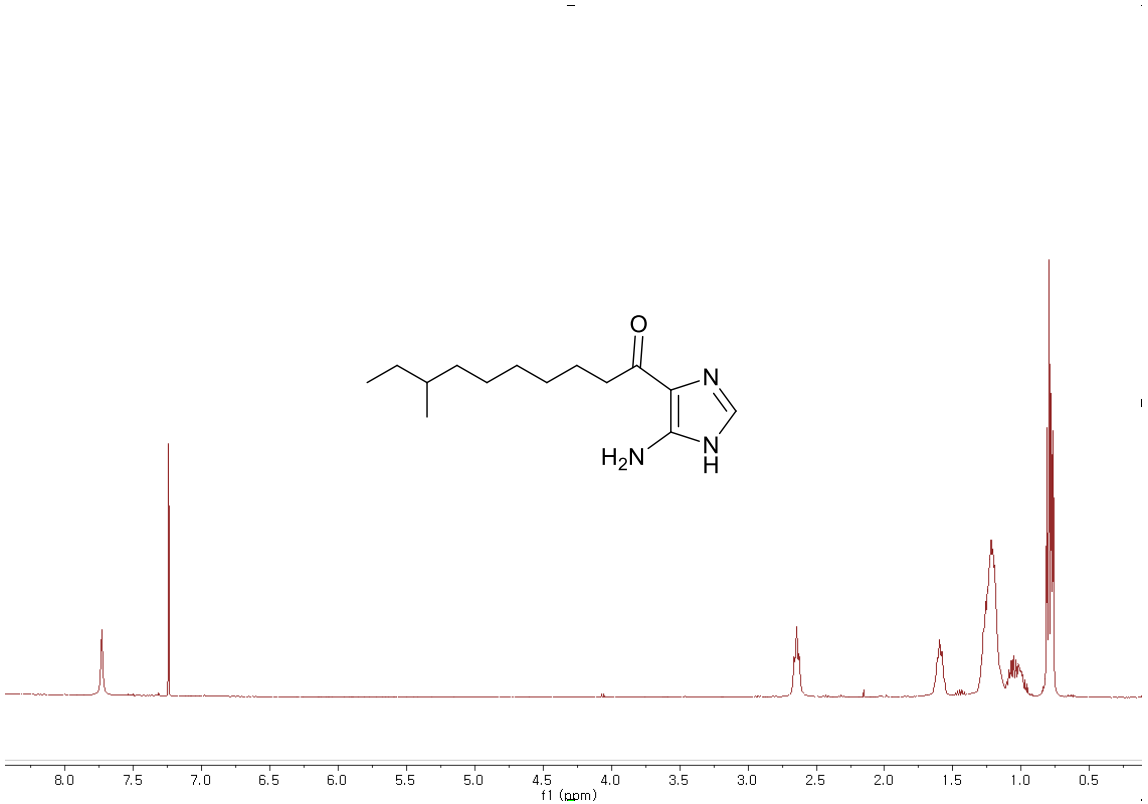

Figure B.1.**7** ^{13}C NMR Spectrum of Nocarimidazol B (**2**) ($CDCl_3$, 125 MHz)

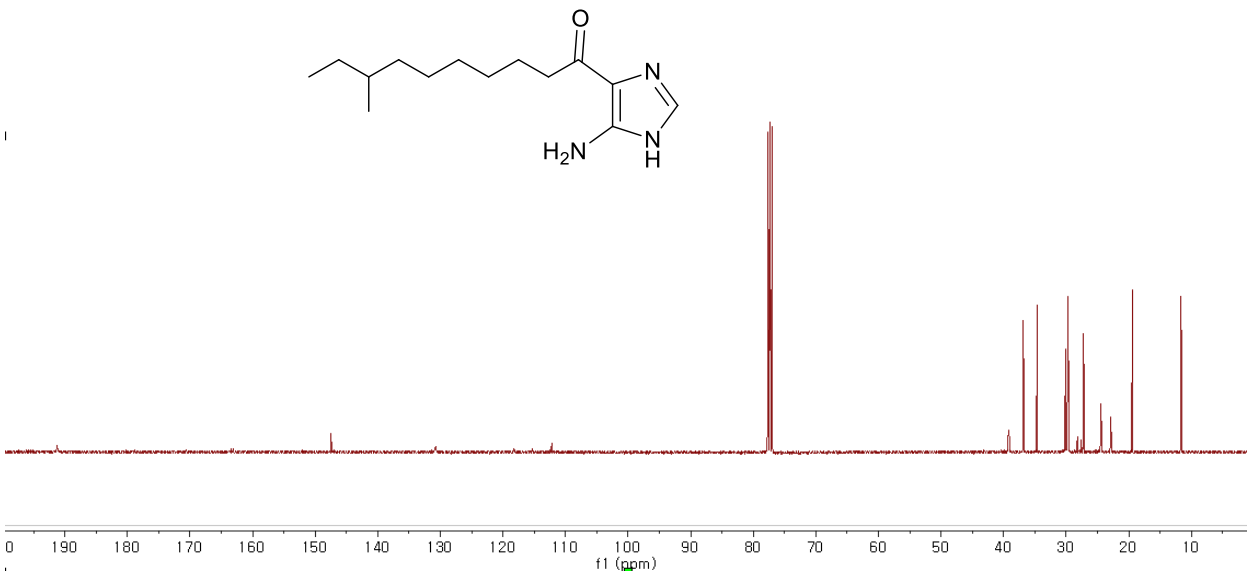

Figure B.1.8 COSY Spectrum of Nocarimidazol B (**2**) ($CDCl_3$, 500 MHz)

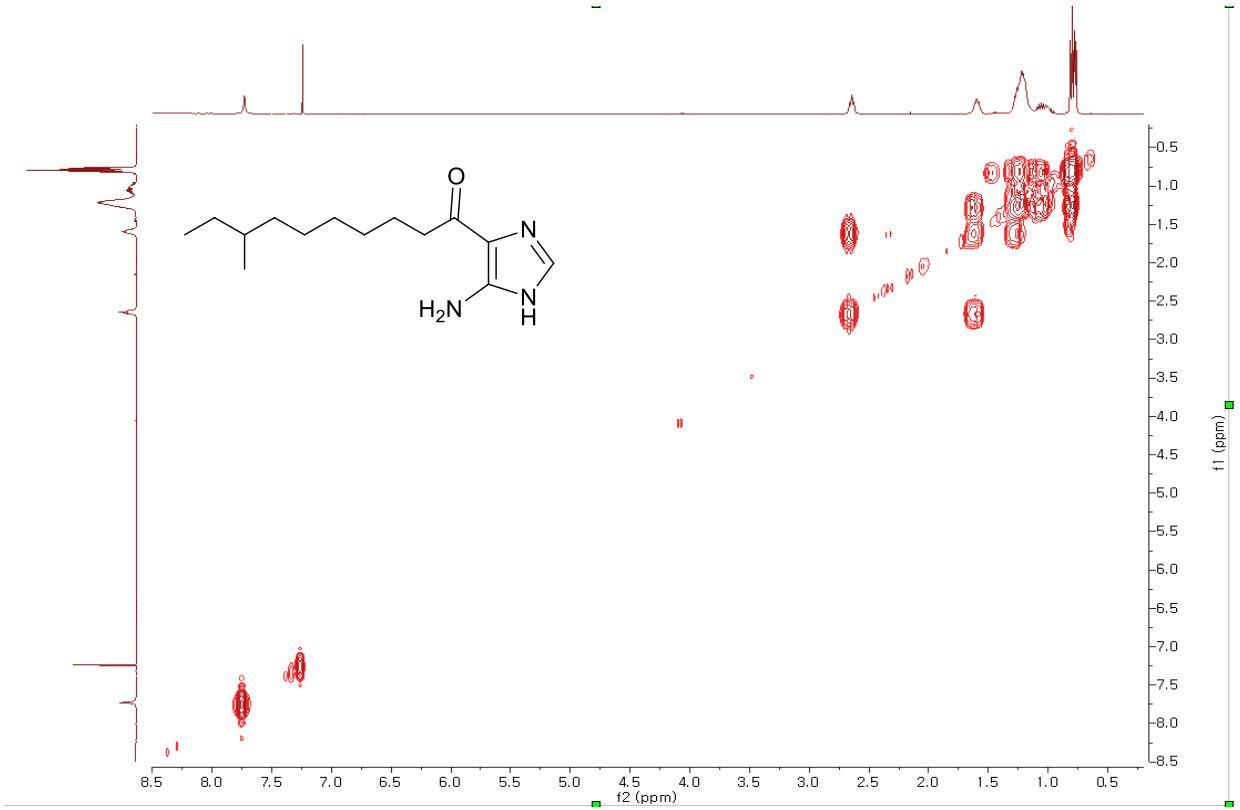

Figure B.1.9 HSQC Spectrum of Nocarimidazol B (**2**) ($CDCl_3$, 500 MHz)

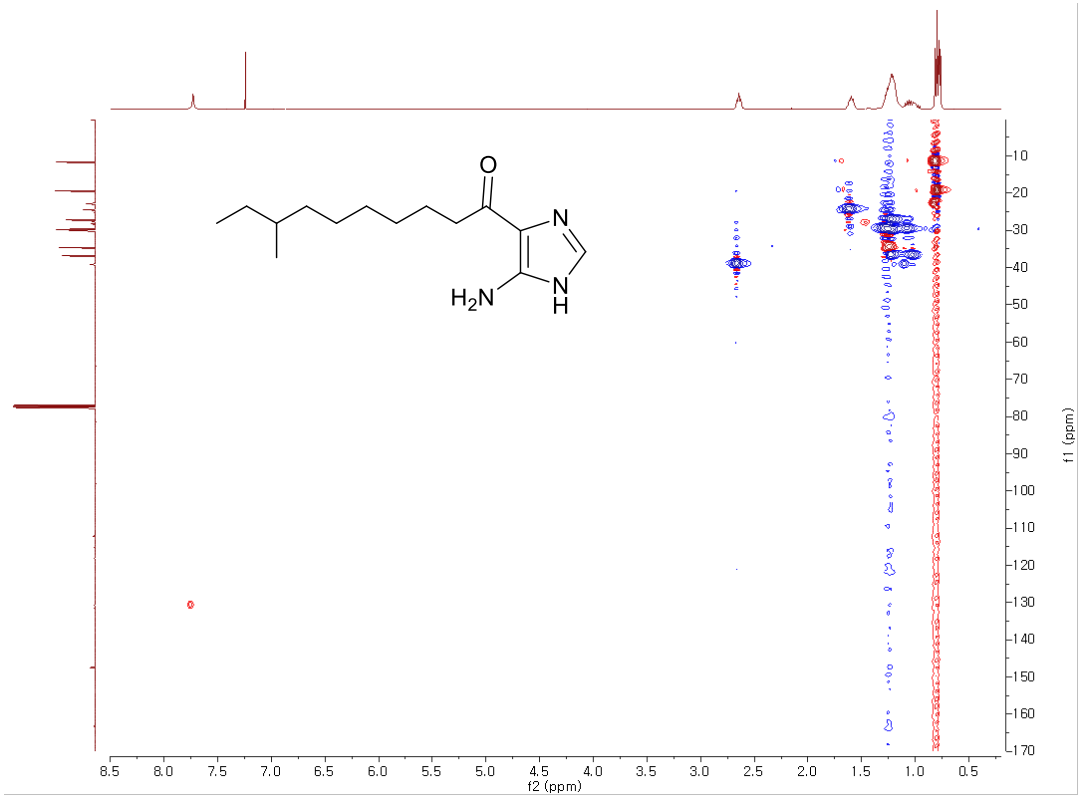

Figure B.1.10 HMBC Spectrum of Nocarimidazol B (**2**) ($CDCl_3$, 500 MHz)

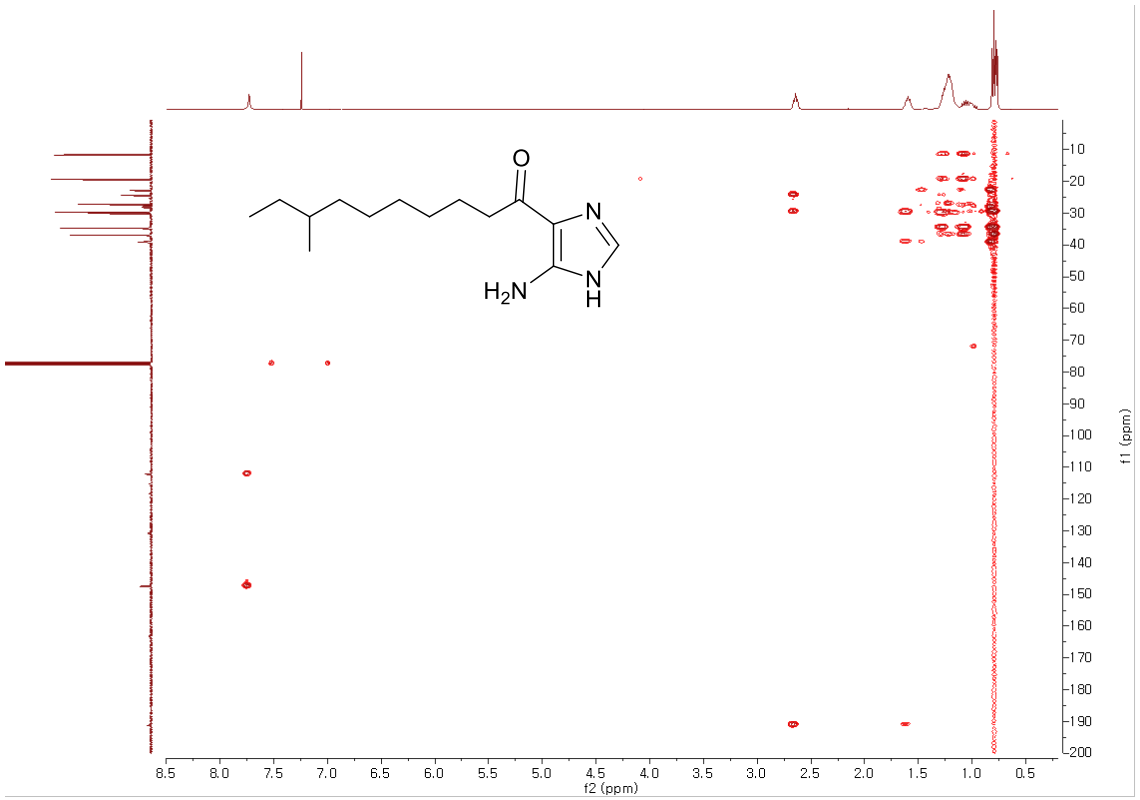

Figure B.1.11 ^{1}H NMR Spectrum of Nocarimidazole B Diazomethane derivative (**3**) ($CDCl_3$, 700 MHz)

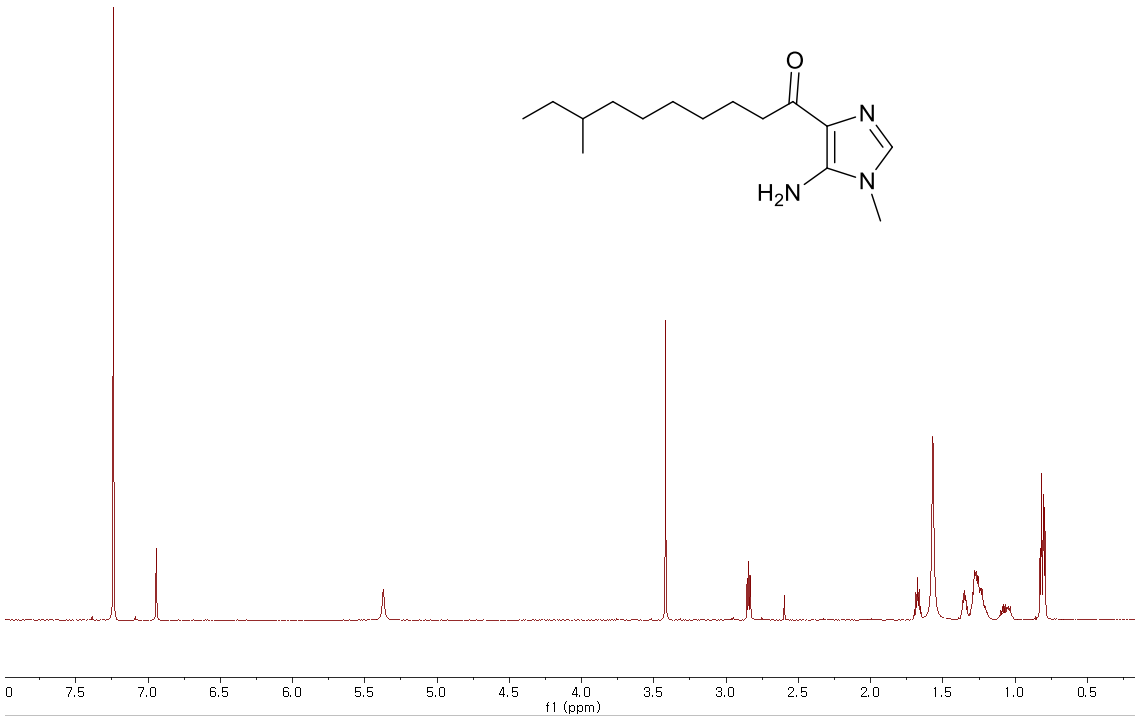

Figure B.1.12 COSY Spectrum of Nocarimidazole B Diazomethane derivative (**3**) ($CDCl_3$, 700 MHz)

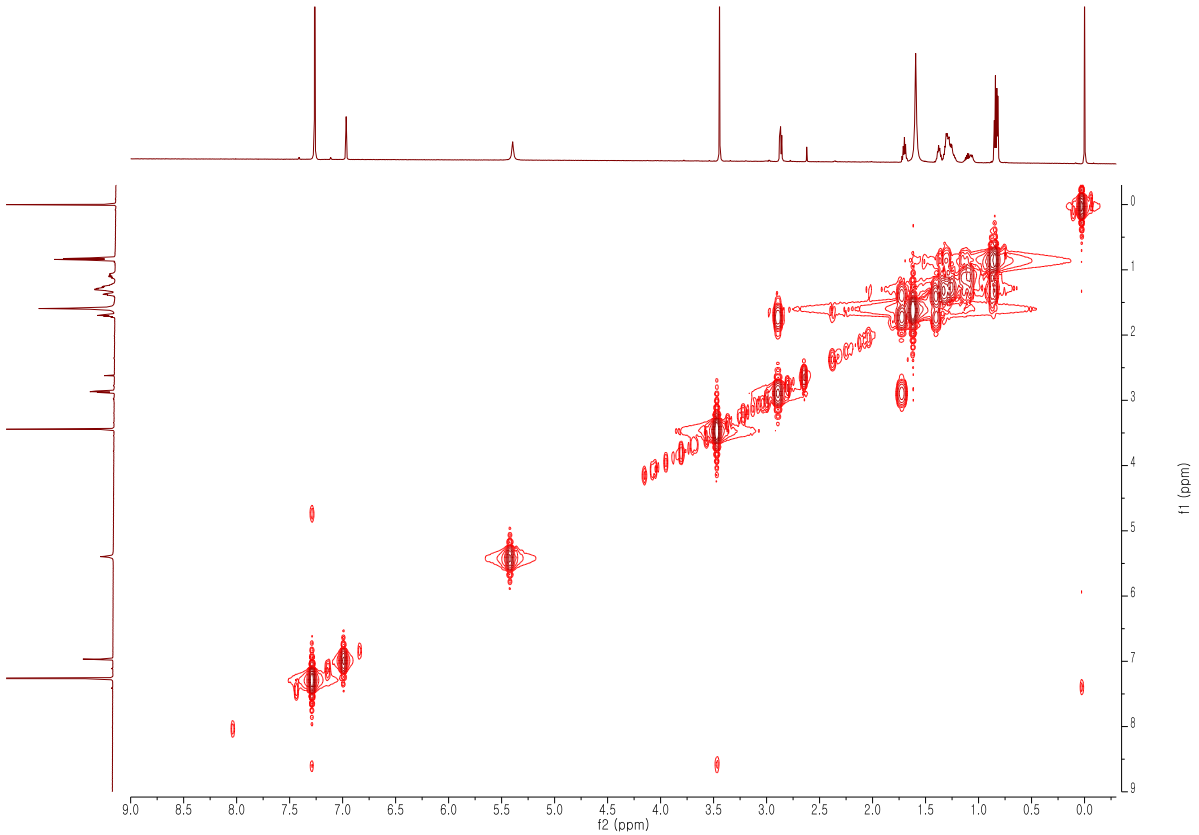

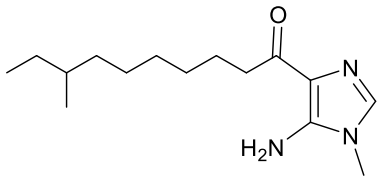

Figure B.1.13 HSQC Spectrum of Nocarimidazole B Diazomethane derivative (**3**) ($CDCl_3$, 700 MHz)

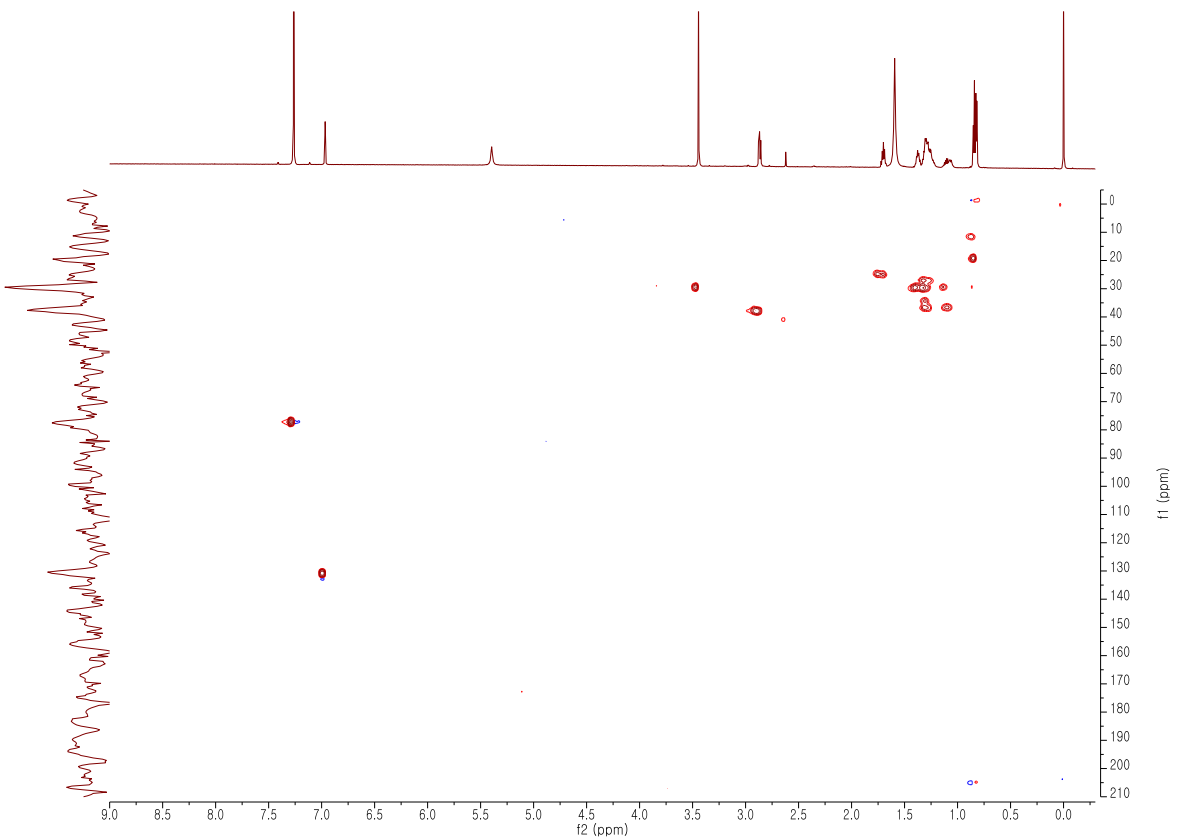

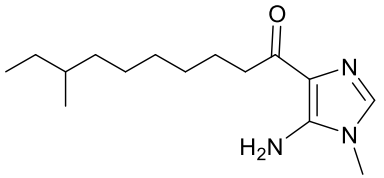

Figure B.1.14 HMBC Spectrum of Nocarimidazole B Diazomethane derivative (**3**) ($CDCl_3$, 700 MHz)

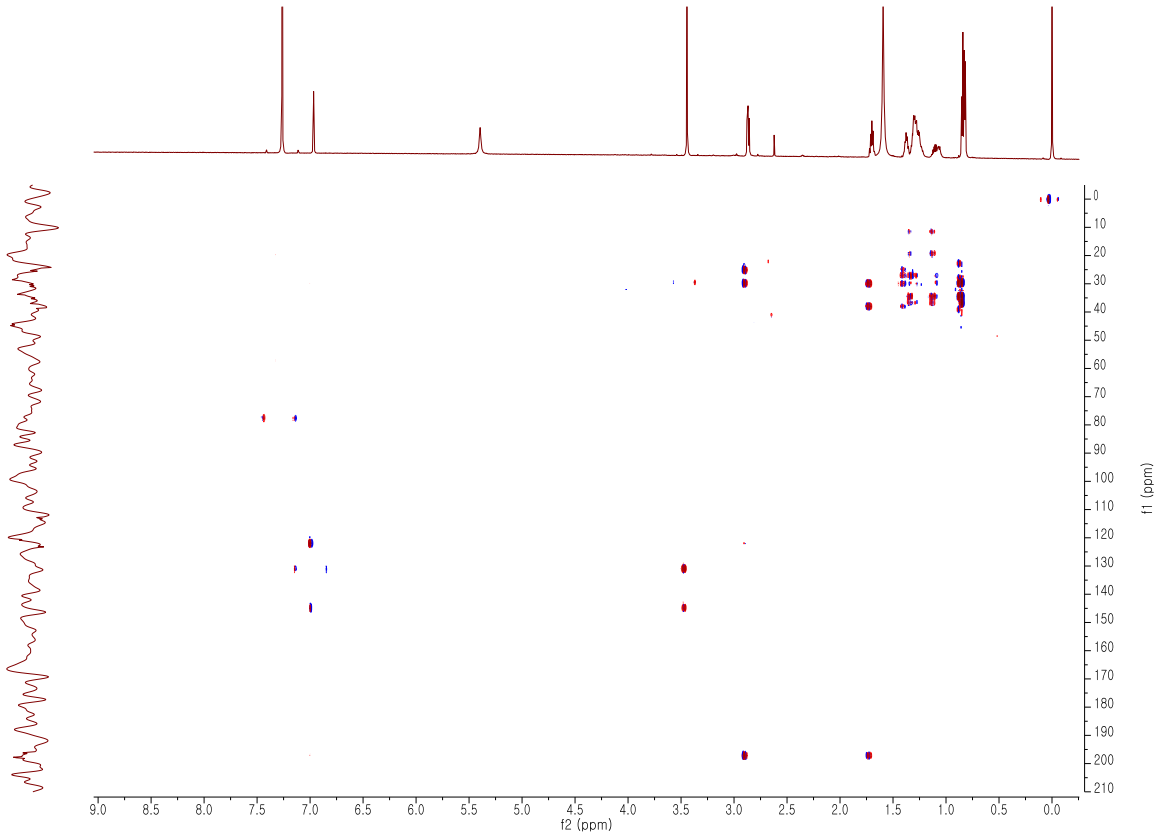

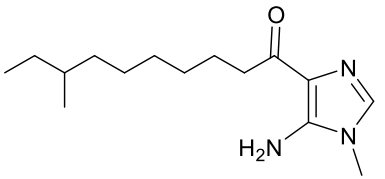

Figure B.1.15 ^{1}H NMR Spectrum of Nocarimidazole B Iodomethane Derivative (**4**) ($CDCl_3$, 700 MHz)

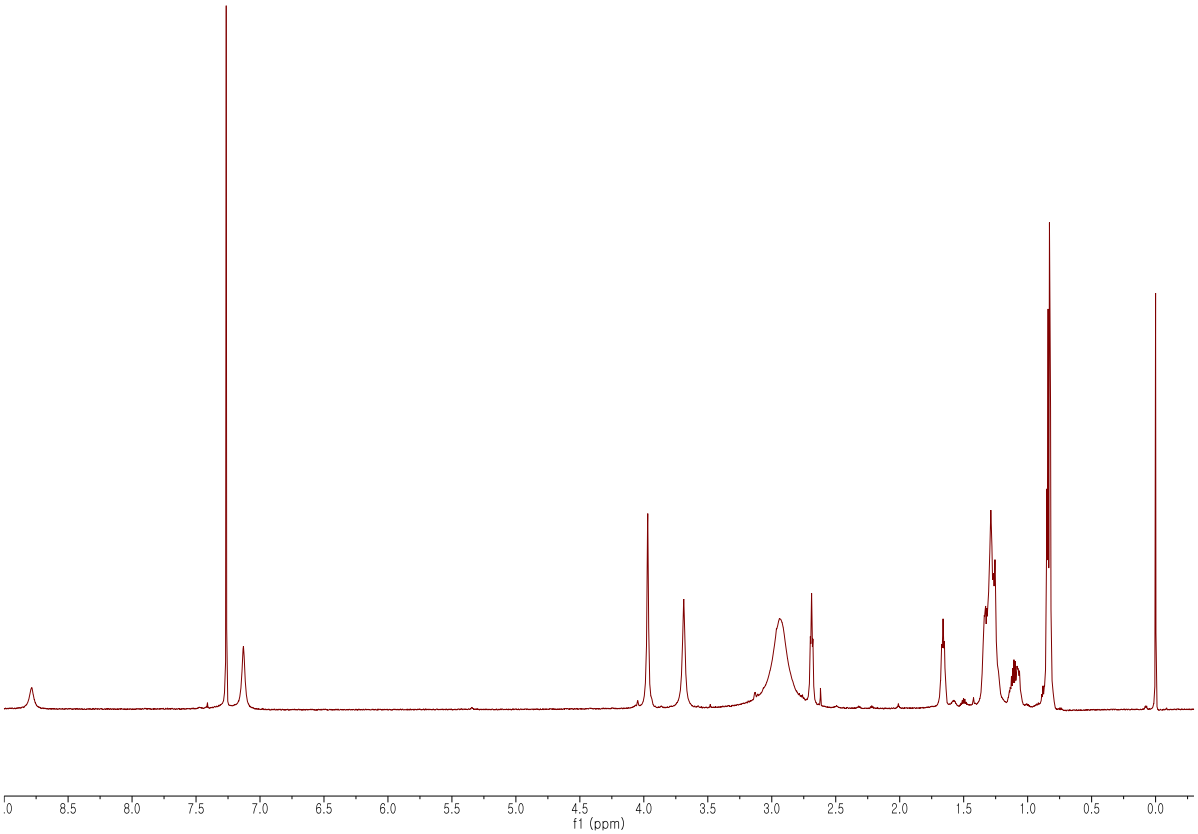

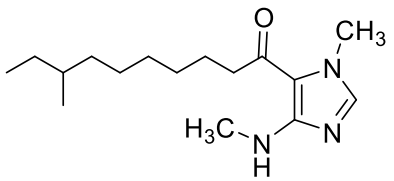

Figure B.1.16 COSY Spectrum of Nocarimidazole B Iodomethane Derivative (**4**) ($CDCl_3$, 700 MHz)

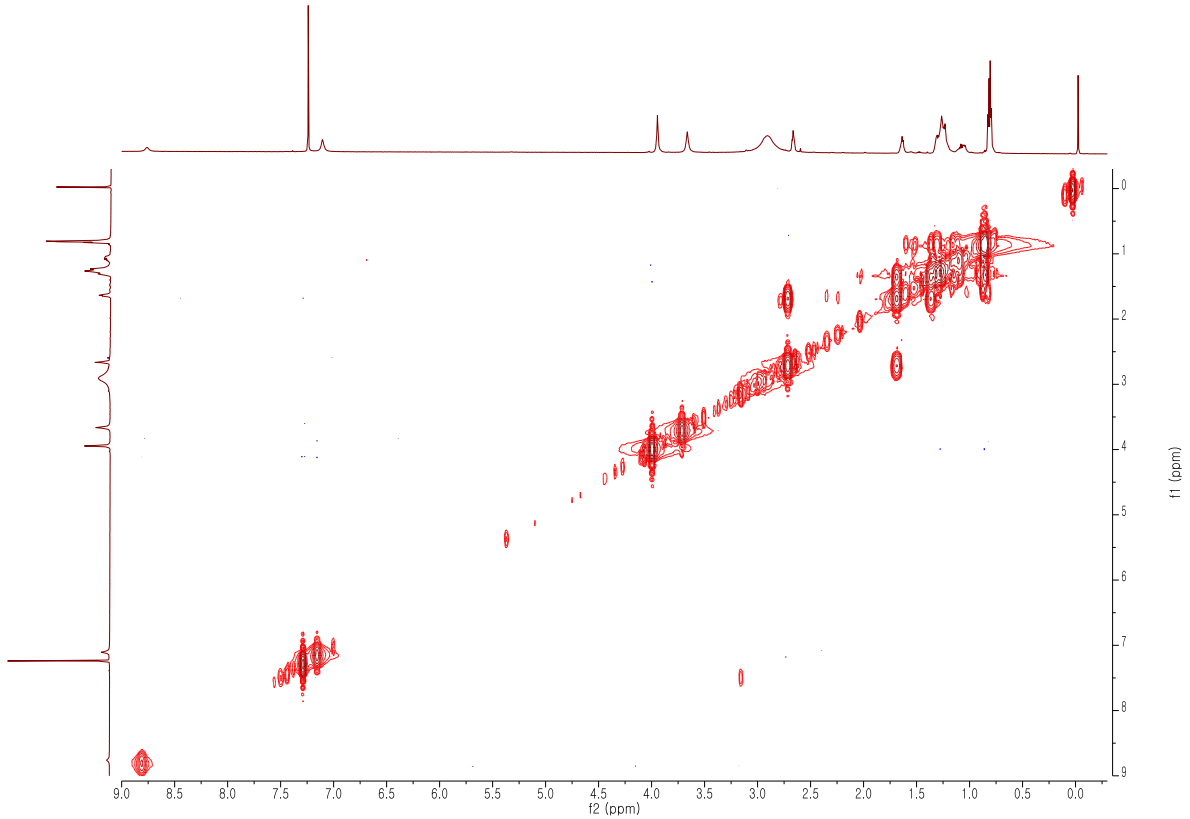

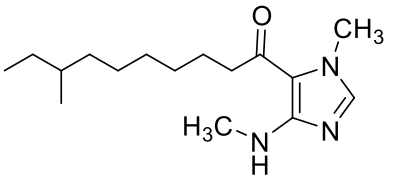

Figure B.1.17 HSQC Spectrum of Nocarimidazole B Iodomethane Derivative (**4**) ($CDCl_3$, 700 MHz)

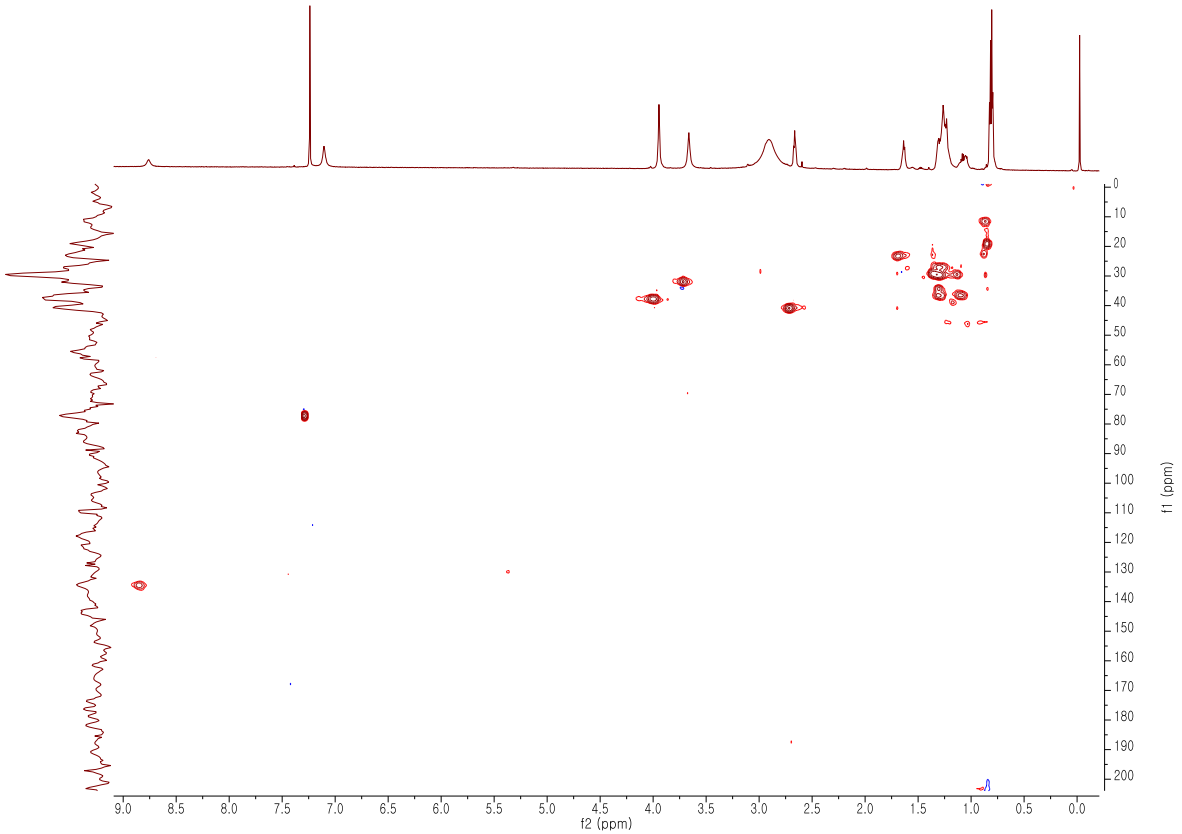

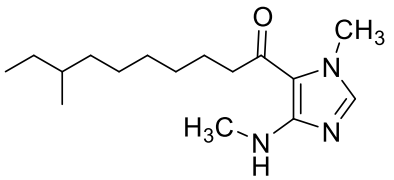

Figure B.1.18 HMBC Spectrum of Nocarimidazole B Iodomethane Derivative (**4**) ($CDCl_3$, 700 MHz)

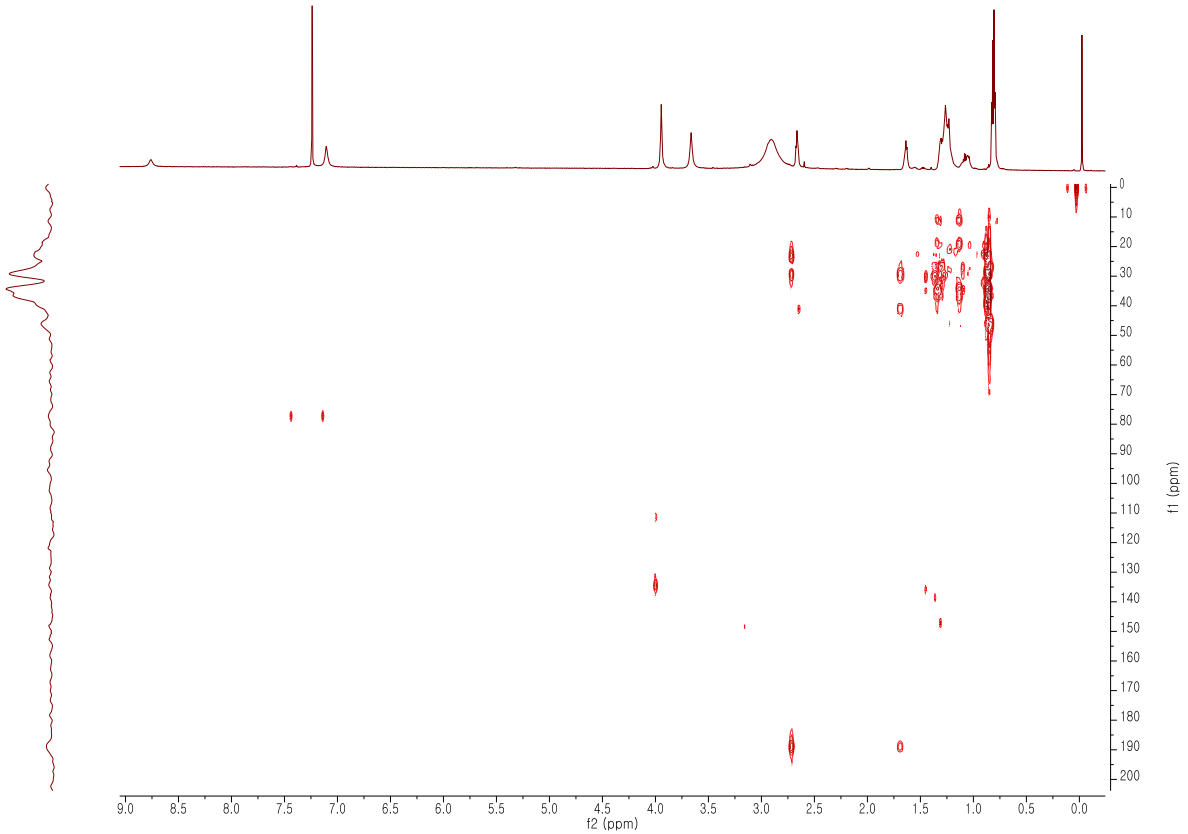

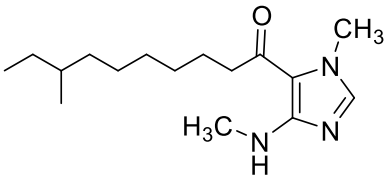

B.2 NMR Spectra of Anithiactins A-D

Figure B.2.1 ^{1}H NMR spectrum of Anithiactin A ($CDCl_3$, 600 MHz)

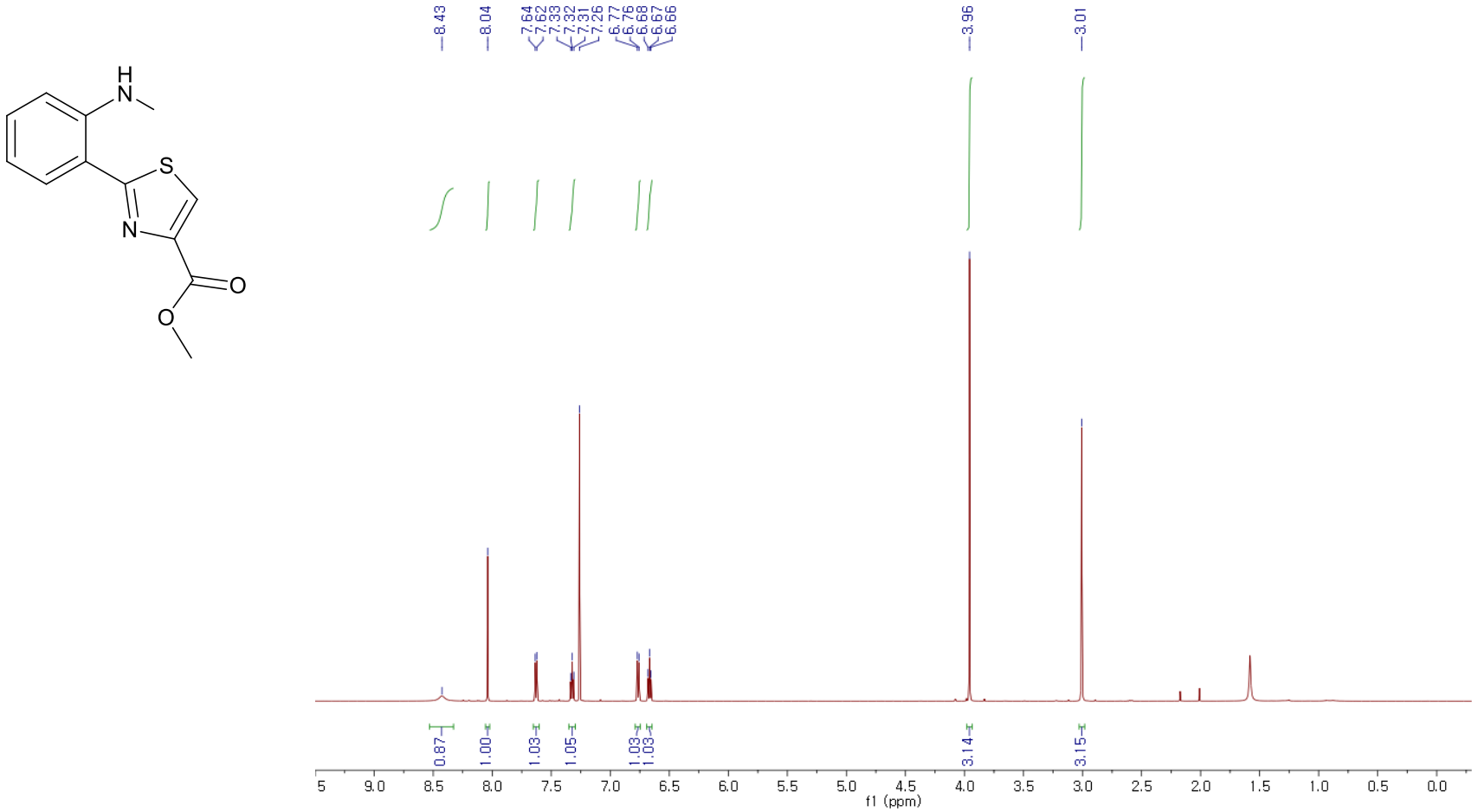

Figure B.2.2 ^{13}C NMR spectrum of Anithiactin A ($CDCl_3$, 600 MHz)

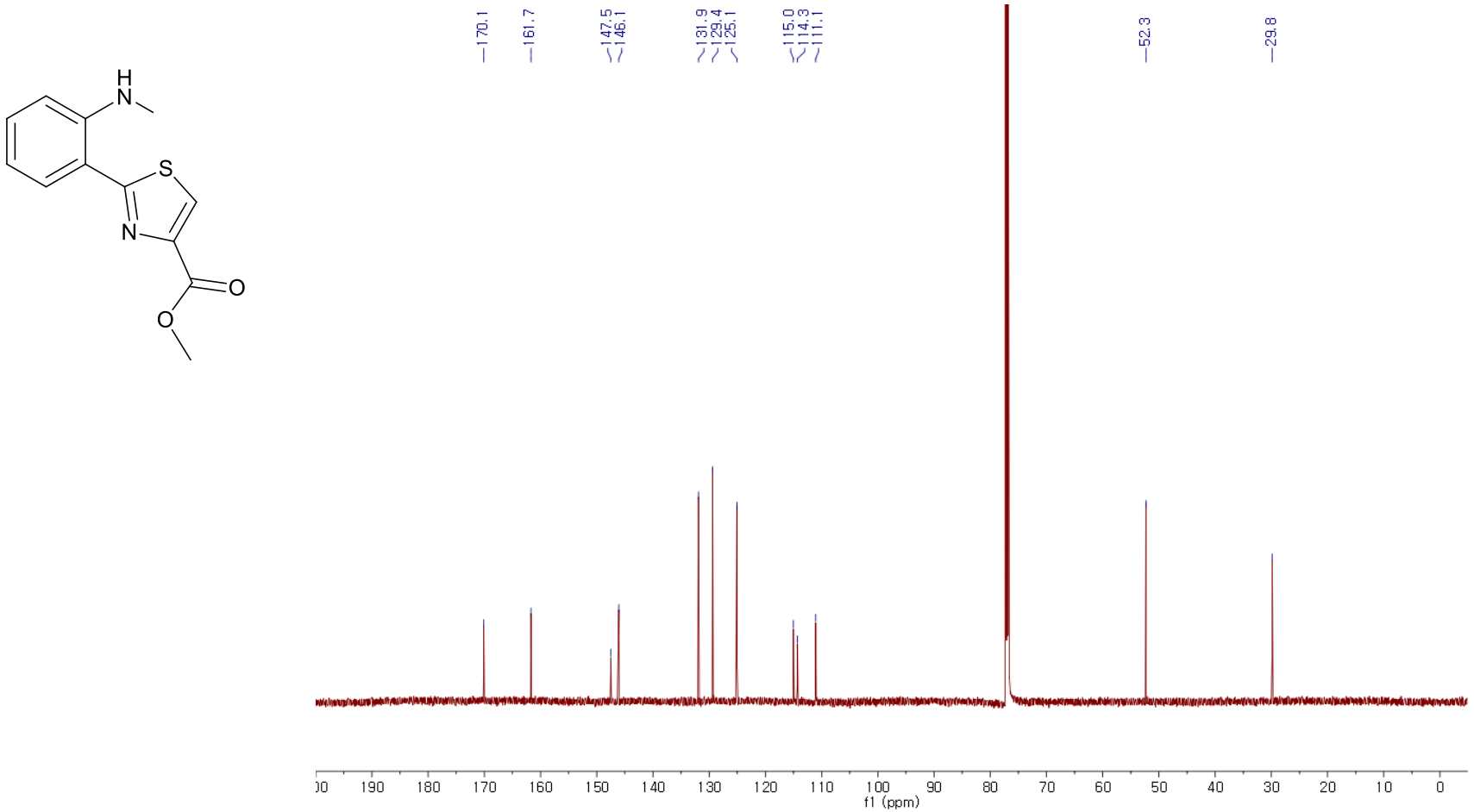

Figure B.2.3 COSY spectrum of Anithiactin A ($CDCl_3$, 600 MHz)

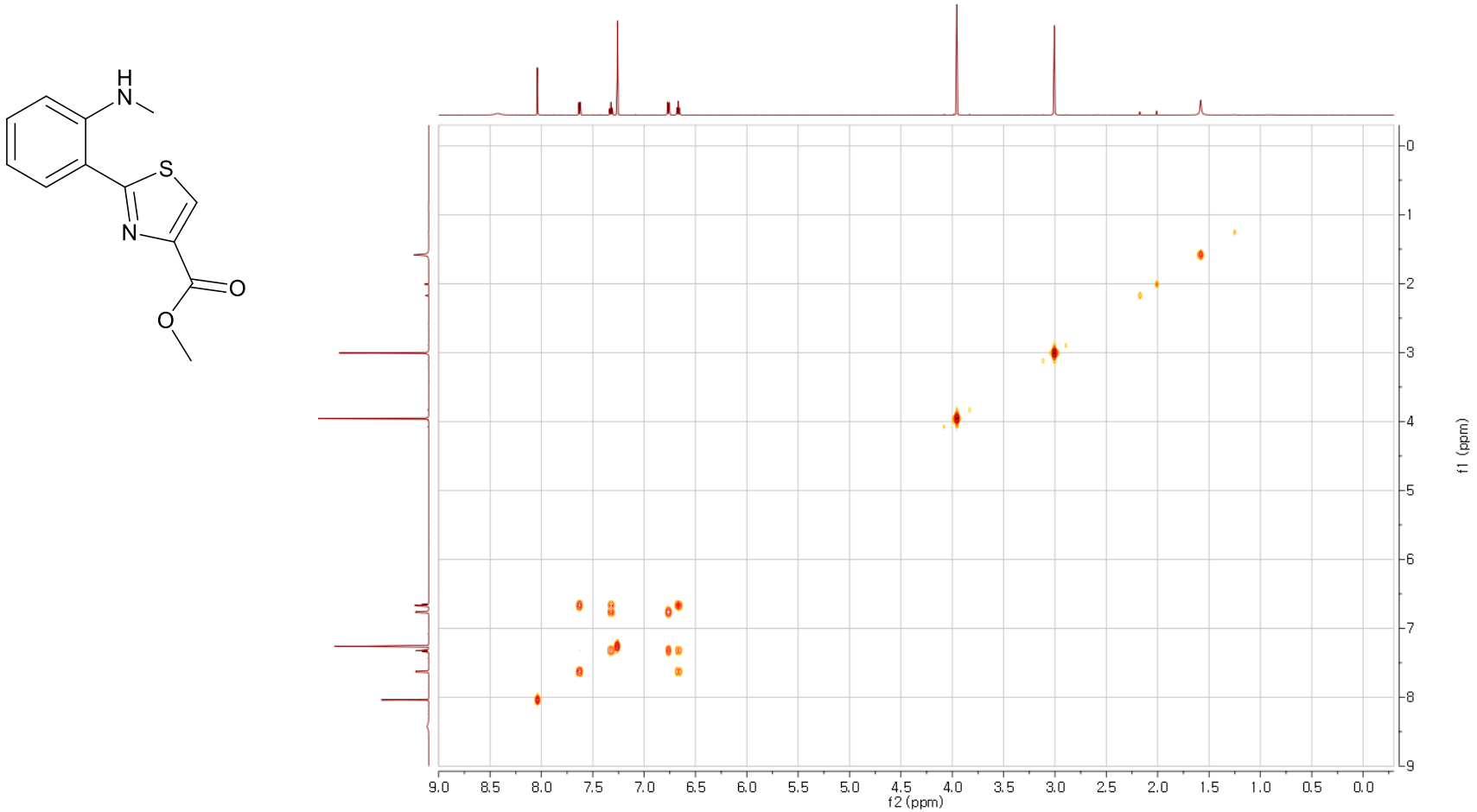

Figure B.2.4 HSQC NMR spectrum of Anithiactin A ($CDCl_3$, 600 MHz)

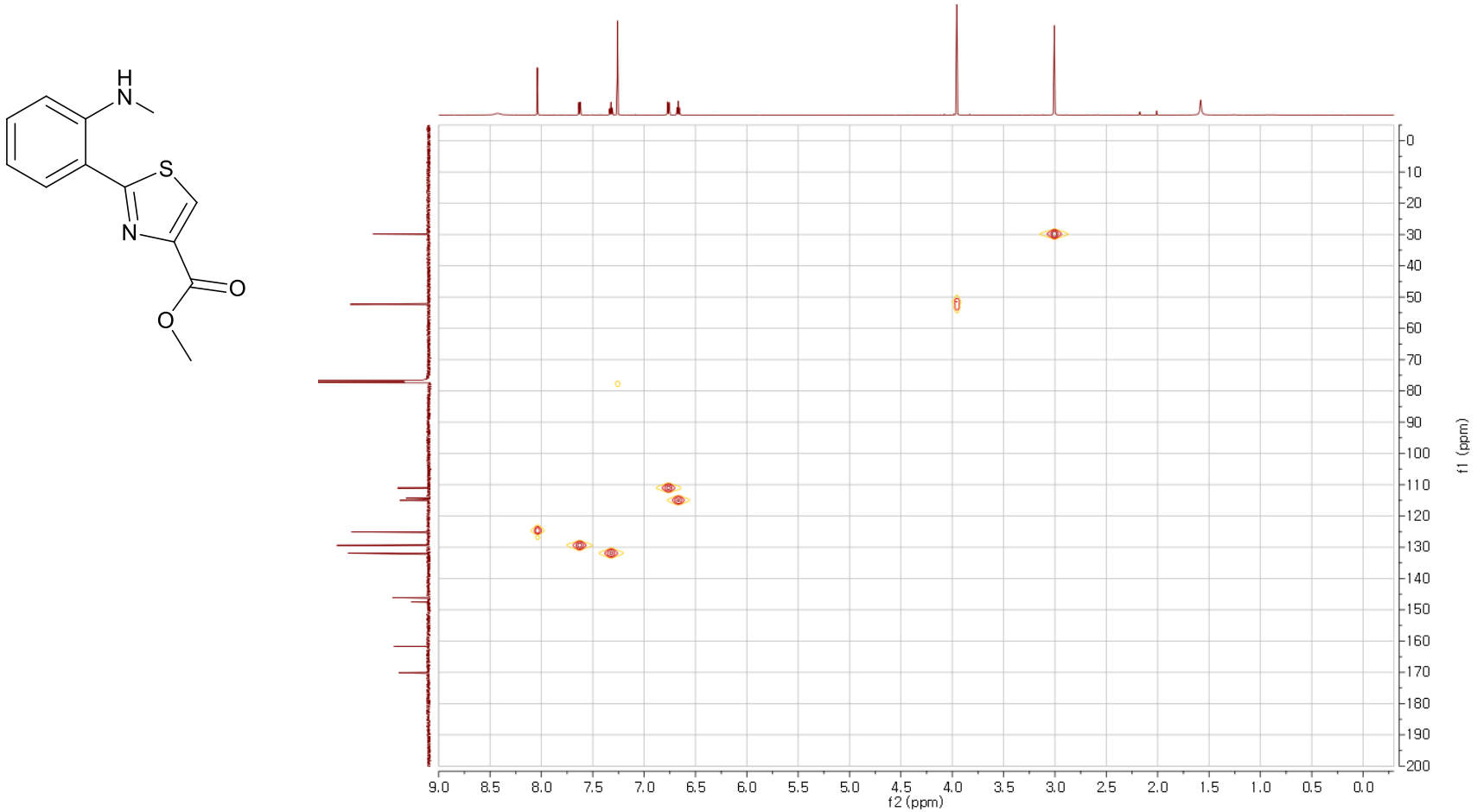

Figure B.2.5 HMBC NMR spectrum of Anithiactin A ($CDCl_3$, 600 MHz)

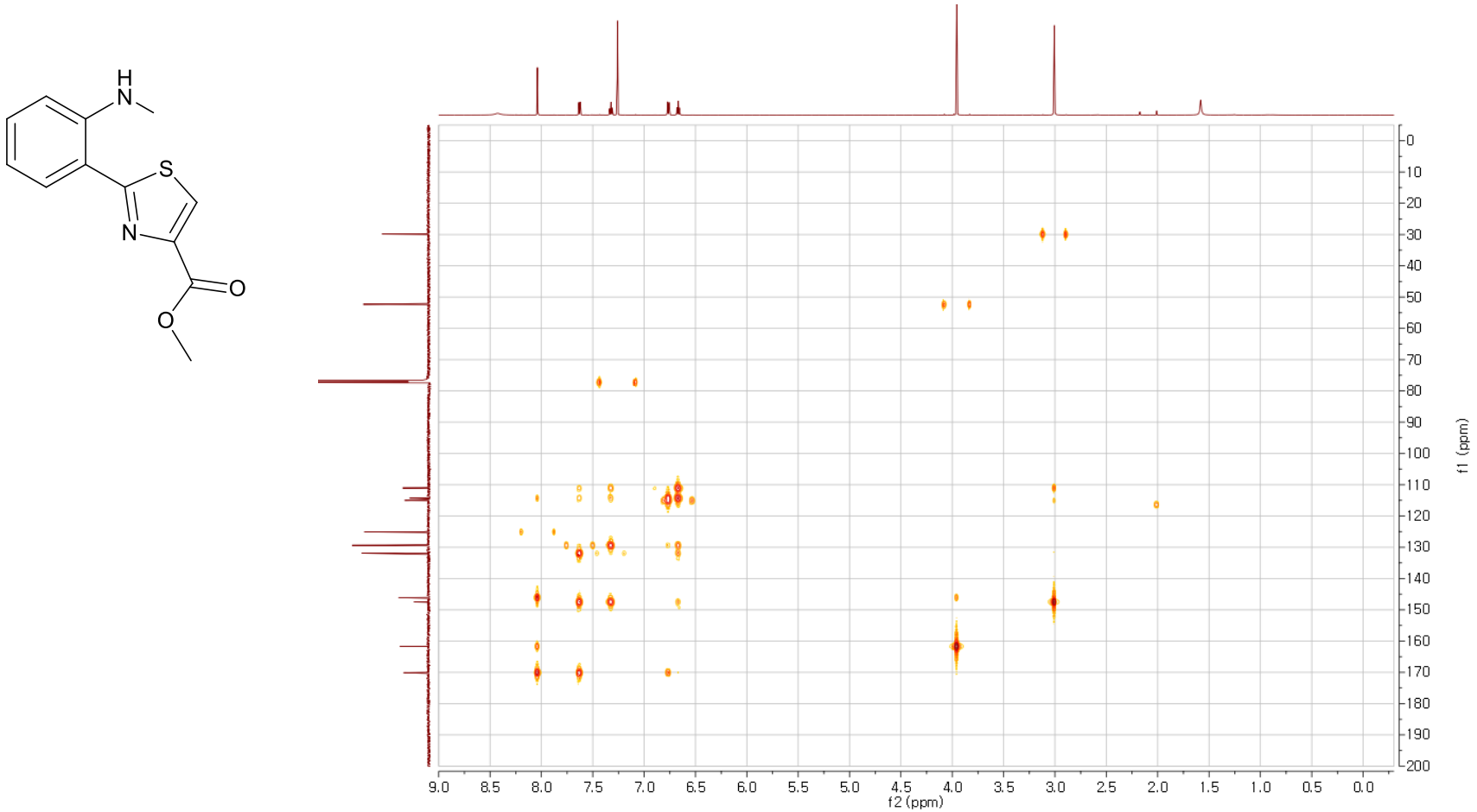

Figure B.2.6 ^{1}H NMR spectrum of Anithiactin B ($CDCl_3$, 600 MHz)

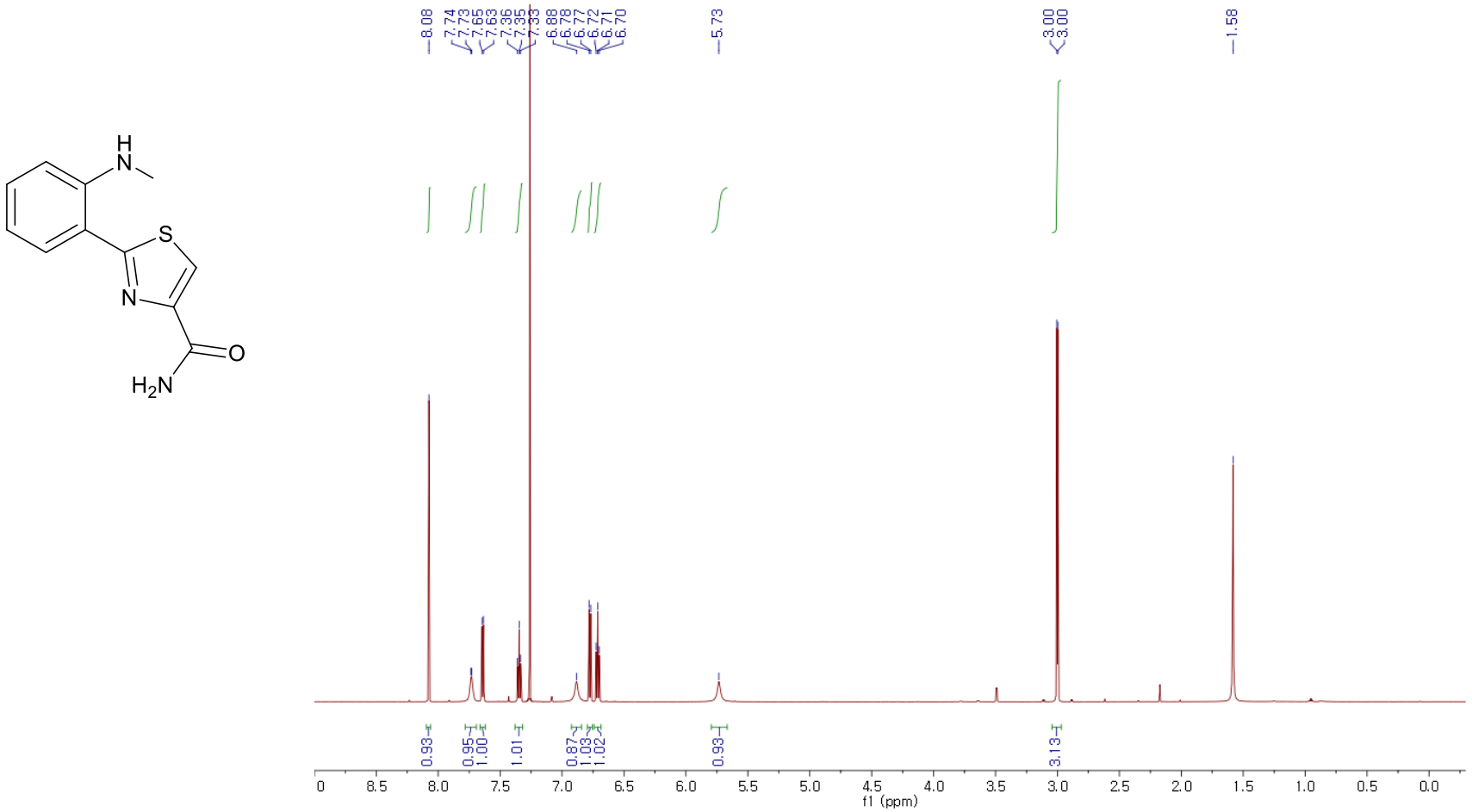

Figure B.2.7 ^{13}C NMR spectrum of Anithiactin B ($CDCl_3$, 600 MHz)

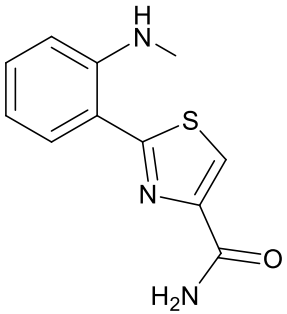

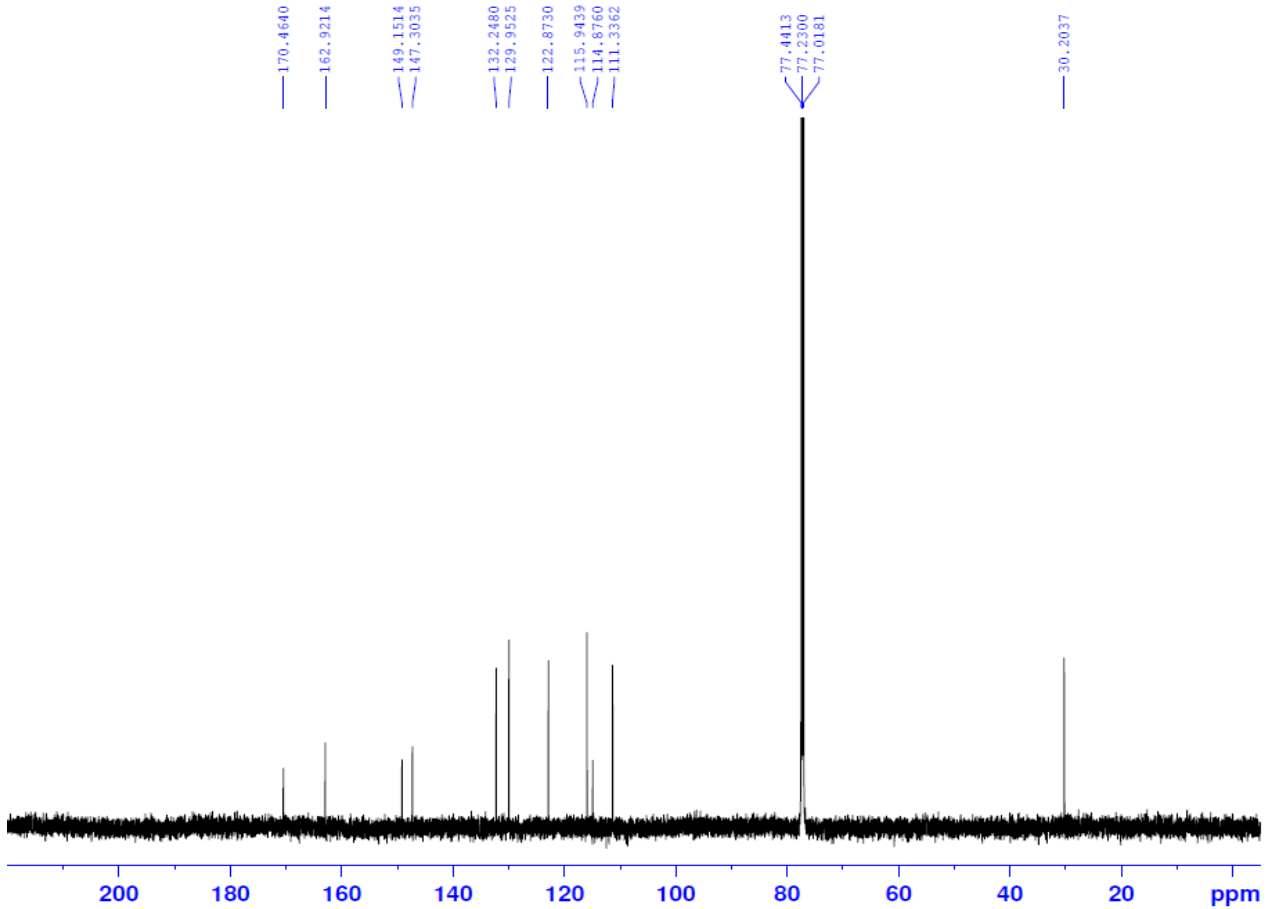

Figure B.2.8 ^{1}H NMR spectrum of Anithiactin C ($CDCl_3$, 600 MHz)

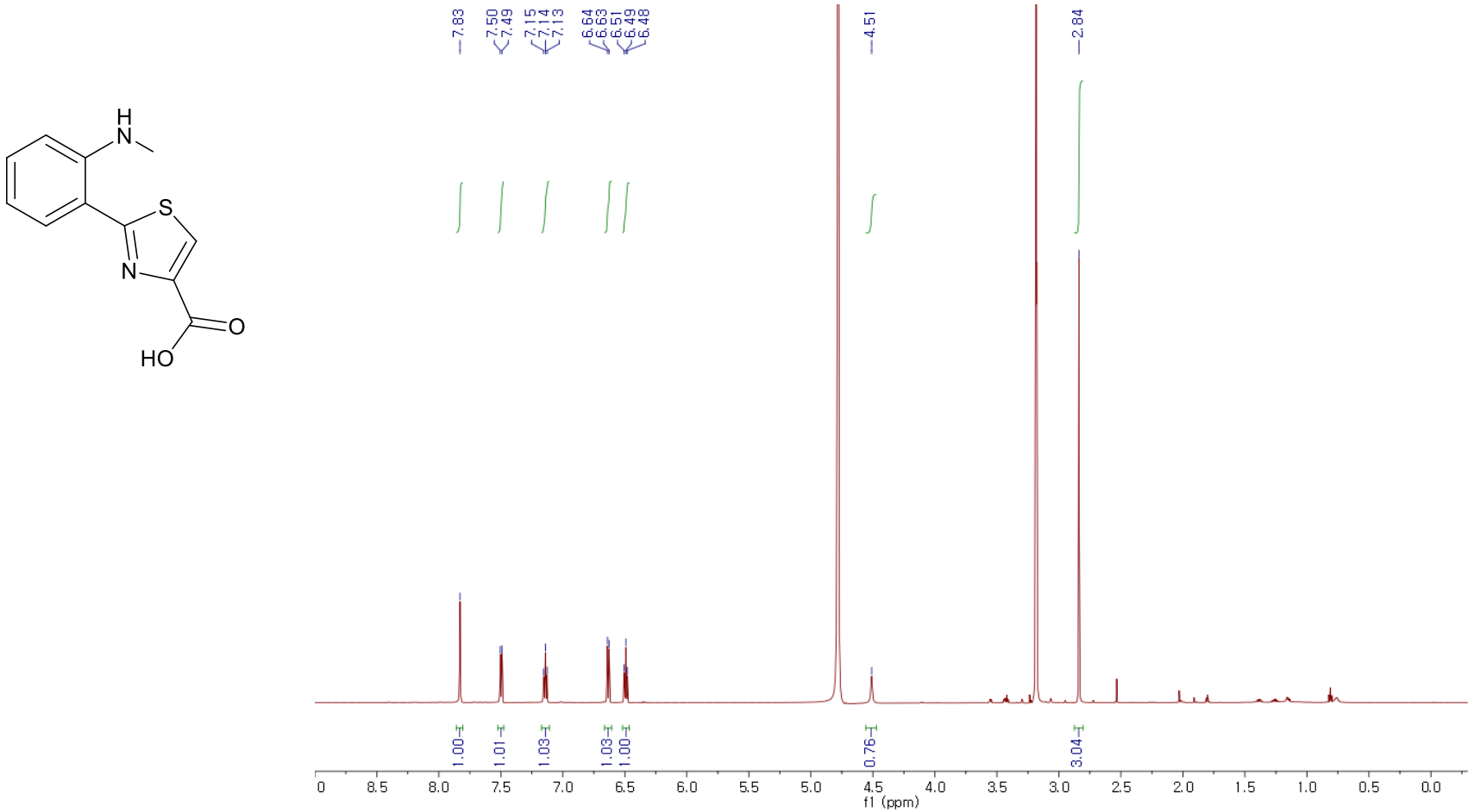

Figure B.2.9 ^{13}C NMR spectrum of Anithiactin C ($CDCl_3$, 600 MHz)

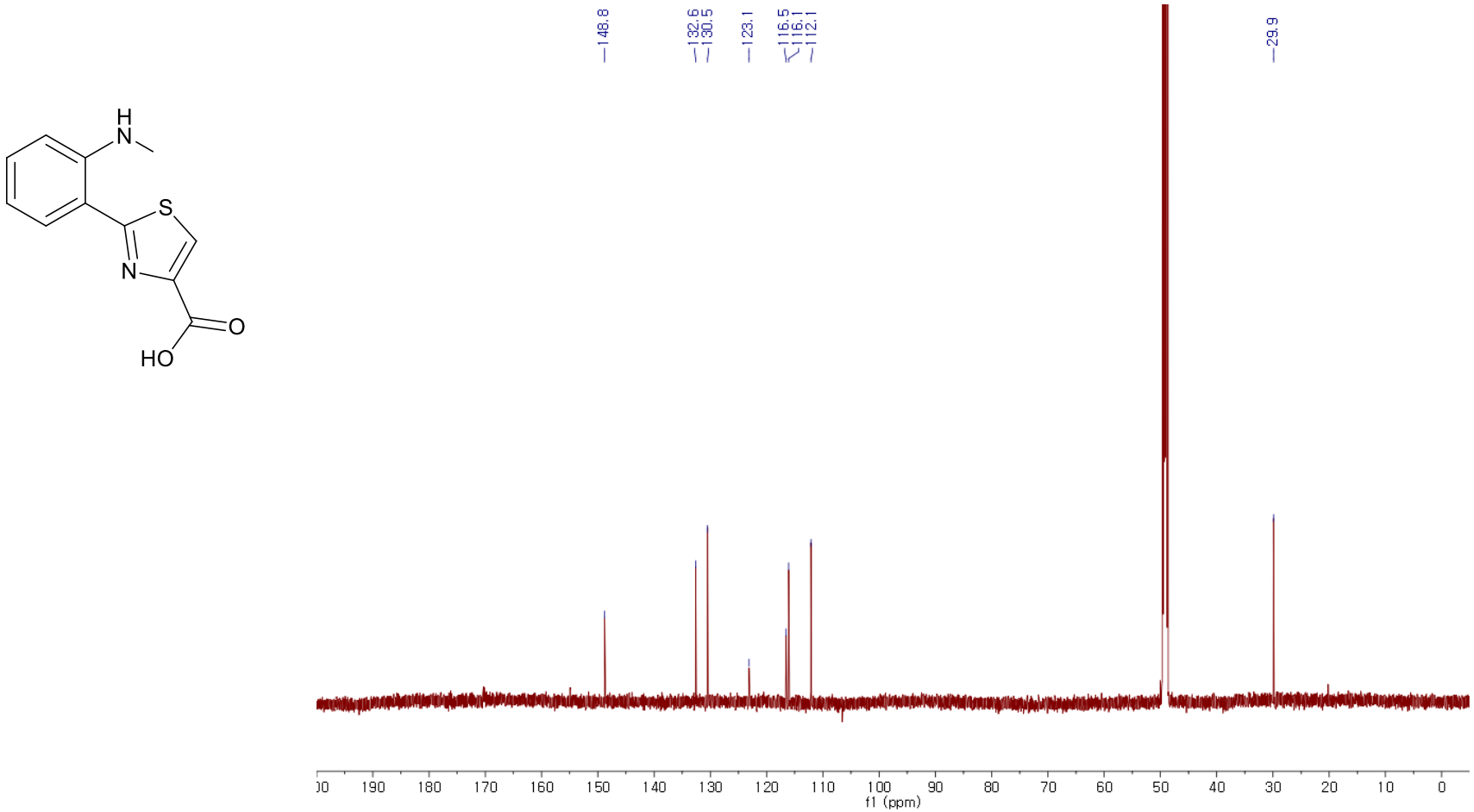

Figure B.2.10 ^{1}H NMR Spectrum of Anithiactin D (CD_3OD, 700 MHz)

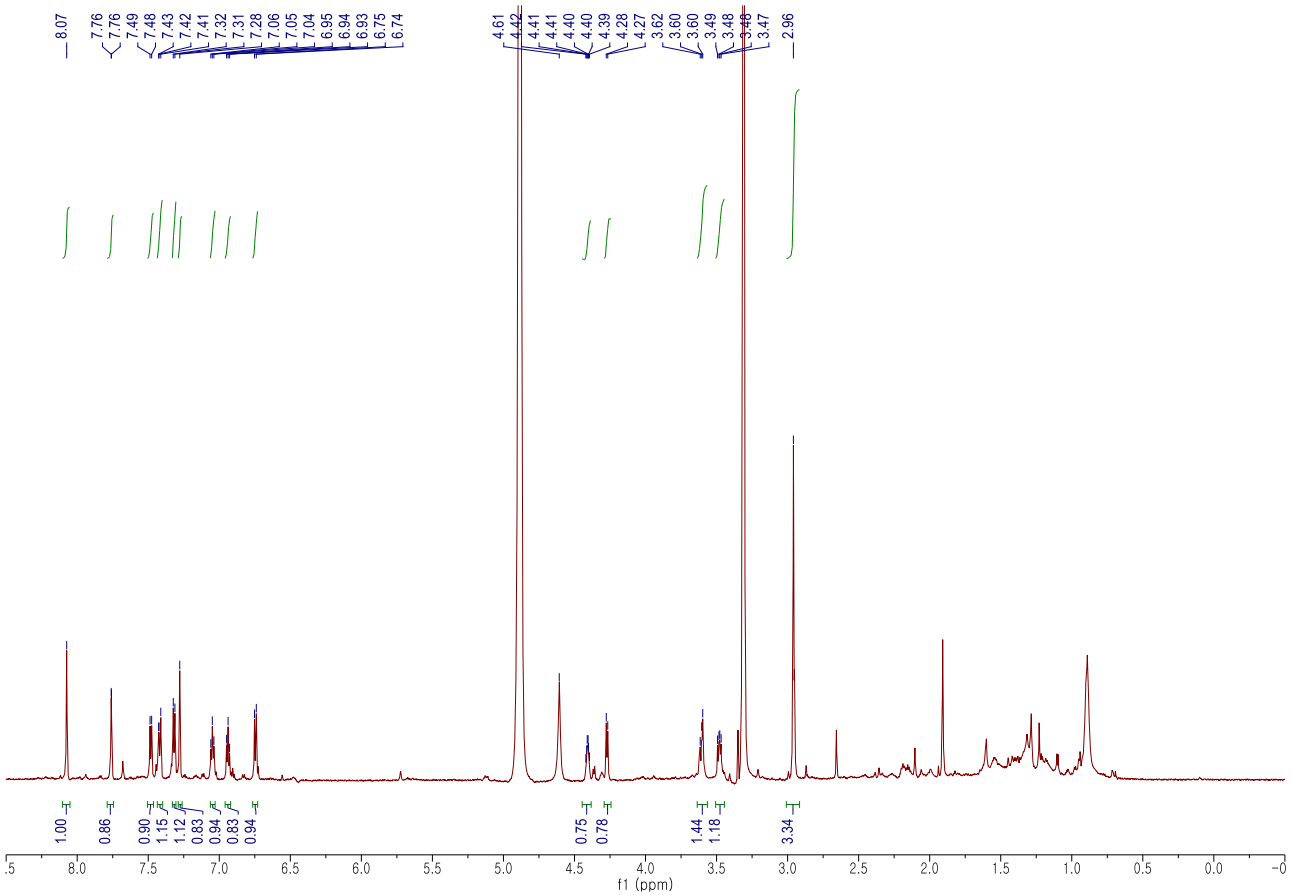

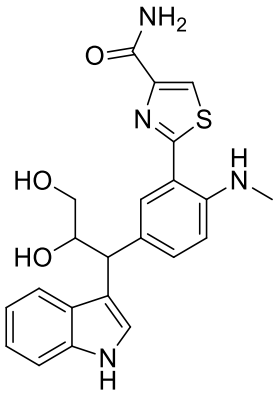

Figure B.2.11 COSY NMR Spectrum of Anithiactin D (CD_3OD, 700 MHz)

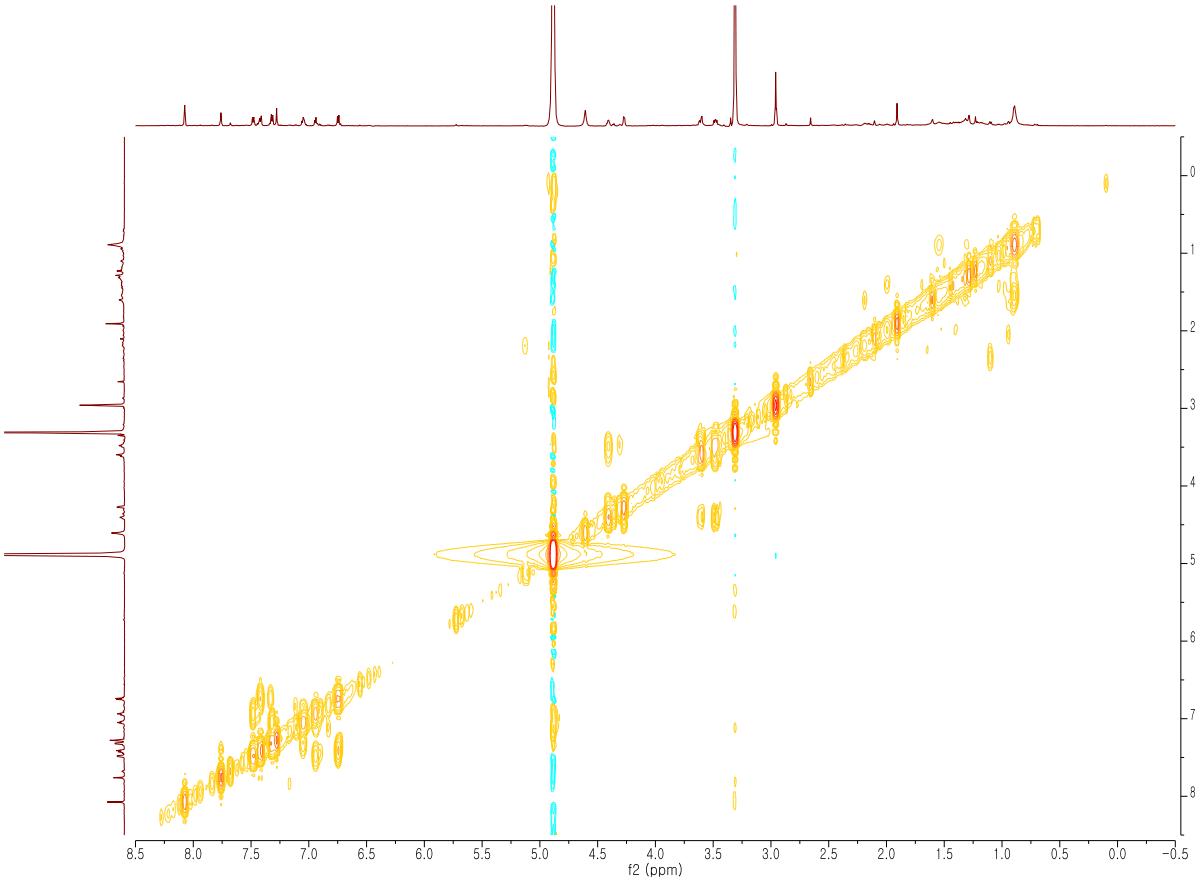

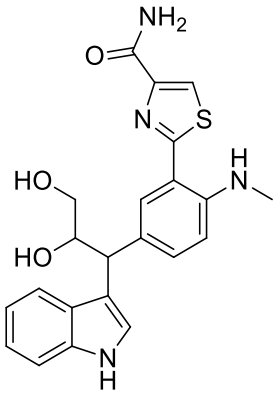

Figure B.2.12 HSQC NMR Spectrum of Anithiactin D (CD_3OD, 700 MHz)

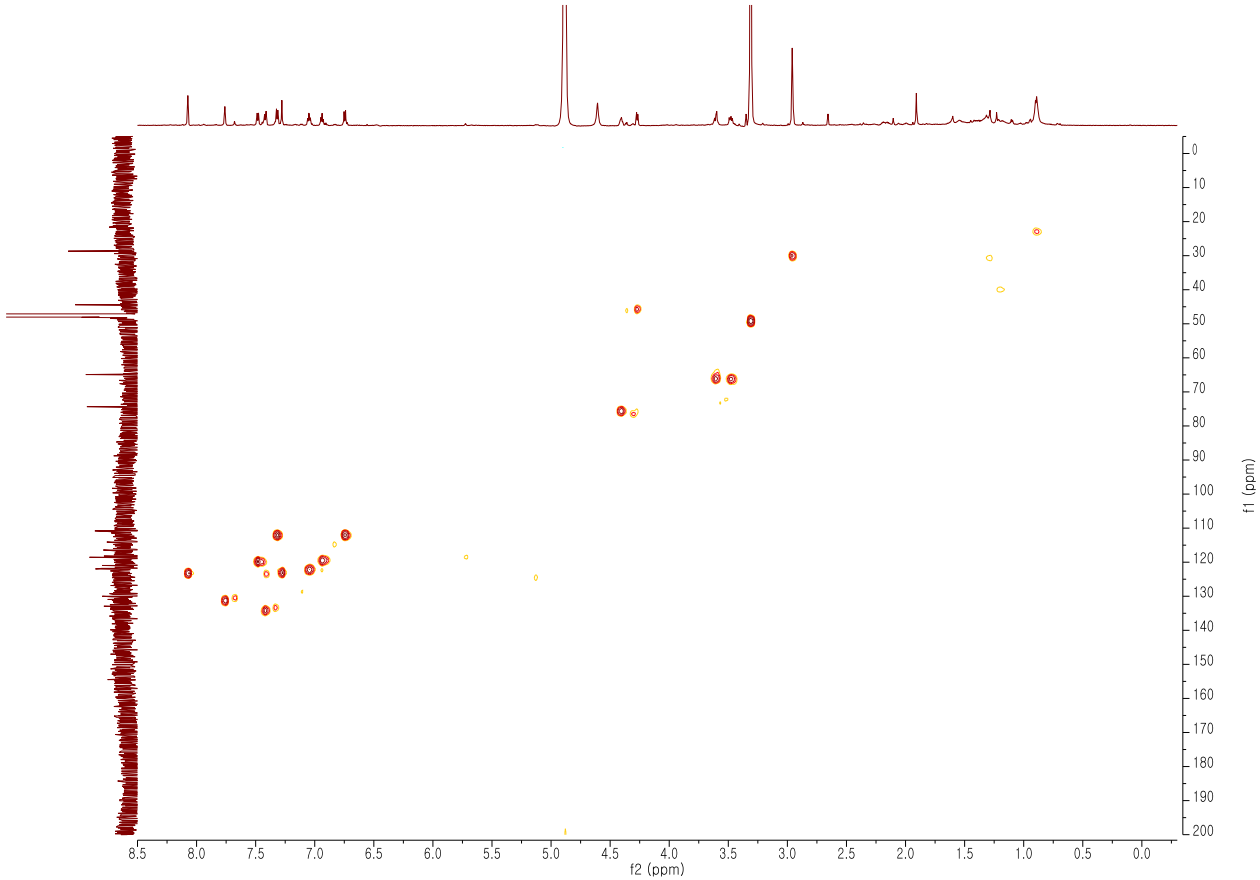

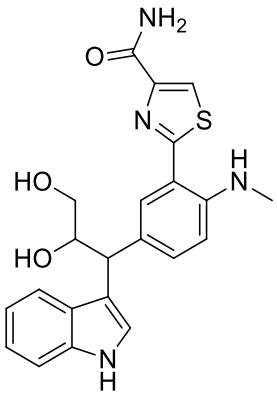

Figure B.2.13 HMBC NMR Spectrum of Anithiactin D (CD_3OD, 700 MHz)

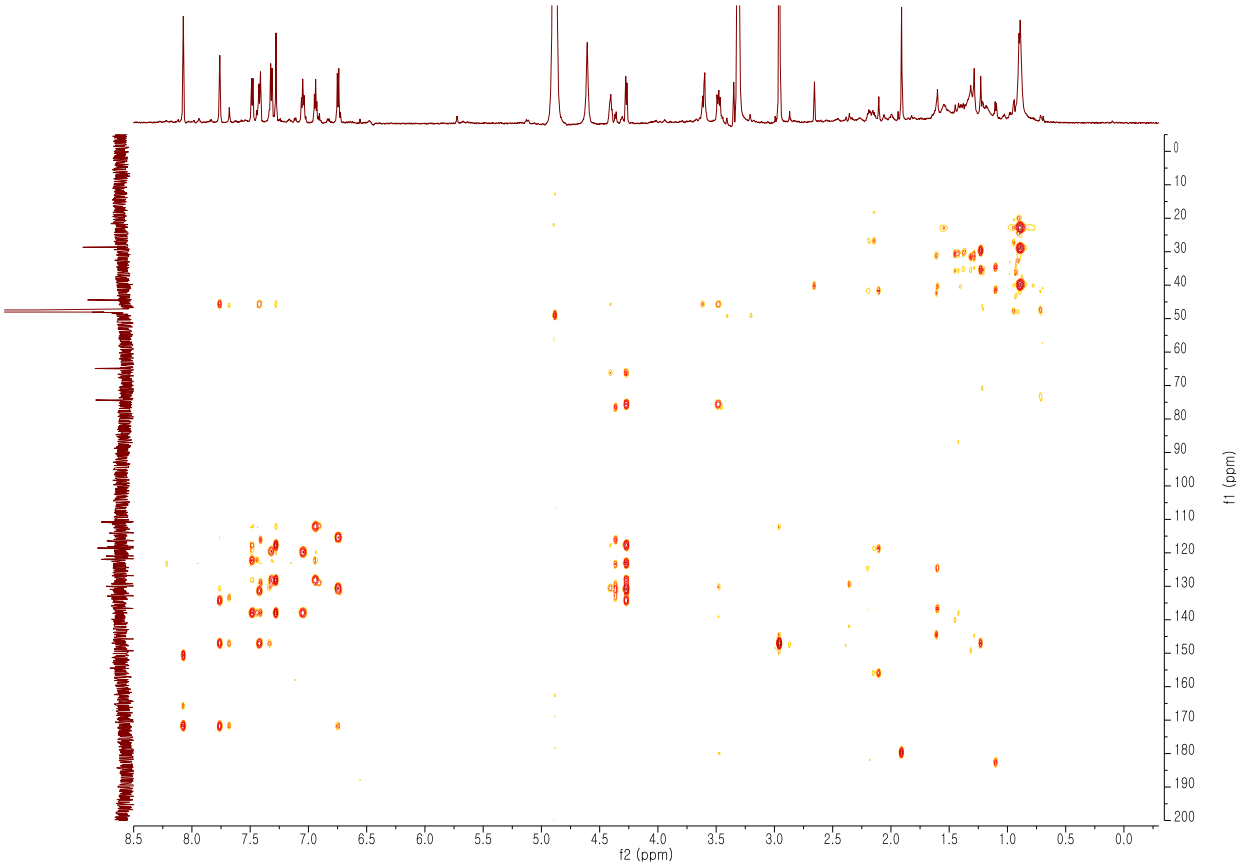

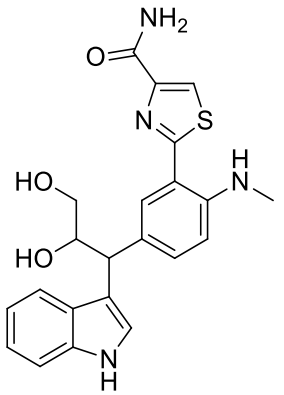

Figure B.2.14 ^{1}H NMR spectrum of synthetic intermediate 6 ($CDCl_3$, 600 MHz)

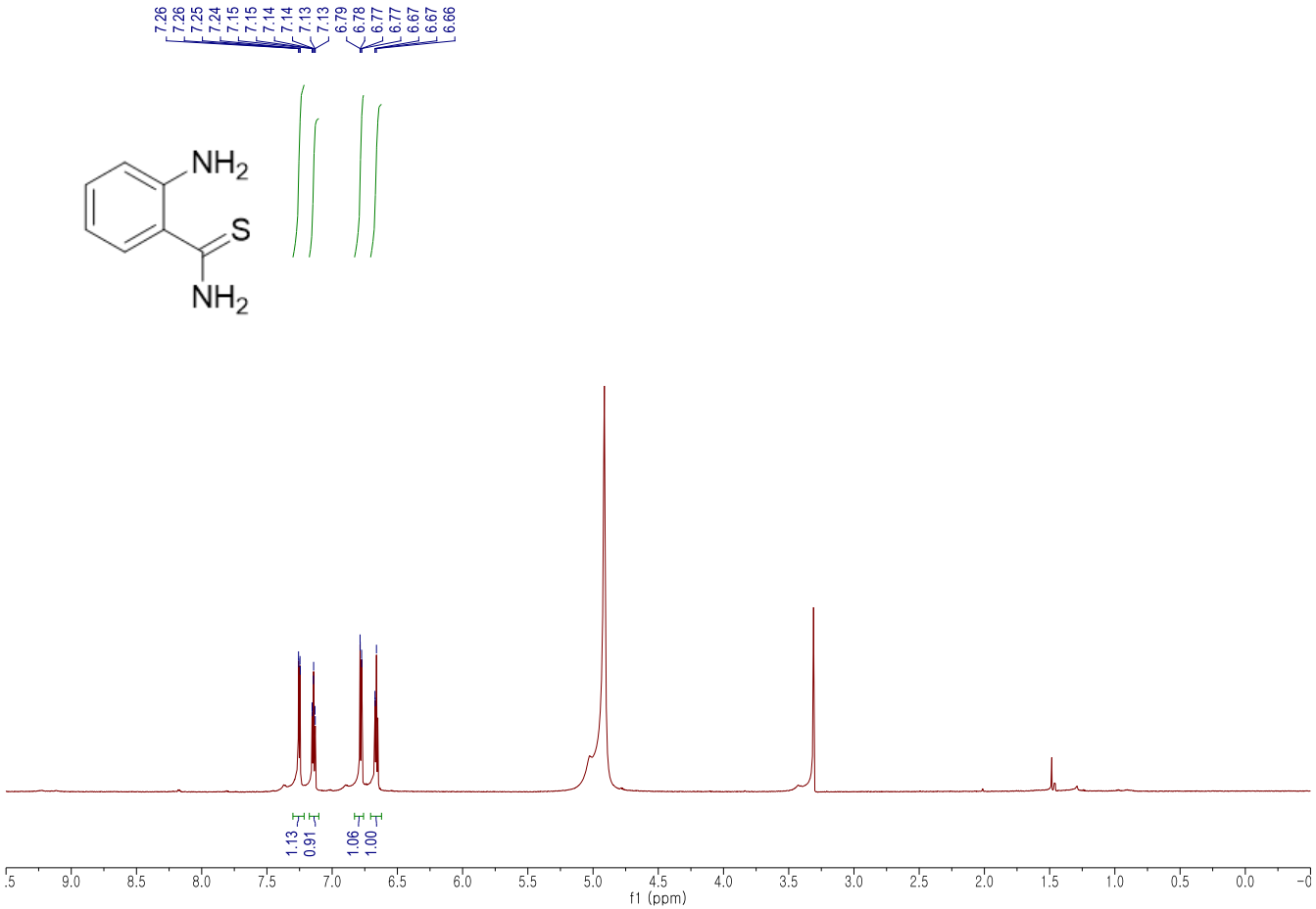

Figure B.2.15 ^{13}C NMR spectrum of synthetic intermediate 6 ($CDCl_3$, 600 MHz)

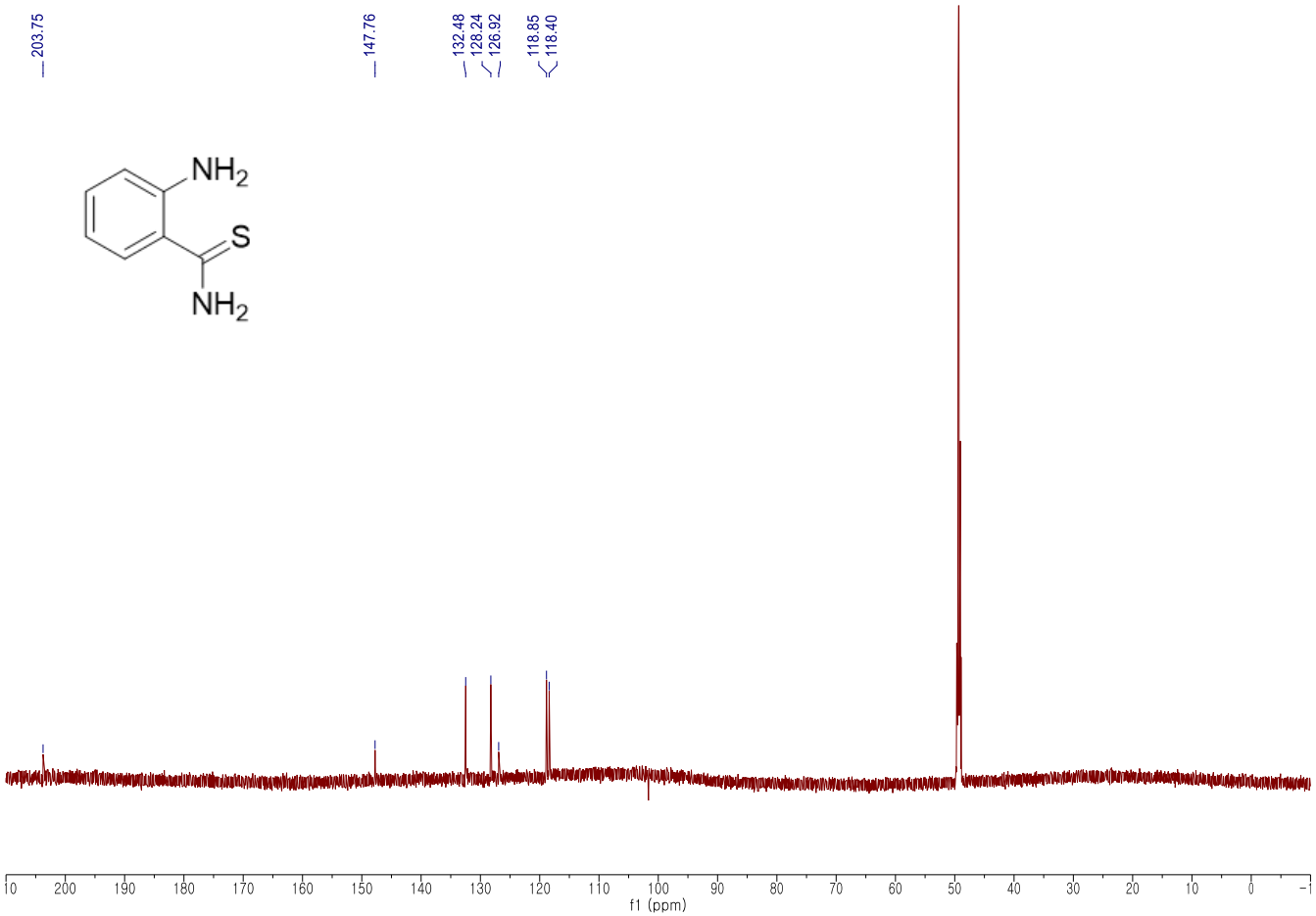

Figure B.2.16 ^{1}H NMR spectrum of synthetic intermediate 7 ($CDCl_3$, 600 MHz)

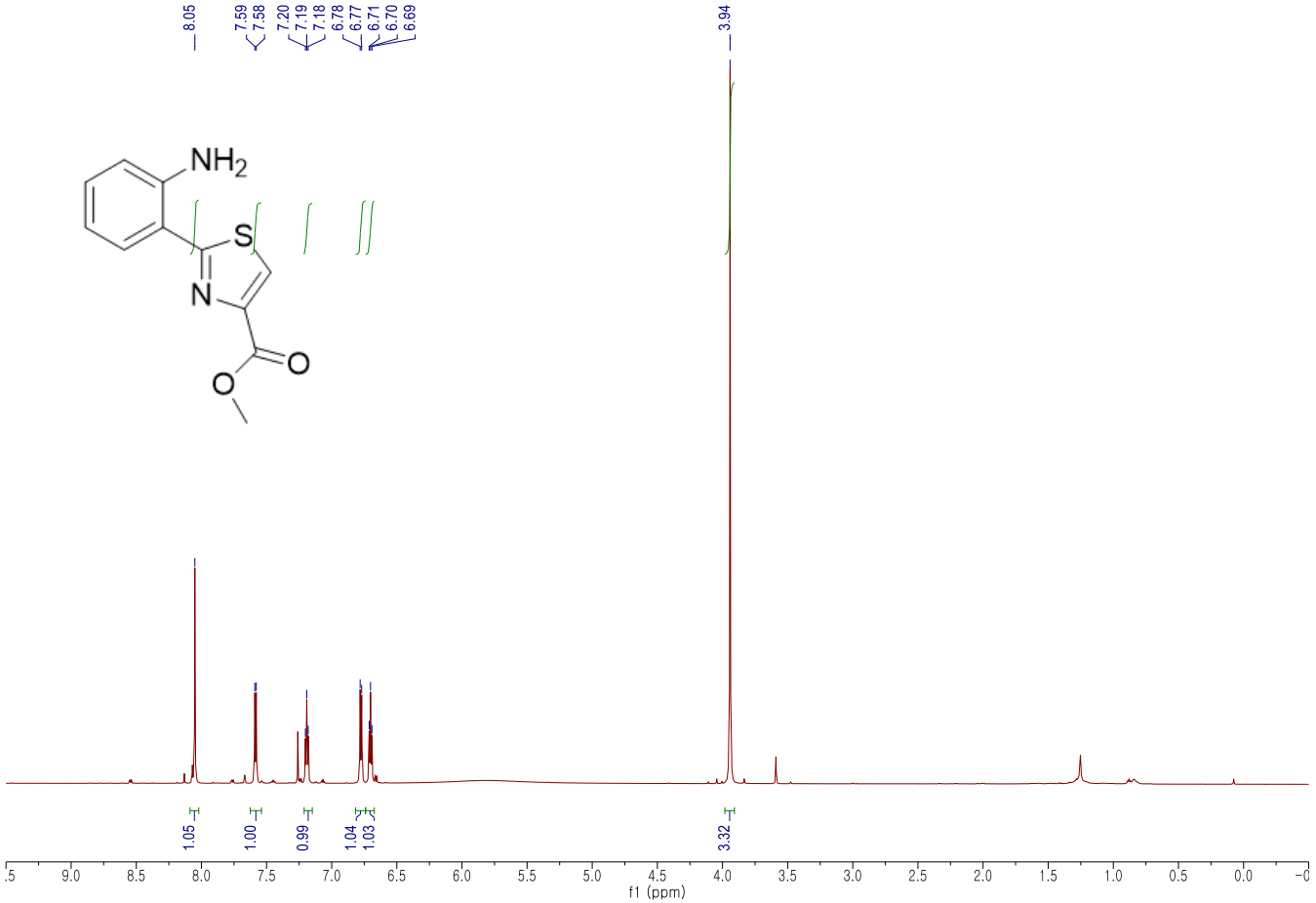

Figure B.2.17 ^{13}C NMR spectrum of synthetic intermediate 7 ($CDCl_3$, 600 MHz)

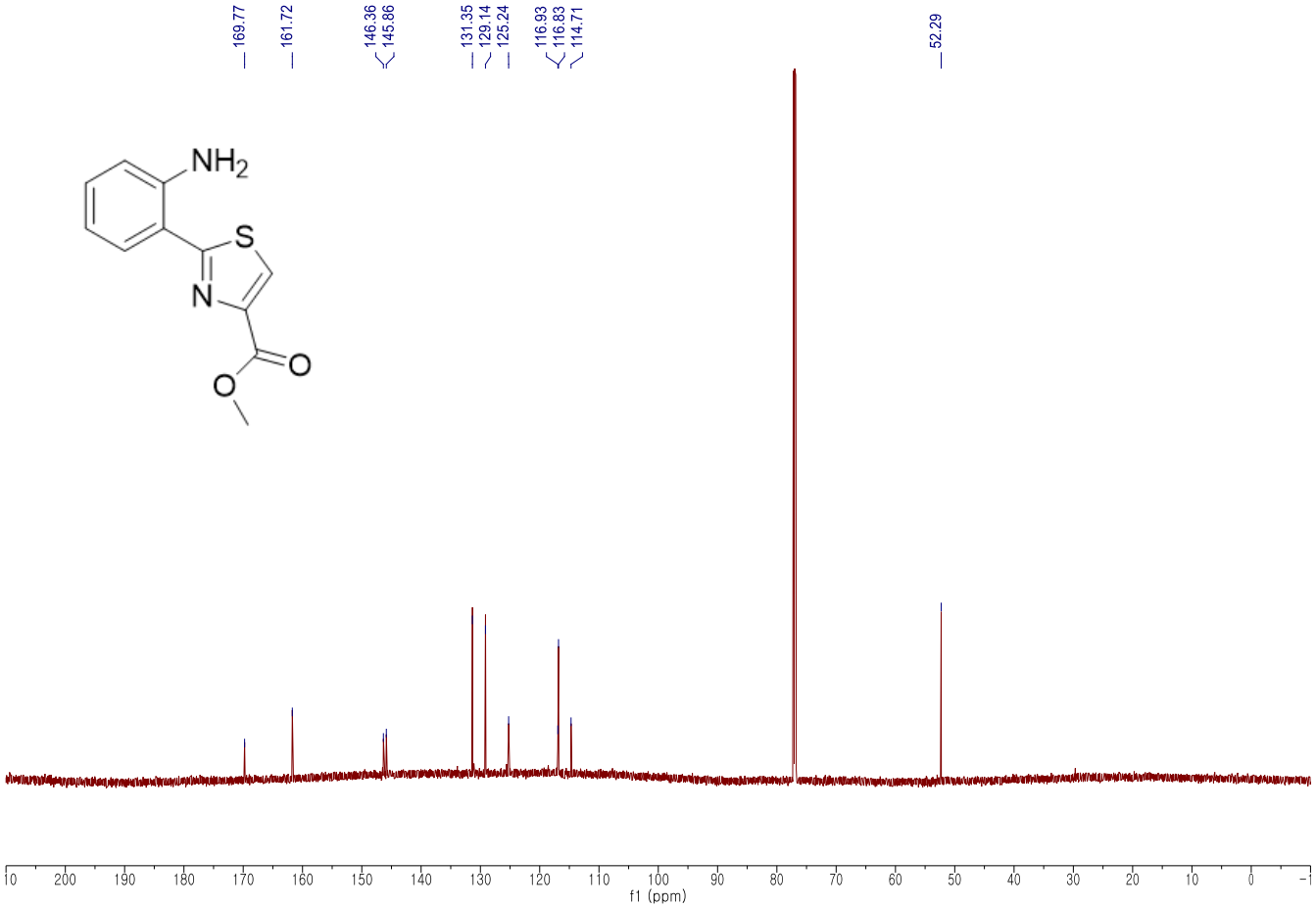

Figure B.2.18 ^{1}H NMR spectrum of synthetic Anithiactin A ($CDCl_3$, 600 MHz)

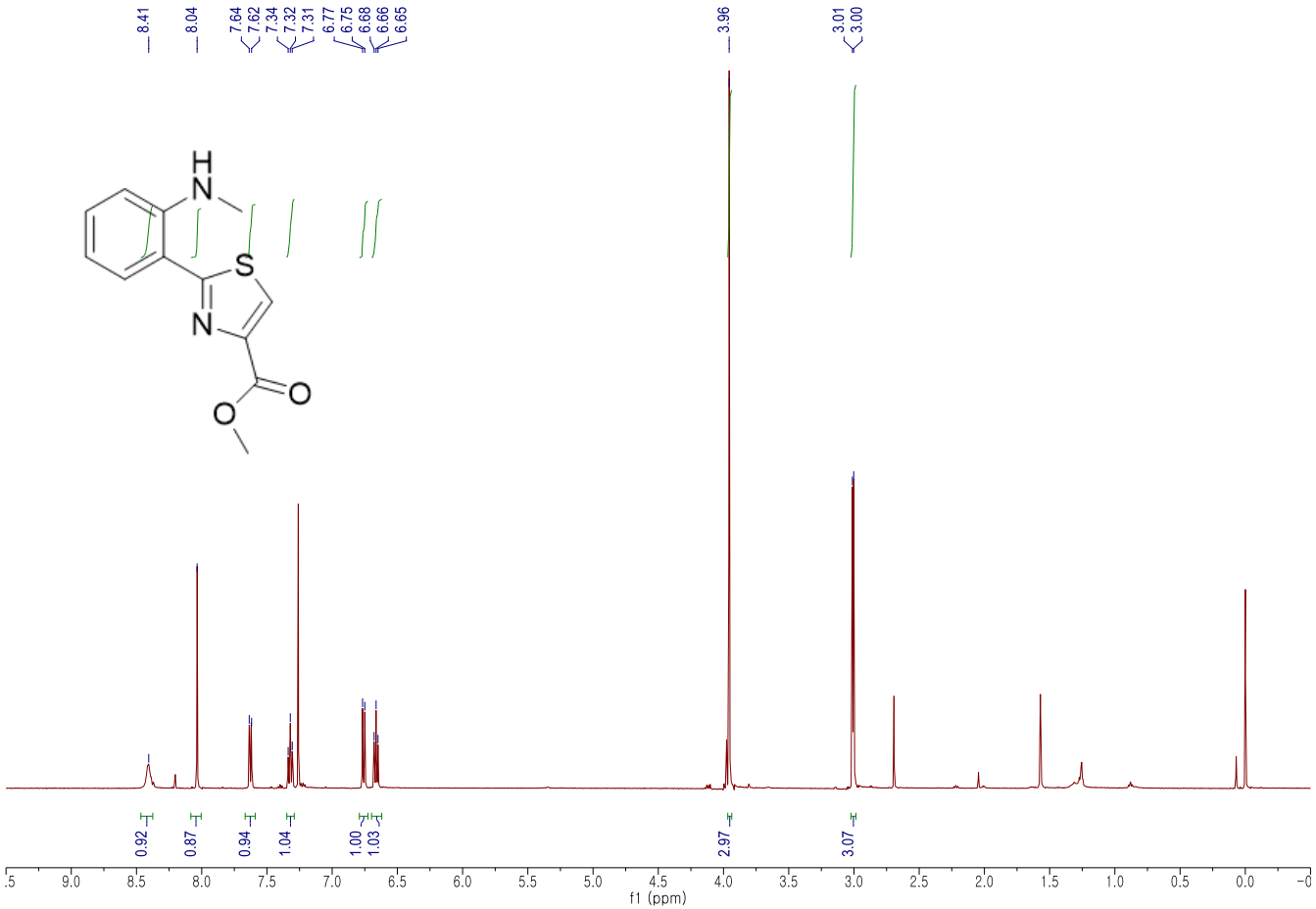

Figure B.2.19 ^{13}C NMR spectrum of synthetic Anithiactin A ($CDCl_3$, 600 MHz)

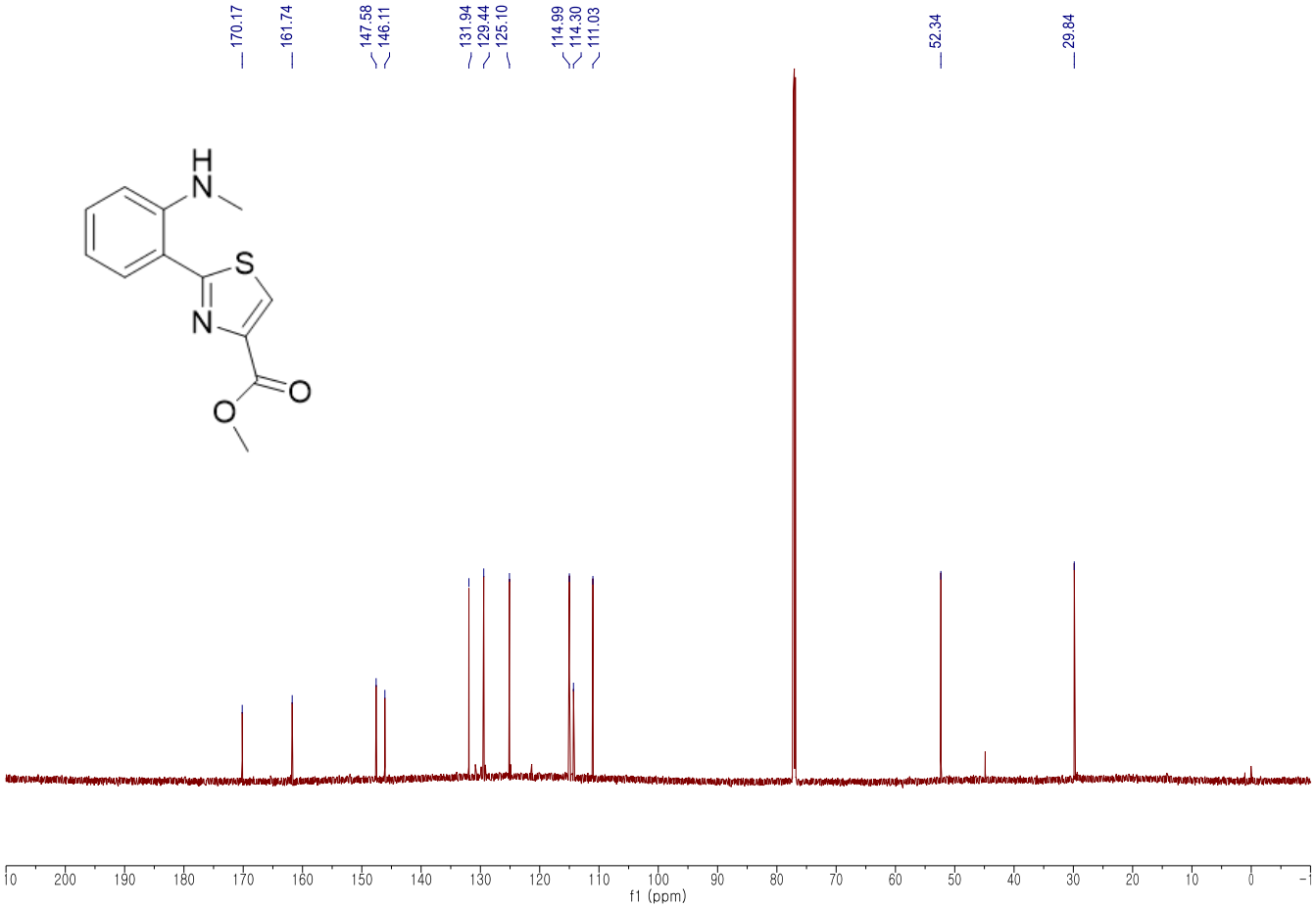

한글초록

해양천연물은 원천생물의 다양성에 기반한 신약후보물질의 새로운 공급원으로 각광받고 있다. 스쿠버다이빙이나 유인잠수정과 같은 기술의 발전에 힘입어 관심이 더해지고 있으며, 현재 8 종의 해양신약이 개발되었다. 대부분의 해양신약은 해양무척추동물로부터 분리된 해양천연물에 기반하여 개발되었으나, 최근에 들어 실제적인 생산자가 해양미생물인 것이 알려지게 되었다. 이 연구에서는 다양한 해양환경에서 분리된 방선균에서 신규한 생리활성 해양천연물을 분리하였다.

미국 캘리포니아 연안의 퇴적물에서 분리한 *Nocardiopsis* sp. CNQ115 에서 2 개의 새로운 이미다졸 천연물인 nocarimidazole A 와 B 를 분리하였다. Nocarimidazole A 와 B 의 화학구조를 NMR 을 이용하여 결정하였다. 항균활성과 항암활성을 확인하였으나, 주목할만하지 않다. 서해의 갯벌에서 *Streptomyces* sp. 10A085 를 분리하여 화학 조성물을 분석하였다. 새로운 티아졸 천연물 anithiactin A - D 를 분리하여 NMR 을 이용하여 화학구조를 결정하였다. Anithiactin B 는 X-ray 결정구조분석을 같이 수행하였다. Anithiactin A - C 는 acetylcholinesterase 를 저해하는 활성을 보였으며, 세포독성은 관찰되지 않았다.